frontiers | Research Topics

Streaming inflammation: From damage to healing and resilience - volume II

Edited by
Pallavi R. Devchand, Garret A. FitzGerald and Eric Schadt

Published in
Frontiers in Pharmacology

ISSN 1664-8714
ISBN 978-2-83252-128-1
DOI 10.3389/978-2-83252-128-1

About Frontiers

Frontiers is more than just an open access publisher of scholarly articles: it is a pioneering approach to the world of academia, radically improving the way scholarly research is managed. The grand vision of Frontiers is a world where all people have an equal opportunity to seek, share and generate knowledge. Frontiers provides immediate and permanent online open access to all its publications, but this alone is not enough to realize our grand goals.

Frontiers journal series

The Frontiers journal series is a multi-tier and interdisciplinary set of open-access, online journals, promising a paradigm shift from the current review, selection and dissemination processes in academic publishing. All Frontiers journals are driven by researchers for researchers; therefore, they constitute a service to the scholarly community. At the same time, the *Frontiers journal series* operates on a revolutionary invention, the tiered publishing system, initially addressing specific communities of scholars, and gradually climbing up to broader public understanding, thus serving the interests of the lay society, too.

Dedication to quality

Each Frontiers article is a landmark of the highest quality, thanks to genuinely collaborative interactions between authors and review editors, who include some of the world's best academicians. Research must be certified by peers before entering a stream of knowledge that may eventually reach the public - and shape society; therefore, Frontiers only applies the most rigorous and unbiased reviews. Frontiers revolutionizes research publishing by freely delivering the most outstanding research, evaluated with no bias from both the academic and social point of view. By applying the most advanced information technologies, Frontiers is catapulting scholarly publishing into a new generation.

What are Frontiers Research Topics?

Frontiers Research Topics are very popular trademarks of the *Frontiers journals series*: they are collections of at least ten articles, all centered on a particular subject. With their unique mix of varied contributions from Original Research to Review Articles, Frontiers Research Topics unify the most influential researchers, the latest key findings and historical advances in a hot research area.

Find out more on how to host your own Frontiers Research Topic or contribute to one as an author by contacting the Frontiers editorial office: frontiersin.org/about/contact

Streaming inflammation: From damage to healing and resilience - volume II

Topic editors

Pallavi R. Devchand — University of Calgary, Canada

Garret A. FitzGerald — University of Pennsylvania, United States

Eric Schadt — Icahn School of Medicine at Mount Sinai, United States

Citation

Devchand, P. R., FitzGerald, G. A., Schadt, E., eds. (2023). *Streaming inflammation: From damage to healing and resilience - volume II*. Lausanne: Frontiers Media SA. doi: 10.3389/978-2-83252-128-1

Table of contents

frontiers | Frontiers in Pharmacology

TYPE Editorial
PUBLISHED 24 March 2023
DOI 10.3389/fphar.2023.1185593

OPEN ACCESS

EDITED AND REVIEWED BY
Dieter Steinhilber,
Goethe University Frankfurt, Germany

*CORRESPONDENCE
Pallavi R. Devchand,
Pallavi.Devchand@ucalgary.ca

SPECIALTY SECTION
This article was submitted to Inflammation Pharmacology, a section of the journal Frontiers in Pharmacology

RECEIVED 13 March 2023
ACCEPTED 20 March 2023
PUBLISHED 24 March 2023

CITATION
Devchand PR, Schadt EE and FitzGerald GA (2023), Editorial: Streaming inflammation: From damage to healing and resilience–Volume II.
Front. Pharmacol. 14:1185593.
doi: 10.3389/fphar.2023.1185593

Editorial: Streaming inflammation: From damage to healing and resilience–Volume II

Pallavi R. Devchand[1]*, Eric E. Schadt[2] and Garret A. FitzGerald[3]

[1]Department of Physiology and Pharmacology, University of Calgary, Calgary, AB, Canada, [2]Department of Genetics and Genomic Sciences, Icahn School of Medicine at Mount Sinai, New York, NY, United States, [3]Department of Systems Pharmacology and Translational Therapeutics, Perelman School of Medicine, University of Pennsylvania, Philadelphia, PA, United States

KEYWORDS

resilience, disease states, drug target, healing, identity, lipid mediators

Editorial on the Research Topic
Streaming inflammation: From damage to healing and resilience–Volume II

> "It takes a very long time to become young."
>
> -*Pablo Ruiz Picasso* (1881-1973)

Age is a kaleidoscope of identity. It mirrors a number, a malady, a development, an insult and . . . even a compliment. In all dimensions of time, age reflects the fine balance between adaptability and integrity. Our first volume on Streaming Inflammation deemed every human as a multiplex of ecosystems (Devchand et al.). Here, we explore the impacts of damage, healing and resilience on the plasticity of identity as we age.

Longitudinal studies emphasize that identity is fluid. Sayah et al. demonstrate how optical coherence tomography imaging coupled with an automated segmentation algorithm can be applied to study dynamic cellular responses during eye development. This non-invasive method coupled with selective-receptor modulation during oxygen-induced retinopathy provides a powerful approach to understanding retinopathy of prematurity in small rodents. In humans, using real-world dynamics of the JIR cohort of patients with pediatric inflammatory diseases, Hentgen et al. tackle the dosing regiment of off-label use of Interleukin-1 inhibitors. Interestingly, in patients with a monogenic auto-inflammatory disease, the actual-doses used in treat-to-target data present an adaptive comparison with that of recommended drug dosage of the medications.

Although identity is personal, what we share in common also provides for targeted intervention in promoting healing. Hickey et al. take a computational approach to the chronic inflammation component of complex diseases. Innovatively applying *GenePlexus* supervised machine learning, they depict disease heterogeneity into gene clusters of disease-specific chronic inflammation. This facilitates imputing drug priority per disease cluster and identifying potential novel therapeutics. Meanwhile, Skaria et al. toggle Wnt-5A signaling to evaluate pharmacokinetics mediated by damage from innate immune responses on primary human coronary artery endothelial cells. Using transcriptomics and gene ontology analysis,

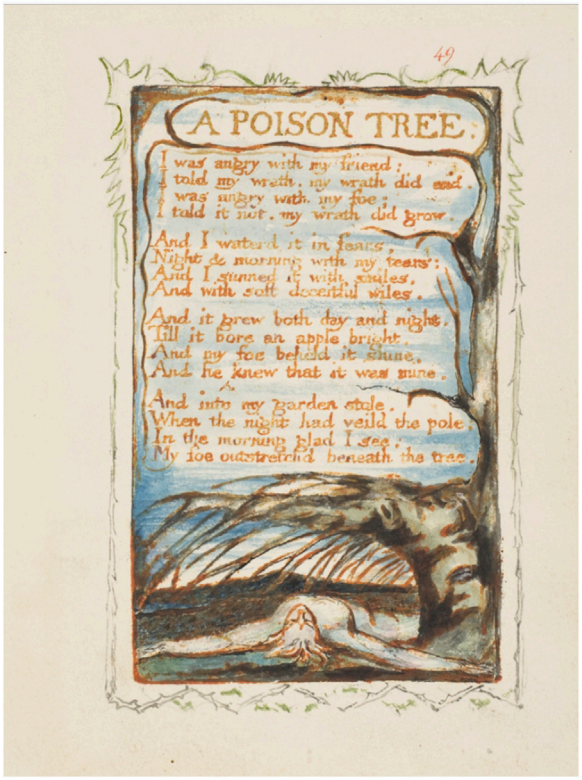

FIGURE 1
Songs of Experience: A Poison Tree. Plate 49. William Blake (British, London 1757-1827). The Metropolitan Museum of Art, New York, Rogers Fund, 1917. www.metmuseum.org. Image obtained under The Met's Open Access progam.

they zone in on the potential need to reflect on the drug-metabolizing cytochrome P450 enzymes, specifically Cyp1A1/Cyp1B1.

Lipid mediators are potent instigators of change in identity. Yamaguchi et al. review the dynamics of bioactive lipids in the blood and vascular wall. The biosynthesis and mechanistic signaling are critically discussed in context of pro- and anti-inflammation. Bergqvist et al. developed a semi-high throughput bioassay measuring prostaglandin E_2 production and IL-8 secretion from whole human blood. Interestingly, this study focus is on key epigenetic modulators and kinase inhibitors within the Structural Genomic Consortium, and aims to identify chemical probes that potentially trigger resolution of chronic inflammation.

Throughout life, the bone is a hub of remodeling of identity. Kalkar et al. focus on the interplay between immune cells and osteoclasts. They reveal an intriguing interplay between a nitrogen-containing bisphosphonate and a glucocorticoid that intersects at interferon-ß expression to inhibit osteoclastogenesis. This work has potential implications on prevention of osteolytic lesions post-chemotherapy.

Dietary intervention of immune activity is a universal story of age. In a didactic exercise, Wang et al. review the concept of trained immunity in atherosclerosis from perspective of metabolic reprogramming, epigenetic reprogramming and promotion of myelopoieisis progenitors. Substantive emphasis is placed on natural products that potentially have anti-atherosclerotic abilities *via* trained monocytes/macrophages. In a different tact, Zhou et al. focus their computational efforts on patients with rosacea. They zone in on an association between keratinocyte autophagy and the mammalian target of rapamycin (mTOR) pathway. After confirming this relationship in a mouse model, they use molecular docking analyses to pinpoint the natural polyphenol EGCG as a candidate lead for mTOR-pathway therapeutics.

Resilience often surfaces in the face of vulnerability. Cheng et al. perform a prospective study on the effective use of vercanozole in treatment of invasive fungal infections. Through stepwise multivariate linear regression analyses of young and elderly patients from a single-center cohort, they identify factors affecting drug trough and metabolite concentrations in plasma. Intriguing prospects for biomarkers are proposed for correlation to predictive effect of the drug.

Age is an art. Blake's bright apple stems from damage, healing and resilience (Figure 1). Picasso's Pomme is a small matter of fluid identity and relativity. And for larger-than-life Miriam Makeba (1932-2008),

> "Age is getting to know all the ways the world turns, so that if you cannot turn the world the way you want, you can at least get out of the way, so you will not get run over."

Author contributions

PD wrote the manuscript, ES and GF contributed to final edits.

Funding

PD is funded in part by a K.A.S.H. Scientific Innovation Award. All authors belong to the PENTACON consortium (funded by the National Institutes of Health HL117798).

Acknowledgments

The editors appreciate the enlightening chapter contributions of the authors and the valuable critiques of the reviewers.

Conflict of interest

The authors declare that the research was conducted in the absence of any commercial or financial relationships that could be construed as a potential conflict of interest.

Publisher's note

frontiers in Pharmacology

BRIEF RESEARCH REPORT
published: 12 March 2020
doi: 10.3389/fphar.2020.00296

Novel Anti-Interleukin-1β Therapy Preserves Retinal Integrity: A Longitudinal Investigation Using OCT Imaging and Automated Retinal Segmentation in Small Rodents

Diane N. Sayah[1,2†], Tianwei E. Zhou[1,2,3†], Samy Omri[1,2], Javier Mazzaferri[1], Christiane Quiniou[4], Maëlle Wirth[1,2], France Côté[1,2], Rabah Dabouz[1,2,3], Michel Desjarlais[1,2], Santiago Costantino[1,2] and Sylvain Chemtob[1,2,4*]*

[1] Hopital Maisonneuve-Rosemont Research Center, Montreal, QC, Canada, [2] Department of Ophthalmology, Faculty of Medicine, Université de Montréal, Montreal, QC, Canada, [3] Faculty of Medicine, McGill University, Montreal, QC, Canada, [4] Department of Pediatrics, Centre Hospitalier Universitaire Sainte-Justine Research Center, Université de Montréal, Montreal, QC, Canada

Retinopathy of prematurity (ROP) is the leading cause of blindness in neonates. Inflammation, in particular interleukin-1β (IL-1β), is increased in early stages of the disorder, and contributes to inner and outer retinal vasoobliteration in the oxygen-induced retinopathy (OIR) model of ROP. A small peptide antagonist of IL-1 receptor, composed of the amino acid sequence, rytvela, has been shown to exert beneficial anti-inflammatory effects without compromising immunovigilance-related NF-κB in reproductive tissues. We conducted a longitudinal study to determine the efficacy of "rytvela" in preserving the integrity of the retina in OIR model, using optical coherence tomography (OCT) which provides high-resolution cross-sectional imaging of ocular structures *in vivo*. Sprague–Dawley rats subjected to OIR and treated or not with "rytvela" were compared to IL-1 receptor antagonist (Kineret). OCT imaging and custom automated segmentation algorithm used to measure retinal thickness (RT) were obtained at P14 and P30; gold-standard immunohistochemistry (IHC) was used to confirm retinal anatomical changes. OCT revealed significant retinal thinning in untreated animals by P30, confirmed by IHC; these changes were coherently associated with increased apoptosis. Both rytvela and Kineret subsided apoptosis and preserved RT. As anticipated, Kineret diminished both SAPK/JNK and NF-κB axes, whereas rytvela selectively abated the former which resulted in preserved monocyte phagocytic function. Altogether, OCT imaging with automated segmentation is a reliable non-invasive approach to study longitudinally retinal pathology in small animal models of retinopathy.

Keywords: rytvela, kineret, anti-interleukin-1β, therapy, oxygen-induced retinopathy, retina, optical coherence tomography, automated segmentation

OPEN ACCESS

Edited by:
Gerard Bannenberg, GOED (Global Orgnization for EPA and DHA Omega-3s), United States

Reviewed by:
Claudio Ferrante, Università degli Studi Gabriele d'Annunzio di Chieti e Pescara, Italy
Luigi Brunetti, Università degli Studi Gabriele d'Annunzio di Chieti e Pescara, Italy

***Correspondence:**
Tianwei E. Zhou
ellen.zhou@umontreal.ca
Sylvain Chemtob
sylvain.chemtob@umontreal.ca

† These authors have contributed equally to this work

Specialty section:
This article was submitted to Inflammation Pharmacology, a section of the journal Frontiers in Pharmacology

Received: *16 November 2019*
Accepted: *27 February 2020*
Published: *12 March 2020*

Citation:
Sayah DN, Zhou TE, Omri S, Mazzaferri J, Quiniou C, Wirth M, Côté F, Dabouz R, Desjarlais M, Costantino S and Chemtob S (2020) Novel Anti-Interleukin-1β Therapy Preserves Retinal Integrity: A Longitudinal Investigation Using OCT Imaging and Automated Retinal Segmentation in Small Rodents. Front. Pharmacol. 11:296. doi: 10.3389/fphar.2020.00296

INTRODUCTION

Retinopathy of prematurity (ROP) is the leading cause of severe visual impairment and blindness in neonates and young children in the western world. In the early stages of the disease, pro-inflammatory IL-1β increases markedly, resulting in microvascular decay which culminates in intravitreal neovascularization predisposing to retinal detachment (Penn et al., 1994; Rivera et al., 2013; Zhou et al., 2016). Recently, rytvela, an Interleukin-1 receptor (IL-1R) allosteric modulator, was shown to be effective in preserving retinal microvascular integrity in ischemic retinopathy induced by postnatal hyperoxia (Rivera et al., 2013) and antenatal inflammation (Beaudry-Richard et al., 2018). Akin to other biologics, IL-1 receptor antagonist (commercialized as Kineret) broadly diminishes immunologic functions of IL-1β, thus increasing the likelihood of serious infections, a major concern for relatively immune incompetent immature neonates. Whereas biased signaling modulation by rytvela targets MAPK and Rho GTPase pathways, while desirably preserving immunovigilant-related NF-κB (Nadeau-Vallee et al., 2015).

Optical coherence tomography (OCT) is now widely used in the clinical setting. Based on low-coherence interferometry, Spectral Domain (SD)-OCT provides high-resolution cross-sectional imaging of ocular structures, permitting the non-invasive observation of retinal layers *in vivo* (Huang et al., 1991). We recently adapted OCT modality to laboratory animals by developing a protocol to efficiently acquire OCT images in small rodents (Zhou et al., 2017). OCT allows to conduct longitudinal studies, accounts for inter-individual variability, and reduces the number of animals required, leading to more robust interpretation of therapeutic pre-clinical trials. In addition, automated segmentation delineates regions in an image using computerized algorithms and allows for more rapid processing of data. In this context, robust segmentation algorithms identify characteristics of a tissue, provide measurements of its dimensions, and compared to manual tracing are efficient, reliable, and objective, as we have demonstrated for human eyes (Beaton et al., 2015; Mazzaferri et al., 2017); OCT and these algorithms can be adapted for small rodents as used herein. Using the oxygen-induced retinopathy (OIR) model of ROP in small rodents, we aim to compare in a longitudinal study using OCT imaging coupled with automatic segmentation the efficacy of rytvela with that of Kineret in preventing retinal damage that follows the OIR-induced vasoobliteration.

Abbreviations: ANOVA, analysis of variance; ART, automatic real time; Iba-1, ionized calcium-binding adaptor molecule 1; IHC, immunohistochemistry; IL-1, interleukin-1; IL-1Ra, interleukin-1 receptor antagonist; IRL, innermost retinal layer; NOR, normal; P14, postnatal day 14; P30, postnatal day 30; OCT, optical coherence tomography; OIR, oxygen-induced retinopathy; ORL, outermost retinal layer; RGC, retinal ganglion cell; RT, retinal thickness; SD-OCT, spectral domain optical coherence tomography; TUNEL, terminal deoxynucleotidyl transferase dUTP nick end labeling.

MATERIALS AND METHODS

This study was carried out in accordance with the principles of the Basel Declaration and Hôpital Maisonneuve-Rosemont Animal Care Committee approved protocols (authorizations 2017-1320, 2016-AV-004), and is adherent to the International Association of Veterinary Editors guidelines.

Oxygen-Induced Retinopathy Model

Newborn Sprague–Dawley rats (Charles River, St-Constant, QC, Canada) were placed under an oxygen concentration protocol cycling between 50 ± 1 and 10 ± 1% every 24 h from postnatal day (P) 0 to P14 (OIR/ROP) (Penn et al., 1994). On P14 rats were returned to room air. This model is characterized by retinal vascular decay (Penn et al., 1994; Rivera et al., 2017) followed by hypoxia-driven inner retinal neovascularization which develops between P14 and P18. Control rats (NOR) were maintained in room air (21% O_2). Rats (n = 4/group), exposed or not to OIR, were randomly assigned to receive from P0 to P14 either twice-daily intraperitoneal injections of rytvela [1 mg/kg; custom synthesized by Elim Pharmaceuticals (>95% purity)], Kineret (20 mg/kg, Biovitrum), or no treatment. The posology of rytvela was based on reported efficacy (Quiniou et al., 2008) and further supported in subsequent studies (Nadeau-Vallee et al., 2015; Beaudry-Richard et al., 2018; Geranurimi et al., 2019).

Longitudinal Study Design

Twenty-four newborn Sprague–Dawley rats were divided equally into six groups. Twelve rats were placed in conditions to develop OIR as explained previously. The healthy control group comprised twelve other rats. In both the OIR and healthy groups, four rats were treated with rytvela, four rats were treated with the Kineret, and four rats received no treatment. Imaging took place at two time points, P14 and P30. On P30, all animals were then sacrificed and eyes were immediately collected and prepared for histological analysis.

Optical Coherence Tomography Imaging

Spectral domain optical coherence tomography (Spectralis OCT, Heidelberg Engineering) imaging was carried out on all rats at P14 and P30 after the careful dosing injection of ketamine-xylazine for anesthesia (Zhou et al., 2017). The anesthetized rats were placed on a plastic horizontal panel in front of the OCT for imaging. The instillation of dilating drops, tropicamide (Mydriacyl) 1.0%, in one or both eyes was done. Additional steps to ensure high-quality OCT images included: (1) placing anesthetized rats on a warming pad (35–37°C) during image acquisition and until they regained full consciousness as advised by the Canadian Council on Animal Care; (2) frequent hydration (every 30 s) of the cornea with artificial tears to restore crispness of fundus and OCT images; and (3) lubricating ointment (Tear Gel, Alcon) application to the unexamined eye during OCT acquisition and to the examined eye immediately post-acquisition.

OCT Parameters

Volume scans of 15° × 5° (7 B-scans 240 microns apart, ART 100 frames including 768 A-scans) were taken in the right eye, by convention. If the imaging was rendered difficult due to rapid breathing or movement that disrupted the eye-tracker, the experimenter held the rat's head in place and applied light pressure to reduce motion and permit proper OCT imaging. All OCT scans were obtained at the temporal side of the optic nerve (equivalent to position of human macula). During acquisition, image quality was determined based on the Spectralis image quality signal as seen on the OCT monitor, as well as subjective appreciation of the resolution of the B-scan and clear visualization of the layers of interest by the examiner.

Automatic Segmentation of OCT Images

Image processing for measuring the thickness of the retina in OCT B-scans of rodent eyes was carried out using a custom-made fully automated segmentation algorithm with Matlab (The Mathworks, Inc.). Essentially, the algorithm segments two layers sequentially: the outermost retinal layer (ORL) and the innermost layer of the retina (IRL) as seen in **Figure 1**. The sclera being the brightest object in the B-scan, this feature was used to coarsely localize it in the image. After smoothing the image with a Gaussian average filter (σ = 20 μm), we located the center of the scleral layer as the absolute intensity maximum in each A-scan (**Figure 1**, center panel). Taking this position as a reference, we located the ORL as the first valley of the intensity slope just above the center of the sclera. Finally, the IRL was obtained as the highest intensity slope peak more than 120 μm above the ORL. The intensity slope was computed after a Gaussian smoothing operation using a filter of $\sigma = 2$ μm.

The retinal thickness (RT) was computed as the distance between the IRL and the ORL. This procedure was performed on every A-scan of each B-scan of each OCT volume scan. The mean thicknesses and their standard deviations were computed for each B-scan, using the results of all A-scans. After discarding B-scans where the percentage error was bigger than 25%, the mean thickness for each map was computed as the weighted average along B-scans, using the inverse of the standard deviation as weight. The final uncertainty of the thickness was computed as the standard error among B-scans.

Ocular Tissue Preparation

Animals were perfused with phosphate buffered saline and 4% paraformaldehyde. For histology sections, eyes were immediately collected, dehydrated by alcohol, and embedded in paraffin. Sagittal sections of 5 μm were cut by microtome (Leica, RM 2145). Eyes for cryo-preparation were further fixed in 4% paraformaldehyde overnight. Posterior eyecups were frozen in optimal cutting temperature medium. Samples were then cut into 10 μm-thick sagittal sections (Microm, HM500O) and processed for IHC.

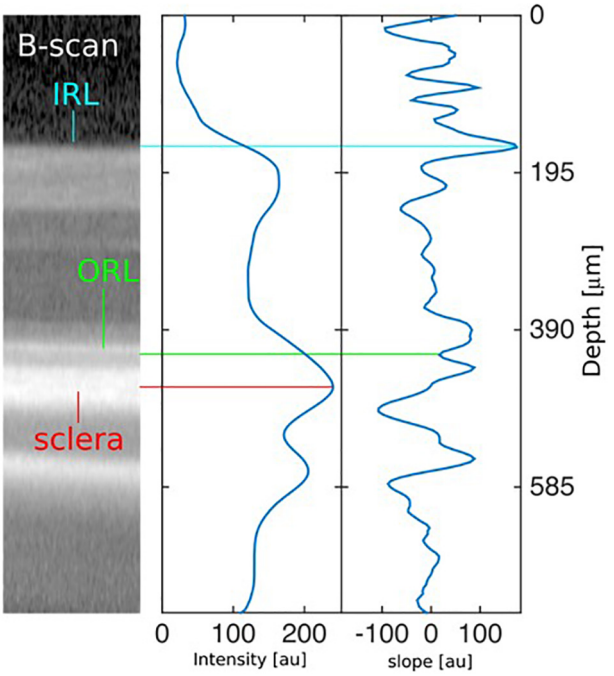

FIGURE 1 | Description of automated segmentation algorithm. Left: Identification of the sclera, the outermost retinal layer (ORL), and the innermost retinal layer (IRL) in a section of a typical rodent eye B-scan. Center: Intensity profile along the center A-scan of the image at the left, averaged with a Gaussian filter (σ = 20 μm). The absolute maximum signals the location of the sclera. Right: First derivative (slope) of the intensity profile along the center A-scan of the image at the left. The first valley above the sclera indicates the ORL, and the highest peak more than 120 μm above it indicates the IRL. The slope is computed after a Gaussian smoothing operation with σ = 2 μm.

Cell Culture

The murine macrophage cell line J774 and RAW264.7, purchased from ATCC, were cultured in Dulbecco's Modified Eagle's Medium (DMEM) (Thermo Fisher Scientific, 11995-065) supplemented with 10% fetal bovine serum (FBS) and 1% penicillin/streptomycin (respectively, 085-150 and 450-201-EL, Wisent Bioproducts).

Phagocytosis Assay Preparation

Mouse macrophages (Raw 264.7 and J774) (100,000 cells) were pre-incubated with rytvela (1 μM), SC-514 (2 μM), or Kineret (1 mg/ml) for 30 min and incubated with IL-1β (100 ng/ml) for 4–24 h. Phagocytosis was determined with the Vybrant Phagocytosis Assay kit from Thermo Scientific (Waltham, MA, United States) according to manufacturer's instructions. Briefly, medium was removed at 4 or 24 h after IL-1β incubation and replaced with Fluorescein-labeled *Escherichia coli* K-12 BioParticles resuspended in HBSS. Two hours later, bioparticles were removed and the signal was quenched by exposing cells to trypan blue for 1 min. Fluorescence intensity was read using 480 nm excitation and 520 nm emission using ClarioStar microplate reader (BMG LabTech; Champigny-sur-Marne, France). The same procedure was repeated using Kineret

and SC-514, an inhibitor of NF-κB and results were compared with those obtained with rytvela.

Immunofluorescence Staining

J774 macrophages were seeded overnight in DMEM containing 10% FBS and 1% penicillin/streptomycin, on round 15 mm cover glass. J774 were pre-incubated with rytvela (1 μM), for 30 min and incubated with IL-1β (100 ng/ml) for 4 h. Then medium was removed and Fluorescein-labeled *Escherichia coli* K-12 BioParticles mix was added with HBSS. Two hours later, cells were washed twice with PBS for 5 min, fixed in 4% PFA for 30 min, and permeabilized in 1.0% Triton X100 and blocked in 10% FBS 1 h. Cells were counterstained with Rhodamine Phalloidin (1:500, 1 h) (Santa Cruz Biotechnology, R415) and DAPI (1:5000; 5 min) (Sigma–Aldrich, D9542) to evidence cell-contour and cell-nuclei. Phagocytosis efficiency was assessed using a confocal microscope (Zeiss, LSM 510).

Statistical Analysis

Results for RT are presented as means ± standard error of the mean. One-way ANOVA with significance ($\alpha = 0.05$) was used for processing data. Bonferroni *post hoc* analysis was used to calculate statistical significance between groups. The graphs showing phagocytosis results were generated using Graph Prism 8. One-way ANOVA with significance ($\alpha = 0.05$) was used for comparing experiment data.

RESULTS

Early Anti-IL-1 β Therapy Preserves Retinal Thickness in OIR Animals

Retinal thickness was defined as that between the IRL and the ORL (**Figure 2A**). No difference in RT between groups was yet detected immediately after vasoobliteration (during hyperoxia) on P14 (**Figure 2B**). By P30, a thinner retina was observed in the untreated OIR group, while RT was preserved in OIR animals that received rytvela or Kineret (**Figures 2A,C**).

Early Anti-IL-1 β Therapy Reduces the Number of Apoptotic Cells and Preserves Retinal Vessels in the Superficial Capillary Plexus of OIR Animals

Diminished RT in OIR was confirmed histologically (**Figure 3**); inhibition of IL-1R with rytvela and Kineret avoided retinal thinning. As anticipated, retinal vessel density in the superficial capillary plexus of the nerve fiber layer was reduced by OIR and preserved by anti-IL-1 receptor treatments (**Figures 3G,H,I,L**). Coherently, microvascular decay which results in the loss of retinal parenchyma was associated with increased apoptosis (TUNEL positivity) mostly observed in the inner retina (**Figures 3A,D**) consisting of the region most affected in OIR; again, both rytvela and Kineret effectively diminished the number of TUNEL-positive apoptotic cells (**Figure 3G**).

Biased Signaling Pathway Selectivity of Rytvela Compared to Kineret

Consistent with previous reports (Nadeau-Vallee et al., 2015), rytvela selectively reduced OIR-generated (augmented) SAPK/JNK pathway while preserving intact the important immuno-vigilant related NF-κB axis as measured directly in retinal tissue (at P30) (**Figure 4** and **Supplementary Material**); in comparison, Kineret inhibited both SAPK/JNK and NF-κB pathways (**Figures 4C,D**). This particularly relevant information results in maintenance of NF-κB-dependent (defense-related) phagocytosis in IL-1β-activated mononuclear myeloid cells by rytvela (**Figures 4E,F**); whereas phagocytosis in mononuclear cells is compromised by Kineret, as seen with the NF-κB inhibitor SC-514 (**Figure 4F**).

DISCUSSION

In this longitudinal study, retinal thinning in OIR animals and the retina-preserving effects of two anti-IL-1β agents, Rytvela and Kineret, were successfully observed using OCT imaging and automated segmentation. Validity of OCT, without established automated segmentation, has been successfully used in assessing retinoblastoma growth (Corson et al., 2014), as well as in evaluating retinal layer injury upon subretinal injections in rats (Becker et al., 2017). The current study extends the reliability of OCT in rodent OIR model. OCT imaging has rapidly become an attractive alternative to current laboratory techniques such as IHC due to its many advantages. First, the traditional IHC to measure RT requires sacrificing animals with significantly longer sample process time. Second, IHC often faces artifacts including tissue shrinkage, swelling, and cracks that are caused by fixation and the postmortem status (Rastogi et al., 2013). In addition, OCT is non-invasive and hence allows longitudinal measurements in the same subject, while conventional IHC protocol requires animal sacrifice at each time point; this translates into a significant reduction of experimental animals needed for longitudinal studies. Lastly, repeated measurements reduce inter-individual variabilities and enhance statistical power. Another strength of this study lies in the use of an automated segmentation protocol which enables timely, rapid, and effective analysis of retinal features, while ensuring objectivity when compared to manual tracing. Accordingly, large amounts of data can be efficiently processed; consistent results can be obtained when repeating iterations on a given dataset, and both inter- and intra-evaluator variabilities are eliminated (Dysli et al., 2015).

A key point to successfully carrying out longitudinal measurements in OCT lies in maintaining a clear cornea in experimental animals. Previous studies have identified a rare but serious side effect of Xylazine (a common anesthetics used in rodent studies)—corneal calcification akin to band keratopathy (Turner and Albassam, 2005; Koehn et al., 2015; Zhou et al., 2017). The dense calcification in the central cornea immediately precluded subsequent OCT experiments. Our group developed a protocol to safely anesthetize animals and achieve long-term, repeated imaging (Zhou et al., 2017). This protocol was applied

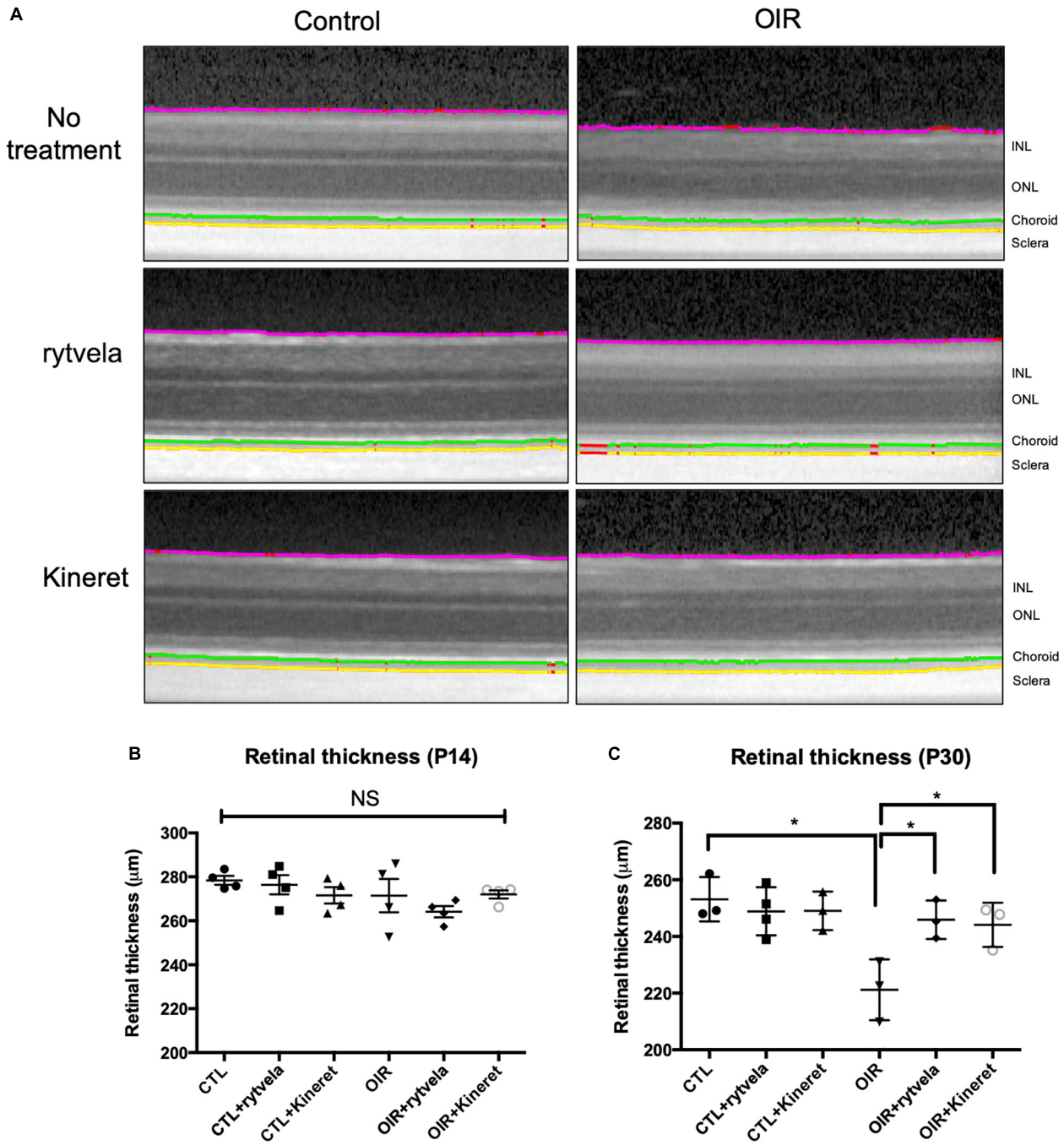

FIGURE 2 | Early anti-IL-1β therapy preserves retinal integrity in OIR subjects. **(A)** Original B-scans overlaid with the innermost layer of the retina (purple), the inner choroid limit (green), and the choroid-sclera interface (yellow) are shown for each sub-group at P30. **(B)** There is no difference in retinal thickness on P14. **(C)** However, OIR retinae become statistically thinner by P30; retinal thickness is preserved by anti-IL-1β. $N = 4$ animals on P14; $N = 3$-4 on P30. Values are mean ± SEM. One-way ANOVA; $^{*}p < 0.05$, $^{**}p < 0.01$, $^{***}p < 0.001$, $^{****}p < 0.0001$ vs corresponding values as indicated.

in our experiments. As expected, results generated by our OCT imaging and automated segmentation are parallel to previous studies that used IHC methods (Dorfman et al., 2008; Dorfman et al., 2010; Rivera et al., 2013); our protocol can thus be readily integrated for reliable longitudinal small animal experimentation.

Anti-IL-1β treatment has been shown to be effective in preventing retinal OIR-elicited vasoobliteration and in turn reduce aberrant pre-retinal neovascularization (Rivera et al., 2013). In this context, it was shown that anti-IL-1 treatment effectively diminishes the release of vaso-repulsive molecule

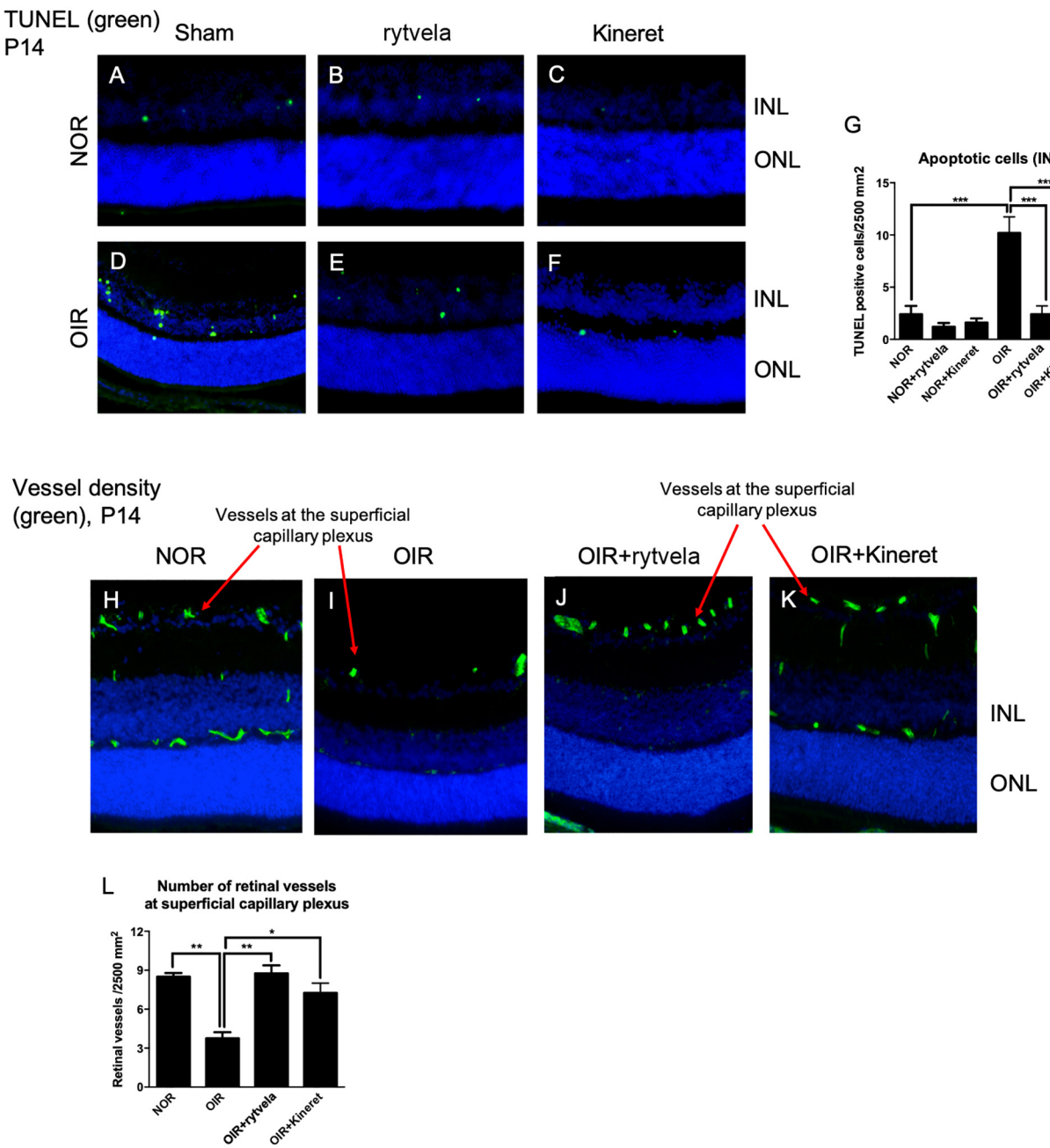

FIGURE 3 | Early anti-IL-1 β therapy reduces the number of apoptotic cells and preserves retinal vessel density at the superficial capillary plexus of OIR subjects. **(A–D)** TUNEL staining show 2–4 positive cells per 2500 mm^2 in P14 control (NOR) animals (with or without anti-IL-1β), compared to ∼10 cells in OIR rats of the same age. **(E,F)** Both IL-1β antagonists effectively diminish TUNEL positive cells in OIR subjects. Statistical analyses are shown in **G**. **(H)** P14 control animals display normal vessel density (green) in the retina. **(I)** P14 OIR rats show reduced vessel density at the superficial plexus. **(J–L)** Rytvela and Kineret preserved retinal vessels at the superficial capillary plexus of OIR rats. N = 3–4 animals per group. Values are mean ± SEM. One-way ANOVA; $^{*}p < 0.05$, $^{**}p < 0.01$, $^{***}p < 0.001$, $^{****}p < 0.0001$ vs corresponding values as indicated.

semaphorin 3A from RGCs (Joyal et al., 2014; Sitaras et al., 2015), thereby facilitating NOR revascularization. The advantage of rytvela, a non-competitive inhibitor of IL-1β receptor, has been previously demonstrated in a model of preterm labor (Nadeau-Vallee et al., 2015). In particular, rytvela preserves NF-κB axis while inhibiting SAPK/JNK and others; this effect was shown *in vivo* herein. This is important in maintaining the multiple functions of the transcription factor NF-κB (Hoesel and Schmid, 2013). NF-κB has a quintessential role in sustaining innate immune surveillance (Hayden et al., 2006) consistent

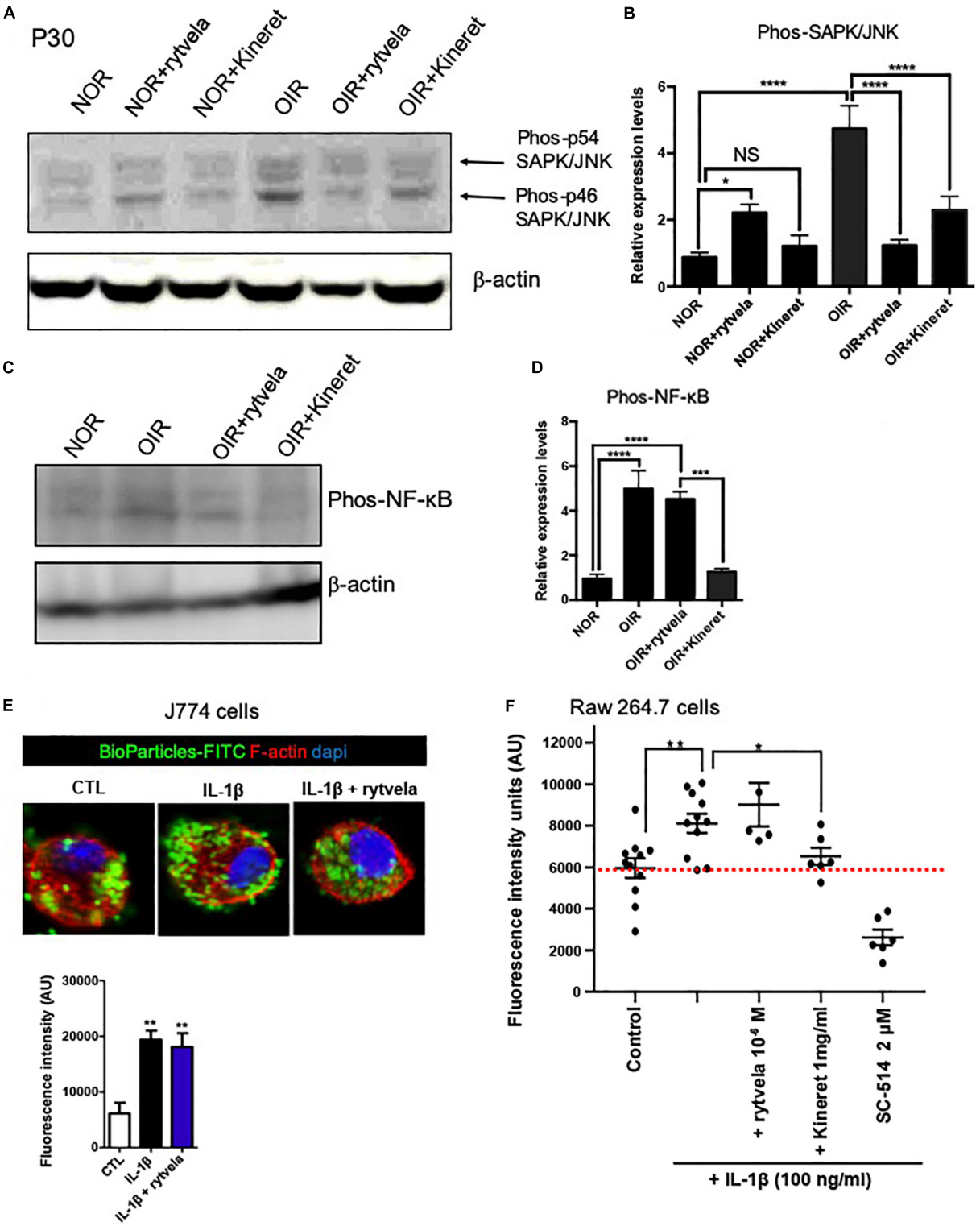

FIGURE 4 | Different inhibition profiles between rytvela and Kineret in retinal tissue at P30 in OIR subjects vs. controls (NOR) and the effect of rytvela on macrophage phagocytosis. **(A,B)** Both rytvela and Kineret abolish SAPK/JNK phosphorylation in OIR subjects. **(C,D)** However, Kineret inhibits NF-κB, whereas rytvela preserves NF-κB pathway. $N = 3$–5 animals. Values are mean ± SEM; $^{*}p < 0.05$, $^{**}p < 0.01$, $^{***}p < 0.001$, $^{****}p < 0.0001$ vs corresponding values as indicated. **(E)** Confocal imaging showing Fluorescein-labeled BioParticles (green) phagocytosed by J774 mononuclear cells counterstained with Rhodamine phalloidin (red) and DAPI (blue). Histogram below immunofluorescent images refer to quantitative analysis using fluorescence intensity plate reading, showing that rytvela does not inhibit IL-1β-induced phagocytosis. **(F)** Quantitative analysis of Raw 264.7 cell phagocytosis activated by IL-1β, showing preservation by rytvela (1 µM) but not by Kineret (1 mg/ml) or the selective NF-kB inhibitor SC-514 (2 µM). $N = 4$–11/group. One-way ANOVA; $^{*}p < 0.05$, $^{**}p < 0.01$, $^{***}p < 0.001$, $^{****}p < 0.0001$ compared to control.

with our findings related to mononuclear cell phagocytosis; this is particularly important for premature newborns as they face complex immunological challenges when they emerge from the sterile *in utero* environment (McDonagh et al., 2004; Marchini et al., 2005). During this period, neonates mainly depend on the innate immunity where Toll-like receptor—NF-κB axis plays a significant role (Kollmann et al., 2012). Therefore, when treating neonatal inflammatory conditions, one must strike a fine balance between adequate immune defense and unrestrained inflammation. Additionally, NF-κB signaling participates in cell proliferation and angiogenesis in the retina (Yoshida et al., 1999; Noort et al., 2014). In ROP, revascularization and restoration of retinal blood flow are prerequisites for the proper development of the premature retina (Wei et al., 2016). Overt inhibition of NF-κB by Kineret may contribute to the absence of revascularization in OIR rats as observed herein. Hence together, rytvela provides a beneficial alternative to Kineret as anti-IL-1β treatment of the neonate.

In summary, OCT imaging coupled with an automated segmentation algorithm represents a non-invasive, reliable, and readily efficient method to study longitudinally retinal pathology and its alteration by drug candidates, in rat OIR model. The present study further establishes that rytvela, a novel biased inhibitor of IL-1β, preserves retinal integrity and restores vascular density in a rodent model of ischemic retinopathy, while conserving innate mononuclear cell phagocytosis.

DATA AVAILABILITY STATEMENT

All datasets analyzed for this study are included in the article/**Supplementary Material**.

ETHICS STATEMENT

The animal study was reviewed and approved by the Hôpital Maisonneuve-Rosemont Animal Care Committee.

AUTHOR CONTRIBUTIONS

DS, TZ, SaC, and SyC contributed to the conception and design of the study. DS, TZ, SO, and CQ carried out the experiments. JM developed the segmentation algorithm. DS and TZ performed the data analyses. DS and TZ wrote the first draft of the manuscript. All authors (including MW, FC, RD, and MD) contributed to interpretation and analysis of data. SaC and SyC provided expert advice and gave important suggestions for improving the manuscript. All authors contributed to manuscript revision and read and approved the submitted version.

FUNDING

TZ is a recipient of Canadian Institutes of Health Research (CIHR) M.D./Ph.D. Scholarship, Fonds Suzanne Véronneau-Troutman, and Fonds de Recherche en Ophtalmologie de l'Université de Montréal (FROUM). DS is a recipient of the Fonds de la Recherche du Québec en Santé (FRQS) Doctoral Training Award, FROUM Scholarship, and Vision Health Research Network (VHRN) Performance Award. SaC was supported by grants from CIHR, NSERC, and FROUM, and received a salary award from FRQS. SyC was supported by grants from CIHR, March of Dimes Birth Defects Foundation, and the FRQS-Antoine Turmel Foundation-VHRN Research Program for Age-Related Macular Degeneration, and also holds a Canada Research Chair (Vision Science) and the Leopoldine Wolfe Chair in translational research in age-related macular degeneration.

SUPPLEMENTARY MATERIAL

The Supplementary Material for this article can be found online at: https://www.frontiersin.org/articles/10.3389/fphar.2020.00296/full#supplementary-material

REFERENCES

Beaton, L., Mazzaferri, J., Lalonde, F., Hidalgo-Aguirre, M., Descovich, D., Lesk, M. R., et al. (2015). Non-invasive measurement of choroidal volume change and ocular rigidity through automated segmentation of high-speed OCT imaging. *Biomed. Opt. Exp.* 6, 1694–1706. doi: 10.1364/BOE.6.001694

Beaudry-Richard, A., Nadeau-Vallee, M., Prairie, E., Maurice, N., Heckel, E., Nezhady, M., et al. (2018). Antenatal IL-1-dependent inflammation persists postnatally and causes retinal and sub-retinal vasculopathy in progeny. *Sci. Rep.* 8:11875. doi: 10.1038/s41598-018-30087-30084

Becker, S., Wang, H., Stoddard, G. J., and Hartnett, M. E. (2017). Effect of subretinal injection on retinal structure and function in a rat oxygen-induced retinopathy model. *Mol. Vis.* 23, 832–843.

Corson, T. W., Samuels, B. C., Wenzel, A. A., Geary, A. J., Riley, A. A., McCarthy, B. P., et al. (2014). Multimodality imaging methods for assessing retinoblastoma orthotopic xenograft growth and development. *PLoS One* 9:e99036. doi: 10.1371/journal.pone.0099036

Dorfman, A., Dembinska, O., Chemtob, S., and Lachapelle, P. (2008). Early manifestations of postnatal hyperoxia on the retinal structure and function of the neonatal rat. *Invest. Ophthalmol. Vis. Sci.* 49, 458–466. doi: 10.1167/iovs.07-0916

Dorfman, A. L., Chemtob, S., and Lachapelle, P. (2010). Postnatal hyperoxia and the developing rat retina: beyond the obvious vasculopathy. *Doc. Ophthalmol.* 120, 61–66. doi: 10.1007/s10633-009-9208-9203

Dysli, C., Enzmann, V., Sznitman, R., and Zinkernagel, M. S. (2015). Quantitative analysis of mouse retinal layers using automated segmentation of spectral domain optical coherence tomography images. *Transl. Vis. Sci. Technol.* 4:9. doi: 10.1167/tvst.4.4.9

Geranurimi, A., Cheng, C. W. H., Quiniou, C., Zhu, T., Hou, X., Rivera, J. C., et al. (2019). Probing anti-inflammatory properties independent of NF-kappaB through conformational constraint of peptide-based interleukin-1 receptor biased ligands. *Front. Chem.* 7:23. doi: 10.3389/fchem.2019.00023

Hayden, M. S., West, A. P., and Ghosh, S. (2006). NF-kappaB and the immune response. *Oncogene* 25, 6758–6780. doi: 10.1038/sj.onc.1209943

Hoesel, B., and Schmid, J. A. (2013). The complexity of NF-kappaB signaling in inflammation and cancer. *Mol. Cancer* 12:86. doi: 10.1186/1476-4598-12-86

Huang, D., Swanson, E. A., Lin, C. P., Schuman, J. S., Stinson, W. G., Chang, W., et al. (1991). Optical coherence tomography. *Science* 254, 1178–1181.

Joyal, J. S., Nim, S., Zhu, T., Sitaras, N., Rivera, J. C., Shao, Z., et al. (2014). Subcellular localization of coagulation factor II receptor-like 1 in neurons governs angiogenesis. *Nat. Med.* 20, 1165–1173. doi: 10.1038/nm.3669

Koehn, D., Meyer, K. J., Syed, N. A., and Anderson, M. G. (2015). Ketamine/Xylazine-induced corneal damage in mice. *PLoS One* 10:e0132804. doi: 10.1371/journal.pone.0132804

Kollmann, T. R., Levy, O., Montgomery, R. R., and Goriely, S. (2012). Innate immune function by toll-like receptors: distinct responses in newborns and the elderly. *Immunity* 37, 771–783. doi: 10.1016/j.immuni.2012.10.014

Marchini, G., Nelson, A., Edner, J., Lonne-Rahm, S., Stavreus-Evers, A., and Hultenby, K. (2005). Erythema toxicum neonatorum is an innate immune response to commensal microbes penetrated into the skin of the newborn infant. *Pediatr. Res.* 58, 613–616. doi: 10.1203/01.pdr.0000176836.27156.32

Mazzaferri, J., Beaton, L., Hounye, G., Sayah, D. N., and Costantino, S. (2017). Open-source algorithm for automatic choroid segmentation of OCT volume reconstructions. *Sci. Rep.* 7:42112. doi: 10.1038/srep42112

McDonagh, S., Maidji, E., Ma, W., Chang, H. T., Fisher, S., and Pereira, L. (2004). Viral and bacterial pathogens at the maternal-fetal interface. *J. Infect. Dis.* 190, 826–834. doi: 10.1086/422330

Nadeau-Vallee, M., Quiniou, C., Palacios, J., Hou, X., Erfani, A., Madaan, A., et al. (2015). Novel noncompetitive IL-1 receptor-biased ligand prevents infection- and inflammation-induced preterm birth. *J. Immunol.* 195, 3402–3415. doi: 10.4049/jimmunol.1500758

Noort, A. R., van Zoest, K. P., Weijers, E. M., Koolwijk, P., Maracle, C. X., Novack, D. V., et al. (2014). NF-kappaB-inducing kinase is a key regulator of inflammation-induced and tumour-associated angiogenesis. *J. Pathol.* 234, 375–385. doi: 10.1002/path.4403

Penn, J. S., Henry, M. M., and Tolman, B. L. (1994). Exposure to alternating hypoxia and hyperoxia causes severe proliferative retinopathy in the newborn rat. *Pediatr. Res.* 36, 724–731. doi: 10.1203/00006450-199412000-199412007

Quiniou, C., Sapieha, P., Lahaie, I., Hou, X., Brault, S., Beauchamp, M., et al. (2008). Development of a novel noncompetitive antagonist of IL-1 receptor. *J. Immunol.* 180, 6977–6987. doi: 10.4049/jimmunol.180.10.6977

Rastogi, V., Puri, N., Arora, S., Kaur, G., Yadav, L., and Sharma, R. (2013). Artefacts: a diagnostic dilemma - a review. *J. Clin. Diagn. Res.* 7, 2408–2413. doi: 10.7860/JCDR/2013/6170.3541

Rivera, J. C., Holm, M., Austeng, D., Morken, T. S., Zhou, T. E., Beaudry-Richard, A., et al. (2017). Retinopathy of prematurity: inflammation, choroidal degeneration, and novel promising therapeutic strategies. *J. Neuroinflamm.* 14:165. doi: 10.1186/s12974-017-0943-941

Rivera, J. C., Sitaras, N., Noueihed, B., Hamel, D., Madaan, A., Zhou, T., et al. (2013). Microglia and interleukin-1beta in ischemic retinopathy elicit microvascular degeneration through neuronal semaphorin-3A. *Arterioscler. Thromb. Vasc. Biol.* 33, 1881–1891. doi: 10.1161/ATVBAHA.113.301331

Sitaras, N., Rivera, J. C., Noueihed, B., Bien-Aime, M., Zaniolo, K., Omri, S., et al. (2015). Retinal neurons curb inflammation and enhance revascularization in ischemic retinopathies via proteinase-activated receptor-2. *Am. J. Pathol.* 185, 581–595. doi: 10.1016/j.ajpath.2014.10.020

Turner, P. V., and Albassam, M. A. (2005). Susceptibility of rats to corneal lesions after injectable anesthesia. *Comp. Med.* 55, 175–182.

Wei, Y., Gong, J., Xu, Z., and Duh, E. J. (2016). Nrf2 promotes reparative angiogenesis through regulation of NADPH oxidase-2 in oxygen-induced retinopathy. *Free Radic. Biol. Med.* 99, 234–243. doi: 10.1016/j.freeradbiomed.2016.08.013

Yoshida, A., Yoshida, S., Ishibashi, T., Kuwano, M., and Inomata, H. (1999). Suppression of retinal neovascularization by the NF-kappaB inhibitor pyrrolidine dithiocarbamate in mice. *Invest. Ophthalmol. Vis. Sci.* 40, 1624–1629.

Zhou, T. E., Rivera, J. C., Bhosle, V. K., Lahaie, I., Shao, Z., Tahiri, H., et al. (2016). Choroidal involution is associated with a progressive degeneration of the outer retinal function in a model of retinopathy of prematurity: early role for IL-1beta. *Am. J. Pathol.* 186, 3100–3116. doi: 10.1016/j.ajpath.2016.08.004

Zhou, T. E., Sayah, D. N., Noueihed, B., Mazzaferri, J., Costantino, S., Brunette, I., et al. (2017). Preventing corneal calcification associated with xylazine for longitudinal optical coherence tomography in young rodents. *Invest. Ophthalmol. Vis. Sci.* 58, 461–469. doi: 10.1167/iovs.16-20526

Conflict of Interest: The authors declare that the research was conducted in the absence of any commercial or financial relationships that could be construed as a potential conflict of interest.

frontiers in Pharmacology

BRIEF RESEARCH REPORT
published: 06 May 2020
doi: 10.3389/fphar.2020.00613

Anti-Inflammatory Properties of Chemical Probes in Human Whole Blood: Focus on Prostaglandin E_2 Production

Filip Bergqvist[1,2]*, *Yvonne Sundström*[1,2], *Ming-Mei Shang*[1,2], *Iva Gunnarsson*[1], *Ingrid E. Lundberg*[1], *Michael Sundström*[1,2], *Per-Johan Jakobsson*[1,2] *and Louise Berg*[1,2]*

[1] Division of Rheumatology, Department of Medicine, Solna, Karolinska Institutet, and Karolinska University Hospital, Stockholm, Sweden, [2] The Structural Genomic Consortium (SGC), Karolinska Institutet, Stockholm, Sweden

OPEN ACCESS

Edited by:
Ulrike Garscha,
Friedrich Schiller University Jena,
Germany

Reviewed by:
Cristina López-Vicario,
Hospital Clínic de Barcelona,
Spain
Giustino Orlando,
Università degli Studi G. d'Annunzio
Chieti e Pescara,
Italy

***Correspondence:**
Filip Bergqvist
Bergqvist.Filip@gmail.com
Louise Berg
Louise.Berg@ki.se

Specialty section:
This article was submitted to Inflammation Pharmacology, a section of the journal Frontiers in Pharmacology

Received: 19 February 2020
Accepted: 20 April 2020
Published: 06 May 2020

Citation:
Bergqvist F, Sundström Y, Shang M-M, Gunnarsson I, Lundberg IE, Sundström M, Jakobsson P-J and Berg L (2020) Anti-Inflammatory Properties of Chemical Probes in Human Whole Blood: Focus on Prostaglandin E_2 Production. Front. Pharmacol. 11:613. doi: 10.3389/fphar.2020.00613

We screened 57 chemical probes, high-quality tool compounds, and relevant clinically used drugs to investigate their effect on pro-inflammatory prostaglandin E_2 (PGE_2) production and interleukin-8 (IL-8) secretion in human whole blood. Freshly drawn blood from healthy volunteers and patients with systemic lupus erythematosus (SLE) or dermatomyositis was incubated with compounds at 0.1 or 1 μM and treated with lipopolysaccharide (LPS, 10 μg/ml) to induce a pro-inflammatory condition. Plasma was collected after 24 h for lipid profiling using liquid chromatography tandem mass spectrometry (LC-MS/MS) and IL-8 quantification using enzyme-linked immunosorbent assay (ELISA). Each compound was tested in at least four donors at one concentration based on prior knowledge of binding affinities and *in vitro* activity. Our screening suggested that PD0325901 (MEK-1/2 inhibitor), trametinib (MEK-1/2 inhibitor), and selumetinib (MEK-1 inhibitor) decreased while tofacitinib (JAK inhibitor) increased PGE_2 production. These findings were validated by concentration–response experiment in two donors. Moreover, the tested MEK inhibitors decreased thromboxane B_2 (TXB_2) production and IL-8 secretion. We also investigated the lysophophatidylcholine (LPC) profile in plasma from treated whole blood as these lipids are potentially important mediators in inflammation, and we did not observe any changes in LPC profiles. Collectively, we deployed a semi-high throughput and robust methodology to investigate anti-inflammatory properties of new chemical probes.

Keywords: prostaglandin E_2, whole blood assay, interleukin-8, inflammation, drug screen

HIGHLIGHTS

- Inhibitors for MEK decreased PGE_2 and TXB_2 production
- Inhibitors for MEK and ERK decreased IL-8 secretion
- JAK inhibitor tofacitinib increased PGE_2 and TXB_2 production

INTRODUCTION

Inflammation is a highly controlled immune response to eliminate the cause of tissue injury or infection and to initiate tissue repair back to homeostasis *via* resolution (Nathan, 2002; Buckley et al., 2013). However, inflammation is not always terminated. Unresolved inflammation causes persistent pain, tissue degeneration, and loss of function. In particular, inflammatory responses drive many autoimmune diseases (McInnes and Schett, 2011) and inflammation is a hallmark of cancer (Hanahan and Weinberg, 2011). Thus, there is a great need for new therapies that are anti-inflammatory and safe.

Prostaglandin E_2 (PGE_2) is a potent lipid mediator of inflammation and immune responses, and PGE_2 is a central mediator of pain, edema, and cartilage erosion typically observed in the joints of rheumatoid arthritis patients (Akaogi et al., 2012; Fattahi and Mirshafiey, 2012). In addition, PGE_2 is a promotor of the immunosuppressive tumor microenvironment with major impact on tumor progression (Wang and Dubois, 2010; Hanahan and Weinberg, 2011; Ricciotti and Fitzgerald, 2011). During inflammation, PGE_2 is synthesized *via* conversion of arachidonic acid by cyclooxygenases (COX-1 and COX-2) into unstable PGH_2 that is further metabolized by the inducible terminal synthase microsomal prostaglandin E synthase-1 (mPGES-1) to generate PGE_2. Multiple non-steroidal anti-inflammatory drugs (NSAIDs) exist in clinical practice that unselectively decrease PGE_2 production *via* inhibition of COX, but these drugs are all associated with adverse effects. Hence, selective inhibition of PGE_2 production with small molecule inhibitors could therefore be a desirable therapeutic strategy in inflammation and cancer (Bergqvist et al., 2020).

Interleukin-8 (IL-8) is a potent chemoattractant and activator of neutrophils. IL-8 signaling is implicated in multiple chronic inflammatory diseases (Russo et al., 2014) and cancer (Waugh and Wilson, 2008). For example, a recent meta-analysis concluded that patients suffering from systemic lupus erythematosus (SLE) have increased levels of circulating IL-8 (Mao et al., 2018). Patients with central neuropsychiatric SLE have increased concentration of IL-8 in cerebrospinal fluid compared to patients with non-central neuropsychiatric SLE (Yoshio et al., 2016). IL-8 is also associated with renal damage and pulmonary fibrosis in SLE patients (Lit et al., 2006; Nielepkowicz-Goździńska et al., 2014). Given that IL-8 is a stimulant for neutrophil activation, which plays a significant role in the pathogenesis of SLE (Kaplan, 2011), targeting IL-8 secretion or signaling could constitute a therapeutic strategy for SLE. A similar role of neutrophils and net formation has been reported in patients with dermatomyositis (DM) (Zhang et al., 2014; Peng et al., 2018). In cancer, IL-8 is highly expressed in several types of cancer tissues (David et al., 2016) and serum concentration of IL-8 correlates with tumor burden (Alfaro et al., 2017). The tumor-favoring actions of IL-8 include promotion of angiogenesis, increased survival of cancer stem cells, and attraction of myeloid cells that indorse the immunosuppressive tumor microenvironment (Alfaro et al., 2017).

In this study, we aimed to evaluate the effect of 57 chemical probes, high-quality tool compounds, and relevant control drugs on eicosanoid production and IL-8 secretion in human whole blood. A chemical probe is defined as "… a selective small-molecule modulator of a protein's function that allows the user to ask mechanistic and phenotypic questions about its molecular target in biochemical, cell-based or animal studies" (Arrowsmith et al., 2015), and these compounds follow the criteria of *in vitro* potency (IC_{50} or Kd <100 nM), high selectivity versus other protein subfamilies (>30-fold), and on-target cell activity at 1 μM. The chemical probes and other high-quality tool compounds included are mainly epigenetic modulators and kinase inhibitors that were produced in academic collaborations or donated by pharmaceutical companies within the Structural Genomic Consortium (SGC, www.thesgc.org), which aims to investigate novel targets for drug development in open science and in collaboration with the pharmaceutical industry. These inhibitors were tested here at one concentration (in triplicates, n = 4–15 donors) based on previous knowledge of binding affinities and toxicity *in vitro*, as assessed using other validated assays in our laboratories (https://ultra-dd.org/tissue-platforms/cell-assay-datasets).

MATERIALS AND METHODS

Ethical Approval and Consent to Participate

Ethical approval for this study was granted by local research ethics committee at Karolinska University hospital (Dnr 02-196) and the Regional Ethical Review Board in Stockholm (Dnr 2015/2001-31/2). Full informed consent according to the Declaration of Helsinki was obtained from all patients.

Collection of Blood

Peripheral venous blood was drawn from 10 females and 6 males, aged between 27 and 81 years. Healthy controls (n = 4) and two patient groups were included: SLE (n = 9) and DM (n = 3). Patients with diagnosis SLE or DM and aged 18 or older were recruited from the Rheumatology Clinic at Karolinska University Hospital. Patients with ongoing treatment including Sendoxan (cyclophosphamide) and Benlysta (belimumab) or with kidney failure as defined by present dialysis or previous kidney transplantation were excluded. Disease activity measurements were not obtained at the time of sampling. For healthy control and patients characteristics, see **Supplementary Table 1**. The blood was collected in tubes containing sodium heparin (1000 U/ml).

Inhibitors

The inhibitors (chemical probes and other high-quality tool compounds) tested here were obtained through the SGC (www.thesgc.org) and supplied by different distributers (**Supplementary Table 2**). Inhibitors and control drugs (**Supplementary Table 2**) were reconstituted at 10 mM in DMSO (D2250, Sigma-Aldrich), aliquoted in Eppendorf tubes or 96-well plates, and kept at −80°C. A fresh aliquot was used at each experiment. Diclofenac (dual COX-1/2 inhibitor) was used

as positive control for inhibition of prostanoid production. Lipopolysaccharide (LPS; L6529, Sigma-Aldrich) was reconstituted in phosphate-buffered saline (PBS) (D8537, Sigma-Aldrich) to a final concentration of 0.1 mg/ml and kept at +8°C.

Whole Blood Assay

Inhibitors and vehicle control (DMSO) were diluted in PBS at room temperature with no direct light on. The treatments were prepared in 25 µl portions to U-shaped 96-well plate and 200 µl of freshly drawn heparin blood (< 2 h at room temperature) was added to the plate. The plate was incubated at 37°C for 30 min and then 25 µl of 0.1 mg/ml LPS in PBS was added followed by pipetting up and down 3 times (final concentration of LPS was 10 µg/ml). The tested concentration for inhibitor was 0.1 or 1 µM (**Supplementary Table 1**). The plate was incubated for 24 h at 37°C and then centrifuged at 3000*g* for 10 min at 4°C. Working on ice, 100 µl plasma was recovered to a new plate (for prostanoid profiling) and from this 20 µl was transferred to a second plate (for IL-8 quantification). The plates were sealed with aluminum foil and stored at -80°C.

Extraction of Lipids

Plasma samples (80–240 µl) were thawed on ice and spiked with 50 µl deuterated internal standard mix containing 17 ng 6-keto-$PGF_{1\alpha}$-d4, 8 ng $PGF_{2\alpha}$-d4, 12 ng PGE_2-d4, 8 ng PGD_2-d4, 8 ng thromboxane B_2 (TXB_2)-d4, and 8 ng 15-deoxy-Δ12,14PGJ_2-d4 (Cayman Chemical Company) prepared in 100% methanol. Protein precipitation was performed by addition of 800 µl 100% methanol, followed by vortexing, and centrifugation at 3000*g* for 10 min at 4°C. The supernatants were collected in a new plate and evaporated under vacuum for 4 h. The evaporated samples (100–200 µl) were diluted to 1 ml with 0.05% formic acid in water and then loaded onto Oasis HLB 1 cc 30 mg plate (Waters Corporation, USA) that had been pre-conditioned with 1 ml of 100% methanol and 1 ml of 0.05% formic acid in water. The plate was washed with 10% methanol, 0.05% formic acid in water and lipids were eluted with 100% methanol. The eluates were dried under vacuum overnight and stored at −20°C until reconstituted in 50 µl of 20% acetonitrile in water prior to analysis with liquid chromatography tandem mass spectrometry (LC-MS/MS).

Lipid Profiling by LC-MS/MS

Lipids were quantified in negative mode with multiple reaction monitoring method, using a triple quadrupole mass spectrometer (Acquity TQ detector, Waters) equipped with an Acquity H-class UPLC (Waters). Eicosanoid were purchased from Cayman Chemicals and individually optimized for based on precursor ion m/z, cone voltage, collision energy, and fragment ion m/z (**Supplementary Table 3**). An eicosanoid mix containing all standards of interest was used to check interference in the LC-MS/MS analysis. Lysophophatidylcholine (LPC)(14:0) and LPC (18:0) were used to set optimal analytical parameters for quantification of LPCs. Separation of lipids was performed on a 50 × 2.1-mm Acquity UPLC BEH C18 column 1.7 µm (Waters) with a 12-min stepwise linear gradient (20%–95%) at a flowrate of 0.6 ml/min with 0.05% formic acid in acetonitrile as mobile phase B and 0.05% formic acid in water as mobile phase A. Data were analyzed using MassLynx software, version 4.1, with internal standard calibration and quantification to external standard curves for prostanoids. LPCs were normalized as area-% within each injection. Only lipids with peaks intensities of signal-to-noise greater than 10 (S/N >10) were considered in our data analysis.

Development of Whole Blood Assay

The whole blood assay was developed to screen for changes in multiple eicosanoids. Each eicosanoid and corresponding deuterated variant were individually optimized in the LC-MS/MS analysis. A dilution curve containing 6-keto $PGF_{1\alpha}$-d4, PGE_2-d4, PGD_2-d4, $PGF_{2\alpha}$-d4, TXB_2-d4, 15d-PGJ_2-d4, LTB_4-d4, LTC_4-d5, LTD_4-d5, 5-HETE-d8, 12-HETE-d8, 15-HETE-d8, and undeuterated variants of 13-HODE, RvD1, RvD2, 17-hydroxy DHA, and protectin DX was spiked into 100 µl plasma at different stages throughout the extraction. A dilution curve was spiked in water at the same step. The dilution curve ranged from 0.006 to 1.5 pmol as final amount injected on the column in the LC-MS/MS analysis. This enabled us to investigate the lower limit of quantification (LLOQ), recovery efficacy, and matrix effect for each eicosanoid. The LLOQ injected on column was considered as great (0.02–0.05 pmol), good (0.1–0.2 pmol), or poor (0.4–1.5 pmol). Eicosanoids with great LLOQ were PGE_2, $PGF_{2\alpha}$, TXB_2, RvD1, RvD2, LTB_4, protectin DX, and 13-HODE; good LLOQ were 6-keto $PGF_{1\alpha}$, PGD_2, 5-HETE, 15-HETE, and LTD_4; poor LLOQ were 15d-PGJ_2, 12-HETE, 17-hydroxy DHA, and LTC_4. The extraction recovery rates were 33%–125%. The response in plasma compared to 20% acetonitrile were 52%–116% due to matrix effects. The estimated LLOQ in 100 µl plasma was approximately 1 ng/ml for the best performing eicosanoids including PGE_2, TXB_2, $PGF_{2\alpha}$, RvD1, RvD2, and protectin DX. We can conclude that the method provided similar quantitative performance in plasma for many eicosanoids.

LPS at 10 µg/ml induced PGE_2 and TXB_2 production in human whole blood, which are the two dominant eicosanoids produced under these conditions (Mazaleuskaya et al., 2016). All other eicosanoids were below the LLOQ. We chose 10 µg/ml of LPS based on the consensus in the literature for this type of assay, yielding a robust amount of PGE_2 (49 ± 4 ng/ml, n = 5 donors) and TXB_2 (24 ± 9 ng/ml, n = 5 donors). The prostanoid production was completely blocked using the dual COX-1/2 inhibitor diclofenac (10 µM). High concentration of DMSO (0.1%) slightly decreased PGE_2 production by 20% (n = 2 donors) while DMSO at 0.01% or 0.001% had no effect. The intra-assay coefficient of variation (CV, n = 20 technical replicates) was 12% and 11% for PGE_2 and TXB_2, respectively. The inter-assay CV for control material (n = 3 donors) was 20% for PGE_2 and 30% for TXB_2. This was performed on blood that was drawn, incubated, extracted, and analyzed at separate occasions. The suppression in signal due to matrix effects and/or recovery efficiency varied between donors and experiments, ranging from 10% to 70% suppression compared to signal in extracted blank (mean ± SD, n = 6 donors, PGE_2: 45% ± 25%,

TXB_2: 40 ± 20%). In summary, 24-h incubation of whole blood with 10 μg/ml LPS resulted in profound induction of the COX-1/2 products PGE_2 and TXB_2 that was efficiently blocked by diclofenac at 10 μM.

Quantification of IL-8

IL-8 was quantified in plasma by human IL-8 (CXCL8) enzyme-linked immunosorbent assay (ELISA) development kit (3560-1H, Mabtech) according to manufacturer's instructions.

Statistical Analyses

Data are presented as mean ± SEM if not stated otherwise. Statistical analyses were performed using GraphPad Prism 6 (GraphPad Software). One-sample t-test and two-sample t-test with Bonferroni correction were used to test significant difference. Statistical significance level was set to $p < 0.05$.

RESULTS

Effect on PGE_2 and TXB_2 Production

Our screening of inhibitors suggested that selected kinase inhibitors affected prostanoid production (**Figure 1**). The strongest reduction in PGE_2 production was observed by MEK-1 inhibitor PD0325901 (31% ± 6%, p = 0.001, n = 4) and MEK-1/2 inhibitor trametinib (34% ± 7%, p < 0.0001, n = 15). Moderate suppression in PGE_2 concentration was found for MEK-1/2 inhibitor selumetinib (65% ± 9%, p = 0.02, n = 5), ERK-1/2 inhibitor SCH772984 (76% ± 11%, p = 0.04, n = 13), and p38 inhibitor skepinone-L (76% ± 8%, p = 0.01, n = 13). However, the tested p38 inhibitor pamapimod did not affect PGE_2 production. Two of these compounds decreased TXB_2 production, namely trametinib (63% ± 6%, p = 0.02, n = 15) and selumetinib (74% ± 7%, p = 0.02, n = 5). Diclofenac, here used as a positive control for inhibition of prostanoid production, blocked the prostanoid production while selective COX-2 inhibitor NS-398 inhibited only PGE_2 production, in agreement with previously reported data for these compounds in whole blood assay (Larsson et al., 2019). The JAK inhibitor tofacitinib increased both PGE_2 (286% ± 51%, p = 0.01, n = 6) and TXB_2 (169% ± 20%, p = 0.02, n = 6) production. The IRAK-1/4 inhibitor I slightly increased the concentrations of PGE_2 (139% ± 15%, p = 0.04, n = 7) and TXB_2 (133% ± 8%, p = 0.008, n = 7).

We chose to investigate the strongest observed effects in more detail by performing concentration–response experiments for PD0325901, trametinib, selumetinib, and tofacitinib. All three MEK inhibitors showed a concentration-dependent response on both PGE_2 and TXB_2 production while tofacitinib showed a concentration-dependent response on PGE_2 production (**Figure 2**).

Effect on IL-8 Secretion

In line with the effect on prostanoid production, reduction in IL-8 secretion was found for PD0325901 (24% ± 9%, p = 0.03, n = 3), trametinib (27% ± 5%, p < 0.0001, n = 13), and selumetinib (45% ± 10%, p = 0.03, n = 3) (**Figure 3**). Moderate reduction in IL-8 secretion was found for SCH772984 (62% ± 9%, p = 0.002, n = 12) and diclofenac (66% ± 8%, p = 0.003, n = 11). We could also observe that tofacitinib increased IL-8 secretion (225% ± 57%, p = 0.16, n = 3), however not with statistical significance.

Effect on LPC Profile

We measured LPC species within our targeted LC-MS/MS analysis. LPCs are mainly generated by metabolism of membrane phosphatidylcholine by cytosolic phospholipase A_2 (Burke and Dennis, 2009). These lipids have been reported to be involved in several cellular processes; sometimes with opposing effect depending on degree of saturation, concentration, and biological context (Sevastou et al., 2013; Drzazga et al., 2014). We observed no difference in total LPC or LPC profile when whole blood was treated with LPS neither did any of the tested inhibitors alter the LPC profile (**Figure 4**).

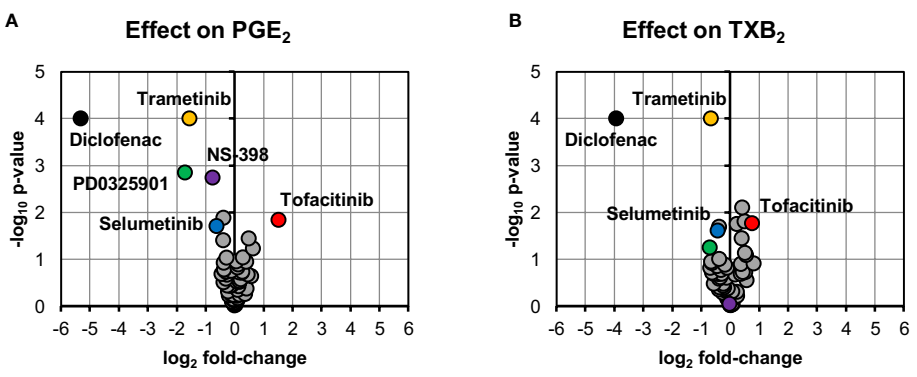

FIGURE 1 | Volcano plots showing effects on PGE_2 **(A)** and TXB_2 **(B)** production in LPS-induced human whole blood. The top altered conditions compared to vehicle control based on fold-change (< 0.5 or >2) and p-value (< 0.05) are highlighted. Each inhibitor was tested in 4–15 donors. Statistical significance was tested using one-sample t-test ($p < 0.05$). PGE_2, prostaglandin E_2; LPS, lipopolysaccharide; TXB_2, thromboxane B_2.

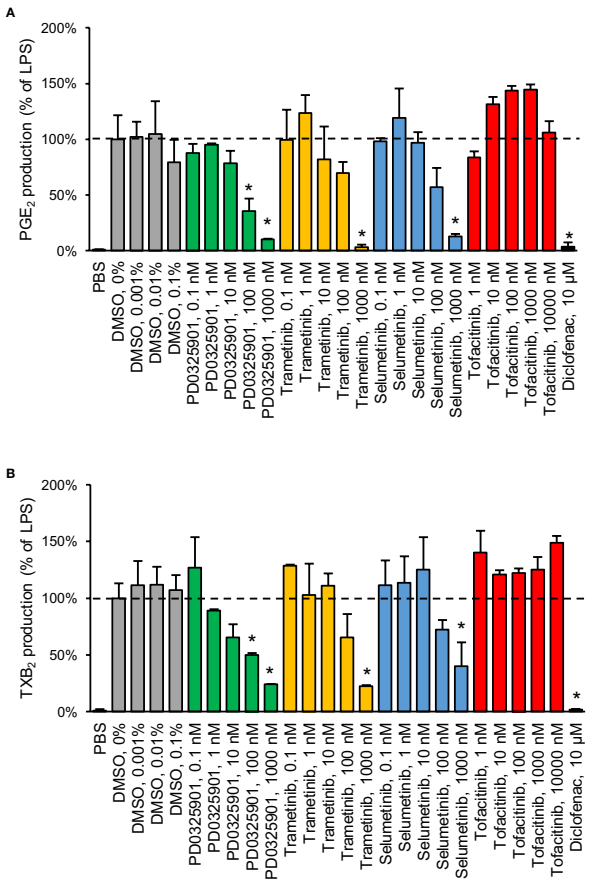

FIGURE 2 | Validation of inhibitory effect on PGE_2 **(A)** and TXB_2 **(B)** production by MEK inhibitors in human whole blood. Diclofenac at 10 µM was used as positive control. Data are presented as mean ± SD of biological replicates (n = 2-6 per condition) from one representative experiment. The absolute prostanoid production in LPS control was 53.3 ± 8.3 ng/ml for PGE_2 and 15.5 ± 2.1 ng/ml for TXB_2. The concentration–response was tested in two donors. Statistical significance was tested using two-sample t-test with Bonferroni correction ($p < 0.05$). The asterisk (*) represents statistical significance to vehicle control.

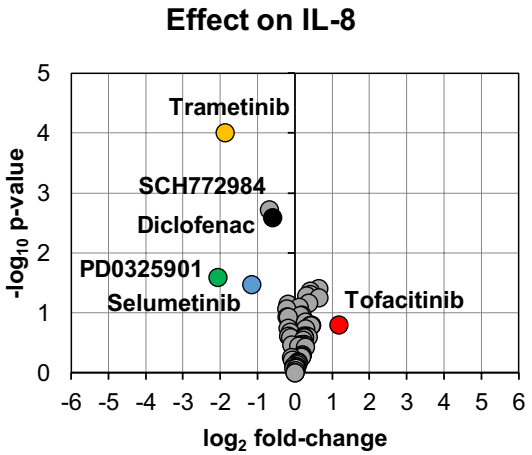

FIGURE 3 | Volcano plot showing effects on IL-8 secretion in LPS-induced human whole blood. The top altered conditions compared to vehicle control based on fold-change (< 0.5 or >2) and p-value (< 0.05) are highlighted. Each inhibitor was tested in 3–13 donors. Statistical significance was tested using one sample t-test ($p < 0.05$). IL-8, interleukin-8.

DISCUSSION

We have tested the inhibitory effect on prostanoid production and IL-8 secretion in human whole blood for 57 high-quality inhibitors with known target specificities and *in vitro* potencies. None of the tested epigenetic modulators, which are acting on demethylases, bromodomains, or methyltransferases, affected PGE_2 or IL-8 concentration. Inhibition of MEK-1/2 or ERK decreased PGE_2 production and IL-8 secretion in this assay. This effect was observed for allosteric inhibitor trametinib (MEK-1/2), non-ATP-competitive inhibitors PD0325901 (MEK-1) and selumetinib (MEK-1/2), and ATP-competitive inhibitor SCH772984 (ERK-1/2). These kinase targets are part of the RAS/RAF/MEK/ERK signaling transduction pathway, where inhibition of MEK prevents the downstream phosphorylation and activation of ERK that ultimately regulates cellular responses such as survival, lipid metabolism, and protein translation (McCubrey et al., 2007). For example, MEK-1/2 inhibitor PD184352 decreased PGE_2 production in melanoma cell line by decreased COX-2 expression due to inhibition of phosphorylation on ERK (Zelenay et al., 2015) and trametinib reduced IL-8 production in melanoma cell line (Hartman et al., 2017). We found that our positive control diclofenac for blocking prostanoid production decreased IL-8 secretion, which is explained by the fact that PGE_2 stimulates IL-8 production in cultured cells (Agro et al., 1996; Caristi et al., 2005; Aso et al., 2012; Venza et al., 2012). While our study mainly focused on identifying inhibitory effects, we observed that JAK inhibitor tofacitinib increased both PGE_2 production and IL-8 secretion. Tofacitinib is used to treat rheumatoid arthritis and it is known that tofacitinib can increase the expression of pro-inflammatory mediators, including PGE_2, in macrophages by acting inhibitory on the expression of anti-inflammatory IL-10 (Kothari et al., 2014). The increased formation of pro-inflammatory PGE_2 and platelet activating thromboxane A_2 (as measured by stable metabolite TXB_2) in human whole blood may be associated with the recently recognized increased risk of thromboembolism associated with JAK inhibitors in treatment of rheumatoid arthritis (Scott et al., 2018). Moreover, we did not observe any changes in LPC profile by LPS alone or the tested compounds. While LPCs can be generated by degradation of phosphatidylcholine, LPCs are continuously incorporated back into the plasma membrane (Law et al., 2019). This would result in no net change in LPCs while other phospholipid species may change in abundance. We acknowledge that the limitation of our study is the usage of one concentration per tested inhibitor.

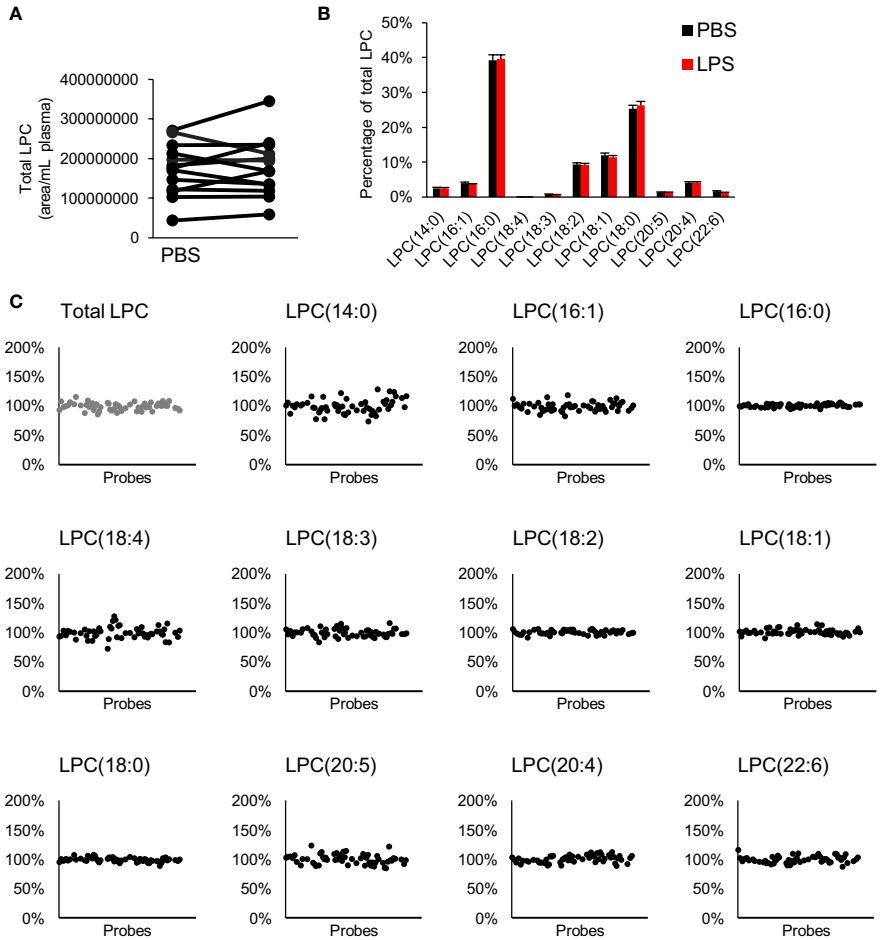

FIGURE 4 | Effect on LPC profile in whole blood. There was no difference in total LPC **(A)** or LPC profile **(B)** with LPS treatment, and none of the tested compounds affected the LPC profile **(C)**. Each inhibitor was tested in 4–15 donors. LPC, lysophophatidylcholine.

However, the used concentrations were based on reported IC_{50} and/or EC_{50} values as well as solid experiences in our laboratories using other validated assay systems (https://ultra-dd.org/index.php/tissue-platforms/cell-assay-datasets). The concentrations were selected to avoid cellular toxicity but we acknowledge that greater concentrations might be of relevance considering the bioavailability in blood. Indeed, we demonstrated in concentration–response experiments that greater inhibitory effect could be achieved by increasing the concentration for the MEK inhibitors. However, this increases the risk of off-target effects and/or introduction of cellular toxicity that needs to be taken into account in experimental design and interpretation of results. In conclusion, we identified inhibitors for MEK or ERK as anti-inflammatory hits in our human whole blood assay. Based on the suppression in PGE_2 production and IL-8 secretion, further investigation of the MEK/ERK signaling pathway may inform future therapeutic strategies to treat inflammatory diseases such as SLE and DM.

DATA AVAILABILITY STATEMENT

The datasets generated for this study are available on request to the corresponding authors.

ETHICS STATEMENT

The studies involving human participants were reviewed and approved by Karolinska University hospital (Dnr 02-196) and the Regional Ethical Review Board in Stockholm (Dnr 2015/2001-31/2). The patients/participants provided their written informed consent to participate in this study.

AUTHOR CONTRIBUTIONS

FB, YS, MS, P-JJ, and LB contributed to study conception and design. FB, YS, and M-MS performed experiments. FB analyzed

data, performed statistical analysis, and drafted the manuscript. IG and IL facilitated administrative, technical, or material support. All authors critically revised and approved the final version of the manuscript.

ACKNOWLEDGMENTS

This work was supported by grants from Innovative Medicines Initiative (EU/EFPIA, ULTRA-DD, grant no. 115766), the Swedish Research Council (grant no. 2017-02577), Stockholm County Council (ALF, grant no. 20160378), The Swedish Rheumatism Association (grant no. R-755861), King Gustaf V's 80 Years Foundation (grant no. n/a), and funds from Karolinska Institutet (grant no. n/a). This manuscript has been released as a preprint at https://doi.org/10.1101/2019.12.30.890715, (Bergqvist et al., 2019).

SUPPLEMENTARY MATERIAL

The Supplementary Material for this article can be found online at: https://www.frontiersin.org/articles/10.3389/fphar.2020.00613/full#supplementary-material

REFERENCES

Agro, A., Langdon, C., Smith, F., and Richards, C. D. (1996). Prostaglandin E 2 enhances interleukin 8 (IL-8) and IL-6 but inhibits GMCSF production by IL-1 stimulated human synovial fibroblasts in vitro. *J. Rheumatol* 23, 862-868.

Akaogi, J., Nozaki, T., Satoh, M., and Yamada, H. (2012). Role of PGE2 and EP Receptors in the Pathogenesis of Rheumatoid Arthritis and as a Novel Therapeutic Strategy. *Endocrine Metab. Immune Disord. - Drug Targets* 6, 383–394. doi: 10.2174/187153006779025711

Alfaro, C., Sanmamed, M. F., Rodríguez-Ruiz, M. E., Teijeira, Á., Oñate, C., González, Á., et al. (2017). Interleukin-8 in cancer pathogenesis, treatment and follow-up. *Cancer Treat Rev*. 60, 24–31. doi: 10.1016/j.ctrv.2017.08.004

Arrowsmith, C. H., Audia, J. E., Austin, C., Baell, J., Bennett, J., Blagg, J., et al. (2015). The promise and peril of chemical probes. *Nat. Chem. Biol*. 11, 536–541. doi: 10.1038/nchembio.1867

Aso, H., Ito, S., Mori, A., Morioka, M., Suganuma, N., Kondo, M., et al. (2012). Prostaglandin e 2 enhances interleukin-8 production via ep4 receptor in human pulmonary microvascular endothelial cells. *Am. J. Physiol. - Lung Cell. Mol. Physiol*. 302, 266–273. doi: 10.1152/ajplung.00248.2011

Bergqvist, F., Sundström, Y., Shang, M., Gunnarsson, I., Lundberg, I. E., Sundström, M., et al. (2019). Anti-inflammatory properties of chemical probes in human whole blood: focus on prostaglandin E2 production. *bioRxiv* doi: 10.1101/2019.12.30.890715

Bergqvist, F., Morgenstern, R., and Jakobsson, P. J. (2020). A review on mPGES-1 inhibitors: From preclinical studies to clinical applications. *Prostaglandins Other Lipid Mediators* 147. doi: 10.1016/j.prostaglandins.2019.106383

Buckley, C. D., Gilroy, D. W., Serhan, C. N., Stockinger, B., and Tak, P. P. (2013). The resolution of inflammation. *Nat. Rev. Immunol*. 13, 59–66. doi: 10.1038/nri3362

Burke, J. E., and Dennis, E. A. (2009). Phospholipase A 2 structure/function, mechanism, and signaling. *J. Lipid Res* 50, S237–S242. doi: 10.1194/jlr.R800033-JLR200

Caristi, S., Piraino, G., Cucinotta, M., Valenti, A., Loddo, S., and Teti, D. (2005). Prostaglandin E2 induces interleukin-8 gene transcription by activating C/EBP homologous protein in human T lymphocytes. *J. Biol. Chem*. 280, 14433–14442. doi: 10.1074/jbc.M410725200

David, J. M., Dominguez, C., Hamilton, D. H., and Palena, C. (2016). The IL-8/IL-8R axis: A double agent in tumor immune resistance. *Vaccines* 4. doi: 10.3390/vaccines4030022

Drzazga, A., Sowińska, A., and Koziołkiewicz, M. (2014). Lysophosphatidylcholine and lysophosphatidylinosiol novel promissing signaling molecules and their possible therapeutic activity. *Acta Poloniae Pharm. - Drug Res*. 71, 887-899.

Fattahi, M. J., and Mirshafiey, A. (2012). Prostaglandins and Rheumatoid Arthritis. *Arthritis*. 2012, 1–7. doi: 10.1155/2012/239310

Hanahan, D., and Weinberg, R. A. (2011). Hallmarks of cancer: The next generation. *Cell* 144, 646–674. doi: 10.1016/j.cell.2011.02.013

Hartman, M. L., Rozanski, M., Osrodek, M., Zalesna, I., and Czyz, M. (2017). Vemurafenib and trametinib reduce expression of CTGF and IL-8 in V600EBRAF melanoma cells. *Lab. Invest*. 97, 217–227. doi: 10.1038/labinvest.2016.140

Kaplan, M. J. (2011). Neutrophils in the pathogenesis and manifestations of SLE. *Nat. Rev. Rheumatol*. 7, 691–699. doi: 10.1038/nrrheum.2011.132

Kothari, P., Pestana, R., Mesraoua, R., Elchaki, R., Khan, K. M. F., Dannenberg, A. J., et al. (2014). IL-6–Mediated Induction of Matrix Metalloproteinase-9 Is Modulated by JAK-Dependent IL-10 Expression in Macrophages. *J. Immunol* 192, 349–357. doi: 10.4049/jimmunol.1301906

Larsson, K., Steinmetz, J., Bergqvist, F., Arefin, S., Spahiu, L., Wannberg, J., et al. (2019). Biological characterization of new inhibitors of microsomal PGE synthase-1 in preclinical models of inflammation and vascular tone. *Br. J. Pharmacol* 176, 4625–4638. doi: 10.1111/bph.14827

Law, S. H., Chan, M. L., Marathe, G. K., Parveen, F., Chen, C. H., and Ke, L. Y. (2019). An updated review of lysophosphatidylcholine metabolism in human diseases. *Int. J. Mol. Sci*. 20. doi: 10.3390/ijms20051149

Lit, L. C. W., Wong, C. K., Tam, L. S., Li, E. K. M., and Lam, C. W. K. (2006). Raised plasma concentration and ex vivo production of inflammatory chemokines in patients with systemic lupus erythematosus. *Ann. Rheumatic Dis*. 65, 209–215. doi: 10.1136/ard.2005.038315

Mao, Y. M., Zhao, C. N., Liu, L. N., Wu, Q., Dan, Y. L., Wang, D. G., et al. (2018). Increased circulating interleukin-8 levels in systemic lupus erythematosus patients: A meta-analysis. *Biomarkers Med*. 12, 1291–1302. doi: 10.2217/bmm-2018-0217

Mazaleuskaya, L. L., Lawson, J. A., Li, X., Grant, G., Mesaros, C., Grosser, T., et al. (2016). A broad-spectrum lipidomics screen of antiinflammatory drug combinations in human blood. *JCI Insight* 1. doi: 10.1172/jci.insight.87031

McCubrey, J. A., Steelman, L. S., Chappell, W. H., Abrams, S. L., Wong, E. W. T., Chang, F., et al. (2007). Roles of the Raf/MEK/ERK pathway in cell growth, malignant transformation and drug resistance. *Biochim. Biophys. Acta - Mol. Cell Res*. 1773, 1263–1284. doi: 10.1016/j.bbamcr.2006.10.001

McInnes, I. B., and Schett, G. (2011). The pathogenesis of rheumatoid arthritis. *New Engl. J. Med*. 365, 2205–2219. doi: 10.1056/NEJMra1004965

Nathan, C. (2002). Points of control in inflammation. *Nature* 420, 846–852. doi: 10.1038/nature01320

Nielepkowicz-Goździńska, A., Fendler, W., Robak, E., Kulczycka-Siennicka, L., Górski, P., Pietras, T., et al. (2014). Exhaled IL-8 in systemic lupus erythematosus with and without pulmonary fibrosis. *Archivum Immunologiae Ther. Exp*. 62, 231–238. doi: 10.1007/s00005-014-0270-5

Peng, Y., Zhang, S., Zhao, Y., Liu, Y., and Yan, B. (2018). Neutrophil extracellular traps may contribute to interstitial lung disease associated with anti-MDA5 autoantibody positive dermatomyositis. *Clin. Rheumatol*. 37, 107–115. doi: 10.1007/s10067-017-3799-y

Ricciotti, E., and Fitzgerald, G. A. (2011). Prostaglandins and inflammation. *Arteriosclerosis Thrombosis Vasc. Biol*. 31, 986–1000. doi: 10.1161/ATVBAHA.110.207449

Russo, R. C., Garcia, C. C., Teixeira, M. M., and Amaral, F. A. (2014). The CXCL8/IL-8 chemokine family and its receptors in inflammatory diseases. *Expert Rev. Clin. Immunol*. 10, 593–619. doi: 10.1586/1744666X.2014.894886

Scott, I. C., Hider, S. L., and Scott, D. L. (2018). Thromboembolism with Janus Kinase (JAK) Inhibitors for Rheumatoid Arthritis: How Real is the Risk? *Drug Safety* 41, 645–653. doi: 10.1007/s40264-018-0651-5

Sevastou, I., Kaffe, E., Mouratis, M. A., and Aidinis, V. (2013). Lysoglycerophospholipids in chronic inflammatory disorders: The PLA 2/LPC and ATX/LPA axes. *Biochim. Biophys. Acta - Mol. Cell Biol. Lipids* 1831, 42–60. doi: 10.1016/j.bbalip.2012.07.019

Venza, I., Visalli, M., Fortunato, C., Ruggeri, M., Ratone, S., Caffo, M., et al. (2012). PGE2 induces interleukin-8 derepression in human astrocytoma through coordinated DNA demethylation and histone hyperacetylation. *Epigenetics* 7, 1315–1330. doi: 10.4161/epi.22446

Wang, D., and Dubois, R. N. (2010). Eicosanoids and cancer. *Nat. Rev. Cancer* 10, 181-193. doi: 10.1038/nrc2809

Waugh, D. J. J., and Wilson, C. (2008). The interleukin-8 pathway in cancer. *Clin. Cancer Res.* 14, 6735–6741. doi: 10.1158/1078-0432.CCR-07-4843

Yoshio, T., Okamoto, H., Kurasawa, K., Dei, Y., Hirohata, S., and Minota, S. (2016). IL-6, IL-8, IP-10, MCP-1 and G-CSF are significantly increased in cerebrospinal fluid but not in sera of patients with central neuropsychiatric lupus erythematosus. *Lupus* 25, 997–1003. doi: 10.1177/0961203316629556

Zelenay, S., Van Der Veen, A. G., Böttcher, J. P., Snelgrove, K. J., Rogers, N., Acton, S. E., et al. (2015). Cyclooxygenase-Dependent Tumor Growth through Evasion of Immunity. *Cell* 162, 1257–1270. doi: 10.1016/j.cell.2015.08.015

Zhang, S., Shu, X., Tian, X., Chen, F., Lu, X., and Wang, G. (2014). Enhanced formation and impaired degradation of neutrophil extracellular traps in dermatomyositis and polymyositis: A potential contributor to interstitial lung disease complications. *Clin. Exp. Immunol.* 177, 134–141. doi: 10.1111/cei.12319

Conflict of Interest: The SGC receives funds from AbbVie, Bayer Pharma, Boehringer Ingelheim, the Canada Foundation for Innovation, the Eshelman Institute for Innovation, Genome Canada, Janssen, Merck (Darmstadt, Germany), MSD, Novartis Pharma, the Ontario Ministry of Economic Development and Innovation, Pfizer, the São Paulo Research Foundation, Takeda and the Wellcome Trust (authors: FB, YS, M-MS, MS, P-JJ, and LB). These funders had no direct role in study conceptualization, design, data collection, analysis, decision to publish, or preparation of the manuscript. P-JJ is member of the board of directors at Gesynta Pharma, a company that develops anti-inflammatory drugs.

The remaining authors declare that the research was conducted in the absence of any commercial or financial relationships that could be construed as a potential conflict of interest.

frontiers in Pharmacology

BRIEF RESEARCH REPORT
published: 11 January 2021
doi: 10.3389/fphar.2020.568865

Long-Term Follow-Up and Optimization of Interleukin-1 Inhibitors in the Management of Monogenic Autoinflammatory Diseases: Real-Life Data from the JIR Cohort

Véronique Hentgen[1], Isabelle Koné-Paut[2], Alexandre Belot[3], Caroline Galeotti[2], Gilles Grateau[4], Aurelia Carbasse[5], Anne Pagnier[6], Pascal Pillet[7], Marc Delord[8], Michael Hofer[9] and Sophie Georgin-Lavialle[4]*

[1]Department of Pediatrics, National Reference Center for Auto-inflammatory Diseases and Amyloidosis, CEREMAIA, Versailles Hospital, Versailles, France, [2]Department of Pediatric Rheumatology National Reference Center for Auto-Inflammatory Diseases and Amyloidosis, CEREMAIA, CHU du Kremlin Bicêtre, University of Paris Sud Saclay, UVSQ, Le Kremlin Bicêtre, France, [3]Pediatric Nephrology, Rheumatology, Dermatology, HFME, Hospices Civils de Lyon, National Referee Centre RAISE, & INSERM U1111, Université de Lyon, Lyon, France, [4]Department of Internal Medicine, National Reference Center for Auto-Inflammatory Diseases and Amyloidosis, CEREMAIA, Tenon Hospital, AP-HP, Sorbonne University, Paris, France, [5]Department of Pediatrics, Hôpital Arnaud de Villeneuve, CHRU Montpellier, Montpellier, France, [6]Department of Pediatrics, CHU de Grenoble, Grenoble, France, [7]Department of Pediatrics, Hôpital des Enfants, CHRU Bordeaux, Bordeaux, France, [8]Direction de La Recherche Clinique et de L'Innovation (DRCI) Versailles Hospital, Versailles, France, [9]Unité Romande D'Immuno-Rhumatologie Pédiatrique, CHUV, University of Lausanne, Lausanne, Switzerland

OPEN ACCESS

Edited by:
Gerard Bannenberg, Global Organization for EPA and DHA Omega-3s (GOED), United States

Reviewed by:
Luca Cantarini, University of Siena, Italy
Selcan Demir, Hacettepe University, Turkey
Joost Frenkel, Utrecht University, Netherlands

***Correspondence:**
Véronique Hentgen
vhentgen@ch-versailles.fr

Specialty section:
This article was submitted to Inflammation Pharmacology, a section of the journal Frontiers in Pharmacology

Received: *02 June 2020*
Accepted: *12 October 2020*
Published: *11 January 2021*

Citation:
Hentgen V, Koné-Paut I, Belot A, Galeotti C, Grateau G, Carbasse A, Pagnier A, Pillet P, Delord M, Hofer M and Georgin-Lavialle S (2021) Long-Term Follow-Up and Optimization of Interleukin-1 Inhibitors in the Management of Monogenic Autoinflammatory Diseases: Real-Life Data from the JIR Cohort. Front. Pharmacol. 11:568865. doi: 10.3389/fphar.2020.568865

Objectives: The major role of interleukin (IL)-1 in the pathogenesis of hereditary recurrent fever syndromes favored the employment of targeted therapies modulating IL-1 signaling. However the best use of IL1 inhibitors in terms of dosage is difficult to define at present.

Methods: In order to better understand the use of IL1 inhibitors in a real-life setting, our study assessed the dosage regimens of French patients with one of the four main hereditary recurrent fever syndromes (Familial Mediterranean Fever (FMF), TNF receptor associated periodic syndrome (TRAPS), cryopyrin associated periodic fever (CAPS) and mevalonate kinase deficiency). The patients were retrieved retrospectively from the JIR cohort, an international platform gathering data of patients with pediatric inflammatory diseases.

Results: Forty five patients of the JIR cohort with a hereditary recurrent fever syndrome had received at least once an IL1 inhibitor (anakinra or canakinumab). Of these, 43% received a lower dosage than the one suggested in the product recommendations, regardless of the type of the IL1 inhibitor. Especially patients with FMF and TRAPS seemed to need lower treatment regimens; in our cohort none of the FMF or TRAPS patients received an intensified dose of IL-inhibitor. On-demand treatment with a short half-life IL-1 inhibitor has also been used successfully for some patients with one of these two conditions The standard dose was given to 42% of the patients; whereas an intensified dose of IL-1 inhibitors was given to 15% of the patients (44% of CAPS patients and 17% of mevalonate kinase deficiency patients). In our cohort each individual patient's need for

treatment seemed highly variable, ranging from on demand treatment regimens to intensified dosage maintenance therapies depending on the activity and the severity of the underlying disease.

Conclusion: IL-1 inhibitors are a good treatment option for patients with a hereditary recurrent fever syndrome, but the individual need of the dosage of IL-1 inhibitors to control the disease effectively seems highly variable. Severity, activity but also the type of the underlying disease, belong to the parameters underpinning the treat-to-target strategy implemented in an everyday life practice.

Keywords: anakinra, canakinumab, cryopyrin-associated periodic syndrome, Tumor Necrosis factor (TNF)-receptor-associated periodic syndrome, mevalonate kinase deficiency, posology, familial mediterranean fever disease, IL-1 inhibitor

INTRODUCTION

Interleukin (IL)-1 is implicated in the pathogenesis of several systemic auto-inflammatory disorders and this recognition has favored the employment of targeted therapies modulating IL-1 signaling in a wide number of diseases (Cavalli and Dinarello, 2015). Several IL-1 inhibitors have been developed, but in France the marketing authorization has been obtained only for two of them, the IL-1 receptor antagonist analog anakinra and the IL-1β selective monoclonal antibody canakinumab. The first one was formerly licensed for rheumatoid arthritis, then cryopyrin-associated periodic syndrome (CAPS), and recently in systemic JIA. The second has an indication in the treatment of systemic JIA and in four hereditary systemic auto-inflammatory disorders (European Medicines Agency, 2018b). In 2018, the pivotal placebo-controlled umbrella study with canakinumab has provided the highest level of evidence for the use of IL-1 blockers to control inflammatory symptoms in 3 diseases other than CAPS: i.e. mevalonate kinase deficiency (MKD), TNF receptor associated periodic syndrome (TRAPS), and familial Mediterranean fever (FMF) (De Benedetti et al., 2018). Anakinra will shortly be licensed in France also for colchicine resistant FMF (crFMF) patients (European Medecines Agency, 2018a).

Despite the studies giving short or medium-term results, the use of IL-1 inhibitors on a long term and especially in real life may differ in terms of both intervals between the injections and dosage. Indeed, patients responding insufficiently to IL-1 inhibition, respond completely to a dose increase or shortening of the interval between the doses (Bodar et al., 2011; Grimwood et al., 2015; Kone-Paut et al., 2017; Deshayes et al., 2018). Conversely, the minimum doses required to treat a patient effectively are less well known, considering that the majority of patients are currently treated with a treat-to-target strategy.

In French tertiary care centers, IL-1 inhibitors have been used off-labeled in theses indications for several years (Meinzer et al., 2011; Stankovic et al.,2012; Rossi-Semerano et al., 2015; Abbara et al., 2017). The analysis of these patients therefore presents an unique opportunity to compare the actual doses received by patients in a nation-wide "real-life" setting to the drug dosage recommended in the product recommendations.

MATERIALS AND METHODS

Study Design and Participants

Patients were identified from the JIR cohort, an international multicenter data repository granted by the Swiss-Children-Rheumatisms foundation, which aims to collect both retrospective and prospective information in a variety of juvenile onset systemic inflammatory disorders (http://www.fondationres.org/fr/jircohorte - NTC02377245). For the purpose of the study, only patients from French centers (pediatric and adult) with complete history data and at least one completed follow-up visit were analyzed. Inclusion criteria to the study were all patients.

1) with a monogenic autoinflammatory recurrent fever syndrome (CAPS, TRAPS, FMF and MKD) according to the EUROFEVER/Printo classification criteria (Gattorno et al., 2019).
2) who received during their follow-up at least one IL-1 inhibitor.

Export of patient's data took place on 12th June 2017, one month before the marketing authorization of canakinumab in France.

Protocol Approvals

This study conformed to the tenets of the Declaration of Helsinki and the protocol was approved by the French Ethic Committee (CCTIRS). Patients were enrolled after comprehensive information checking that they (or their legal guardian) were not opposed to the study and the storage of their personal data. The electronic case report form has been the object of an approval of the national commission for Data Protection and Liberties (CNIL).

Aims and Endpoints

The primary objective of the study was to evaluate the consistence of dosing of IL1inhibitors in HRFs based on European Medicines Agency labeled recommendations.

The secondary aims were 1) to analyze the reasons for discrepancies with the product recommendations and 2) to assess the overall safety profile of IL-1 inhibitors in HRFs.

TABLE 1 | Patients characteristics and received IL1inhibitor.

Disease/Patient *N*°	Mutation (HGVS name)	First line IL1 inhibitor			Second line IL1 inhibitor			Third line IL1 inhibitor	
		Drug	Dosing group	Medication stopped? Y/N Reason	Drug	Dosing group	Medication stopped? Y/N Reason	Drug	Dosing group
CAPS 1	T348M (*p.Thr348Met*)	CAN	Std	Y Patient's choice					
CAPS 2	D303N (*p.Asp303Asn*)	ANA	Std	Y Scheduled switch from ANA to CAN	CAN	Int	N		
CAPS 3	Y859C (*p.Tyr859Cys*)	CAN	Int	N					
CAPS 4	R260W (*p.Arg260Trp*)	CAN	Std	Y Adverse event (infection)	CAN	Std	N		
CAPS 5	R260W (*p.Arg260Trp*)	CAN	Int	Y Adverse event (metabolic disorder)	CAN	Int	Y Adverse event (nervous system disorder)	CAN	Int
CAPS 6	R260W (*p.Arg260Trp*)	CAN	Std	N					
CAPS 7	T348M (*p.Thr348Met*)	ANA	Std	Y Scheduled switch from ANA to CAN	CAN	Std	N		
CAPS 8	R260W (*p.Arg260Trp*)	CAN	Std	N					
CAPS 9	A352V (*p.Ala352Val*)	CAN	Std	N					
CAPS 10	R260W (*p.Arg260Trp*)	CAN	Int	N					
CAPS 11	R260W (*p.Arg260Trp*)	ANA	Std	Y Scheduled switch from ANA to CAN	CAN	Int	N		
CAPS 12	T348M (*p.Thr348Met*)	CAN	Std	N					
CAPS 13	R260W (*p.Arg260Trp*)	CAN	Int	N					
CAPS 14	T348M (*p.Thr348Met*)	CAN	Int	N					
CAPS 15	R260W (*p.Arg260Trp*)	CAN	Int	N					
CAPS 16	R260W (*p.Arg260Trp*)	ANA	Std	Y Burden of injections	CAN	Std	Y Patient's choice	CAN	Std
CAPS 17	R260W (*p.Arg260Trp*)	CAN	Std	N					
CAPS 18	R260W (*p.Arg260Trp*)	CAN	Std	N					
TRAPS 1	C29S (*p.Cys58Ser*)	ANA	Std	Y Scheduled switch from ANA to CAN	CAN	Low	N		
TRAPS 2	C70Y (*p.Cys99Tyr*)	ANA	Low	Y Not effective (on demand)	CAN	Low	N		
TRAPS 3	D42E (*p.Asp71Glu*)	ANA	Low	N					
TRAPS 4	Y20C (*p.Thy49Cys*)	ANA	Low	Y Scheduled switch from ANA to CAN	CAN	Low	N		
TRAPS 5	T50M (*p.Thr79Met*)	ANA	Low	N					
TRAPS 6	C43F (*p.Cys72Phe*)	ANA	Low	N					
TRAPS 7	D42E (*p.Asp42Glu*)	ANA	Low	N					
TRAPS 8	R92Q (p.Arg121Gln)	ANA	Std	Y Not effective (on demand)	CAN	Std	Y not effective	Other	
FMF 1	I692*/V726A (*p.Ile692Del/p.Val726Ala*)	ANA	Std	Y Adverse event (skin disorder)	CAN	Low	N		
FMF 2	M694V/M694V (*p.Met694Val/p.Met694Val*)	ANA	Low	Y Adverse event (hepatitis)	CAN	Low	N		
FMF 3	M694V/M694V (*p.Met694Val/p.Met694Val*)	CAN	Low	N					
FMF 4	M694V/WT (*p.Met694Val/WT*)	ANA	Low	Y Not effective	CAN	Std	N		
FMF 5	M694V/M694V (*p.Met694Val/p.Met694Val*)	ANA	Std	Y Remission					
FMF 6	M694V/WT (*p.Met694Val/WT*)	ANA	Low	N					
FMF 7	M694V/M694V (*p.Met694Val/p.Met694Val*)	CAN	Low	N					
FMF 8	M694V/M694V (*p.Met694Ile/p. Met694Ile*)	ANA	Low	N					
FMF 9	M694V/WT (*p.Met694Val/WT*)	CAN	Low	N					
FMF 10	M694V/WT (*p.Met694Val/WT*)	ANA	Low	N					
FMF 11	M694V/M694V (*p.Met694Val/p.Met694Val*)	ANA	Std	Y Burden of injections	CAN	Low	Y Remission	CAN	Low
FMF 12	M694V/M694V (*p.Met694Val/p.Met694Val*)	CAN	Low	Y Adverse event (infection)					
FMF 13	M694I/M694I (*p.Met694Ile/p.Met694Ile*)	ANA	Std	Y Not effective	Other				
MKD 1	K13Q/N205D (*p.Lys13Gln/p.Asn205Asp*)	ANA	Std	Y Remission	CAN	Low	N		
MKD 2	D204E/V377I (*p.Asp204Glu/p.Val377Ile*)	ANA	Std	Y Scheduled switch from ANA to CAN	CAN	Low	N		
MKD 3	I268T/V377I (*p.Ile268Thr/p.Val377Ile*)	CAN	Low	N					

(Continued on following page)

TABLE 1 | (*Continued*) Patients characteristics and received IL1inhibitor.

Disease/Patient N°	Mutation (HGVS name)	First line IL1 inhibitor			Second line IL1 inhibitor			Third line IL1 inhibitor	
		Drug	Dosing group	Medication stopped? Y/N Reason	Drug	Dosing group	Medication stopped? Y/N Reason	Drug	Dosing group
MKD 4	G309S/R388X (*p.Gly309Ser/p.Arg388**)	CAN	Low	N					
MKD 5	G311R/V377I (*p.Gly311Arg/p.Val377Ile*)	ANA	Std	Y Scheduled switch from ANA to CAN	CAN	Std	N		
MKD 6	L51F/WT (*p.Leu51Phe/WT*)	CAN	Int	N					

Low = group 1: patient receiving lower than recommended dosage.
Std = group 2: patient receiving standard dosage.
Int = group 3: patient receiving an intensified dosage of IL-1 inhibitor.
ANA = anakinra. CAN = canakinumab.
The treatment group of the patients (low, standard or intensified) was defined on the dosage received at the last visit (or at the last visit before discontinuation of the studied IL-1 inhibitor).

Assessment of the Accordance of the Received Dosage of Medication with the Recommended Dosing Regimen

All the patients who received at least one IL1 inhibitor for colchicine resistant FMF, MKD, TRAPS and CAPS were assessed. Starting and ending date of the IL-1 inhibition were notified so that total exposure time for each IL-1 inhibitor, expressed in patient-years, could be calculated.

To study the different dosage regimens, we considered the dosage of IL-1 inhibitor received at the last visit (or at the last visit before discontinuation of the studied IL-1 inhibitor). Patients were classified into three groups: group 1/lower than recommended dosage, group 2/standard dosage and group 3/ intensified dosage. For anakinra, standard dose was defined as 100 mg/day (among adults) or 2 (±0.5) mg/kg/day (among children) (European Medicines Agency, 2018a). For canakinumab the standard dose depended on the indication: for CAPS-patients the standard dose was defined as 150 mg (or 2 (±0.5) mg/kg) every 8 weeks, whereas the standard dose for crFMF, MKD and TRAPS patient was the dose recommended by the European Medicines Agency: 150 mg (or 2 (±0.5) mg/kg) every 4 weeks (European Medicines Agency, 2018b). Patients treated with lower or less frequent injections were considered as receiving lower than recommended doses, whereas those receiving higher dosages or more frequent injections were considered as receiving intensified dosages of canakinumab.

Analysis of the Reasons for Discrepancies with the Product Recommendations

To analyze the reasons for accordance or discrepancies of the different dosage regimens with the product recommendations, a descriptive analysis of the treatment modalities of the patients treated with IL-1 inhibitors was performed.

Assessment of the Overall Safety Profile of IL-1 Inhibitors

Frequency and description of adverse events were retrieved according to the medDRA terminology. For each adverse event, investigators had to indicate the intensity among "no effect", "mild", "moderate", "severe" and "very severe," the seriousness with the necessity of an hospitalization or not, the relationship between the medication and the event among "not related," "not likely," "possible," "probable," and "definitely" and the consequence on the administration of the treatment among "no action," "drug interrupted," "drug discontinued," "dose reduced". Adverse events were expressed both as absolute number of events during the whole follow-up and as number of events/100 patients/year.

RESULTS

Forty-five French patients who received at least once an IL-1 inhibitor, either anakinra or canakinumab or both, were identified in the JIR cohort and included for analysis. **Table 1** summarizes patient's characteristics with their treatments. Anakinra was the most given treatment (25/45 – 56%),

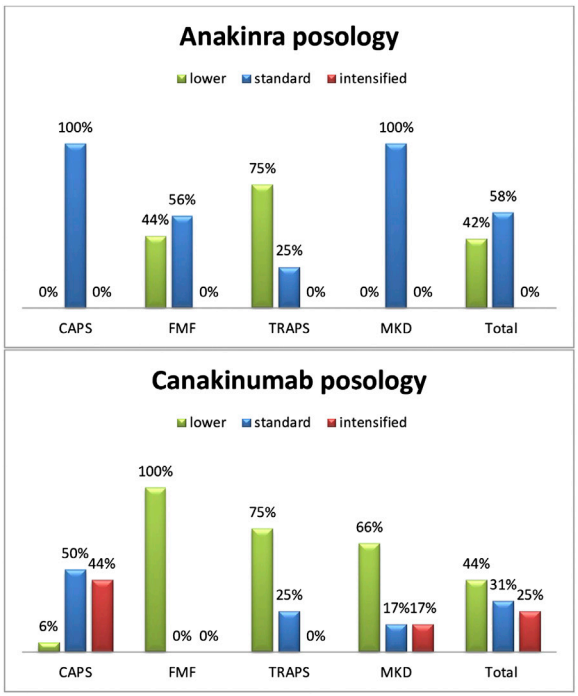

Figure: Actual posology received by the patients compared to recommended doses in the summary of product characteristics

Lower: percentage of patients receiving lower doses than recommended in the summary of product characteristics (SPC), Standard: percentage of patients receiving doses as recommended in the SPC; Intensified: percentage of patients receiving the intensified dose of the recommendations in the SPC

CAPS: cryopyrin associated periodic syndrome

FMF: familial Mediterranean fever

TRAPS: TNF receptor associated periodic syndrome

MKD: mevalonate kinase deficiency

FIGURE 1 | Actual posology received by the patients compared to recommended doses in the summary of product characteristics.

especially in FMF (9/13 – 69%) and TRAPS (8/8 – 100%) patients. The total treatment exposure to anakinra and canakinumab represented 54 and 202.9 patient-years respectively.

Figure 1 summarizes the actual doses received at the last visit (or at the last visit before discontinuation of the studied IL-1 inhibitor) according to the different diseases. Group 1 (lower dosage than in product recommendations) constituted 43% of the patients, regardless the type of IL-1 inhibitor. This was especially true for FMF, TRAPS and MKD patients on canakinumab with 100%, 75%, and 66% of patients respectively who received less than standard dose (i.e. 150 mg or 2 mg/kg every 4 weeks). Group 2 (standard dose) concerned 42% of the patients; whereas an intensified dose of IL-1 inhibitors (group 3) was given to 15% of the patients: 44% of CAPS patients and 17% of MKD patients received in our cohort higher doses than the recommended standard dose whereas neither FMF nor TRAPS patients required the intensified maintenance dose (i.e. 300 mg or 4 mg/kg every 4 weeks).

The lower dosages in our cohort than the ones recommended in the summary of product characteristics (SPC) were explained by different treatment regimens:

- Fifty percent of the patients (i.e 2 FMF and 3 TRAPS patients) treated with anakinra who received less than the recommended dose were treated with an on-demand regimen (anakinra administration only during flares), the other half received either a maintenance treatment by injections every other day instead of daily injections, or lower daily doses.
- Administration modalities for canakinumab also varied: One CAPS and one FMF patient received an "on-demand" regimen, i.e., an injection of canakinumab only if clinical and biological symptoms appeared. The other lower dose regimens involved patients with the new indication of canakinumab (i.e., FMF, TRAPS and MKD): they received less frequent injections than those stipulated in the SCP, varying from an injection every 10 weeks to every 6 weeks.

Concerning reported adverse eventsoccuring while on IL1 inhibitors (**Table 2**), 6 led to a therapeutic discontinuation, whereas 40 other adverse events possibly, probably or certainly related to IL1 inhibition were reported. The global incidence of adverse events with IL1 inhibition was 17.1 per 100 patient/years. No significant difference in the incidence of adverse events was found between anakinra or canakinumab therapy ($p = 0.55$). No link could be established between the frequency of adverse events and the dosage of IL1 inhibitor received. Especially of the nine patients with a side effect considered as serious or very serious by the investigator, three received an intensified dosage regimen. No life-threatening adverse events were retrieved in our study.

The global drug retention rate was higher for canakinumab than anakinra (**Figure 2**): 33 out of 36 patients (92%) that ever received canakinumab continued the treatment at the end of the study period, whereas this was only the case for 7 out of 25 (29%) of anakinra treated patients ($p < 0.0001$).

TABLE 2 | Reported side effects with IL1 inhibitors during the study period.

	Anakinra (24 patients 54 pts/year)	Canakinumab (36 patients/202,9 pts/year)
Infections/infestations	7	26
Hepatobiliary disorders	1	1
Metabolism and/or nutrition disorders	0	1
Nervous system disorders	0	3
Skin and/or subcutaneous tissue disorders	3	1
Surgical and/or medical procedures	0	2
Vascular disorders	0	1
Total	11	35

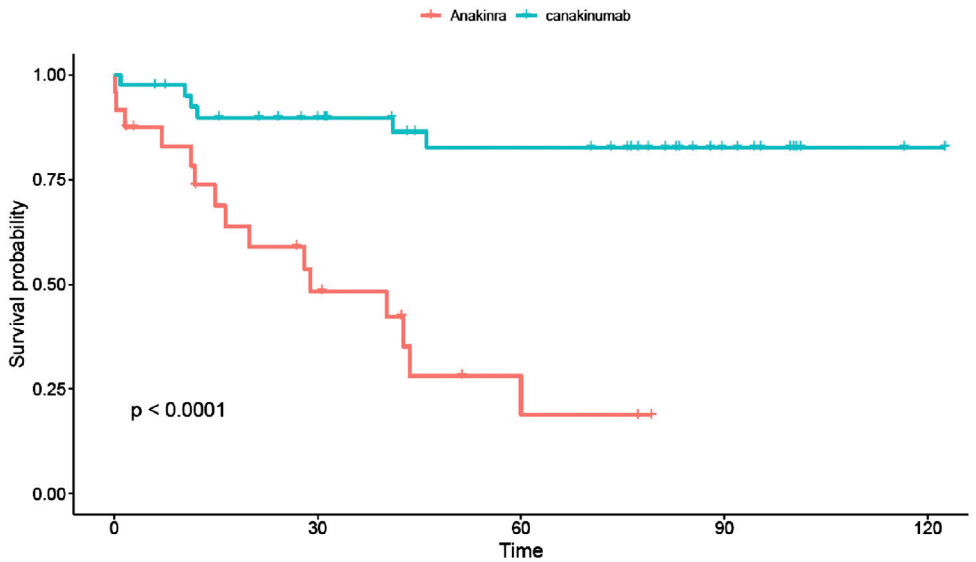

FIGURE 2 | Drug survival curves for anakinra (red line) and canakinumab (blue line). The retention rate for canakinumab was significantly higher than for anakinra. Time expressed in months.

DISCUSSION

This study assessed the dosing regimen of IL-1 inhibitors in patients with a monogenic auto-inflammatory disease. During the study period, in France licensed use of IL-1 inhibitors was possible only in CAPS patients. Nevertheless the French healthcare organization enables physicians belonging to secondary or tertiary care centers for rare diseases to prescribe off labeled drugs and our study focused on these patients.

Almost half of the patients received lower dosages of IL-1 inhibitors than the recommended standard dose. These lower dosage regimens concerned 60% of the patients with the more recent licensed indications of IL1-inhibitors: crFMF, TRAPS and MKD (De Benedetti et al., 2018; European Medicines Agency, 2018b). Especially, canakinumab injections rate was far lower and varied greatly from one patient to another with injections ranging from every 6 to every 10 weeks. This was probably due to the fact that patients received doses based upon the licensed use of canakinumab (ie CAPS, in whom the standard dose is lower than in the other recurrent autoinflammatory fever syndromes). Indeed the publication of the phase 3 Canakinumab Pivotal Umbrella Study in Three Hereditary Periodic Fevers (CLUSTER) study (De Benedetti et al., 2018), defining the standard dose of 150 mg (or 2 mg/kg) every 4 weeks, occurred after the end of our study. Nevertheless it is a striking finding that in a real-life setting, lower doses than the anticipated standard dose seem sufficient to control the disease. Moreover it seems to show that the need for IL1 inhibitors is not uniform: while 100% of patients with crFMF responded to low doses of interleukin 1 inhibition, patients with MKD required overall higher doses, with a need of intensified doses observed only in this group. TRAPS patients seem to display an intermediate profile of interleukin 1 thresholds, with more various needs of the level of IL-1 inhibition to control the disease. Thus results show that the optimal dosage for properly treating any of these diseases is not yet fully defined.

The other main reason for lower dosages was an on-demand treatment strategy in FMF and TRAPS patients. An on-demand

strategy was previously described only in 3 studies with anakinra (Bodar et al., 2011; Grimwood et al., 2015; Babaoglu et al., 2019). In a real life setting, this strategy seems to be a realistic treatment option for selected patients (equally well with anakinra than canakinumab), as 5 out of 7 patients still received an on-demand regimen at the end of the study period. Both patients not responding to an on demand treatment with anakinra switched to a maintenance therapy with canakinumab with – according to the including physician – a good response.

The global incidence rate of adverse events in our study was slightly higher than in an Italian study (17.1 per 100 patient/years in our study vs. 8.4 in the Italian study) (Sota et al., 2018), but only already known side effects were described by the participating physicians (**Table 2**), with mainly–as anticipated-infectious complications (~11 per 100 patient/years). Most adverse events were considered to be mild and could be managed with minimal treatment modifications. No death, no neoplasm, no *tuberculosis* infection or reactivation, nor opportunistic infections were reported in our study. Our observations are comforting about the safety profile of IL1 inhibitors in HRFs and support the hypothesis that severe adverse events with IL1 inhibitors are preferentially related to the underlying diseases requiring IL1 inhibition and to the poor general clinical condition, rather than to an actual effect of IL-1 blockade (Sota et al., 2018).

We show a far better drug retention for canakinumab than for anakinra, whereas side effects seemed equally frequent in both groups. Our hypothesis is that the ease of treatment may be the most important point for treatment persistence in patients. It is worth noting, that during the scheduled switch from anakinra to canakinumab, none of the attending physicians pointed out that anakinra was not sufficiently effective to justify changing the medication. Similarly, patients with on-demand anakinra therapy with inadequate disease control switched directly to canakinumab–and not daily anakinra - maintenance therapy. These observations suggest that the ease of treatment is also a major argument guiding the choice of the drug for the prescribing physician.

The major flaw of our study is that due to the retrospective design of our study; we were not able to retrieve a standardized disease activity score and consequently we were not able to link the disease activity of the patients to their treatment regimens. However we consider that we can infer the control of disease activity indirectly by assuming that the adaptations of therapies decided by the investigating physician were made because of criteria related to the severity and the control of the disease. The observed highly variable treatment regimens, ranging from on demand treatment regimens to intensified dosage maintenance therapies, reflects in our opinion that in daily life the investigating physicians adapts drug dosages as closely as possible to disease activity. This is all the more true since our study took place before the French marketing authorization for IL1-inhibitors in HRFs, at a time when dosages had not yet been standardized by the SCP.

A second bias of our study concerns the heterogeneity of our sample, particularly concerning pathologies. However, this heterogeneity also highlighted that individual treatment needs are highly variable. Future studies should focus on identifying and refining the parameters underpinning the treat-to-target strategy practiced in HRFs.

Key Messages

- IL-1 inhibitors are a good treatment option for patients with a hereditary recurrent fever syndrome.
- The individual need of the dosage of IL-1 inhibitors to control the disease effectively seems highly variable, with about 45% of patients responding well to low dosages of IL-1 inhibitors.
- On-demand treatment with a short half-life IL-1 inhibitor may be a treatment option for some selected patients with a recurrent hereditary fever syndrome.

DATA AVAILABILITY STATEMENT

The raw data supporting the conclusions of this article will be made available by the authors, without undue reservation.

ETHICS STATEMENT

The studies involving human participants were reviewed and approved by French Ethic Committee (CCTIRS). Patients were enrolled after comprehensive information checking that they (or their legal guardian) were not opposed to the study and the storage of their personal data.

AUTHOR CONTRIBUTIONS

VH and SG-L were involved in the conception and design of the study. VH, SG-L, IK-P, AB, CG, GG, AC, AP, MH, and PP organized the data base. VH and MD analyzed the data. VH wrote the first draft of the manuscript. All authors contributed to the manuscript revision, read and approved the submitted version.

FUNDING

No specific funding was received from any bodies in the public, commercial or not-for-profit sectors to carry out the work described in this article.

ACKNOWLEDGMENTS

The authors express their sincere thanks to François Hofer for the technical management of the JIR cohort and the help for preparing the data. The authors thank the Fondation Rhumatisme Suisse for hosting the JIR data base.

REFERENCES

Abbara, S., Georgin-Lavialle, S., Stankovic Stojanovic, K., Bachmeyer, C., Senet, P., Buob, D., et al. (2017). Association of hidradenitis suppurativa and familial Mediterranean fever: a case series of 6 patients. *Jt. Bone Spine Rev. Rhum.* 84, 159–162. doi:10.1016/j.jbspin.2016.02.021

Babaoglu, H., Varan, O., Kucuk, H., Atas, N., Satis, H., Salman, R., et al. (2019). On demand use of anakinra for attacks of familial Mediterranean fever (FMF). *Clin. Rheumatol.* 38, 577–581. doi:10.1007/s10067-018-4230-z

Bodar, E. J., Kuijk, L. M., Drenth, J. P. H., van der Meer, J. W. M., Simon, A., and Frenkel, J. (2011). On-demand anakinra treatment is effective in mevalonate kinase deficiency. *Ann. Rheum. Dis.* 70, 2155–2158. doi:10.1136/ard.2011.149922

Cavalli, G., and Dinarello, C. A. (2015). Treating rheumatological diseases and co-morbidities with interleukin-1 blocking therapies. *Rheumatol. Oxf. Engl.* 54, 2134–2144. doi:10.1093/rheumatology/kev269

De Benedetti, F., Gattorno, M., Anton, J., Ben-Chetrit, E., Frenkel, J., Hoffman, H. M., et al. (2018). Canakinumab for the treatment of autoinflammatory recurrent fever syndromes. *N. Engl. J. Med.* 378, 1908–1919. doi:10.1056/NEJMoa1706314

Deshayes, S., Georgin-Lavialle, S., Hot, A., Durel, C-A., Hachulla, E., Rouanes, N., et al. (2018). Efficacy of continuous interleukin 1 blockade in mevalonate kinase deficiency: a multicenter retrospective study in 13 adult patients and literature review. *J. Rheumatol.* 45, 425–429. doi:10.3899/jrheum.170684

European Medicines Agency (2018a). Available at: https://www.ema.europa.eu/en/medicines/human/EPAR/kineret (Accessed April 19, 2020).

European Medicines Agency (2018b). Ilaris: summary of product characteristics. Available at: http://www.ema.europa.eu/docs/en_GB/document_library/EPAR_-_Product_Information/human/001109/WC500031680.pdf (Accessed July 14, 2018).

Gattorno, M., Hofer, M., Federici, S., Vanoni, F., Bovis, F., Aksentijevich, I., et al. (2019). Classification criteria for autoinflammatory recurrent fevers. *Ann. Rheum. Dis.* 78 (8), 1025–1032. doi:10.1136/annrheumdis-2019-215048

Grimwood, C., Despert, V., Jeru, I., and Hentgen, V. (2015). On-demand treatment with anakinra: a treatment option for selected TRAPS patients. *Rheumatol. Oxf. Engl.* 54, 1749–1751. doi:10.1093/rheumatology/kev111

Kone-Paut, I., Quartier, P., Fain, O., Grateau, G., Pillet, P., Le Blay, P., et al. (2017). Real-world experience and impact of canakinumab in cryopyrin-associated periodic syndrome: results from a French observational study. *Arthritis Care Res.* 69, 903–911. doi:10.1002/acr.23083

Laskari, K., Boura, P., Dalekos, G. N., Garyfallos, A., Karokis, D., Pikazis, D., et al. (2017). Longterm beneficial effect of canakinumab in colchicine-resistant familial Mediterranean fever. *J. Rheumatol.* 44, 102–109. doi:10.3899/jrheum.160518

Meinzer, U., Quartier, P., Alexandra, J-F., Hentgen, V., Retornaz, F., and Koné-Paut, I. (2011). Interleukin-1 targeting drugs in familial Mediterranean fever: a case series and a review of the literature. *Semin. Arthritis Rheum.* 41, 265–271. doi:10.1016/j.semarthrit.2010.11.003

Rossi-Semerano, L., Fautrel, B., Wendling, D., Hachulla, E., Galeotti, C., Semerano, L., et al. (2015). Tolerance and efficacy of off-label anti-interleukin-1 treatments in France: a nationwide survey. *Orphanet J. Rare Dis.* 10, 19. doi:10.1186/s13023-015-0228-7

Sota, J., Vitale, A., Insalaco, A., Sfriso, P., Lopalco, G., Emmi, G., et al. (2018). Safety profile of the interleukin-1 inhibitors anakinra and canakinumab in real-life clinical practice: a nationwide multicenter retrospective observational study. *Clin. Rheumatol.* 37 (8), 2233–2240. doi:10.1007/s10067-018-4119-x

Stankovic Stojanovic, K., Delmas, Y., Torres, P. U., Peltier, J., Pelle, G., Jéru, I., et al. (2012). Dramatic beneficial effect of interleukin-1 inhibitor treatment in patients with familial Mediterranean fever complicated with amyloidosis and renal failure. *Nephrol. Dial. Transplant.* 27, 1898–1901. doi:10.1093/ndt/gfr528

Conflict of Interest: VH, IK, GG, MH, and SG-L received personal fees and non-financial support from Novartis and SOBI; CG and AB received non-financial support from Novartis; AP received non-financial support from SOBI.

The remaining authors declare that the research was conducted in the absence of any commercial or financial relationships that could be construed as a potential conflict of interest.

frontiers in Pharmacology

BRIEF RESEARCH REPORT
published: 17 May 2021
doi: 10.3389/fphar.2021.619588

Transcriptional Regulation of Drug Metabolizing CYP Enzymes by Proinflammatory Wnt5A Signaling in Human Coronary Artery Endothelial Cells

Tom Skaria[1,2], *Esther Bachli*[3] *and Gabriele Schoedon*[1]*

[1]Inflammation Research Unit, Division of Internal Medicine, University Hospital Zürich, Zürich, Switzerland, [2]School of Biotechnology, National Institute of Technology Calicut, Kerala, India, [3]Department of Medicine, Uster Hospital, Uster, Switzerland

OPEN ACCESS

Edited by:
Daniel Merk,
Goethe University Frankfurt, Germany

Reviewed by:
Wen-Bin Wu,
Fu Jen Catholic University, Taiwan
Wageh Darwish,
Zagazig University, Egypt

***Correspondence:**
Gabriele Schoedon
klinsog@usz.uzh.ch

Specialty section:
This article was submitted to Inflammation Pharmacology, a section of the journal Frontiers in Pharmacology

Received: 20 October 2020
Accepted: 29 March 2021
Published: 17 May 2021

Citation:
Skaria T, Bachli E and Schoedon G (2021) Transcriptional Regulation of Drug Metabolizing CYP Enzymes by Proinflammatory Wnt5A Signaling in Human Coronary Artery Endothelial Cells. Front. Pharmacol. 12:619588. doi: 10.3389/fphar.2021.619588

Downregulation of drug metabolizing enzymes and transporters by proinflammatory mediators in hepatocytes, enterocytes and renal tubular epithelium is an established mechanism affecting pharmacokinetics. Emerging evidences indicate that vascular endothelial cell expression of drug metabolizing enzymes and transporters may regulate pharmacokinetic pathways in heart to modulate local drug bioavailability and toxicity. However, whether inflammation regulates pharmacokinetic pathways in human cardiac vascular endothelial cells remains largely unknown. The lipid modified protein Wnt5A is emerging as a critical mediator of proinflammatory responses and disease severity in sepsis, hypertension and COVID-19. In the present study, we employed transcriptome profiling and gene ontology analyses to investigate the regulation of expression of drug metabolizing enzymes and transporters by Wnt5A in human coronary artery endothelial cells. Our study shows for the first time that Wnt5A induces the gene expression of CYP1A1 and CYP1B1 enzymes involved in phase I metabolism of a broad spectrum of drugs including chloroquine (the controversial drug for COVID-19) that is known to cause toxicity in myocardium. Further, the upregulation of CYP1A1 and CYP1B1 expression is preserved even during inflammatory crosstalk between Wnt5A and the prototypic proinflammatory IL-1β in human coronary artery endothelial cells. These findings stimulate further studies to test the critical roles of vascular endothelial cell CYP1A1 and CYP1B1, and the potential of vascular-targeted therapy with CYP1A1/CYP1B1 inhibitors in modulating myocardial pharmacokinetics in Wnt5A-associated inflammatory and cardiovascular diseases.

Keywords: inflammation, Wnt5A, transcriptome profiling, pharmacokinetic pathways, cardiac vascular endothelial cells

INTRODUCTION

Inflammation is the first line innate immune response to protect the host from infections or tissue injury. It involves highly coordinated interaction of antigen-activated immune cells and their soluble inflammatory products with vascular endothelial cells, inducing a procoagulant, immune cell adhesive and hyperpermeable phenotype in vascular endothelial cells, followed by the movement of immune cells, soluble inflammatory mediators and other plasma proteins across vascular endothelial cells to the site of infection or injury to minimize tissue damage (Pober and Sessa, 2007). Although an orchestrated inflammatory response is crucial for efficient immunity, uncontrolled or sustained inflammation becomes pathogenic and causes tissue destruction, impairs organ function and affects drug pharmacokinetics (Morgan, 2009; Netea et al., 2017). The importance of deregulated immune defense is obvious even in the current pandemic COVID-19 where, endotheliitis, for example in the heart leads to local thrombosis (Varga et al., 2020). Drug pharmacokinetics is affected when locally produced proinflammatory cytokines enter systemic circulation and exert inflammatory responses in hepatocytes, enterocytes and renal tubular epithelium, which represent the classical sites for action of drug metabolizing enzymes and transporters. It was shown that proinflammatory cytokines such as interleukin (IL)-1β and tumor necrosis factor-α downregulate the transcription of cytochrome P450 (CYP) enzymes involved in phase I oxidative metabolism, and membrane protein drug transporters such as Organic Anion Transporting Polypeptide (OATP)- 1 and 2 in hepatocytes, enterocytes and renal tubular epithelium. This results in decreased hepatic clearance and enhanced oral bioavailability increasing the incidence of adverse events. In case of prodrugs activated by metabolism, decreased activities of CYP enzymes may reduce their therapeutic efficiency (Morgan, 2009; König et al., 2013; Wu and Lin, 2019).

Emerging evidences indicate that cardiac vascular endothelial cell expression of drug and xenobiotic metabolizing enzymes and transporters, involved in local metabolic homeostasis, can also modulate pharmacokinetics in the heart muscle. It is shown that organic cation transporter novel type 2, a sodium dependent transport protein for carnitine, is expressed and localized in normal cardiac endothelial cells. Its cardiac expression regulates cardiac delivery of spironolactone or mildronate during congestive heart failure. High variability in its cardiac expression among individuals is linked to variable response to its substrate drugs in clinical setting (Grube et al., 2006). Similarly, multidrug resistance protein 1 (MDR1), a drug efflux pump, is expressed in normal cardiac endothelial cells, and modulates myocardial uptake of its substrates talinolol and celiprolol. Further, cardiac vascular endothelial expression of MDR1 may mediate inter-individual variability observed for the positive inotropic effects of its another substrate digoxin (Meissner et al., 2002; Hausner et al., 2019). In addition to their effects on drugs, cardiac vascular endothelial expression of drug/xenobiotic metabolizing enzymes and transporters also modulates disease modifying endobiotic transformations. Blocking CYP2C9 activity using sulfaphenazole decreased experimentally induced infarct size and post-ischemic vascular superoxide generation, and enhanced post-ischemic coronary flow (Granville et al., 2004; Hunter et al., 2005; Michaud et al., 2010). All these recent findings clearly reveal a critical role for the intrinsic activity of cardiac vascular endothelial cell-expressed drug metabolizing enzymes and transporters in modulating drug and xenobiotic concentrations in myocardium. However, there has been no study performed yet to investigate whether inflammation that has an established role in affecting pharmacokinetics pathways in hepatocytes, enterocytes and renal tubular epithelium (Morgan, 2009; König et al., 2013; Wu and Lin, 2019), regulates the expression of drug and xenobiotic metabolizing enzymes and transporters in human cardiac vascular endothelial cells. In precision medicine, a comprehensive knowledge of the regulation of pharmacokinetic pathways in vascular endothelial cells by specific inflammatory mediators is crucial for developing vascular-targeted therapy to reduce inter-individual variability in drug response and local and systemic toxicity (Eelen et al., 2015; Fatunde and Brown, 2020; Glassman et al., 2020).

In the present study, we employed whole genome expression profiling to investigate whether Wnt5A, an emerging inflammatory mediator in vascular system (Blumenthal et al., 2006; Pereira et al., 2008; Schulte et al., 2012; Skaria and Schoedon, 2017; Choi et al., 2020), regulates the expression of drug metabolizing enzymes and transporters in immunocompetent, primary, human coronary artery endothelial cells (HCAEC; Skaria et al., 2017; Skaria et al., 2019). In our present study, Wnt5A treatments of HCAEC were conducted for 4 h. We chose 4 h treatment in this study because several previous independent studies established that the effects of Wnt5A are time-dependent in different cell types (Valencia et al., 2014; Shojima et al., 2015; Huang et al., 2017). Here, we find that in HCAEC, Wnt5A critically modulates myocardium-specific pharmacokinetic pathways by upregulating the transcription of CYP enzymes that are known to metabolize a broad spectrum of drugs including those used in immune system and cardiovascular diseases.

MATERIALS AND METHODS

Primary Cell Culture

HCAEC were propagated, and treated with vehicle (sterile, pyrogen free, 0.1% human serum albumin in 0.9% NaCl) and recombinant human/mouse Wnt5A (250 ng/ml, R&D systems) alone or combined with recombinant human IL-1β (20 U/ml, PeproTech) for 4 h as described (Skaria et al., 2017; Skaria et al., 2019) (detailed in **Supplementary Material**). Specific information about vascular endothelial cell characterization is provided in **Supplementary Material**.

Whole Genome Expression Profiling and Gene Ontology Analysis

Differential gene expression profiling using microarray analysis, and scanning, feature extraction, and data normalization of

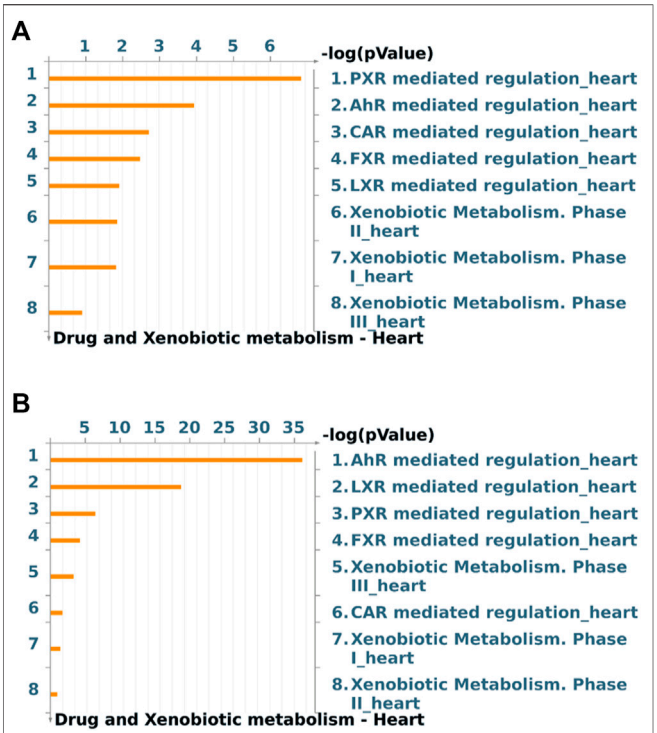

FIGURE 1 | Drug and xenobiotic metabolism pathways most significantly ($p < 0.05$) regulated by 4 h Wnt5A **(A)** and Wnt5A/IL-1β combination **(B)** treatment in HCAEC. Pathways represented as histograms are ranked by the–log value (p value). Data are from 3 independent experiments.

microarrays were performed using established methods (Skaria et al., 2017; Skaria et al., 2019) (detailed in **Supplementary Material**). Complete data sets of Wnt5A and Wnt5A/IL-1β combination transcriptomes in HCAEC are accessible in the NCBI GEO data repository through accession numbers GSE145987 and GSE62281, and GSE146691 respectively (refer **Supplementary Material** for particulars about accession numbers). Linear-lowess normalized microarray data were further analyzed using GeneSpring GX 9.0 Software (Agilent Tech. Inc.), and gene ontology analysis to identify drug and xenobiotic metabolism pathways significantly ($p < 0.05$) enriched in microarray data were performed using MetaCoreTM GeneGO software (Thomson Reuters, http://portal.genego.com) as described (Skaria et al., 2017; Skaria et al., 2019) with modifications (detailed in **Supplementary Material**).

RESULTS

Global gene expression profile of 4 h Wnt5A treated HCAEC was compared with that of vehicle-treated HCAEC by whole human genome microarrays. Genes of Wnt5A-treated HCAEC which are significantly differentially regulated after linear-lowess normalization (refer **Supplementary Material**) and consistently showing at least two-fold change in expression in subsequent GeneSpring analysis compared with vehicle-treated HCAEC were identified (**Supplementary Table S1**) and screened with MetaCoreTM GeneGO software for their involvement in regulating drug and xenobiotic metabolism pathways. PXR mediated regulation_heart, AhR mediated regulation_heart, CAR mediated regulation_heart, FXR mediated regulation_heart, LXR mediated regulation_heart, Xenobiotic Metabolism- phase II_heart, Xenobiotic Metabolism- phase I_heart, and Xenobiotic Metabolism- phase III_heart were the drug and xenobiotic metabolism pathways significantly enriched in 4 h Wnt5A transcriptome of HCAEC (**Figure 1A**). Genes of these statistically significant, enriched pathways upregulated by Wnt5A include those encoding intracellular enzymes CYP1A1 and CYP1B1 involved in phase I oxidation, and the transmembrane peptide SLCO2B1 transporting large hydrophobic organic anions, cations and neutral compounds (**Table 1**). Abundant protein expression of CYP1A1, CYPB1 and SLCO2B1 has been verified in human myocardium (**Table 1**). CYP1A1 is reported to metabolize compounds such as the antiarrhythmic drug amiodarone, antimicrobial erythromycin, antimalarial and immunomodulatory chloroquine (controversial in use against COVID-19 as an agent preventing the entry of SARS-CoV-2 through ACE2 receptor), nonsteroidal anti-inflammatory diclofenac, anti-psychotic haloperidol, steroid hormone estradiol and the chemotherapeutic agent daunorubicin in humans (**Supplementary Table S2**). Chloroquine, with active metabolites and long half-life, can prolong the QT interval that could trigger ventricular arrhythmias including torsades de pointes (Kamp et al., 2020). Haloperidol is still used in treating delirium in septic patients admitted in ICU and is associated with QT interval prolongation (Huffman and Stern, 2003). CYP1B1 metabolizes drugs including the anticancer procarbazine, theophylline and the most prescribed cholesterol lowering drug rosuvastatin in humans (**Supplementary Table S2**). SLCO2B1 can transport drugs such as the leukotriene receptor antagonist montelukast used for asthma, the antirheumatic, immunosuppressive sulfasalazine and a number of drugs acting on the cardiovascular system such as aliskiren, antihypertensive drugs of the sartan group (telmisartan) and a number of cholesterol lowering agents (rosuvastatin, atorvastatin, pravastatin) (**Supplementary Table S2**). Genes of significantly enriched pharmacokinetic pathways downregulated by Wnt5A include UDP-glucuronosyltransferases (UGT)-1A4 and 1A6 (**Table 1**) involved in phase II drug metabolism of drugs such as the anticonvulsant lamotrigine and anti-atherosclerotic/analgesic aspirin respectively (Bigler et al., 2001; Reimers et al., 2016).

During inflammatory diseases such as sepsis and atherosclerosis, vascular endothelial cells may not be exposed to a single inflammatory mediator, rather, different inflammatory mediators such as Wnt5A and the prototypic proinflammatory prothrombotic proatherogenic IL-1β simultaneously act paracrinically on vascular endothelial cells and their crosstalk may modulate inflammatory responses in vascular endothelial cells (Pereira et al., 2008; Bhatt et al., 2012; Schulte et al., 2012; Gatica-Andrades et al., 2017; Skaria and Schoedon, 2017). This prompted us to test whether the regulation of expression of CYP

TABLE 1 | Genes of statistically significant ($p < 0.05$) drug and xenobiotic metabolism pathways regulated by 4 h Wnt5A treatment in HCAEC. Data are from 3 independent array experiments.

Gene symbol	Protein name	Class	Regulation
CCNC[a,b,c,e,i]	Cyclin C	Generic binding protein	Down
CEACAM3[b,i]	Carcinoembryonic antigen-related cell adhesion molecule 3	Generic protein	Down
CHI3L1[b,e,i]	Chitinase-3-like protein 1	Generic enzyme	Down
CYP1A1[a,b,c,g,i]	Cytochrome P450 1A1	Generic enzyme	Up
CYP1B1[b,e,g,i]	Cytochrome P450 1B1	Generic enzyme	Up
DCHS2[b]	Protocadherin-23	Generic binding protein	Down
EDNRA[a,b,e,i]	Endothelin-1 receptor	G protein-coupled receptor	Up
EDNRB[a,b,e,i]	Endothelin receptor type B	G protein-coupled receptor	Down
GNAO1[b,i]	Guanine nucleotide-binding protein G(o) subunit alpha	G-alpha	Down
HNF4A[a,d]	Hepatocyte nuclear factor 4-alpha	Transcription factor	Down
IGF2[a,i]	Insulin-like growth factor II	Receptor ligand	Down
IL2[b]	Interleukin-2	Receptor ligand	Down
ITGA4[b,i]	Integrin alpha-4	Generic receptor	Up
ITGB6[b]	Integrin beta-6	Generic receptor	Down
KCTD12[b,e,i]	BTB/POZ domain-containing protein KCTD12	Voltage-gated ion-channel	Up
KLK12[c,e]	Kallikrein-12	Generic protease	Down
LILRB4[e,i]	Leukocyte immunoglobulin-like receptor subfamily B member 4	Generic receptor	Down
MS4A2[e,i]	High affinity immunoglobulin epsilon receptor subunit beta	Generic receptor	Up
NDUFS7[b,e,i]	NADH dehydrogenase [ubiquinone] iron-sulfur protein 7, mitochondrial	Generic enzyme	Down
OR4C16[a]	Olfactory receptor 4C16	G protein-coupled receptor	Down
OR4D2[a]	Olfactory receptor 4D2	G protein-coupled receptor	Down
OR4F4[a]	Olfactory receptor 4F4	G protein-coupled receptor	Down
OR6Y1[a]	Olfactory receptor 6Y1	G protein-coupled receptor	Up
OR8J1[a]	Olfactory receptor 8J1	G protein-coupled receptor	Up
OR9G4[a]	Olfactory receptor 9G4	G protein-coupled receptor	Down
PSG5[b]	Pregnancy-specific beta-1-glycoprotein 5	Generic protein	Up
SLC16A2[h,i]	Monocarboxylate transporter 8	Transporter	Up
SLCO2B1[a,b,e,h,i]	Solute carrier organic anion transporter family member 2B1	Transporter	Up
SYT6[b]	Synaptotagmin-6	Generic receptor	Down
TCTN3[b,i]	Tectonic-3	Generic protein	Down
TFAP2D[d]	Transcription factor AP-2-delta	Transcription factor	Down
TIMP1[d,e,i]	Metalloproteinase inhibitor 1	Generic binding protein	Down
UGT1A4[a,b,c,d,f]	UDP-glucuronosyltransferase 1-4	Generic enzyme	Down
UGT1A6[a,b,c,d,f]	UDP-glucuronosyltransferase 1-6	Generic enzyme	Down

[a]*Genes regulated in PXR mediated regulation_heart.*
[b]*Genes regulated in AhR mediated regulation_heart.*
[c]*Genes regulated in CAR mediated regulation_heart.*
[d]*Genes regulated in FXR mediated regulation_heart.*
[e]*Genes regulated in LXR mediated regulation_heart.*
[f]*Genes regulated in Xenobiotic Metabolism. Phase II_heart.*
[g]*Genes regulated in Xenobiotic Metabolism. Phase I_heart.*
[h]*Genes regulated in Xenobiotic Metabolism. Phase III_heart.*
[i]*Protein expression verified in normal human myocardium as shown in The Human Protein Atlas (accessed on 03.08.2020).*

enzymes, known to metabolize broad spectrum of drug substrates (**Supplementary Table S2**) and found regulated by sole Wnt5A treatment in this study (**Table 1**; **Supplementary Table S1**), is preserved during crosstalk between Wnt5A and IL-1β in HCAEC. CYP1A1 and CYP1B1 remained upregulated by Wnt5A/IL-1β combination treatment in HCAEC (**Supplementary Tables S3, S4**). Further, Wnt5A/IL-1β signaling interaction upregulated the gene encoding an additional member of CYP enzyme family CYP7A1 (**Supplementary Tables S3, S4**). Protein expression of CYP7A1 has been verified in normal human myocardium (**Supplementary Table S4**), however its substrates in humans remain largely unidentified. Moreover, Wnt5A/IL-1β combination treatment significantly enhanced enrichment of genes in AhR mediated regulation_heart and LXR mediated regulation_heart pharmacokinetic pathways in HCAEC compared with Wnt5A or IL-1β alone treatments (**Figure 1B**; **Supplementary Figure S1**; **Supplementary Table S4**).

DISCUSSION

Transcriptional downregulation of expression of drug metabolizing enzymes and transporters by the systemic action of proinflammatory mediators in hepatocytes, enterocytes and renal tubular epithelium is an established mechanism affecting pharmacokinetics during inflammation (Morgan, 2009; Wu and Lin, 2019). Additionally, increasing evidences indicate that vascular endothelial expression of drug metabolizing enzymes and transporters may regulate pharmacokinetic pathways in

heart to modulate local drug bioavailability and toxicity in humans (Meissner et al., 2002; Grube et al., 2006; Hausner et al., 2019). However, whether inflammatory activation regulates pharmacokinetic pathways in human cardiac vascular endothelial cells remained largely unknown. This study investigated for the first time the regulation of expression of drug metabolizing enzymes and transporters by proinflammatory mediator Wnt5A in human coronary artery endothelial cells. It reveals that Wnt5A upregulates the mRNA expression of CYP1A1 and CYP1B1; enzymes with known role in phase I metabolism of a broad of spectrum of drugs and their protein expression established in human myocardium. Further, it reveals that upregulated CYP1A1 and CYP1B1 expression is preserved during inflammatory crosstalk between Wnt5A and proinflammatory IL-1β in human coronary artery endothelial cells. This novel finding from human vascular endothelial cells isolated from coronary artery, a primary cell system retaining original tissue characteristics (Franscini et al., 2004; Skaria et al., 2017; Skaria et al., 2019), is in accordance with previous findings that proinflammatory cytokines, in contrast to their suppressive effects on drug metabolizing pathways in hepatocytes (Morgan, 2009; Wu and Lin, 2019), stimulate the transcription of CYP enzymes in extrahepatic cell systems (Smerdová et al., 2014; Alhouayek et al., 2018).

Previous studies showed that CYP1A1, involved in transformation of xenobiotics to toxic metabolites, also metabolizes a broad spectrum of drugs and consequently account for drugs' adverse effects. CYP1A1 metabolizes the class III antiarrhythmic drug amiodarone to desethyl amiodarone, the latter causes toxicity in multiple organs (Wu et al., 2016). Another substrate of CYP1A1 is the macrolide erythromycin used as an antiinfection agent or for gastrointestinal disease in ICUs (Zhou et al., 2019). Overexpression of CYP1A1 by Wnt5A may enhance erythromycin's metabolism and thus affects its half-life leading to the persistence of infection and lack of drug efficiency. Likewise, enhanced CYP1A1 activity may increase the clearance of theophylline used in treatment of obstructive pulmonary disease (Sarkar and Jackson, 1994). In pathological states such as sepsis, cardiac arrhythmia associated with hypertension and chronic obstructive lung diseases, Wnt5A signaling is activated in the cardiovascular system (Pereira et al., 2008; Schulte et al., 2012; Daud et al., 2016; Abraityte et al., 2017a; Baarsma et al., 2017; Abraityte et al., 2017b). This stimulates further investigations to determine whether circulating Wnt5A concentration correlates with myocardial CYP1A1/CYP1B1 activity, drug availability and cardiotoxicity in these diseases.

A previous study showed transcriptional downregulation of CYP1B1 and upregulation of CYP1A1 in endothelial cells with homozygous null mutation of the β-catenin gene, isolated from E9.5 embryos (Ziegler et al., 2016). Several independent, previous studies established that endothelial cells derived from embryo exhibit high plasticity and therefore significantly differs in morphology and in response to signaling molecules compared with adult human vascular endothelial cells (Risau, 1995; Invernici et al., 2005; Földes et al., 2010). Accordingly, the aforesaid study involving endothelial cells from E9.5 embryos additionally demonstrated upregulation of CYP1B1 and unaltered expression of CYP1A1 in response to canonical Wnt3A conditioned medium by mouse brain microvascular endothelial cells. Furthermore, the aforesaid study showed that mouse brain microvascular endothelial cells respond to non-canonical Wnt5A-conditioned medium by decreasing CYP1B1 transcription (Ziegler et al., 2016). As the above study itself and several other previous studies proved, Wnt ligands regulate multiple signaling pathways depending on the availability of specific receptors and other mediators of the signaling pathway, cellular conditions, and the presence of natural inhibitors like sFRP and WIF1 (Pukrop and Binder, 2008; Kikuchi et al., 2012; Ziegler et al., 2016). In this manuscript, we show the transcriptional upregulation of CYP1A1 and CYP1B1 by exogenous Wnt5A in primary, coronary artery endothelial cells derived from adult human myocardium. Primary, coronary artery endothelial cells derived from adult human myocardium was chosen in this study to assess how Wnt5A regulates the drug metabolizing potential of myocardial vasculature because it is well established that vascular endothelial cells from different anatomical locations like brain and heart significantly differ in their response to signaling molecules (Aird, 2007).

In precision medicine, therapeutically modulating a specific characteristic of inflamed vascular endothelial cells by vascular-targeted nanocarriers is a potential strategy to reduce inter-individual variability in drug response and local toxicity (Eelen et al., 2015; Glassman et al., 2020). Therefore, targeting vascular endothelial CYP1A1 and CYP1B1 by their inhibitors loaded in nanocarriers conjugated with affinity ligands of inflamed endothelial markers may be a potential strategy to modulate myocardial pharmacokinetics of CYP1A1 and CYPB1 substrates in diseases associated with Wnt5A. Further, a precise knowledge on the regulation of pharmacokinetic pathways by specific inflammatory mediators may enable adapting drug dosage regimens according to the changes in inflammatory status of patients (Morgan, 2009) as has been postulated even in the case of emerging COVID-19 pandemic (El-Ghiaty et al., 2020). Most interesting in the latter context is the fact that medication proposed to target ACE2 (Wang et al., 2020) are metabolized through CYP1A1, and our observation that CYP1A1 but not ACE2 expression, is a target for transcriptional modulation by Wnt5A. Most recently, Wnt5A has been found significantly elevated in severe cases of COVID-19 (Choi et al., 2020), and endotheliitis was observed as major pathology in severe COVID-19 (Varga et al., 2020). Therefore, while targeting ACE2 with drugs that are substrates for CYP1A1, the modulation of those drugs' pharmacokinetics by Wnt5A-inflamed cardiac vascular endothelial cells might occur and must be a focus of future studies. Drug metabolizing enzymes and transporters are also transcriptionally regulated by the xenobiotic receptors (XR) such as constitutive androstane receptor (CAR), the pregnane X receptor (PXR) and the aryl hydrocarbon receptor (AhR), which are mainly expressed in the liver

(Mackowiak and Wang, 2016). It is noteworthy that their expression has been reported in vascular endothelial cells (Agbor et al., 2011). Therefore, whether their activation by endogenous compounds and drugs or xenobiotics transcriptionally regulate the phase I and phase II metabolizing enzymes or drug transporters in vascular endothelial cells during inflammation warrants further investigations. Moreover, in light of emerging evidences indicating that cytokine signaling pathways activate XR even in the absence of their xenobiotic activators (Mackowiak and Wang, 2016), the ability of Wnt5A/IL-1 signaling pathways to mediate XR activation in the absence of drugs/metabolites in pathological states needs to be further investigated.

In conclusion, this study shows for the first time that the proinflammatory mediator Wnt5A upregulates human coronary artery endothelial expression of CYP1A1 and CYP1B1 enzymes involved in phase I metabolism of a broad spectrum of drugs. Upregulated CYP1A1 and CYP1B1 expression is preserved during inflammatory crosstalk between Wnt5A and proinflammatory IL-1β in human coronary artery endothelial cells. These preliminary findings presented in this brief research report stimulate further studies on the critical roles of drug metabolizing potential of Wnt5A-inflamed adult human myocardial vasculature and the therapeutic benefits of vascular-targeted inhibitors of CYP1A1/CYP1B1 in modulating myocardial pharmacokinetics in Wnt5A-associated inflammatory diseases.

DATA AVAILABILITY STATEMENT

The datasets presented in this study can be found in online repositories. The names of the repository/repositories and accession number(s) can be found in the article/ **Supplementary Material**.

AUTHOR CONTRIBUTIONS

TS, EB and GS conceived and designed the research. TS performed the experiments. TS and GS analyzed the data. TS, GS and EB wrote the manuscript. All authors read and approved the final manuscript.

FUNDING

This study was supported by the Swiss National Science Foundation No. 31-124861 to Gabriele Schoedon.

SUPPLEMENTARY MATERIAL

The Supplementary Material for this article can be found online at: https://www.frontiersin.org/articles/10.3389/fphar.2021.619588/full#supplementary-material.

REFERENCES

Abraityte, A., Lunde, I. G., Askevold, E. T., Michelsen, A. E., Christensen, G., Aukrust, P., et al. (2017a). Wnt5a is associated with right ventricular dysfunction and adverse outcome in dilated cardiomyopathy. *Sci. Rep.* 7, 3490. doi:10.1038/s41598-017-03625-9

Abraityte, A., Vinge, L. E., Askevold, E. T., Lekva, T., Michelsen, A. E., Ranheim, T., et al. (2017b). Wnt5a is elevated in heart failure and affects cardiac fibroblast function. *J. Mol. Med.* 95, 767–777. doi:10.1007/s00109-017-1529-1

Agbor, L. N., Elased, K. M., and Walker, M. K. (2011). Endothelial cell-specific aryl hydrocarbon receptor knockout mice exhibit hypotension mediated, in part, by an attenuated angiotensin II responsiveness. *Biochem. Pharmacol.* 82, 514–523. doi:10.1016/j.bcp.2011.06.011

Aird, W. C. (2007). Phenotypic heterogeneity of the endothelium. *Circ. Res.* 100, 158–173. doi:10.1161/01.res.0000255691.76142.4a

Alhouayek, M., Gouveia-Figueira, S., Hammarström, M.-L., and Fowler, C. J. (2018). Involvement of CYP1B1 in interferon γ-induced alterations of epithelial barrier integrity. *Br. J. Pharmacol.* 175, 877–890. doi:10.1111/bph.14122

Baarsma, H. A., Skronska-Wasek, W., Mutze, K., Ciolek, F., Wagner, D. E., John-Schuster, G., et al. (2017). Noncanonical WNT-5A signaling impairs endogenous lung repair in COPD. *J. Exp. Med.* 214, 143–163. doi:10.1084/jem.20160675

Bhatt, P. M., Lewis, C. J., House, D. L., Keller, C. M., Kohn, L. D., Silver, M. J., et al. (2012). Increased Wnt5a mRNA expression in advanced atherosclerotic lesions, and oxidized LDL treated human monocyte-derived macrophages. *Open Circ. Vasc. J.* 5, 1–7. doi:10.2174/1877382601205010001

Bigler, J., Whitton, J., Lampe, J. W., Fosdick, L., Bostick, R. M., and Potter, J. D. (2001). CYP2C9 and UGT1A6 genotypes modulate the protective effect of aspirin on colon adenoma risk. *Cancer Res.* 61, 3566–3569.

Blumenthal, A., Ehlers, S., Lauber, J., Buer, J., Lange, C., Goldmann, T., et al. (2006). The Wingless homolog WNT5A and its receptor Frizzled-5 regulate inflammatory responses of human mononuclear cells induced by microbial stimulation. *Blood* 108, 965–973. doi:10.1182/blood-2005-12-5046

Choi, E. Y., Park, H. H., Kim, H., Kim, H. N., Kim, I., Jeon, S., et al. (2020). Wnt5a and Wnt11 as acute respiratory distress syndrome biomarkers for SARS-CoV-2 patients. *Eur. Respir. J.* 56, 2001531. doi:10.1183/13993003.01531-2020

Daud, T., Parmar, A., Sutcliffe, A., Choy, D., Arron, J., Amrani, Y., et al. (2016). The role of WNT5a in Th17 asthma. *Eur. Respir. J.* 48, PA3416. doi:10.1183/13993003

Eelen, G., De Zeeuw, P., Simons, M., and Carmeliet, P. (2015). Endothelial cell metabolism in normal and diseased vasculature. *Circ. Res.* 116, 1231–1244. doi:10.1161/circresaha.116.302855

El-Ghiaty, M. A., Shoieb, S. M., and El-Kadi, A. O. S. (2020). Cytochrome P450-mediated drug interactions in COVID-19 patients: current findings and possible mechanisms. *Med. Hypotheses* 144, 110033. doi:10.1016/j.mehy.2020.110033

Fatunde, O. A., and Brown, S. A. (2020). The role of CYP450 drug metabolism in precision cardio-oncology. *Int. J. Mol. Sci.* 21. doi:10.3390/ijms21020604

Földes, G., Liu, A., Badiger, R., Paul-Clark, M., Moreno, L., Lendvai, Z., et al. (2010). Innate immunity in human embryonic stem cells: comparison with adult human endothelial cells. *PLoS One* 5, e10501. doi:10.1371/journal.pone.0010501

Franscini, N., Bachli, E. B., Blau, N., Leikauf, M.-S., Schaffner, A., and Schoedon, G. (2004). Gene expression profiling of inflamed human endothelial cells and influence of activated protein C. *Circulation* 110, 2903–2909. doi:10.1161/01.cir.0000146344.49689.bb

Gatica-Andrades, M., Vagenas, D., Kling, J., Nguyen, T. T. K., Benham, H., Thomas, R., et al. (2017). WNT ligands contribute to the immune response during septic shock and amplify endotoxemia-driven inflammation in mice. *Blood Adv.* 1, 1274–1286. doi:10.1182/bloodadvances.2017006163

Glassman, P. M., Myerson, J. W., Ferguson, L. T., Kiseleva, R. Y., Shuvaev, V. V., Brenner, J. S., et al. (2020). Targeting drug delivery in the vascular system: focus on endothelium. *Adv. Drug Deliv. Rev.* 157, 96–117. doi:10.1016/j.addr.2020.06.013

Granville, D. J., Tashakkor, B., Takeuchi, C., Gustafsson, A. B., Huang, C., Sayen, M. R., et al. (2004). Reduction of ischemia and reperfusion-induced myocardial damage by cytochrome P450 inhibitors. *Proc. Natl. Acad. Sci.* 101, 1321–1326. doi:10.1073/pnas.0308185100

Grube, M., Meyer Zu Schwabedissen, H. E. U., Präger, D., Haney, J., Möritz, K.-U., Meissner, K., et al. (2006). Uptake of cardiovascular drugs into the human heart. *Circulation* 113, 1114–1122. doi:10.1161/circulationaha.105.586107

Hausner, E. A., Elmore, S. A., and Yang, X. (2019). Overview of the components of cardiac metabolism. *Drug Metab. Dispos* 47, 673–688. doi:10.1124/dmd.119.086611

Huang, G., Chubinskaya, S., Liao, W., and Loeser, R. F. (2017). Wnt5a induces catabolic signaling and matrix metalloproteinase production in human articular chondrocytes. *Osteoarthritis and Cartilage* 25, 1505–1515. doi:10.1016/j.joca.2017.05.018

Huffman, J. C., and Stern, T. A. (2003). QTc prolongation and the use of antipsychotics: a case discussion. *Prim. Care Companion J. Clin. Psychiatry* 05, 278–281. doi:10.4088/pcc.v05n0605

Hunter, A. L., Bai, N., Laher, I., and Granville, D. J. (2005). Cytochrome p450 2C inhibition reduces post-ischemic vascular dysfunction. *Vasc. Pharmacol.* 43, 213–219. doi:10.1016/j.vph.2005.07.005

Invernici, G., Ponti, D., Corsini, E., Cristini, S., Frigerio, S., Colombo, A., et al. (2005). Human microvascular endothelial cells from different fetal organs demonstrate organ-specific CAM expression. *Exp. Cel Res.* 308, 273–282. doi:10.1016/j.yexcr.2005.04.033

Kamp, T. J., Hamdan, M. H., and January, C. T. (2020). Chloroquine or hydroxychloroquine for COVID-19: is cardiotoxicity a concern?. *J. Am. Heart Assoc.* 9, e016887. doi:10.1161/JAHA.120.016887

Kikuchi, A., Yamamoto, H., Sato, A., and Matsumoto, S. (2012). Wnt5a: its signalling, functions and implication in diseases. *Acta Physiol. (Oxf)* 204, 17–33. doi:10.1111/j.1748-1716.2011.02294.x

König, J., Müller, F., and Fromm, M. F. (2013). Transporters and drug-drug interactions: important determinants of drug disposition and effects. *Pharmacol. Rev.* 65, 944–966. doi:10.1124/pr.113.007518

Mackowiak, B., and Wang, H. (2016). Mechanisms of xenobiotic receptor activation: direct vs. indirect. *Biochim. Biophys. Acta (Bba) - Gene Regul. Mech.* 1859, 1130–1140. doi:10.1016/j.bbagrm.2016.02.006

Meissner, K., Sperker, B., Karsten, C., zu Schwabedissen, H. M., Seeland, U., Böhm, M., et al. (2002). Expression and localization of P-glycoprotein in human heart. *J. Histochem. Cytochem.* 50, 1351–1356. doi:10.1177/002215540205001008

Michaud, V., Frappier, M., Dumas, M. C., and Turgeon, J. (2010). Metabolic activity and mRNA levels of human cardiac CYP450s involved in drug metabolism. *PLoS One* 5, e15666. doi:10.1371/journal.pone.0015666

Morgan, E. (2009). Impact of infectious and inflammatory disease on cytochrome P450-mediated drug metabolism and pharmacokinetics. *Clin. Pharmacol. Ther.* 85, 434–438. doi:10.1038/clpt.2008.302

Netea, M. G., Balkwill, F., Chonchol, M., Cominelli, F., Donath, M. Y., Giamarellos-Bourboulis, E. J., et al. (2017). A guiding map for inflammation. *Nat. Immunol.* 18, 826–831. doi:10.1038/ni.3790

Pereira, C., Schaer, D. J., Bachli, E. B., Kurrer, M. O., and Schoedon, G. (2008). Wnt5A/CaMKII signaling contributes to the inflammatory response of macrophages and is a target for the antiinflammatory action of activated protein C and interleukin-10. *Arterioscler. Thromb. Vasc. Biol.* 28, 504–510. doi:10.1161/atvbaha.107.157438

Pober, J. S., and Sessa, W. C. (2007). Evolving functions of endothelial cells in inflammation. *Nat. Rev. Immunol.* 7, 803–815. doi:10.1038/nri2171

Pukrop, T., and Binder, C. (2008). The complex pathways of Wnt 5a in cancer progression. *J. Mol. Med.* 86, 259–266. doi:10.1007/s00109-007-0266-2

Reimers, A., Sjursen, W., Helde, G., and Brodtkorb, E. (2016). Frequencies of UGT1A4*2 (P24T) and *3 (L48V) and their effects on serum concentrations of lamotrigine. *Eur. J. Drug Metab. Pharmacokinet.* 41, 149–155. doi:10.1007/s13318-014-0247-0

Risau, W. (1995). Differentiation of endothelium. *FASEB j.* 9, 926–933. doi:10.1096/fasebj.9.10.7615161

Sarkar, M. A., and Jackson, B. J. (1994). Theophylline N-demethylations as probes for P4501A1 and P4501A2. *Drug Metab. Dispos* 22, 827–834.

Schulte, D. M., Müller, N., Neumann, K., Oberhäuser, F., Faust, M., Güdelhöfer, H., et al. (2012). Pro-inflammatory wnt5a and anti-inflammatory sFRP5 are differentially regulated by nutritional factors in obese human subjects. *PLoS One* 7, e32437. doi:10.1371/journal.pone.0032437

Shojima, K., Sato, A., Hanaki, H., Tsujimoto, I., Nakamura, M., Hattori, K., et al. (2015). Wnt5a promotes cancer cell invasion and proliferation by receptor-mediated endocytosis-dependent and -independent mechanisms, respectively. *Sci. Rep.* 5, 8042. doi:10.1038/srep08042

Skaria, T., Bachli, E., and Schoedon, G. (2019). Gene ontology analysis for drug targets of the whole genome transcriptome of human vascular endothelial cells in response to proinflammatory IL-1. *Front. Pharmacol.* 10. doi:10.3389/fphar.2019.00414

Skaria, T., Bachli, E., and Schoedon, G. (2017). Wnt5A/Ryk signaling critically affects barrier function in human vascular endothelial cells. *Cell Adhes. Migration* 11, 24–38. doi:10.1080/19336918.2016.1178449

Skaria, T., and Schoedon, G. (2017). Inflammatory Wnt5A signalling pathways affecting barrier function of human vascular endothelial cells. *J. Inflamm. (Lond)* 14, 15. doi:10.1186/s12950-017-0163-6

Smerdová, L., Šmerdová, J., Kabátková, M., Kohoutek, J., Blažek, D., Machala, M., et al. (2014). Upregulation of CYP1B1 expression by inflammatory cytokines is mediated by the p38 MAP kinase signal transduction pathway. *Carcinogenesis* 35, 2534–2543. doi:10.1093/carcin/bgu190

Valencia, J., Martínez, V. G., Hidalgo, L., Hernández-López, C., Canseco, N. M., Vicente, Á., et al. (2014). Wnt5a signaling increases IL-12 secretion by human dendritic cells and enhances IFN-γ production by CD4+ T cells. *Immunol. Lett.* 162, 188–199. doi:10.1016/j.imlet.2014.08.015

Varga, Z., Flammer, A. J., Steiger, P., Haberecker, M., Andermatt, R., Zinkernagel, A. S., et al. (2020). Endothelial cell infection and endotheliitis in COVID-19. *The Lancet* 395, 1417–1418. doi:10.1016/s0140-6736(20)30937-5

Wang, N., Han, S., Liu, R., Meng, L., He, H., Zhang, Y., et al. (2020). Chloroquine and hydroxychloroquine as ACE2 blockers to inhibit viropexis of 2019-nCoV Spike pseudotyped virus. *Phytomedicine* 79, 153333. doi:10.1016/j.phymed.2020.153333

Wu, K.-C., and Lin, C.-J. (2019). The regulation of drug-metabolizing enzymes and membrane transporters by inflammation: evidences in inflammatory diseases and age-related disorders. *J. Food Drug Anal.* 27, 48–59. doi:10.1016/j.jfda.2018.11.005

Wu, Q., Ning, B., Xuan, J., Ren, Z., Guo, L., and Bryant, M. S. (2016). The role of CYP 3A4 and 1A1 in amiodarone-induced hepatocellular toxicity. *Toxicol. Lett.* 253, 55–62. doi:10.1016/j.toxlet.2016.04.016

Zhou, X., Su, L.-X., Zhang, J.-H., Liu, D.-W., and Long, Y. (2019). Rules of anti-infection therapy for sepsis and septic shock. *Chin. Med. J. (Engl)* 132, 589–596. doi:10.1097/cm9.0000000000000101

Ziegler, N., Awwad, K., Fisslthaler, B., Reis, M., Devraj, K., Corada, M., et al. (2016). β-Catenin is required for endothelial Cyp1b1 regulation influencing metabolic barrier function. *J. Neurosci.* 36, 8921–8935. doi:10.1523/jneurosci.0148-16.2016

Conflict of Interest: The authors declare that the research was conducted in the absence of any commercial or financial relationships that could be construed as a potential conflict of interest.

frontiers | Frontiers in Pharmacology

TYPE Review
PUBLISHED 27 September 2022
DOI 10.3389/fphar.2022.997403

OPEN ACCESS

EDITED BY
Pallavi R. Devchand,
University of Calgary, Canada

REVIEWED BY
Hong Yong Peh,
Brigham and Women's Hospital and Harvard Medical School, United States
Angelo Sala,
University of Milan, Italy

*CORRESPONDENCE
Michael Holinstat,
mholinst@umich.edu

SPECIALTY SECTION
This article was submitted to Inflammation Pharmacology, a section of the journal Frontiers in Pharmacology

RECEIVED 18 July 2022
ACCEPTED 05 September 2022
PUBLISHED 27 September 2022

CITATION
Yamaguchi A, Botta E and Holinstat M (2022), Eicosanoids in inflammation in the blood and the vessel.
Front. Pharmacol. 13:997403.
doi: 10.3389/fphar.2022.997403

Eicosanoids in inflammation in the blood and the vessel

Adriana Yamaguchi[1], Eliana Botta[1] and Michael Holinstat[1,2]*

[1]Department of Pharmacology, University of Michigan Medical School, Ann Arbor, MI, United States, [2]Department of Internal Medicine, Division of Cardiovascular Medicine, University of Michigan Medical School, Ann Arbor, MI, United States

Polyunsaturated fatty acids (PUFAs) are structural components of membrane phospholipids in cells. PUFAs regulate cellular function through the formation of derived lipid mediators termed eicosanoids. The oxygenation of 20-carbon PUFAs via the oxygenases cyclooxygenases, lipoxygenases, or cytochrome P450, generates a class of classical eicosanoids including prostaglandins, thromboxanes and leukotrienes, and also the more recently identified hydroxy-, hydroperoxy-, epoxy- and oxo-eicosanoids, and the specialized pro-resolving (lipid) mediators. These eicosanoids play a critical role in the regulation of inflammation in the blood and the vessel. While arachidonic acid-derived eicosanoids are extensively studied due to their pro-inflammatory effects and therefore involvement in the pathogenesis of inflammatory diseases such as atherosclerosis, diabetes mellitus, hypertension, and the coronavirus disease 2019; in recent years, several eicosanoids have been reported to attenuate exacerbated inflammatory responses and participate in the resolution of inflammation. This review focused on elucidating the biosynthesis and the mechanistic signaling of eicosanoids in inflammation, as well as the pro-inflammatory and anti-inflammatory effects of these eicosanoids in the blood and the vascular wall.

KEYWORDS

eicosanoids, inflammation, oxygenases, blood, blood vessel

1 Introduction

Eicosanoids are a family of fatty acid metabolites generated from 20-carbon polyunsaturated fatty acids (PUFAs) synthesized by enzymatic oxygenation pathways involving a distinct family of enzymes, the oxygenases (Khanapure et al., 2007). Eicosanoids are not stored, but promptly synthesized *de novo* after cell activation (Bozza et al., 2011) through a highly regulated event, primarily involving three oxygenases: cyclooxygenases (COXs), P450 cytochrome epoxygenases (CYP450), and lipoxygenases (LOXs) (Alvarez and Lorenzetti, 2021). The formed eicosanoids function to regulate a physiological response, including tissue homeostasis, pain, host defense, and inflammation (Esser-von Bieren, 2019). Due to the observed critical role of eicosanoids in physiological and pathological inflammation, they have been implicated in the pathogenesis of major diseases including cardiovascular disease, diabetes mellitus, hypertension, and more recently, the coronavirus disease 2019 (COVID-19) (Wang and Dubois, 2010; Fava and Bonafini, 2018; Hammock et al., 2020; Bosma et al., 2022).

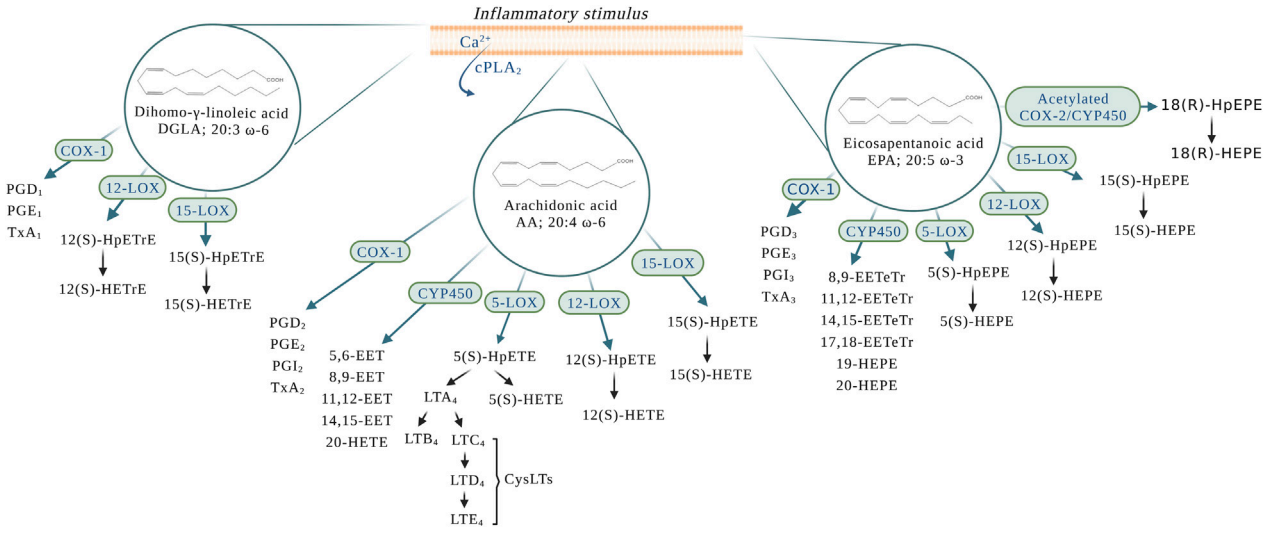

FIGURE 1
Eicosanoid biosynthesis in the blood and the vessel upon an inflammatory stimulus. *AA*: arachidonic acid; *COX-1*: cyclooxygenase-1; *COX-2*: cyclooxygenase-2; *cPLA$_2$*: cytoplasmic phospholipase A$_2$; *CYP450:* P450 cytochrome epoxygenase; *CysLTs:* cysteinyl leukotrienes; *DGLA*: dihomo-γ-linolenic acid; *EPA*: eicosapentaenoic acid; *LTA$_4$*: leukotriene A$_4$; *LTB$_4$*: leukotriene B$_4$; *LTC$_4$*: leukotriene C$_4$; *LTD$_4$*: leukotriene D$_4$; *LTE$_4$*: leukotriene E$_4$; *PGD$_1$*: prostaglandin D$_1$; *PGD$_2$*: prostaglandin D$_2$; *PGD$_3$*: prostaglandin D$_3$; *PGE$_1$*: prostaglandin E$_1$; *PGE$_2$*: prostaglandin E$_2$; *PGE$_3$*: prostaglandin E$_3$; *PGI$_2$*: prostaglandin I$_2$ or prostacyclin; *PGI$_3$*: prostaglandin I$_3$; *TxA$_1$*: thromboxane A$_1$; *TxA$_2$*: thromboxane A$_2$; *TxA$_3$*: thromboxane A$_3$; *5(S)-HEPE*: 5(S)-hydroxyeicosapentaenoic acid; *5(S)-HpEPE*: 5(S)-hydroperoxyeicosapentaenoic acid; *5(S)-HETE:* 5(S)-hydroxyeicosatetraenoic acid; *5(S)-HpETE:* 5(S)-hydroperoxyeicosatetraenoic acid; *5-LOX:* 5-lipoxygenase; *5,6-EET*: 5,6-epoxyeicosatrienoic acid; *8,9-EET*: 8,9-epoxyeicosatrienoic acid; *8,9-EETeTr*: 8,9-epoxyeicosatetraenoic acid; *11,12-EET*: 11,12-epoxyeicosatrienoic acid; *11,12-EETeTr*: 11,12-epoxyeicosatetraenoic acid; *12(S)-HETE: 12*(S)-hydroxyeicosatetraenoic acid; *12(S)-HpETE: 12*(S)-hydroperoxyeicosatetraenoic acid; *12(S)-HETE: 12*(S)-hydroxyeicosatetraenoic acid; *12(S)-HpETE: 12*(S)-hydroperoxyeicosatetraenoic acid; *12(S)-HETrE:* 12(S)-hydroxyeicosatrienoic acid; *12(S)-HpETrE:* 12(S)-hydroperoxyeicosatrienoic acid; *12-LOX:* 12-lipoxygenase; *14,15-EET*: 14,15-epoxyeicosatrienoic acid; *14,15-EETeTr*: 14,15-epoxyeicosatetraenoic acid; *15-LOX:* 15-lipoxygenase; *15(S)-HETE: 15*(S)-hydroxyeicosatetraenoic acid; *15(S)-HpETE: 15*(S)-hydroperoxyeicosatetraenoic acid; *15(S)-HETE: 15*(S)-hydroxyeicosatetraenoic acid; *15(S)-HpETE: 15*(S)-hydroperoxyeicosatetraenoic acid; *15(S)-HETrE:* 15(S)-hydroxyeicosatrienoic acid; *15(S)-HpETrE:* 15(S)-hydroperoxyeicosatrienoic acid; *17,18-EETeTr*: 17,18-epoxyeicosatetraenoic acid; *18(R)HpEPE:* 18(R)-hydroperoxyeicosapentaenoic acid; *18(R)-HEPE:* 18(R)-hydroxyeicosapentaenoic acid; *19-HEPE*: 19-hydroxyeicosapentaenoic acid; *20-HEPE*: 20-hydroxyeicosapentaenoic acid; *20-HETE*: 20-hydroxyeicosatetraenoic acid.

Although eicosanoids are usually associated with pro-inflammatory responses (Aoki and Narumiya, 2012), they are also known to play a key role in reducing inflammation by promoting the resolution of inflammation (Pan et al., 2022), limiting immune cell infiltration, and initiating tissue repair mechanisms (Serhan and Levy, 2018; Díaz Del Campo et al., 2022). This review focuses on the role of eicosanoids on inflammation in the blood and the vascular wall and discusses key discoveries related to the regulatory mechanism of these lipid mediators in inflammation in the blood vessel.

2 Eicosanoid biosynthesis

The superclass of eicosanoids expressed in the blood includes classical eicosanoids, prostaglandins (PGs), leukotrienes (LTs), and thromboxanes (Txs), and the more recently discovered, specialized pro-resolving (lipid) mediators (SPMs), as well as hydroxy-, hydroperoxy-, epoxy-, and oxoeicosanoids (Fahy et al., 2009). The SPMs include lipoxins (LXs), resolvins, protectins (PD), their aspirin-triggered (AT) isomers, and maresins (MaR) (Chiang and Serhan, 2020). One of the best-studied classes of these lipid mediators are the eicosanoids derived from the 20-carbon PUFAs such as eicosapentaenoic acid (EPA; 20:5 ω-3), dihomo-γ-linolenic acid (DGLA; 20:3 ω-6), and arachidonic acid (AA; 20:4 ω-6) (Astarita et al., 2015) (Figure 1), with the last being the most abundant PUFA in the phospholipid of human cell membranes (Sonnweber et al., 2018). Regarding the newly discovered SPMs, LXs are generated from AA, E-series resolvins (RvEs) are synthesized from EPA, and D-series resolvins (RvDs), PDs, and MaRs are formed from docosahexaenoic acid (DHA; 22:6 ω-3) (Calder, 2020a; Chiang and Serhan, 2020) (Figure 2). The initial event of eicosanoid biosynthesis consists of cellular activation which leads to an increased influx of calcium; and subsequently, the translocation of cytoplasmic phospholipase A$_2$ (cPLA$_2$) to the membrane resulting in the cleavage of the PUFA from the *sn*-2 position of the glycerophospholipid (Dennis et al., 2011) to be further oxygenated by respective enzymes. Eicosanoid biosynthesis differs between the type of PUFA being oxidized and the enzymes metabolizing those PUFAs.

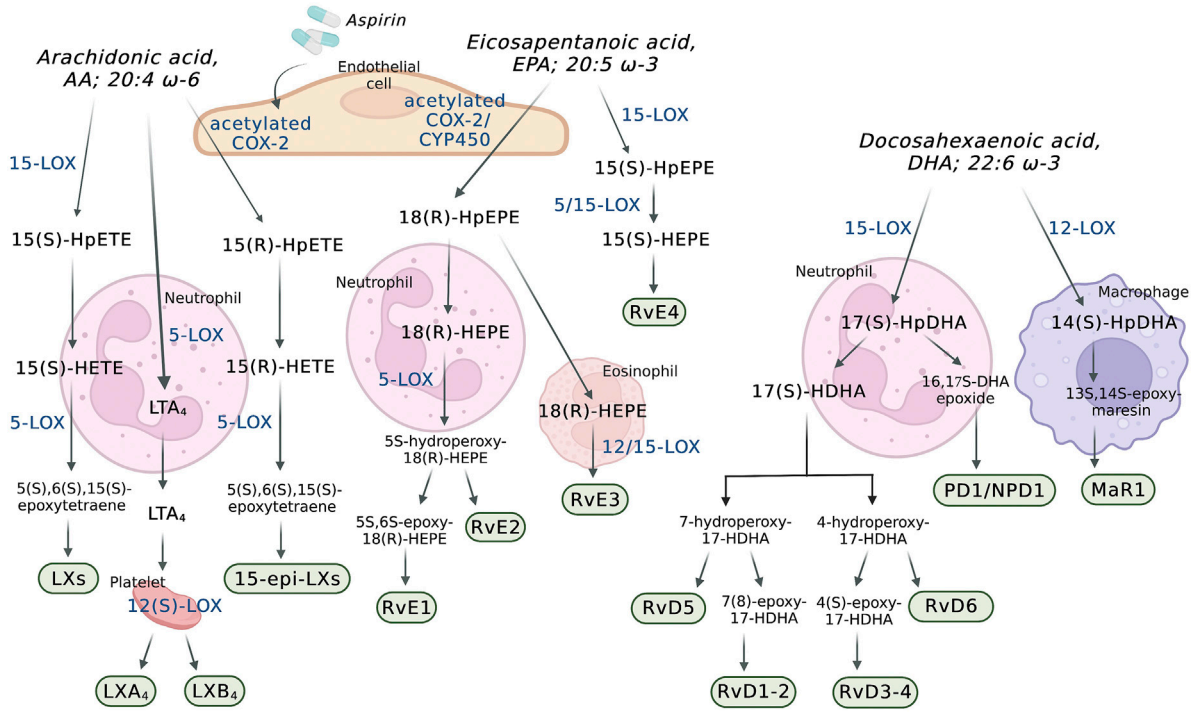

FIGURE 2
Transcellular biosynthesis of eicosanoids in the blood and the vascular wall. *AA*: arachidonic acid; *COX-2:* cyclooxygenase-2; *CYP450:* P450 cytochrome epoxygenase; *DHA:* docosahexaenoic acid; *EPA*: eicosapentaenoic acid; *LTA_4:* leukotriene A_4; *LXs:* lipoxins; *LXA_4:* lipoxin A_4; *LXB_4:* lipoxin B_4; *MaR1:* maresin 1; *PD1/NPD1:* protectin D1/neuroprotectin D1; RvD1-2: resolvin D1-2; RvD3-4: resolvin D3-4; RvD5: resolvin D5; RvD6: resolvin D6; *RvE1:* resolvin E1; *RvE2:* resolvin E2; *RvE3:* resolvin E3; *RvE4:* resolvin E4; *5-LOX:* 5-lipoxygenase; *12(S)-LOX:* 12(S)-lipoxygenase; *14(S)-HpDHA:* 14(S)-hydroperoxydocosahexaenoic acid; *15-LOX:* 15-lipoxygenase; *15(S)-HEPE*: 15(S)-hydroxyeicosapentaenoic acid; *15(S)-HpEPE*: 15(S)-hydroperoxyeicosapentaenoic acid; *15(S)-HETE: 15*(S)-hydroxyeicosatetraenoic acid; *15(S)-HpETE: 15*(S)-hydroperoxyeicosatetraenoic acid; *15-epi-LX_s:* 15-epi-lipoxins; *17(S)-HDHA:* 17(S)-hydroxydocosahexaenoic acid; *17(S)-HpDHA:* 17(S)-hydroperoxydocosahexaenoic acid; *18(R)-HEPE*: 18(R)-hydroxyeicosapentaenoic acid; *18(R)-HpEPE*: 18(R)-hydroperoxyeicosapentaenoic acid.

The freed PUFAs can be oxygenated by several enzymes including COXs, LOXs and CYP450s (Hajeyah et al., 2020) (Figure 1). An alternative biosynthesis pathway forming the AT-isomers can be triggered by aspirin. For example, in the presence of aspirin, AA and EPA form 15(R)-HpETE and 18(R)-HpEPE, respectively (Calder, 2020a) (Figure 2).

2.1 The cyclooxygenase-dependent synthesis

Cyclooxygenases are a widely distributed enzyme in mammalian tissues and exist in two isoforms, COX-1 and COX-2 (Vane et al., 1998). The activation of COX leads to the generation of PGs and Txs, which are collectively named as prostanoids. COX oxygenates AA into series 2 PGs (PGD_2, PGE_2, PGI_2, and TxA_2) (Figure 1). Series 1 PGs (PGD_1, PGE_1, and TxA_1) and series 3 PGs (PGD_3, PGE_3, PGI_3, and TxA_3,) are produced from the oxygenation of DGLA and EPA, respectively (Lagarde et al., 2013; Sergeant et al., 2016) (Figure 1).

In patients taking aspirin, COX-2 is involved in the formation of LXs and RvEs through transcellular biosynthesis (Figure 2). In endothelial cells, aspirin causes an irreversible acetylation of COX-2, which oxygenates AA to form 15(R)-hydroxyeicosatetraenoic acid (15(R)-HETE) and EPA to form 18(R)-hydroxyeicosapentaenoic acid (18(R)-HEPE). While 15(R)-HETE is further used by adherent leukocyte and other endothelial cells to form the 15-epimeric-LXs (15-epi-LXs) (Fu et al., 2020), 18(R)-HEPE is further metabolized into RvE1 and RvE2. It is important to mention that 18(R)-HEPE can also be formed through oxygenation of EPA by CYP450s (Serhan and Petasis, 2011).

2.2 The lipoxygenase-dependent synthesis

Lipoxygenases are a family of nonheme iron-containing enzymes (Kuhn et al., 2015) which are categorized accordingly to their positional specificity of AA oxygenation: 5-LOX, 12-LOX,

and 15-LOX. LOX isozymes are further characterized by tissue expression and stereospecificity (S or R), such as the platelet-type 12-(S)-LOX and the epithelial 12-(R)-LOX (Brash, 1999), as an example. Regarding the expression of LOXs in the blood, 12(S)-LOX is only expressed in platelets and 15-LOX-1 is expressed in eosinophils, monocytes, macrophages, and reticulocytes (Jiang et al., 2006). The expression of 5-LOX is found in myeloid cells including neutrophils, macrophages, monocytes and basophils (Yeung et al., 2017).

The LOXs are able to oxygenate AA to form hydroperoxyeicosatetraenoic acids (HpETEs) (Figure 1), which are rapidly converted to hydroxy derivative HETEs in the blood (Tourdot and Holinstat, 2017). In a similar manner, the LOX-derived eicosanoids from DGLA and EPA are converted to hydroperoxyeicosatrienoic acids (HpETrEs) and hydroperoxyeicosapentaenoic acids (HpEPEs), which are further hydrolyzed to hydroxyeicosatrienoic acids (HETrEs) and hydroxyeicosapentaenoic acids (HEPEs), respectively (Yeung et al., 2017). 5-LOX is best known for its ability to produce LTs (Figure 1). The oxygenation of AA by 5-LOX generates 5(S)-HpETE, which is further converted to the unstable leukotriene A_4 (LTA_4). This intermediate eicosanoid is either converted to the leukotriene B_4 (LTB_4) or leukotriene C4 (LTC_4) in cells that possess LTC_4 synthase activity, such as platelets and endothelial cells, and sequential degradation of the LTC_4 by peptidases forms LTD_4 and LTE_4 (Figure 1). These three products, LTC_4, LTD_4, and LTE_4, are collectively named cysteinyl LTs (cysLTs). The production of cysLTs appears to be restricted to leukocytes, including eosinophils, basophils, and macrophages. However, under inflammatory stimulus, transcellular activity can result in cysLTs formation in endothelial cells (Feinmark and Cannon, 1986). This mechanism favors cells unable to produce LTA_4, such as vascular endothelial cells, platelets and blood peripheral monocytes, to use LTA_4 generated from surrounding cells (such as leukocytes) to produce LTC_4 and the other cysLTs (Colazzo et al., 2017). LTA_4 can also be used by other cells in the blood to form the LXs. Lipoxins A (LXA_4) and B (LXB_4) are formed through a transcellular mechanism between polymorphonuclear leukocytes (PMNs) (5-LOX) and platelets (12(S)-LOX) (Recchiuti and Serhan, 2012). In addition to the transcellular mechanism, lipoxins are synthesized from AA via 15-LOX in neutrophils and monocytes. In these cells, AA is converted to 15(S)-hydroperoxyeicosatetraenoic acid (15(S)-HpETE), which is subsequently converted to lipoxins A and B (Chandrasekharan and Sharma-Walia, 2015) (Figure 2).

The LOXs are also involved in the biosynthesis of others SPMs derived from DHA and EPA. The D-series resolvins 1–6 (RvD1-RvD6) are SPMs derived from the DHA-derived 17(S)-hydroperoxydocosahexaenoic acid (17(S)-HpDHA), which is synthesized through the oxygenation of DHA by 5-LOX in PMNs and macrophages (Serhan and Levy, 2018) (Figure 2). DHA is also a precursor for the maresins (MaR) and protectins. Maresin 1 (MaR1) is generated from the precursor DHA-derived 14(S)-hydroperoxydocosahexaenoic acid (14(S)-HpDHA) and its biosynthesis was first described in human macrophages via 12-LOX-mediated biosynthesis (Serhan et al., 2009). MaR1 is also synthesized during platelet-PMN interactions (Serhan and Levy, 2018). In leukocytes, the biosynthesis of the protectin D1/neuroprotectin D1 (PD1/NPD1) has the DHA-derived 17(S)-HpDHA as the intermediate precursor and it occurs via a 15-LOX-mediated pathway (Serhan et al., 2015; Chiang and Serhan, 2020) (Figure 2). Also in leukocytes, aspirin triggers the biosynthesis of the DHA-derived aspirin-triggered neuroprotection D1/protectin D1 [AT-(NPD1/PD1)] (Serhan et al., 2011a; Serhan et al., 2015). The E-series resolvins 1–4 (RvE1-4) are generated from a common precursor, the EPA-derived 18(R)-hydroxyeicosapentaenoic acid (18(R)-HEPE) (Figure 2). RvE1 and RvE2 are synthesized by PMNs via the 5-LOX pathway, whereas RvE3 is synthesized by eosinophils via the 12/15-LOX pathways (Serhan and Petasis, 2011; Isobe et al., 2012). Currently, the synthesis of RvE4 has only been shown in *in vitro* studies using purified recombinant human 5-LOX and 15-LOX (Serhan and Petasis, 2011; Libreros et al., 2020).

2.3 The cytochrome P450-dependent synthesis

CYP450s belong to a family of heme-containing monooxygenases (Cook et al., 2016) that are known for their role in the metabolism of eicosanoids from PUFAs (Zhao et al., 2021). CYP epoxygenase metabolizes AA into epoxyeicosatrienoic acids (EETs) (Figure 1). Four regioisomeric cis-epoxyeicosatrienoic acids have been described: 5.6-, 8.9-, 11.12-, and 14,15-EET. Upon hydration by soluble epoxide hydrolase (sEH), EETs are rapidly converted to more stable and less biologically active metabolites, dihydroxyeicosatrienoic acids (DHETs) (Spiecker and Liao, 2005). Additionally, members of the CYP4A and CYP4F subfamilies also oxygenate AA to produce 20-hydroxyeicosatetraenoic acid (20-HETE) (Arnold et al., 2010) (Figure 1), which undergoes additional oxidation to 20-hydroxy-prostaglandin G_2 and H_2 (Schwartzman et al., 1989; Kaduce et al., 2004; Hoxha and Zappacosta, 2020). EPA can also be a substrate for CYP450 catalysis. The major CYP450-dependent metabolites derived from EPA include epoxyeicosatetraenoic acids (EETeTrs, 5.6-, 8.9-, 11.12-, and 14,15-EETeTrs), 19- and 20-hydroxyeicosapentaenoic acids (19- and 20-HEPE) (Figure 1).

3 Eicosanoid mode of action

3.1 Prostanoid receptors

PGs exert their biological effects in the blood in an autocrine and paracrine manner by activating their respective cell surface G protein-coupled receptors (GPCRs) (Ricciotti and FitzGerald,

TABLE 1 The signal transduction of the eicosanoid receptors.

Eicosanoid	Receptor Subtype	G-protein coupled	Intracellular signaling
PGE_2	EP1	$G_{\alpha q}$	↑ IP_3, ↑ Ca^{2+}
	EP2	$G_{\alpha s}$	AC activation, ↑ cAMP, PKA activation
	EP3	$G_{\alpha i}$ or $G_{\alpha 12}$	↑ Ca^{2+}, Rho activation
	EP4	$G_{\alpha s}$	AC activation, ↑ cAMP, PKA activation
PGD_2	DP1	$G_{\alpha s}$	AC activation, ↑ cAMP, PKA activation
	DP2 (CRTH/DP2)	$G_{\alpha i}$	↓ cAMP, ↑ Ca^{2+}
$PGF_{2\alpha}$	FP_A, FP_B	$G_{\alpha q}$	↑ IP_3, ↑ Ca^{2+}
		$G_{\alpha 12/13}$	Rho activation
PGI_2	IP	$G_{\alpha s}$	AC activation, ↑ cAMP, PKA activation
TxA_2	TP_α, TP_β	$G_{\alpha q}$	↑ IP_3, ↑ Ca^{2+}
		$G_{\alpha 12/13}$	Rho activation
LTB_4	BLT_1	$G_{\alpha i}$	↑ Ca^{2+}
LTB_4, 12-HHT, HETEs	BLT_2	$G_{\alpha i}$	Phosphorylation of MAPKs and PI3K/Akt, NF-kB activation
LTC_4, LTD_4	$CysLT_1$	$G_{\alpha i/o}$	PLCβ activation, ↑ Ca^{2+}, ERK phosphorylation
	$CysLT_2$	$G_{\alpha q/11}$	PLCβ activation, ↑ IP_3, ↑ Ca^{2+}
EETs	PPARγ	-	NF-κB inhibition, STAT3 activation
12(S)-HETrE	IP	$G_{\alpha s}$	AC activation, ↑ cAMP, PKA activation
12(S)-HETE	GPR31	$G_{\alpha i}$	AC inhibition, Rap1 and p38 activation
20-HETE	GPR75	$G_{\alpha q/11}$	IP_3, ↑ Ca^{2+}, activation of Rho kinase, NF-κB and MAPK/ERK pathway
11(S)-$HpDPA_{\omega\text{-}6}$, 14(S)-$HpDPA_{\omega\text{-}6}$	PPARα	-	PKC inhibition, ↓ Ca^{2+}
RvE1	BLT_1	ND	Phosphorylation of rS6
	ERV1/ChemR23	ND	Phosphorylation of Akt and rS6
RvD1, LXs	ALX/FPR2, **GPR32**	ND	ND
RvD2	GPR18	ND	↑ cAMP, ↑ CREB and STAT3 phosphorylation
RvD5	GPR32	ND	↓ Expression of NF-kB
MaR1	LGR6	ND	↑ CREB and ERK phosphorylation, NF-κB inhibition
PD1/NPD1	GPR37	ND	↑ Ca^{2+}

Note: *AC:* adenylyl cyclase; *Akt:* protein kinase B; *BLT:* leukotriene B_4 receptor; *cAMP:* cyclic adenosine monophosphate; *ALX/FPR2:* formyl peptide receptor 2; *ChemR23:* chemokine-like receptor 1; *CREB:* cAMP-response element binding protein; *CRTH:* chemoattractant receptor-homologous molecule; *CysLT:* cysteinyl leukotriene receptor; *DP:* prostaglandin D receptor; *EETs:* epoxyeicosatrienoic acids; *EP:* E prostanoid receptor; *ERK:* extracellular signal-regulated kinase; *ERV1:* resolvin E1 receptor; *FP:* prostaglandin F receptor; *GPR18:* G-protein coupled receptor 18; *GPR31:* G protein-coupled receptor 31; *GPR32:* G protein-coupled receptor 32; *GPR37:* G protein-coupled receptor 37; *GPR75:* G protein-coupled receptor 75; *HETE:* hydroxyeicosatetraenoic; *IP:* prostacyclin receptor; *IP_3:* inositol triphosphate; *LGR6:* leucine-rich repeat-containing G protein-coupled receptor 6; *LTB_4:* leukotriene B_4; *LTC_4:* leukotriene C_4; *LTD_4:* leukotriene D_4; *LXs:* lipoxins; *MAPK:* mitogen-activated protein kinase; *MaR1:* maresin 1; *ND:* non-determined in cells in the blood or the vessel; *NF-κB:* nuclear factor kappa B; *PD1/NPD1:* protectin D1/neuroprotectin D1; *PGD_2:* prostaglandin D_2; *PGE_2:* prostaglandin E_2; *$PGF_{2\alpha}$:* prostaglandin $F_{2\alpha}$; *PGI_2:* prostaglandin I_2 or prostacyclin; *PI3K:* phosphatidylinositol 3-kinase; *PKA:* protein kinase A; *PKC:* protein kinase C; *PLCβ:* phospholipase Cβ; *PPARα:* peroxisome proliferator-activated receptor α; *PPARγ:* peroxisome proliferator-activated receptor γ; *Rap1:* Ras-related protein 1; *Rho:* Ras homologous; *rS6:* ribosomal protein S6; *RvD1:* resolvin D1; *RvD2:* resolvin D2; *RvD5:* resolvin D5; *RvE1:* resolvin E1; *STAT3:* signal transducer and activator of transcription 3; *TP:* thromboxane receptor; *TxA_2:* thromboxane A_2; *12-HHT:* 12-hydroxyheptadecatrienoic acid; *11(S)-$HpDPA_{\omega\text{-}6}$:* 11(S)-hydroperoxydocosapentaenoic acid; *12(S)-HETrE:* 12(S)-hydroxyeicosatrienoic acid; *12(S)-HETE:* 12(S)-hydroxyeicosatetraenoic acid; *14(S)-$HpDPA_{\omega\text{-}6}$:* 14(S)-hydroperoxydocosapentaenoic acid; *20-HETE:* 20-hydroxyeicosatetraenoic acid.

2011; Biringer, 2021). There are at least eight known prostanoid receptor subfamilies in the blood and the vascular wall (Funk, 2001) (Table 1). Four of the receptor subtypes bind PGE_2, E prostanoid receptor (EP) 1, EP2, EP3, and EP4 in platelets and vascular smooth muscle cells (VSMCs) and two bind PGD_2 (DP1 and DP2) (Aoki and Narumiya, 2012). While $PGF_{2\alpha}$ binds to FP, the PGI_2 and TxA_2 receptors are known as IP and TP, respectively (Wang and Dubois, 2010). The IP is expressed in the endothelium, VSMCs and platelets. There are two isoforms of human TP (TP_α, TP_β) in platelets, vascular smooth muscle cells, and macrophages, and FP (FP_A, FP_B) in VSMCs (Ricciotti and FitzGerald, 2011; Gilroy and Bishop-Bailey, 2019). DP2 is also known as a chemoattractant receptor-homologous molecule (CRTH/DP2) expressed in T helper 2 cells, that responds to PGD_2 but belongs to the family of chemokine receptors (Ricciotti and FitzGerald, 2011; Aoki and Narumiya, 2012).

The prostanoid receptors couple to a range of intracellular signaling pathways that mediate the effects of receptor activation in the cell (Table 1). While EP2, EP4, IP, and DP1 receptors activate adenylyl cyclase (AC) via $G_{\alpha s}$, increasing intracellular cyclic adenosine monophosphate (cAMP) and protein kinase A (PKA) activity, EP1, FP, and

TP activate phosphatidylinositol metabolism via $G_{\alpha q}$, leading to the formation of inositol triphosphate (IP_3) via the mobilization of intracellular free calcium (Ca^{2+}) (Huang et al., 2004a). In addition to signaling through $G_{\alpha q}$, the FP and TP receptors couples to the small G-protein Rho via a $G_{\alpha 12/13}$-dependent mechanism (Ricciotti and FitzGerald, 2011). EP3 isoforms can couple via $G_{\alpha i}$ or $G_{\alpha 12}$ to elevate intracellular Ca^{2+}, inhibit cAMP generation, and activate Rho (Ricciotti and FitzGerald, 2011). The DP2 couples to a $G_{\alpha i}$ to inhibit cAMP synthesis and increase intracellular Ca^{2+} (Schuligoi et al., 2010).

3.2 Leukotriene receptors

There are four known LT receptors subfamilies (Table 1). Two GPCRs are known to be associated with LTB_4, leukotriene B_4 receptor (BLT) BLT_1 and BLT_2. While BLT_1 is known to be expressed on a number of blood cells including leukocytes (Yokomizo et al., 1997), eosinophils (Tager et al., 2000), cluster of differentiation (CD) 4^+ and $CD8^+$ effector T cells (Goodarzi et al., 2003; Tager et al., 2003), dendritic cells (Toda et al., 2010) and macrophages (Serezani et al., 2011), BLT_2 is expressed ubiquitously in leukocytes, with high expression in mononuclear cells, such as $CD8^+$ and $CD4^+$ T-cells, and $CD14^+$ monocytes (Toda et al., 2002). In leukocytes, BLT_1 is coupled to the pertussis toxin-sensitive G protein ($G_{\alpha i}$) and its activation by LTB_4 promotes Ca^{2+} mobilization, leukocyte chemotactic migration and lysosomal release (Goldman et al., 1985). In monocytes, both BLT_1 and BLT_2 have been reported to couple to $G_{\alpha i}$ to induce phosphorylation of mitogen-activated protein kinases (MAPKs) and PI3K/Akt (phosphatidylinositol 3-kinase/protein kinase B, Akt is also known as protein kinase B (PKB)), and nuclear factor-κB (NF-κB) activation (Sánchez-Galán et al., 2009). However, in human umbilical vein endothelial cells (HUVECs) LTB_4 increases HUVEC adhesiveness for polymorphonuclear neutrophils (PMNs) through the increase of intracellular Ca^{2+}, but it does not depend on pertussis toxin-sensitive G proteins (Palmblad et al., 1994). The BLT_2 receptor is considered to be a receptor for several oxidized fatty acids, including 12-hydroxyheptadecatrienoic acid (12-HHT) and hydroxyeicosatetraenoic acids (HETEs) (Yokomizo et al., 2000) and in the blood vessel, BLT_2 is expressed in endothelial cells (Yokomizo et al., 2018).

CysLTs regulate cell function through the cysteinyl leukotriene receptors $CysLT_1$ and $CysLT_2$ (Funk, 2001) (Table 1). $CysLT_1$ is known as a high-affinity receptor for LTD_4, whereas $CysLT_2$ has similar affinity to LTC_4 and LTD_4 (Woszczek et al., 2007). Duah et al. (Duah et al., 2013) has demonstrated that while $CysLT_1$ activation elicits proliferation of endothelial cells via extracellular signal-regulated kinase (ERK) phosphorylation, activation of $CysLT_2$ increases intracellular Ca^{2+} and leads to endothelial cell contraction and barrier disruption via the Rho kinase pathway. Moreover, the *in vitro* activation of $CysLT_1$ by LTD_4 in monocyte/macrophage U937 cells produces second intracellular messengers through phospholipase Cβ (Crooke et al., 1989). LTD_4 induces Ca^{2+} response via the pertussis toxin-sensitive G protein ($G_{\alpha i/o}$) in these cells (Pollock and Creba, 1990; Capra, 2004). In addition, LTC_4 has been shown to activate $CysLT_2$ in mouse platelets *ex vivo* to induce α-granule and TxA_2 secretion (Capra et al., 2003; Cummings et al., 2013). In endothelial cells, $CysLT_2$ couples to $G_{\alpha q/11}$ to activates PLCβ and IP_3 signaling, and increase intracellular Ca^{2+} release, in response to interferon-γ (IFN-γ) stimulation *in vitro* (Woszczek et al., 2007).

3.3 Epoxyeicosatrienoic acid receptors

The CYP-derived epoxyeicosatrienoic acids (EETs) activates peroxisome proliferator-activated receptor γ (PPARγ) in endothelial cells in the presence of an epoxide hydrolase-specific inhibitor (Liu et al., 2005). Additionally, EETs inhibit the NF-κB activation and attenuate the NF-κB-dependent inflammatory responses by reducing cytokine-induced leukocyte adhesion to the vasculature (Node et al., 1999). Some vascular-related actions of the EETs include the activation of the signal transducer and activator of transcription 3 (STAT3) (Table 1). Specifically, 14,15-EET stimulates the tyrosine phosphorylation of STAT3 and its translocation from the cytoplasm to the nucleus to bind to vascular endothelial growth factor (VEGF) promoter in a Src-STAT3 activation signaling-dependent manner, which leads to VEGF expression and angiogenesis (Cheranov et al., 2008).

3.4 Hydroxyeicosanoid receptors

Hydroxyeicosanoids are known to activate cells through a number of mechanisms including activation of GPCRs. The ω-6-derived 12(S)-HETrE inhibits platelet function through selectively binding to the $G_{\alpha s}$-coupled prostacyclin receptor and activates a PKA-dependent signaling pathway (Tourdot et al., 2017) (Table 1). More recently, Cebo et al. has suggested that 12(S)-HETrE promotes C-X-C chemokine receptor type 7 (ACKR3, also known as CXCR7) ligation coordinated with IP to trigger the cAMP-PKA signaling pathway. Enhanced platelet expression of the chemokine receptor ACKR3/CXCR7 has been reported in coronary artery disease patients with reduced platelet aggregation (Cebo et al., 2022).

The eicosanoid 12(S)-HETE acts through binding to the G-coupled protein receptor 31 (GPR31) in platelets and human umbilical vein endothelial cells (HUVECs) (Van Doren et al., 2021) (Table 1). In platelets, 12(S)-HETE-GPR31 signals through $G_{\alpha i}$ to induce platelet activation and thrombosis. Activation of the GPR31 inhibits AC activity and

results in Ras-related protein 1 (Rap1) and p38 activation (Van Doren et al., 2019). 20-HETE affects vascular function by binding to G-protein coupled receptor 75 (GPR75) coupled to $G_{\alpha q/11}$ in endothelial cells which results in PLC-IP_3-mediated increases in intracellular Ca^{2+} (Garcia et al., 2017), activation of the Rho kinase (Randriamboavonjy et al., 2003) and the mitogen activated protein (MAP) kinase pathways (Muthalif et al., 2000) (Table 1). Additionally, studies have demonstrated that 20-HETE stimulates the production of inflammatory cytokines, including interleukin-8 (IL-8), IL-13, IL-4, and PGE_2, in endothelial cells via activation of NF-kB and MAPK/ERK signaling pathways (Ishizuka et al., 2008), resulting in endothelial cell activation and endothelial dysfunction (Singh et al., 2007). In addition to regulation of the cells through activation of GPCRs, hydroxyeicosanoids, such as 11(S)-$HpDPA_{\omega-6}$ and 14(S)-$HpDPA_{\omega-6}$ selectively activate PPARα in platelets *ex vivo* which results in inhibition of PKC activity and reduction in Ca^{2+} mobilization (Yeung et al., 2020) (**Table 1**).

3.5 Specialized pro-resolving (lipid) mediator receptors

Recent studies have shown that the SPMs also exert their effects in the blood to regulate inflammation through GPCRs (Table 1). These receptors are typically able to interact with more than one SPM and conversely some SPMs are able to interact with several receptors, leading to some overlapping downstream signals and pathways. RvE1 binds to BLT_1 on neutrophils (Arita et al., 2007), to the chemokine-like receptor 1 (ChemR23) and to the resolvin E1 receptor (ERV1) on monocyte/macrophages (Freire et al., 2017), platelets (Fredman et al., 2010), neutrophils (Chiang and Serhan, 2020), and VSMCs (Ho et al., 2010). The activation of BLT_1 by RvE1 induces phosphorylation of the ribosomal protein S6 (rS6) in neutrophils (Freire et al., 2017), as well as RvE1 activation of ERV1/ChemR23, which results in phosphorylation of Akt and rS6 to enhance phagocytosis by human macrophages (Ohira et al., 2010). Additionally, treatment of HEK-ChemR23 cells with pertussis toxin inhibited RvE1-dependent ERK activation (Serhan et al., 2011b). Although it was shown in HEK cells, the pertussis toxin-sensitive G protein ($G\alpha_{i/o}$)-dependent pathway has already been shown to be activated by LTD_4 in macrophages, suggesting that ChemR23 might couple to a $G\alpha_{i/o}$ to activate intracellular signaling in cells in the blood.

Regarding the D-series resolvins, while in human VSMCs RvD1 binds to the formyl peptide receptor 2 (ALX/FPR2) (also known as LXA_4 receptor) (Ho et al., 2010), studies have suggested that RvD1 may interact with two GPCRs the ALX/FPR2 and the G-protein coupled receptor 32 (GPR32) in leukocytes and platelets (Krishnamoorthy et al., 2010; Lannan et al., 2017). Notably, lipoxins have been found to interact with the same receptors as RvD1, the ALX/FPR2 and GPR32 receptors (Chandrasekharan and Sharma-Walia, 2015). Recently, RvD2 was shown to bind to the G protein-coupled receptor 18 (GRP18) in leukocytes, including PMN, monocytes, and macrophages (Chiang et al., 2015). In macrophages, activation of GRP18 by RvD2 leads to cAMP release and phosphorylation of select kinases and transcription factors, such as cAMP-response element binding protein (CREB) and STAT3 (Chiang and Serhan, 2020). The RvD5 was described to activate the RvD1 receptor GPR32 in leukocytes and macrophages to reduce the expression of NF-κB (Chiang et al., 2012) (Table 1).

The MaR1 activates the leucine-rich repeat-containing G protein-coupled receptor 6 (LGR6) in neutrophils and macrophages/monocytes to increase the phosphorylation of CREB and ERK (Chiang et al., 2019; Chiang and Serhan, 2020). Moreover, studies have shown that MaR1 suppresses NF-κB activation in VSMC and vascular endothelial cells *in vitro* (Chatterjee et al., 2014; Akagi et al., 2015). PD1/NPD1 binds to the G protein-coupled receptor 37 (GPR37) to increase intracellular Ca^{2+} in macrophages (Chiang and Serhan, 2020) (Table 1).

4 Pro-inflammatory eicosanoids in the blood and the vessel

4.1 Prostaglandin E_2

PGs play a key role in the generation of the inflammatory response (Ricciotti and FitzGerald, 2011). They are ubiquitously produced and act as autocrine and paracrine lipid mediators to maintain local hemostasis in the body (Funk, 2001). While PG production is generally very low in uninflamed tissues, it increases immediately in acute inflammation before the recruitment of leukocytes and the infiltration of immune cells (Ricciotti and FitzGerald, 2011). In the blood vessel, one member of the PG family, PGE_2, is synthesized mainly by platelets and macrophages (Cook, 2005). PGE_2 has vasodilation effects and increases the permeability of postcapillary venules, early events in the inflammatory response (Funk, 2001) (Figure 3). Furthermore, PGs may synergize in the blood vessel with other pro-inflammatory mediators, such as histamine or bradykinin, to increase vascular permeability and promote edema (Funk, 2001; Khanapure et al., 2007).

4.2 Thromboxane A_2

TxA_2 is synthesized by macrophages and monocytes on the blood, and in large quantities by platelets (Cook, 2005;

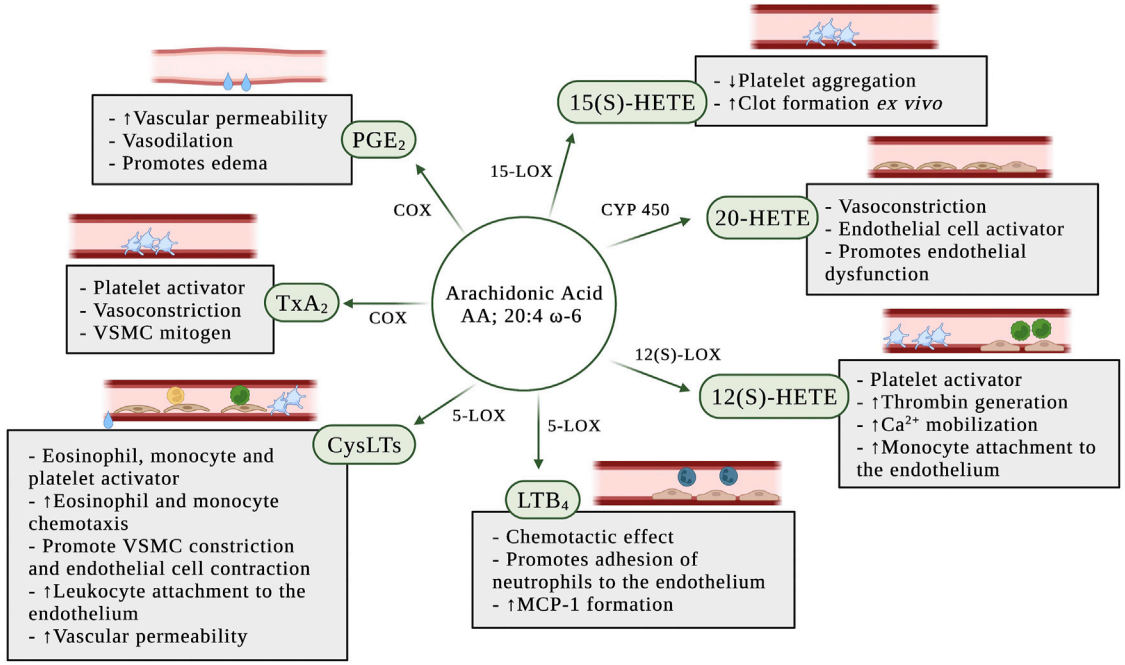

FIGURE 3
Pro-inflammatory effects of eicosanoids in the blood and the vascular wall. *AA:* arachidonic acid; *COX:* cyclooxygenase; *CYP450:* P450 cytochrome epoxygenase; *CysLTs:* cysteinyl leukotrienes; *LTB_4:* leukotriene B_4; *MCP-1:* monocyte chemoattractant protein-1; *PGE_2:* prostaglandin E_2; *TxA_2:* thromboxane A_2; *VSMC:* vascular smooth muscle cell; *5-LOX:* 5-lipoxygenase; *12(S)-LOX:* 12(S)-lipoxygenase; *12(S)-HETE:* 12(S)-hydroxyeicosatetraenoic acid; *15-LOX:* 15-lipoxygenase; *15(S)-HETE:* 15(S)-hydroxyeicosatetraenoic acid; *20-HETE*: 20-hydroxyeicosatetraenoic acid.

Ricciotti and FitzGerald, 2011; Yeung and Holinstat, 2011). Although TxA_2 is an unstable compound with a half-life of 20–30 s (Cook, 2005), it has a wide range of effects on the blood vessel (Figure 3). TxA_2 is a potent vasoconstrictor and VSMC mitogen. It is produced by aggregating platelets and acts as a direct platelet activator in addition to amplifying the platelet response to other platelet agonists (Praticò and Dogné, 2009).

4.3 Leukotrienes

4.3.1 Cysteinyl leukotrienes

CysLTs are potent pro-inflammatory mediators produced during vascular injury (Colazzo et al., 2017). The cysLTs induce eosinophil and monocyte chemotaxis and activation (Funk, 2001), potentiate platelet activation (Yeung et al., 2017), promote vascular smooth muscle constriction and increase vascular permeability in post-capillary venules (Poeckel and Funk, 2010) (Figure 3). Duah et al. (Duah et al., 2013) demonstrated that LTC_4 and LTD_4 regulate endothelial cell function *in vitro* through the increase of endothelial contraction and induction of barrier disruption in the endothelial cell monolayer. In the same study, they also demonstrated that the cysLTs are able to promote attachment of leukocytes to the endothelial monolayer.

4.3.2 Leukotriene B_4

Although most attention has been focused on the COX-dependent pathway of the prostanoids' biosynthesis, the 5-LOX-catalyzed oxygenation of AA play a role in inflammation through the formation of LTs (Poeckel and Funk, 2010). The 5-LOX pathway has long been recognized as a pro-inflammatory cascade and LTs are lipid mediators involved in inflammation and chemotaxis (Funk, 2001). Expression of 5-LOX is usually absent under normal physiologic conditions, but is induced by pro-inflammatory stimuli. Leukotriene B_4 (LTB_4) is a potent chemotactic effect on leukocytes (Yokomizo et al., 2018) and has been implicated in atherosclerosis (Bäck et al., 2005; Ketelhuth et al., 2015). *In vivo* and *in vitro* studies have shown that LTB_4 promotes neutrophil chemotaxis, traffic and adhesion of monocytes to vascular endothelial cells (Friedrich et al., 2003), and increases the formation of monocyte chemoattractant protein-1 (MCP-1) (Huang et al., 2004b) (Figure 3).

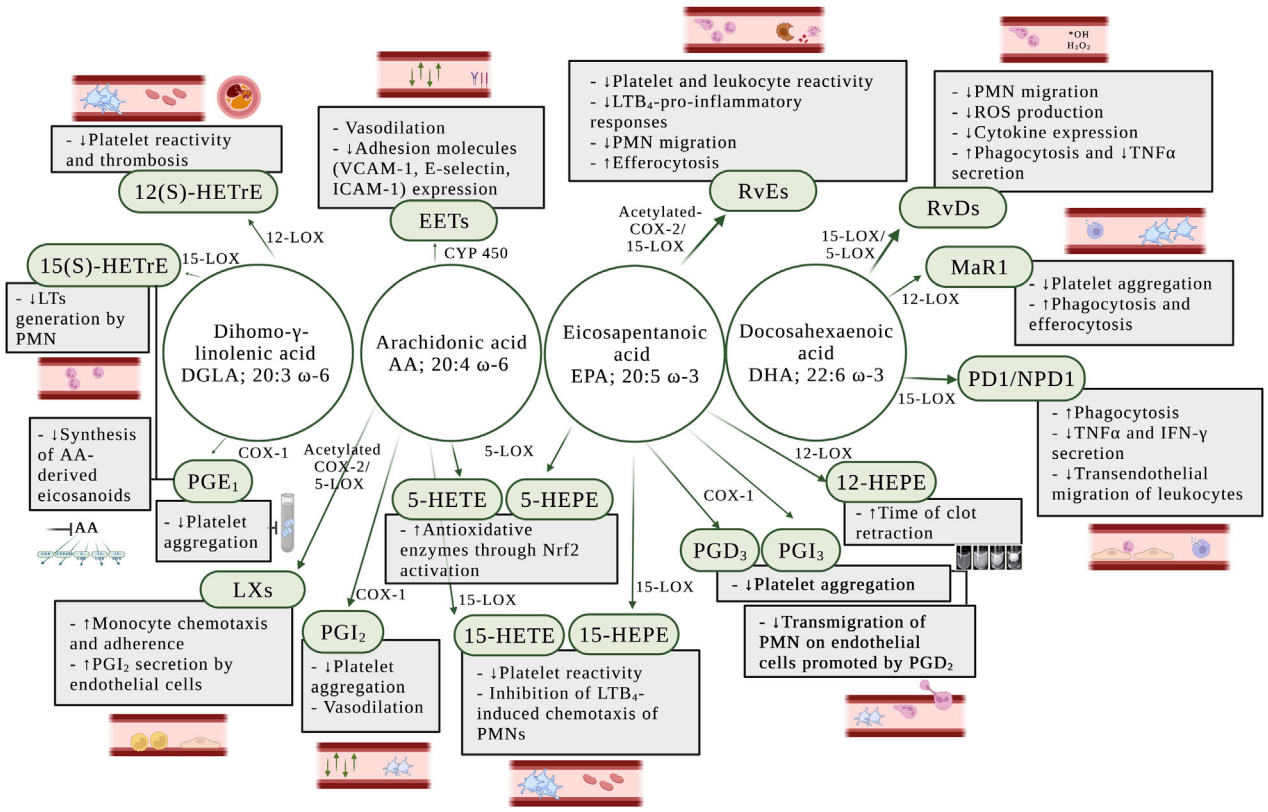

FIGURE 4
Anti-inflammatory effects of eicosanoids in the blood and the vessel wall. *AA:* arachidonic acid; *DGLA:* dihomo-γ-linolenic acid; *DHA:* docosahexaenoic acid; *EETs:* epoxyeicosatrienoic acids; *EPA:* eicosapentaenoic acid; *COX:* cyclooxygenase; *COX-1:* cyclooxygenase-1; *COX-2:* cyclooxygenase-2; *CYP450:* cytochrome epoxygenase; *ICAM-1:* intercellular adhesion molecule 1; *IFN-γ:* interferon-γ; *LTs:* leukotrienes; LTB_4: leukotriene B_4; *LXs:* lipoxins; *MaR1:* maresin 1; Nrf2: nuclear factor-erythroid factor 2-related factor 2; *PD1/NPD1:* protectin D1/neuroprotectin D1; PGD_2: prostaglandin D_2; PGD_3: prostaglandin D_3; PGE_1: prostaglandin E_1; PGI_2: prostaglandin I_2 or prostacyclin; PGI_3: prostaglandin I_3; *PMN:* polymorphonuclear leukocytes; *RvDs:* D-series resolvins; *RvEs:* E-series resolvins; *ROS:* reactive oxygen species; *TNFα:* tumor necrosis factor α; *VCAM-1:* vascular cell adhesion molecule 1; *12-HEPE*: 12-hydroxyeicosapentaenoic acid; *15-HEPE*: 15-hydroxyeicosapentaenoic acid; *5-HETE:* 5-hydroxyeicosatetraenoic acid; *5-LOX:* 5-lipoxygenase; *12-LOX:* 12-lipoxygenase; *12(S)-HETrE:* 12(S)-hydroxyeicosatrienoic acid; *15-LOX:* 15-lipoxygenase; *15-HEPE*: 15(S)-hydroxyeicosapentaenoic acid; *15-HETE: 15*(S)-hydroxyeicosatetraenoic acid; *15(S)-HETrE:* 15(S)-hydroxyeicosatrienoic acid.

4.4 Hydroxyeicosanoids

4.4.1 *12(S)-Hydroxyeicosatetraenoic acid*

The early studies with 12(S)-hydroxyeicosatetraenoic acid (12(S)-HETE) had described anti-inflammatory, antiplatelet and anti-thrombotic effects (Fonlupt et al., 1991; Lagarde et al., 2018). However, most recent studies have shown that 12(S)-HETE potentiates platelet activation, thrombin generation, and calcium mobilization in the platelet (Yeung and Holinstat, 2011) (Figure 3). Furthermore, *in vitro* treatment of human aortic endothelial cells with 12(S)-HETE increased monocyte binding to endothelial cells (Patricia et al., 1999).

4.4.2 20-Hydroxyeicosatetraenoic acid

The role of 20-hydroxyeicosatetraenoic acid (20-HETE) in the regulation of vascular tone and homeostasis promoting a prohypertensive response is due to its potent vasoactive effect (Miyata and Roman, 2005). 20-HETE causes vasoconstriction through its regulation of intracellular signaling (Muthalif et al., 2000) and membrane depolarization (Obara et al., 2002) in smooth muscle cells. Furthermore, studies have demonstrated that 20-HETE stimulates the production of inflammatory cytokines, including IL-8, IL-13, IL-4, and PGE_2, in endothelial cells (Ishizuka et al., 2008) resulting in endothelial cell activation and endothelial dysfunction (Singh et al., 2007) (Figure 3).

5 Anti-inflammatory eicosanoids in the blood and the vessel

5.1 Prostaglandins

Prostacyclin (PGI_2) has been characterized to inhibit platelet aggregation and exerts vasodilator functions, as well as counterbalancing the actions of TxA_2 (Schmid and Brüne, 2021) (Figure 4). It is produced primarily by vascular endothelial and VSMCs, but other cells such as fibroblasts and dendritic cells also synthesize PGI_2 (Dorris and Peebles, 2012). PGI_2 inhibits LPS-induced expression of pro-inflammatory cytokines in macrophages, dendritic cells, T cells and endothelial cells (Luttmann et al., 1996; Zhou et al., 2007a; Zhou et al., 2007b; Di Francesco et al., 2009). PGI_2 can synergize with the anti-inflammatory cytokines IL-4 and IL-13 to selectively inhibit the release of pro-inflammatory cytokines from human peripheral mononuclear blood cells (Luttmann et al., 1999). Under inflammatory conditions including atherosclerosis, the production of PGI_2 may increase, and this has been commonly considered a protective mechanism. Nonetheless, due to PGI_2 acting mainly on TP receptors in vessels with limited IP receptor expression, an increase of its synthesis may lead to increased endothelium-derived vasoconstrictor activity (Luo et al., 2016).

Series 1 and series 3 PGs are well-known to inhibit platelet activity both *in vivo* and *in vitro* (Lagarde et al., 2013; Sergeant et al., 2016). PGE_1 has been considered of biological interest as strong inhibitor of platelet function (Minno et al., 1979; Colman and Figures, 1984), whereas PGD_3 effectively oppose the transmigration of neutrophils on endothelial cells promoted by PGD_2 (Tull et al., 2009). Thus, PGD_3 and PGI_3 have been exhibited potent anti-aggregatory effect *in vitro* in human platelet experiments (Whitaker et al., 1979; Fischer and Weber, 1985) (Figure 4).

5.2 Specialized pro-resolving (lipid) mediators

5.2.1 Lipoxins

The lipoxins A (LXA_4) and B (LXB_4) were two of the first SPMs to be identified and play a critical role in the down-regulation of acute inflammation and enhancement of resolution (Serhan, 2005). LXs increase monocyte chemotaxis and adherence, without causing degranulation or elevation of reactive oxygen species (ROS) (Scalia et al., 1997). It has been established that LXs regulate anti-inflammatory signaling in vascular homeostasis through the stimulation of PGI_2 secretion by human endothelial cells (Brezinski et al., 1989) (Figure 4).

5.2.2 D-series resolvins

Upon vascular injury, the resolvins D1 (RvD1) and D2 (RvD2) have been shown to regulate VSMC phenotypic response, including inhibition of proliferation, migration, monocyte adhesion, ROS production, and inflammatory cytokine expression (Miyahara et al., 2013) (Figure 4). Using mass spectrometry approaches, Cherpokova et al. (Cherpokova et al., 2019) has identified the kinetics of the formation of SPMs in the clot using a deep vein thrombosis animal model. In the same study, administration of RvD4 reduced thrombus burden, with less neutrophil infiltration and more pro-resolving monocytes in the clot. RvD5 promotes pro-resolving effects through enhancement of phagocytosis and reduction of expression of tumor necrosis factor α (TNFα) in neutrophils and macrophages (Chiang et al., 2012; Werz et al., 2018).

5.2.3 E-series resolvins

The resolvin E1 (RvE1) was the first isolated and studied E-series resolvin and possesses anti-inflammatory and pro-resolving actions (Serhan and Petasis, 2011). In the blood, RvE1 has been shown to negatively regulate leukocytes *in vivo* and platelets *ex vivo* (Figure 4), by reducing U46619-, a TP receptor agonist, and ADP-stimulated platelet aggregation, and TxA_2 generation (Dona et al., 2008), suggesting that RvE1 might inhibit $P2Y_{12}$ receptor in platelets. Currently, $P2Y_{12}$ receptor antagonists are used in association with aspirin as the most widely used antiplatelet therapy in cardiovascular diseases (Jackson and Schoenwaelder, 2003). In addition, RvE1 initiates resolution of inflammation through repolarization of human M1 macrophages toward resolution-type macrophages (Herová et al., 2015). Since RvE1 activates the BLT_1 receptor in neutrophils, LTB_4 action is inhibited which reduces LTB_4-pro-inflammatory responses (Arita et al., 2007) (Figure 4).

RvE2 has also been reported to promote anti-inflammatory and pro-resolving effects through *ex vivo* inhibition of PMN chemotaxis and enhancement of nonphlogistic phagocytosis by macrophages (Oh et al., 2012). Recently, the inhibitory effect of RvE3 on neutrophil chemotaxis *in vitro* has been demonstrated (Isobe et al., 2012) and a new member of the EPA-derived resolvins E has been identified and termed resolvin E4 (RvE4). RvE4 is produced under physiologic hypoxia and has a resolving function. It stimulates human M2 macrophage efferocytosis of senescent erythrocytes and apoptotic neutrophils *in vitro* (Libreros et al., 2020) (Figure 4).

5.2.4 Maresin 1

Maresin 1 (MaR1) plays a role in the resolution of inflammation by reducing platelet aggregation *ex vivo*

(Freedman et al., 2020) and stimulating phagocytosis and efferocytosis in human and mouse phagocytes (Chiang and Serhan, 2020) (Figure 4).

5.2.5 Protectin D1/Neuroprotectin D1

Studies have demonstrated that protectin D1/Neuroprotection D1 (PD1/NPD1) increases phagocytosis in macrophages, regulates TNFα and IFNγ secretion by activated T cells *in vitro* (Ariel et al., 2005), and limits transendothelial migration of leukocytes to prevent the infiltration of leukocytes into sites of inflammation (Serhan et al., 2015; Calder, 2020a; Chiang and Serhan, 2020) (Figure 4). Moreover, synthetic PD1/NPD1 attenuated human PMN transmigration *in vivo* and *in vitro* in response to LTB_4 and T cells (Serhan et al., 2015).

Human leukocytes can form AT-(NPD1/PD1) via aspirin-acetylated COX-2 (Serhan et al., 2015). Studies have demonstrated that AT-(NPD1/PD1) has potent protective actions comparable to NPD1/PD1 *in vitro* and *in vivo*, reducing transendothelial PMN migration and enhancing efferocytosis of apoptotic human PMN by macrophages (Serhan et al., 2011a).

5.3 Hydroxyeicosanoids

5.3.1 5-Hydroxyeicosanoids

In neutrophils, EPA and AA are metabolized by 5-LOX to form 5-hydroxyeicosatetraenoic acid (5-HEPE) and 5-hydroxyeicosatetraenoic acid (5-HETE), respectively. Both 5-HEPE and 5-HETE have been shown to induce antioxidative enzymes in vascular endothelial cells through activation of a nuclear factor-erythroid factor 2-related factor 2 (Nrf2)-dependent mechanism through their metabolites, 5-oxo-EPE and 5-oxo-HETE (Nagahora et al., 2017) (Figure 4).

5.3.2 12(S)-Hydroxyeicosanoids

The 12(S)-hydroxyeicosapentaenoic acid (12(S)-HEPE) is the eicosanoid formed through oxygenation of EPA by 12(S)-LOX. Pre-treatment of whole blood with EPA prolonged the time of clot retraction *ex vivo* (Figure 4), suggesting that EPA-derived eicosanoids, such as 12(S)-HEPE, might regulate blood clotting and play a role in clot resolution (Ikei et al., 2012).

DGLA is an ω-6 fatty acid that is oxidized in the platelet by 12(S)-LOX to form 12(*S*)-HETrE. This metabolite has been shown to attenuate platelet activity and thrombosis (Ikei et al., 2012). The antiplatelet role of 12-HETrE was determined by demonstrating its ability to inhibit platelet aggregation *in vitro* and attenuate clot formation *in vivo* (Figure 4) through selective activation of the prostacyclin receptor in platelets (Yeung et al., 2016; Tourdot et al., 2017; Yeung and Holinstat, 2017).

5.3.3 15-Hydroxyeicosanoids

The 15-LOX-derived eicosanoids from AA, DGLA, and EPA are 15(S)-hydroxyeicosatetraenoic acid (15(S)-HETE), 15-hydroxyeicosatrienoic acid (15(S)-HETrE), and 15(S)-hydroxyeicosapentaenoic acid (15(S)-HEPE), respectively. While 15(S)-HETrE, 15(S)-HETE and 15(S)-HEPE have been shown to inhibit platelet reactivity (Guichardant et al., 1988; Vanderhoek et al., 1991) (Figure 4), other studies have observed a pro-aggregatory effect of 15(S)-HETE on platelet function (Setty and Stuart, 1986; Vijil et al., 2014) and an increase of clot formation in human whole blood pre-treated *ex vivo* with 15(S)-HETE (Lundqvist et al., 2016) (Figure 3).

Moreover, studies have suggested that DGLA inhibits the synthesis *in vitro* of LTB_4 in neutrophils through the formation of 15(S)-HETrE (Iversen et al., 1991; Chilton-Lopez et al., 1996) (Figure 4). Additionally, 15(S)-HETE has been shown to inhibit LTB_4-induced chemotaxis of PMNs *in vitro* (Ternowitz et al., 1988; Takata et al., 1994).

5.4 Epoxyeicosatrienoic acids

Epoxyeicosatrienoic acids (EETs) are generated from AA by CYP450 enzymes and promote the active termination of inflammation by a broad array of anti-inflammatory and pro-resolving actions. EETs were found to have direct effects on the large-conductance Ca^{2+}-activated potassium (K^+) channels in vascular smooth muscle cells (Campbell and Harder, 1999). This mechanism contributes to the effect of EETs as endothelium-derived hyperpolarizing factor to hyperpolarize and relax arterial smooth muscle (Li and Campbell, 1997). EETs present functional relevance in vascular inflammation primarily due to their role in the reduction of vascular cell adhesion molecule 1 (VCAM-1), E-selectin and intercellular adhesion molecule 1 (ICAM-1) expression, and prevention of leukocyte adhesion to the vascular wall (Node et al., 1999) (Figure 4).

6 Discussion

Polyunsaturated fatty acids and their bioactive eicosanoids play a critical role in human health and diseases through regulating inflammation in the blood and the vessel. The role of the ω-6 PUFA AA in inflammation through formation of eicosanoids is well established. While the AA-derived eicosanoids, including PGE_2, TxA_2 and LTs, are well-known as pro-inflammatory mediators in the blood, the COX-derived PGs PGI_2 from AA, and the PGs series 1 and 3 from EPA and DGLA, respectively, have a critical role in counterbalancing pro-inflammatory states to attenuate inflammation in the blood and the vascular wall. More recently, studies in the eicosanoid-inflammation field have additionally identified a wide class of bioactive metabolites and SPMs derived from AA, DGLA, EPA, and DHA. As the classic eicosanoids (PGs, LTs and Txs), the bioactive metabolites have pro- or anti-inflammatory effects,

whereas the SPMs are currently extensively studied due to their effects on the attenuation of pro-inflammatory eicosanoid actions and active contribution to the resolution of inflammatory tissue. This review has outlined the function of COX-, LOX- and CYP 450-derived eicosanoids from PUFAs and elucidated their mechanistic regulation of the inflammation process in the blood and the vessel.

As a result of their widespread expression in the blood and the vascular wall, eicosanoids and their metabolites are involved in the pathogenesis and the development of inflammatory diseases such as atherosclerosis, hypertension, diabetes mellitus and more recently, COVID-19. As an example, alterations in the formation of bioactive metabolites, such as 20-HETE, have been reported in inflammatory diseases such as hypertension, diabetes (Miyata and Roman, 2005) and cardiovascular disease (Zu et al., 2016). Due to their critical involvement in eicosanoid biosynthesis, alterations in the expression of oxygenases also play a role in the pathogenesis of inflammatory diseases such as atherosclerosis and diabetes. While the upregulation of 5-LOX expression, leading to production of Cys-LTs and LTB_4, has been reported at the site of atherosclerotic plaques (Whatling et al., 2007; Riccioni et al., 2010), increased 12-LOX activity or expression has been implicated in the functional loss of insulin secretion or production in beta-cells of the pancreatic islets, which may impair blood glucose regulation leading to the development of diabetes (Ma et al., 2010). Synthesis of PGE_2 has also been suggested to be up-regulated in atherosclerosis. Using an animal model of atherosclerosis, Gross et al. have shown that PGE_2 is produced in the arterial wall in response to inflammation and is detected in atherosclerotic plaques. In addition, the authors have demonstrated that PGE_2 enhances atherothrombosis *in vivo* (Gross et al., 2007). Increased production of PGE_2 was recently identified in the blood of COVID-19 patients. These patients were found to have higher PGE_2 levels which were correlated positively with the severity of the disease (Ricke-Hoch et al., 2021). Coronavirus infection activates endoplasmic reticulum stress signaling, which, in turn, can induce the biosynthesis of PGE_2 (Chopra et al., 2019). Thus, an increased level of PGE_2 may be involved in the hyperinflammatory response in COVID 19 infection (Hammock et al., 2020).

Due to their effects on promoting inflammation, the eicosanoids are potential targets for the treatment of these diseases, as well as the enzymes and receptors implicated in their formation. For example, the inhibition of 12-LOX in platelets, using the pharmacological inhibitor ML355, reduces platelet aggregation *ex vivo* and impairs clot formation *in vivo* (Adili et al., 2017). The prostacyclin analogs, such as iloprost and selexipag, are used to treat pulmonary arterial hypertension due to their vasodilatory and anti-platelet effects through activation of the prostacyclin receptor (Sitbon et al., 2015; Mandras et al., 2021). The inhibition of pro-aggregatory effects of TxA_2 through acetylation of COX-1 in platelets is the pharmacological basis for aspirin, used in association with a $P2Y_{12}$ receptor antagonist in dual antiplatelet therapy to treat cardiovascular diseases and prevent the recurrence of major cardiovascular events due to thrombosis (Schrör and Rauch, 2015). The role of TxA_2 in the impairing endothelial function is highly associated with pathogenesis of atherosclerosis. Studies have shown that mice deficient in TP and IP demonstrated an accelerated atherogenesis in the blood vessel (Kobayashi et al., 2004). Notably, the acetylation of COX by aspirin can trigger alternative biosynthesis pathways forming bioactive metabolites and SPMs (Figure 2) which might provide additional anti-inflammatory effects promoted by aspirin treatment.

Studies have shown that increased intake of ω-3 PUFAs (EPA and DHA) results in increased amounts of these fatty acids in blood lipids, leukocytes and platelets (Browning et al., 2012). The increased level of ω-3 PUFAs in leukocytes and platelets has been demonstrated to result in a reduction of the capacity of these cells to produce pro-inflammatory eicosanoids from AA, such as PGs and LTs (Calder, 2020b), and to regulate the function of these cells by attenuating platelet reactivity and increasing leukocyte response to inflammation (Faber et al., 2011; Yamaguchi et al., 2022). Notably, the concentration of several bioactive metabolites, including hydroxy- and epoxyeicosanoids derived from AA, EPA and DHA, were increased in the plasma of normo- and hyperlipidemic patients following supplementation with EPA and DHA (Schuchardt et al., 2014; Schmöcker et al., 2018). Moreover, studies have detected higher levels of the SPMs, such as RvD1 and RvD2, in the plasma and serum of individuals with an increased intake of EPA and DHA (Calder, 2020a). Thus, given the evidence of diverse supplementary studies, modulating the levels of PUFAs mediated by ingestion or supplementation might provide beneficial effects in attenuating the inflammation process in the blood and the vessel.

The SPMs have been recently described as positive modulators on resolution and termination of inflammation. Studies have indicated that RvE1 might control vascular inflammation in atherosclerosis. RvE1 has been shown to protect against atherogenesis in an animal model of atherosclerosis (Hasturk et al., 2015) and Laguna-Fernandez et al. (Laguna-Fernandez et al., 2018) have demonstrated that targeted deletion of the RvE1 receptor ERV1/Chem23 in a hyperlipidemic animal model was associated with proatherogenic signaling in macrophages, increased oxidized low-density lipoprotein uptake, reduced phagocytosis, and increased atherosclerotic plaque size and necrotic core formation, suggesting that RvE1 might have protective effects during atheroprogression (Salic et al., 2016). Additionally, the administration of the D-series resolvin RvD4 to mice of a deep vein thrombosis model has been shown to reduce thrombus formation and improve clot resolution (Cherpokova et al., 2019), suggesting that the delivery of SPMs might help to regulate

thrombosis and inflammation in cardiovascular diseases. Thus, SPMs may be considered as potential therapeutic approaches for prevention or resolution of inflammation or insult in the vessel.

The discovery of SPMs was first reported in exudates (Serhan et al., 2011b) and the investigation of the effects of SPMs on the blood and the vessel is currently in early stages. Studies using *in vitro* assays and animal models have described the SPMs' ability to contribute to resolution of inflammation through regulation of cell function in the blood and the vessel (see review (Chiang and Serhan, 2020)), but the physiological relevance of these effects depends on the endogenous concentration of SPM *in vivo*. The biosynthesis of SPMs has been characterized using *in vitro* studies (Isobe et al., 2012; Libreros et al., 2020; Perry et al., 2020) and other studies have demonstrated the ability of blood cells such as neutrophils and macrophages to form SPMs *in vitro* (Werz et al., 2018; Mainka et al., 2022). In addition, despite several studies having detected SPMs in human samples including plasma and serum (see review (Calder, 2020a)), the concentration of SPMs was at low levels (picogram/picomolar to nanogram/nanomolar range) (Mainka et al., 2022; Schebb et al., 2022) and the analysis of low concentrations of low SPMs can be an analytical challenge and it may affect the detection and quantification process of these metabolites in the sample. Indeed, there is a current controversy in the field based on differences in the methodology and analytical instrumentation used to detect the SPMs in biological samples (Schebb et al., 2022), which demonstrates that a deeper investigation is warranted to provide a better understanding of the concentration range of SPMs circulating in the human bloodstream and whether SPMs at these concentrations are able to regulate resolution of inflammation in the blood and the vessel.

The studies using *in vitro* and *in vivo* approaches in cellular and animal models, and the analysis of samples collected from humans, have significantly contributed to the current understanding of the mechanistic regulation of eicosanoids in inflammation. It resulted in a large body of evidence about the role of the classical pro- and anti-inflammatory eicosanoids derived from the 20-carbon PUFAs AA, DGLA and EPA, in inflammation in the blood. However, a better understanding of the mechanistic regulatory effects of the most recently discovered eicosanoids, including SPMs and bioactive metabolites, in the regulation of inflammatory states and their contribution to the resolution of inflammation in the blood and the vascular wall is warranted. Furthermore, it is important to highlight that, although there is evidence of the synthesis of SPMs by cells in the blood, whether the biosynthesis of some SPMs occurs in the blood and the biological relevance of this process still need to be further elucidate. Hence, the role of eicosanoids in inflammation in the blood and the vessel is currently a focus of much research in the inflammation field which might help to position the anti-inflammatory bioactive eicosanoids as a novel therapeutic approach to treat inflammatory diseases that affects the blood and the vascular wall.

Author contributions

AY and EB performed literature search, wrote the manuscript and created figures. MH wrote and edited the manuscript. MH, AY, and EB proofed the manuscript.

Funding

This study was supported by NIH grants R35 GM131835 (MH), T32 HL007853 (AY), and UL1 TR002240 (MH and AY).

Conflict of interest

MH is a consultant and equity holder for Veralox therapeutics and Cereno Scientific.

The remaining authors declare that the research was conducted in the absence of any commercial or financial relationships that could be construed as a potential conflict of interest.

Publisher's note

References

Adili, R., Tourdot, B. E., Mast, K., Yeung, J., Freedman, J. C., Green, A., et al. (2017). First selective 12-LOX inhibitor, ML355, impairs thrombus formation and vessel occlusion *in vivo* with minimal effects on hemostasis. *Arterioscler. Thromb. Vasc. Biol.* 37 (10), 1828–1839. doi:10.1161/ATVBAHA.117.309868

Akagi, D., Chen, M., Toy, R., Chatterjee, A., and Conte, M. S. (2015). Systemic delivery of proresolving lipid mediators resolvin D2 and maresin 1 attenuates intimal hyperplasia in mice. *Faseb J.* 29 (6), 2504–2513. doi:10.1096/fj.14-265363

Alvarez, M. L., and Lorenzetti, F. (2021). Role of eicosanoids in liver repair, regeneration and cancer. *Biochem. Pharmacol.* 192, 114732. doi:10.1016/j.bcp.2021.114732

Aoki, T., and Narumiya, S. (2012). Prostaglandins and chronic inflammation. *Trends Pharmacol. Sci.* 33 (6), 304–311. doi:10.1016/j.tips.2012.02.004

Ariel, A., Li, P. L., Wang, W., Tang, W. X., Fredman, G., Hong, S., et al. (2005). The docosatriene protectin D1 is produced by TH2 skewing and promotes human T cell apoptosis via lipid raft clustering. *J. Biol. Chem.* 280 (52), 43079–43086. doi:10.1074/jbc.M509796200

Arita, M., Ohira, T., Sun, Y-P., Elangovan, S., Chiang, N., and Serhan, C. N. (2007). Resolvin E1 selectively interacts with leukotriene B4 receptor BLT1 and ChemR23 to regulate inflammation. *J. Immunol.* 178 (6), 3912–3917. doi:10.4049/jimmunol.178.6.3912

Arnold, C., Konkel, A., Fischer, R., and Schunck, W-H. (2010). Cytochrome P450-dependent metabolism of ω-6 and ω-3 long-chain polyunsaturated fatty acids. *Pharmacol. Rep.* 62 (3), 536–547. doi:10.1016/s1734-1140(10)70311-x

Astarita, G., Kendall, A. C., Dennis, E. A., and Nicolaou, A. (2015). Targeted lipidomic strategies for oxygenated metabolites of polyunsaturated fatty acids. *Biochim. Biophys. Acta* 1851 (4), 456–468. doi:10.1016/j.bbalip.2014.11.012

Bäck, M., Bu, D-X., Bränström, R., Sheikine, Y., Yan, Z-Q., and Hansson, G. K. (2005). Leukotriene B4 signaling through NF-κB-dependent BLT1 receptors on vascular smooth muscle cells in atherosclerosis and intimal hyperplasia. *Proc. Natl. Acad. Sci.* 102 (48), 17501–17506.

Biringer, R. G. (2021). A review of prostanoid receptors: Expression, characterization, regulation, and mechanism of action. *J. Cell Commun. Signal* 15 (2), 155–184. doi:10.1007/s12079-020-00585-0

Bosma, K. J., Kaiser, C. E., Kimple, M. E., and Gannon, M. (2022). Effects of arachidonic acid and its metabolites on functional beta-cell mass. *Metabolites* 12 (4), 342. doi:10.3390/metabo12040342

Bozza, P. T., Bakker-Abreu, I., Navarro-Xavier, R. A., and Bandeira-Melo, C. (2011). Lipid body function in eicosanoid synthesis: An update. *Prostagl. Leukot. Essent. Fat. Acids* 85 (5), 205–213. doi:10.1016/j.plefa.2011.04.020

Brash, A. R. (1999). Lipoxygenases: Occurrence, functions, catalysis, and acquisition of substrate. *J. Biol. Chem.* 274 (34), 23679–23682. doi:10.1074/jbc.274.34.23679

Brezinski, M. E., Gimbrone, M. A., Nicolaou, K., and Serhan, C. N. (1989). Lipoxins stimulate prostacyclin generation by human endothelial cells. *FEBS Lett.* 245 (1-2), 167–172. doi:10.1016/0014-5793(89)80214-5

Browning, L. M., Walker, C. G., Mander, A. P., West, A. L., Madden, J., Gambell, J. M., et al. (2012). Incorporation of eicosapentaenoic and docosahexaenoic acids into lipid pools when given as supplements providing doses equivalent to typical intakes of oily fish. *Am. J. Clin. Nutr.* 96 (4), 748–758. doi:10.3945/ajcn.112.041343

Calder, P. C. (2020). n-3 PUFA and inflammation: from membrane to nucleus and from bench to bedside. *Proc. Nutr. Soc.* 79 (4), 1–13. doi:10.1017/S0029665120007077

Calder, P. C. (2020). Eicosapentaenoic and docosahexaenoic acid derived specialised pro-resolving mediators: Concentrations in humans and the effects of age, sex, disease and increased omega-3 fatty acid intake. *Biochimie* 178, 105–123. doi:10.1016/j.biochi.2020.08.015

Campbell, W. B., and Harder, D. R. (1999). Endothelium-derived hyperpolarizing factors and vascular cytochrome P450 metabolites of arachidonic acid in the regulation of tone. *Circ. Res.* 84 (4), 484–488. doi:10.1161/01.res.84.4.484

Capra, V., Accomazzo, M. R., Ravasi, S., Parenti, M., Macchia, M., Nicosia, S., et al. (2003). Involvement of prenylated proteins in calcium signaling induced by LTD4 in differentiated U937 cells. *Prostagl. Other Lipid Mediat* 71 (3-4), 235–251. doi:10.1016/s1098-8823(03)00045-5

Capra, V. (2004). Molecular and functional aspects of human cysteinyl leukotriene receptors. *Pharmacol. Res.* 50 (1), 1–11. doi:10.1016/j.phrs.2003.12.012

Cebo, M., Dittrich, K., Fu, X., Manke, M. C., Emschermann, F., Rheinlaender, J., et al. (2022). Platelet ACKR3/CXCR7 favors antiplatelet lipids over an atherothrombotic lipidome and regulates thromboinflammation. *J. Am. Soc. Hematol.* 139 (11), 1722–1742. doi:10.1182/blood.2021013097

Chandrasekharan, J. A., and Sharma-Walia, N. (2015). Lipoxins: nature's way to resolve inflammation. *J. Inflamm. Res.* 8, 181–192. doi:10.2147/JIR.S90380

Chatterjee, A., Sharma, A., Chen, M., Toy, R., Mottola, G., and Conte, M. S. (2014). The pro-resolving lipid mediator maresin 1 (MaR1) attenuates inflammatory signaling pathways in vascular smooth muscle and endothelial cells. *PLoS One* 9 (11), e113480. doi:10.1371/journal.pone.0113480

Cheranov, S. Y., Karpurapu, M., Wang, D., Zhang, B., Venema, R. C., and Rao, G. N. (2008). An essential role for SRC-activated STAT-3 in 14,15-EET-induced VEGF expression and angiogenesis. *Blood* 111 (12), 5581–5591. doi:10.1182/blood-2007-11-126680

Cherpokova, D., Jouvene, C. C., Libreros, S., DeRoo, E. P., Chu, L., de la Rosa, X., et al. (2019). Resolvin D4 attenuates the severity of pathological thrombosis in mice. *Blood* 134 (17), 1458–1468. doi:10.1182/blood.2018886317

Chiang, N., Dalli, J., Colas, R. A., and Serhan, C. N. (2015). Identification of resolvin D2 receptor mediating resolution of infections and organ protection. *J. Exp. Med.* 212 (8), 1203–1217. doi:10.1084/jem.20150225

Chiang, N., Fredman, G., Bäckhed, F., Oh, S. F., Vickery, T., Schmidt, B. A., et al. (2012). Infection regulates pro-resolving mediators that lower antibiotic requirements. *Nature* 484 (7395), 524–528. doi:10.1038/nature11042

Chiang, N., Libreros, S., Norris, P. C., de la Rosa, X., and Serhan, C. N. (2019). Maresin 1 activates LGR6 receptor promoting phagocyte immunoresolvent functions. *J. Clin. Invest* 129 (12), 5294–5311. doi:10.1172/JCI129448

Chiang, N., and Serhan, C. N. (2020). Specialized pro-resolving mediator network: An update on production and actions. *Essays Biochem.* 64 (3), 443–462. doi:10.1042/EBC20200018

Chilton-Lopez, L., Surette, M. E., Swan, D. D., Fonteh, A. N., Johnson, M. M., and Chilton, F. H. (1996). Metabolism of gammalinolenic acid in human neutrophils. *J. Immunol.* 156 (8), 2941–2947.

Chopra, S., Giovanelli, P., Alvarado-Vazquez, P. A., Alonso, S., Song, M., Sandoval, T. A., et al. (2019). IRE1α-XBP1 signaling in leukocytes controls prostaglandin biosynthesis and pain. *Science* 365 (6450), eaau6499. doi:10.1126/science.aau6499

Colazzo, F., Gelosa, P., Tremoli, E., Sironi, L., and Castiglioni, L. (2017). Role of the cysteinyl leukotrienes in the pathogenesis and progression of cardiovascular diseases. *Mediat. Inflamm.* 2017, 2432958. doi:10.1155/2017/2432958

Colman, R. W., and Figures, W. R. (1984). Characteristics of an ADP receptor mediating platelet activation. *Mol. Cell Biochem.* 59 (1), 101–111. doi:10.1007/BF00231307

Cook, D., Finnigan, J., Cook, K., Black, G., and Charnock, S. (2016). Cytochromes P450: History, classes, catalytic mechanism, and industrial application. *Adv. Protein Chem. Struct. Biol.* 105, 105–126. doi:10.1016/bs.apcsb.2016.07.003

Cook, J. A. (2005). *Eicosanoids. Crit. Care Med.* 33 (1), S488–S491. doi:10.1097/01.ccm.0000196028.19746.42

Crooke, S. T., Mattern, M., Sarau, H. M., Winkler, J. D., Balcarek, J., Wong, A., et al. (1989). The signal transduction system of the leukotriene D4 receptor. *Trends Pharmacol. Sci.* 10 (3), 103–107. doi:10.1016/0165-6147(89)90206-x

Cummings, H. E., Liu, T., Feng, C., Laidlaw, T. M., Conley, P. B., Kanaoka, Y., et al. (2013). Cutting edge: Leukotriene C4 activates mouse platelets in plasma exclusively through the type 2 cysteinyl leukotriene receptor. *J. Immunol.* 191 (12), 5807–5810. doi:10.4049/jimmunol.1302187

Dennis, E. A., Cao, J., Hsu, Y-H., Magrioti, V., and Kokotos, G. (2011). Phospholipase A2 enzymes: Physical structure, biological function, disease implication, chemical inhibition, and therapeutic intervention. *Chem. Rev.* 111 (10), 6130–6185. doi:10.1021/cr200085w

Di Francesco, L., Totani, L., Dovizio, M., Piccoli, A., Di Francesco, A., Salvatore, T., et al. (2009). Induction of prostacyclin by steady laminar shear stress suppresses tumor necrosis factor-alpha biosynthesis via heme oxygenase-1 in human endothelial cells. *Circ. Res.* 104 (4), 506–513. doi:10.1161/CIRCRESAHA.108.191114

Díaz Del Campo, L. S., Rodrigues-Díez, R., Salaices, M., Briones, A. M., and García-Redondo, A. B. (2022). Specialized pro-resolving lipid mediators: New therapeutic approaches for vascular remodeling. *Int. J. Mol. Sci.* 23 (7).

Dona, M., Fredman, G., Schwab, J. M., Chiang, N., Arita, M., Goodarzi, A., et al. (2008). Resolvin E1, an EPA-derived mediator in whole blood, selectively counterregulates leukocytes and platelets. *Blood* 112 (3), 848–855. doi:10.1182/blood-2007-11-122598

Dorris, S. L., and Peebles, R. S. (2012). PGI2 as a regulator of inflammatory diseases. *Mediat. Inflamm.* 2012, 926968. doi:10.1155/2012/926968

Duah, E., Adapala, R. K., Al-Azzam, N., Kondeti, V., Gombedza, F., Thodeti, C. K., et al. (2013). Cysteinyl leukotrienes regulate endothelial cell inflammatory and proliferative signals through $CysLT_2$ and $CysLT_1$ receptors. *Sci. Rep.* 3, 3274. doi:10.1038/srep03274

Esser-von Bieren, J. (2019). Eicosanoids in tissue repair. *Immunol. Cell Biol.* 97 (3), 279–288. doi:10.1111/imcb.12226

Faber, J., Berkhout, M., Vos, A. P., Sijben, J. W., Calder, P. C., Garssen, J., et al. (2011). Supplementation with a fish oil-enriched, high-protein medical food leads to rapid incorporation of EPA into white blood cells and modulates immune responses within one week in healthy men and women. *J. Nutr.* 141 (5), 964–970. doi:10.3945/jn.110.132985

Fahy, E., Subramaniam, S., Murphy, R. C., Nishijima, M., Raetz, C. R., Shimizu, T., et al. (2009). Update of the LIPID MAPS comprehensive classification system for lipids. *J. Lipid Res.* 50 Suppl, S9–S14. doi:10.1194/jlr.R800095-JLR200

Fava, C., and Bonafini, S. (2018). Eicosanoids via CYP450 and cardiovascular disease: Hints from genetic and nutrition studies. *Prostagl. Other Lipid Mediat* 139, 41–47. doi:10.1016/j.prostaglandins.2018.10.001

Feinmark, S. J., and Cannon, P. J. (1986). Endothelial cell leukotriene C4 synthesis results from intercellular transfer of leukotriene A4 synthesized by polymorphonuclear leukocytes. *J. Biol. Chem.* 261 (35), 16466–16472. doi:10.1016/s0021-9258(18)66589-5

Fischer, S., and Weber, P. C. (1985). Thromboxane (TX)A3 and prostaglandin (PG)I3 are formed in man after dietary eicosapentaenoic acid: Identification and quantification by capillary gas chromatography-electron impact mass spectrometry. *Biomed. Mass Spectrom.* 12 (9), 470–476. doi:10.1002/bms.1200120905

Fonlupt, P., Croset, M., and Lagarde, M. (1991). 12-HETE inhibits the binding of PGH2/TXA2 receptor ligands in human platelets. *Thromb. Res.* 63 (2), 239–248. doi:10.1016/0049-3848(91)90287-7

Fredman, G., Van Dyke, T. E., and Serhan, C. N. (2010). Resolvin E1 regulates adenosine diphosphate activation of human platelets. *Arterioscler. Thromb. Vasc. Biol.* 30 (10), 2005–2013. doi:10.1161/ATVBAHA.110.209908

Freedman, C., Tran, A., Tourdot, B. E., Kalyanaraman, C., Perry, S., Holinstat, M., et al. (2020). Biosynthesis of the maresin intermediate, 13S,14S-Epoxy-DHA, by human 15-lipoxygenase and 12-lipoxygenase and its regulation through negative allosteric modulators. *Biochemistry* 59 (19), 1832–1844. doi:10.1021/acs.biochem.0c00233

Freire, M. O., Dalli, J., Serhan, C. N., and Van Dyke, T. E. (2017). Neutrophil resolvin E1 receptor expression and function in type 2 diabetes. *J. Immunol.* 198 (2), 718–728. doi:10.4049/jimmunol.1601543

Friedrich, E. B., Tager, A. M., Liu, E., Pettersson, A., Owman, C., Munn, L., et al. (2003). Mechanisms of leukotriene B4--triggered monocyte adhesion. *Arterioscler. Thromb. Vasc. Biol.* 23 (10), 1761–1767. doi:10.1161/01.ATV.0000092941.77774.3C

Fu, T., Mohan, M., Brennan, E. P., Woodman, O. L., Godson, C., Kantharidis, P., et al. (2020). Therapeutic potential of lipoxin A4 in chronic inflammation: Focus on cardiometabolic disease. *ACS Pharmacol. Transl. Sci.* 3 (1), 43–55. doi:10.1021/acsptsci.9b00097

Funk, C. D. (2001). Prostaglandins and leukotrienes: Advances in eicosanoid biology. *Science* 294 (5548), 1871–1875. doi:10.1126/science.294.5548.1871

Garcia, V., Gilani, A., Shkolnik, B., Pandey, V., Zhang, F. F., Dakarapu, R., et al. (2017). 20-HETE signals through G-protein-coupled receptor GPR75 (gq) to affect vascular function and trigger hypertension. *Circ. Res.* 120 (11), 1776–1788. doi:10.1161/CIRCRESAHA.116.310525

Gilroy, D. W., and Bishop-Bailey, D. (2019). Lipid mediators in immune regulation and resolution. *Br. J. Pharmacol.* 176 (8), 1009–1023. doi:10.1111/bph.14587

Goldman, D. W., Chang, F. H., Gifford, L. A., Goetzl, E. J., and Bourne, H. R. (1985). Pertussis toxin inhibition of chemotactic factor-induced calcium mobilization and function in human polymorphonuclear leukocytes. *J. Exp. Med.* 162 (1), 145–156. doi:10.1084/jem.162.1.145

Goodarzi, K., Goodarzi, M., Tager, A. M., Luster, A. D., and von Andrian, U. H. (2003). Leukotriene B4 and BLT1 control cytotoxic effector T cell recruitment to inflamed tissues. *Nat. Immunol.* 4 (10), 965–973. doi:10.1038/ni972

Gross, S., Tilly, P., Hentsch, D., Vonesch, J-L., and Fabre, J-E. (2007). Vascular wall-produced prostaglandin E2 exacerbates arterial thrombosis and atherothrombosis through platelet EP3 receptors. *J. Exp. Med.* 204 (2), 311–320. doi:10.1084/jem.20061617

Guichardant, M., Naltachayan-Durbin, S., and Lagarde, M. (1988). Occurrence of the 15-hydroxy derivative of dihomogammalinolenic acid in human platelets and its biological effect. *Biochim. Biophys. Acta* 962 (1), 149–154. doi:10.1016/0005-2760(88)90106-3

Hajeyah, A. A., Griffiths, W. J., Wang, Y., Finch, A. J., and O'Donnell, V. B. (2020). The biosynthesis of enzymatically oxidized lipids. *Front. Endocrinol.* 11, 910. doi:10.3389/fendo.2020.591819

Hammock, B. D., Wang, W., Gilligan, M. M., and Panigrahy, D. (2020). Eicosanoids: The overlooked storm in coronavirus disease 2019 (COVID-19)? *Am. J. Pathol.* 190 (9), 1782–1788. doi:10.1016/j.ajpath.2020.06.010

Hasturk, H., Abdallah, R., Kantarci, A., Nguyen, D., Giordano, N., Hamilton, J., et al. (2015). Resolvin E1 (RvE1) attenuates atherosclerotic plaque formation in diet and inflammation-induced atherogenesis. *Arterioscler. Thromb. Vasc. Biol.* 35 (5), 1123–1133. doi:10.1161/ATVBAHA.115.305324

Herová, M., Schmid, M., Gemperle, C., and Hersberger, M. (2015). ChemR23, the receptor for chemerin and resolvin E1, is expressed and functional on M1 but not on M2 macrophages. *J. Immunol.* 194 (5), 2330–2337. doi:10.4049/jimmunol.1402166

Ho, K. J., Spite, M., Owens, C. D., Lancero, H., Kroemer, A. H., Pande, R., et al. (2010). Aspirin-triggered lipoxin and resolvin E1 modulate vascular smooth muscle phenotype and correlate with peripheral atherosclerosis. *Am. J. Pathol.* 177 (4), 2116–2123. doi:10.2353/ajpath.2010.091082

Hoxha, M., and Zappacosta, B. (2020). CYP-Derived eicosanoids: Implications for rheumatoid arthritis. *Prostagl. Other Lipid Mediat* 146, 106405. doi:10.1016/j.prostaglandins.2019.106405

Huang, J. S., Ramamurthy, S. K., Lin, X., and Le Breton, G. C. (2004). Cell signalling through thromboxane A2 receptors. *Cell Signal* 16 (5), 521–533. doi:10.1016/j.cellsig.2003.10.008

Huang, L., Zhao, A., Wong, F., Ayala, J. M., Struthers, M., Ujjainwalla, F., et al. (2004). Leukotriene B4 strongly increases monocyte chemoattractant protein-1 in human monocytes. *Arterioscler. Thromb. Vasc. Biol.* 24 (10), 1783–1788. doi:10.1161/01.ATV.0000140063.06341.09

Ikei, K. N., Yeung, J., Apopa, P. L., Ceja, J., Vesci, J., Holman, T. R., et al. (2012). Investigations of human platelet-type 12-lipoxygenase: Role of lipoxygenase products in platelet activation. *J. Lipid Res.* 53 (12), 2546–2559. doi:10.1194/jlr.M026385

Ishizuka, T., Cheng, J., Singh, H., Vitto, M. D., Manthati, V. L., Falck, J. R., et al. (2008). 20-Hydroxyeicosatetraenoic acid stimulates nuclear factor-kappaB activation and the production of inflammatory cytokines in human endothelial cells. *J. Pharmacol. Exp. Ther.* 324 (1), 103–110. doi:10.1124/jpet.107.130336

Isobe, Y., Arita, M., Matsueda, S., Iwamoto, R., Fujihara, T., Nakanishi, H., et al. (2012). Identification and structure determination of novel anti-inflammatory mediator resolvin E3, 17,18-dihydroxyeicosapentaenoic acid. *J. Biol. Chem.* 287 (13), 10525–10534. doi:10.1074/jbc.M112.340612

Iversen, L., Fogh, K., Bojesen, G., and Kragballe, K. (1991). Linoleic acid and dihomogammalinolenic acid inhibit leukotriene B4 formation and stimulate the formation of their 15-lipoxygenase products by human neutrophils *in vitro*. Evidence of formation of antiinflammatory compounds. *Agents Actions* 33 (3-4), 286–291. doi:10.1007/BF01986575

Jackson, S. P., and Schoenwaelder, S. M. (2003). Antiplatelet therapy: In search of the 'magic bullet'. *Nat. Rev. Drug Discov.* 2 (10), 775–789. doi:10.1038/nrd1198

Jiang, W. G., Watkins, G., Douglas-Jones, A., and Mansel, R. E. (2006). Reduction of isoforms of 15-lipoxygenase (15-LOX)-1 and 15-LOX-2 in human breast cancer. *Prostagl. Leukot. Essent. Fat. Acids* 74 (4), 235–245. doi:10.1016/j.plefa.2006.01.009

Kaduce, T. L., Fang, X., Harmon, S. D., Oltman, C. L., Dellsperger, K. C., Teesch, L. M., et al. (2004). 20-hydroxyeicosatetraenoic acid (20-HETE) metabolism in coronary endothelial cells. *J. Biol. Chem.* 279 (4), 2648–2656. doi:10.1074/jbc.M306849200

Ketelhuth, D. F., Hermansson, A., Hlawaty, H., Letourneur, D., Yan, Z-Q., and Bäck, M. (2015). The leukotriene B4 receptor (BLT) antagonist BIIL284 decreases atherosclerosis in ApoE-/- mice. *Prostagl. Other Lipid Mediat* 121, 105–109. doi:10.1016/j.prostaglandins.2015.05.007

Khanapure, S. P., Garvey, D. S., Janero, D. R., and Letts, L. G. (2007). Eicosanoids in inflammation: Biosynthesis, pharmacology, and therapeutic frontiers. *Curr. Top. Med. Chem.* 7 (3), 311–340. doi:10.2174/156802607779941314

Kobayashi, T., Tahara, Y., Matsumoto, M., Iguchi, M., Sano, H., Murayama, T., et al. (2004). Roles of thromboxane A(2) and prostacyclin in the development of atherosclerosis in apoE-deficient mice. *J. Clin. Invest* 114 (6), 784–794. doi:10.1172/JCI21446

Krishnamoorthy, S., Recchiuti, A., Chiang, N., Yacoubian, S., Lee, C. H., Yang, R., et al. (2010). Resolvin D1 binds human phagocytes with evidence for proresolving receptors. *Proc. Natl. Acad. Sci. U. S. A.* 107 (4), 1660–1665. doi:10.1073/pnas.0907342107

Kuhn, H., Banthiya, S., and van Leyen, K. (2015). Mammalian lipoxygenases and their biological relevance. *Biochim. Biophys. Acta* 1851 (4), 308–330. doi:10.1016/j.bbalip.2014.10.002

Lagarde, M., Bernoud-Hubac, N., Calzada, C., Véricel, E., and Guichardant, M. (2013). Lipidomics of essential fatty acids and oxygenated metabolites. *Mol. Nutr. Food Res.* 57 (8), 1347–1358. doi:10.1002/mnfr.201200828

Lagarde, M., Guichardant, M., Bernoud-Hubac, N., Calzada, C., and Véricel, E. (2018). Oxygenation of polyunsaturated fatty acids and oxidative stress within blood platelets. *Biochim. Biophys. Acta Mol. Cell Biol. Lipids* 1863 (6), 651–656. doi:10.1016/j.bbalip.2018.03.005

Laguna-Fernandez, A., Checa, A., Carracedo, M., Artiach, G., Petri, M. H., Baumgartner, R., et al. (2018). ERV1/ChemR23 signaling protects against atherosclerosis by modifying oxidized low-density lipoprotein uptake and phagocytosis in macrophages. *Circulation* 138 (16), 1693–1705. doi:10.1161/CIRCULATIONAHA.117.032801

Lannan, K. L., Spinelli, S. L., Blumberg, N., and Phipps, R. P. (2017). Maresin 1 induces a novel pro-resolving phenotype in human platelets. *J. Thromb. Haemost.* 15 (4), 802–813. doi:10.1111/jth.13620

Li, P-L., and Campbell, W. B. (1997). Epoxyeicosatrienoic acids activate K+ channels in coronary smooth muscle through a guanine nucleotide binding protein. *Circ. Res.* 80 (6), 877–884. doi:10.1161/01.res.80.6.877

Libreros, S., Shay, A. E., Nshimiyimana, R., Fichtner, D., Martin, M. J., Wourms, N., et al. (2020). A new E-series resolvin: RvE4 stereochemistry and function in efferocytosis of inflammation-resolution. *Front. Immunol.* 11, 631319. doi:10.3389/fimmu.2020.631319

Liu, Y., Zhang, Y., Schmelzer, K., Lee, T. S., Fang, X., Zhu, Y., et al. (2005). The antiinflammatory effect of laminar flow: The role of PPARgamma, epoxyeicosatrienoic acids, and soluble epoxide hydrolase. *Proc. Natl. Acad. Sci. U. S. A.* 102 (46), 16747–16752. doi:10.1073/pnas.0508081102

Lundqvist, A., Sandstedt, M., Sandstedt, J., Wickelgren, R., Hansson, G. I., Jeppsson, A., et al. (2016). The arachidonate 15-lipoxygenase enzyme product 15-HETE is present in Heart tissue from patients with ischemic Heart disease and enhances clot formation. *PLoS One* 11 (8), e0161629. doi:10.1371/journal.pone.0161629

Luo, W., Liu, B., and Zhou, Y. (2016). The endothelial cyclooxygenase pathway: Insights from mouse arteries. *Eur. J. Pharmacol.* 780, 148–158. doi:10.1016/j.ejphar.2016.03.043

Luttmann, W., Herzog, V., Matthys, H., Thierauch, K-H., Virchow, J. C., and Kroegel, C. (1999). Modulation of cytokine release from mononuclear cells by prostacyclin, IL-4 and IL-13. *Cytokine* 11 (2), 127–133. doi:10.1006/cyto.1998.0410

Luttmann, W., Herzog, V., Virchow, J-C., Jr, Matthys, H., Thierauch, K-H., and Kroegel, C. (1996). Prostacyclin modulates granulocyte/macrophage colony-stimulating factor release by human blood mononuclear cells. *Pulm. Pharmacol.* 9 (1), 43–48. doi:10.1006/pulp.1996.0005

Ma, K., Nunemaker, C. S., Wu, R., Chakrabarti, S. K., Taylor-Fishwick, D. A., and Nadler, J. L. (2010). 12-Lipoxygenase products reduce insulin secretion and {beta}-Cell viability in human islets. *J. Clin. Endocrinol. Metab.* 95 (2), 887–893. doi:10.1210/jc.2009-1102

Mainka, M., George, S., Angioni, C., Ebert, R., Goebel, T., Kampschulte, N., et al. (2022). On the biosynthesis of specialized pro-resolving mediators in human neutrophils and the influence of cell integrity. *Biochim. Biophys. Acta Mol. Cell Biol. Lipids* 1867 (3), 159093. doi:10.1016/j.bbalip.2021.159093

Mandras, S., Kovacs, G., Olschewski, H., Broderick, M., Nelsen, A., Shen, E., et al. (2021). Combination therapy in pulmonary arterial hypertension-targeting the nitric oxide and prostacyclin pathways. *J. Cardiovasc Pharmacol. Ther.* 26 (5), 453–462. doi:10.1177/10742484211006531

Minno, G. D., Silver, M., and Gaetano, G. D. (1979). Prostaglandins as inhibitors of human platelet aggregation. *Br. J. Haematol.* 43 (4), 637–647. doi:10.1111/j.1365-2141.1979.tb03797.x

Miyahara, T., Runge, S., Chatterjee, A., Chen, M., Mottola, G., Fitzgerald, J. M., et al. (2013). D-series resolvin attenuates vascular smooth muscle cell activation and neointimal hyperplasia following vascular injury. *Faseb J.* 27 (6), 2220–2232. doi:10.1096/fj.12-225615

Miyata, N., and Roman, R. J. (2005). Role of 20-hydroxyeicosatetraenoic acid (20-HETE) in vascular system. *J. Smooth Muscle Res.* 41 (4), 175–193. doi:10.1540/jsmr.41.175

Muthalif, M. M., Benter, I. F., Khandekar, Z., Gaber, L., Estes, A., Malik, S., et al. (2000). Contribution of Ras GTPase/MAP kinase and cytochrome P450 metabolites to deoxycorticosterone-salt-induced hypertension. *Hypertension* 35 (1), 457–463. doi:10.1161/01.hyp.35.1.457

Nagahora, N., Yamada, H., Kikuchi, S., Hakozaki, M., and Yano, A. (2017). Nrf2 activation by 5-lipoxygenase metabolites in human umbilical vascular endothelial cells. *Nutrients* 9 (9), 1001. doi:10.3390/nu9091001

Node, K., Huo, Y., Ruan, X., Yang, B., Spiecker, M., Ley, K., et al. (1999). Anti-inflammatory properties of cytochrome P450 epoxygenase-derived eicosanoids. *Science* 285 (5431), 1276–1279. doi:10.1126/science.285.5431.1276

Obara, K., Koide, M., and Nakayama, K. (2002). 20-Hydroxyeicosatetraenoic acid potentiates stretch-induced contraction of canine basilar artery via PKC alpha-mediated inhibition of KCa channel. *Br. J. Pharmacol.* 137 (8), 1362–1370. doi:10.1038/sj.bjp.0704960

Oh, S. F., Dona, M., Fredman, G., Krishnamoorthy, S., Irimia, D., and Serhan, C. N. (2012). Resolvin E2 formation and impact in inflammation resolution. *J. Immunol.* 188 (9), 4527–4534. doi:10.4049/jimmunol.1103652

Ohira, T., Arita, M., Omori, K., Recchiuti, A., Van Dyke, T. E., and Serhan, C. N. (2010). Resolvin E1 receptor activation signals phosphorylation and phagocytosis. *J. Biol. Chem.* 285 (5), 3451–3461. doi:10.1074/jbc.M109.044131

Palmblad, J., Lerner, R., and Larsson, S. H. (1994). Signal transduction mechanisms for leukotriene B4 induced hyperadhesiveness of endothelial cells for neutrophils. *J. Immunol.* 152 (1), 262–269.

Pan, W. H., Hu, X., Chen, B., Xu, Q. C., and Mei, H. X. (2022). The effect and mechanism of lipoxin A4 on neutrophil function in LPS-induced Lung injury. *Inflammation* 1, 1. doi:10.1007/s10753-022-01666-5

Patricia, M. K., Kim, J. A., Harper, C. M., Shih, P. T., Berliner, J. A., Natarajan, R., et al. (1999). Lipoxygenase products increase monocyte adhesion to human aortic endothelial cells. *Arterioscler. Thromb. Vasc. Biol.* 19 (11), 2615–2622. doi:10.1161/01.atv.19.11.2615

Perry, S. C., Kalyanaraman, C., Tourdot, B. E., Conrad, W. S., Akinkugbe, O., Freedman, J. C., et al. (2020). 15-Lipoxygenase-1 biosynthesis of 7S,14S-diHDHA implicates 15-lipoxygenase-2 in biosynthesis of resolvin D5. *J. Lipid Res.* 61 (7), 1087–1103. doi:10.1194/jlr.RA120000777

Poeckel, D., and Funk, C. D. (2010). The 5-lipoxygenase/leukotriene pathway in preclinical models of cardiovascular disease. *Cardiovasc Res.* 86 (2), 243–253. doi:10.1093/cvr/cvq016

Pollock, K., and Creba, J. (1990). Leukotriene D4 induced calcium changes in U937 cells may utilize mechanisms additional to inositol phosphate production that are pertussis toxin insensitive but are blocked by phorbol myristate acetate. *Cell Signal* 2 (6), 563–568. doi:10.1016/0898-6568(90)90078-o

Praticò, D., and Dogné, J-M. (2009). Vascular biology of eicosanoids and atherogenesis. *Expert Rev. Cardiovasc Ther.* 7 (9), 1079–1089. doi:10.1586/erc.09.91

Randriamboavonjy, V., Busse, R., and Fleming, I. (2003). 20-HETE-induced contraction of small coronary arteries depends on the activation of Rho-kinase. *Hypertension* 41 (1), 801–806. doi:10.1161/01.HYP.0000047240.33861.6B

Recchiuti, A., and Serhan, C. N. (2012). Pro-resolving lipid mediators (SPMs) and their actions in regulating miRNA in novel resolution circuits in inflammation. *Front. Immunol.* 3, 298. doi:10.3389/fimmu.2012.00298

Riccioni, G., Bäck, M., and Capra, V. (2010). Leukotrienes and atherosclerosis. *Curr. Drug Targets* 11 (7), 882–887. doi:10.2174/138945010791320881

Ricciotti, E., and FitzGerald, G. A. (2011). Prostaglandins and inflammation. *Arterioscler. Thromb. Vasc. Biol.* 31 (5), 986–1000. doi:10.1161/ATVBAHA.110.207449

Ricke-Hoch, M., Stelling, E., Lasswitz, L., Gunesch, A. P., Kasten, M., Zapatero-Belinchón, F. J., et al. (2021). Impaired immune response mediated by prostaglandin E2 promotes severe COVID-19 disease. *PloS one* 16 (8), e0255335. doi:10.1371/journal.pone.0255335

Salic, K., Morrison, M. C., Verschuren, L., Wielinga, P. Y., Wu, L., Kleemann, R., et al. (2016). Resolvin E1 attenuates atherosclerosis in absence of cholesterol-lowering effects and on top of atorvastatin. *Atherosclerosis* 250, 158–165. doi:10.1016/j.atherosclerosis.2016.05.001

Sánchez-Galán, E., Gómez-Hernández, A., Vidal, C., Martín-Ventura, J. L., Blanco-Colio, L. M., Muñoz-García, B., et al. (2009). Leukotriene B4 enhances the activity of nuclear factor-kappaB pathway through BLT1 and BLT2 receptors in atherosclerosis. *Cardiovasc Res.* 81 (1), 216–225.

Scalia, R., Gefen, J., Petasis, N. A., Serhan, C. N., and Lefer, A. M. (1997). Lipoxin A4 stable analogs inhibit leukocyte rolling and adherence in the rat mesenteric microvasculature: Role of P-selectin. *Proc. Natl. Acad. Sci. U. S. A.* 94 (18), 9967–9972. doi:10.1073/pnas.94.18.9967

Schebb, N. H., Kühn, H., Kahnt, A. S., Rund, K. M., O'Donnell, V. B., Flamand, N., et al. (2022). Formation, signaling and occurrence of specialized pro-resolving lipid mediators-what is the evidence so far? *Front. Pharmacol.* 13, 838782. doi:10.3389/fphar.2022.838782

Schmid, T., and Brüne, B. (2021). Prostanoids and resolution of inflammation–beyond the lipid-mediator class switch. *Front. Immunol.* 12, 2838. doi:10.3389/fimmu.2021.714042

Schmöcker, C., Zhang, I. W., Kiesler, S., Kassner, U., Ostermann, A. I., Steinhagen-Thiessen, E., et al. (2018). Effect of omega-3 fatty acid supplementation on oxylipins in a routine clinical setting. *Int. J. Mol. Sci.* 19 (1), 180. doi:10.3390/ijms19010180

Schrör, K., and Rauch, B. H. (2015). Aspirin and lipid mediators in the cardiovascular system. *Prostagl. Other Lipid Mediat* 121 (1), 17–23.

Schuchardt, J. P., Schmidt, S., Kressel, G., Willenberg, I., Hammock, B. D., Hahn, A., et al. (2014). Modulation of blood oxylipin levels by long-chain omega-3 fatty acid supplementation in hyper- and normolipidemic men. *Prostagl. Leukot. Essent. Fat. Acids* 90 (2-3), 27–37. doi:10.1016/j.plefa.2013.12.008

Schuligoi, R., Sturm, E., Luschnig, P., Konya, V., Philipose, S., Sedej, M., et al. (2010). CRTH2 and D-type prostanoid receptor antagonists as novel therapeutic agents for inflammatory diseases. *Pharmacology* 85 (6), 372–382. doi:10.1159/000313836

Schwartzman, M. L., Falck, J., Yadagiri, P., and Escalante, B. (1989). Metabolism of 20-hydroxyeicosatetraenoic acid by cyclooxygenase. Formation and identification of novel endothelium-dependent vasoconstrictor metabolites. *J. Biol. Chem.* 264 (20), 11658–11662. doi:10.1016/s0021-9258(18)80115-6

Serezani, C. H., Lewis, C., Jancar, S., and Peters-Golden, M. (2011). Leukotriene B4 amplifies NF-κB activation in mouse macrophages by reducing SOCS1 inhibition of MyD88 expression. *J. Clin. Invest* 121 (2), 671–682. doi:10.1172/JCI43302

Sergeant, S., Rahbar, E., and Chilton, F. H. (2016). Gamma-linolenic acid, dihommo-gamma linolenic, eicosanoids and inflammatory processes. *Eur. J. Pharmacol.* 785, 77–86. doi:10.1016/j.ejphar.2016.04.020

Serhan, C. N., Dalli, J., Colas, R. A., Winkler, J. W., and Chiang, N. (2015). Protectins and maresins: New pro-resolving families of mediators in acute inflammation and resolution bioactive metabolome. *Biochim. Biophys. Acta* 1851 (4), 397–413. doi:10.1016/j.bbalip.2014.08.006

Serhan, C. N., Fredman, G., Yang, R., Karamnov, S., Belayev, L. S., Bazan, N. G., et al. (2011). Novel proresolving aspirin-triggered DHA pathway. *Chem. Biol.* 18 (8), 976–987. doi:10.1016/j.chembiol.2011.06.008

Serhan, C. N., Krishnamoorthy, S., Recchiuti, A., and Chiang, N. (2011). Novel anti-inflammatory--pro-resolving mediators and their receptors. *Curr. Top. Med. Chem.* 11 (6), 629–647. doi:10.2174/1568026611109060629

Serhan, C. N., and Levy, B. D. (2018). Resolvins in inflammation: Emergence of the pro-resolving superfamily of mediators. *J. Clin. Invest* 128 (7), 2657–2669. doi:10.1172/JCI97943

Serhan, C. N. (2005). Lipoxins and aspirin-triggered 15-epi-lipoxins are the first lipid mediators of endogenous anti-inflammation and resolution. *Prostagl. Leukot. Essent. Fat. Acids* 73 (3-4), 141–162. doi:10.1016/j.plefa.2005.05.002

Serhan, C. N., and Petasis, N. A. (2011). Resolvins and protectins in inflammation resolution. *Chem. Rev.* 111 (10), 5922–5943. doi:10.1021/cr100396c

Serhan, C. N., Yang, R., Martinod, K., Kasuga, K., Pillai, P. S., Porter, T. F., et al. (2009). Maresins: Novel macrophage mediators with potent antiinflammatory and proresolving actions. *J. Exp. Med.* 206 (1), 15–23. doi:10.1084/jem.20081880

Setty, B. N., and Stuart, M. J. (1986). 15-Hydroxy-5,8,11,13-eicosatetraenoic acid inhibits human vascular cyclooxygenase. Potential role in diabetic vascular disease. *J. Clin. Invest* 77 (1), 202–211. doi:10.1172/JCI112277

Singh, H., Cheng, J., Deng, H., Kemp, R., Ishizuka, T., Nasjletti, A., et al. (2007). Vascular cytochrome P450 4A expression and 20-hydroxyeicosatetraenoic acid synthesis contribute to endothelial dysfunction in androgen-induced hypertension. *Hypertension* 50 (1), 123–129. doi:10.1161/HYPERTENSIONAHA.107.089599

Sitbon, O., Channick, R., Chin, K. M., Frey, A., Gaine, S., Galiè, N., et al. (2015). Selexipag for the treatment of pulmonary arterial hypertension. *N. Engl. J. Med.* 373 (26), 2522–2533. doi:10.1056/NEJMoa1503184

Sonnweber, T., Pizzini, A., Nairz, M., Weiss, G., and Tancevski, I. (2018). Arachidonic acid metabolites in cardiovascular and metabolic diseases. *Int. J. Mol. Sci.* 19 (11), 3285. doi:10.3390/ijms19113285

Spiecker, M., and Liao, J. K. (2005). Vascular protective effects of cytochrome p450 epoxygenase-derived eicosanoids. *Arch. Biochem. Biophys.* 433 (2), 413–420. doi:10.1016/j.abb.2004.10.009

Tager, A. M., Bromley, S. K., Medoff, B. D., Islam, S. A., Bercury, S. D., Friedrich, E. B., et al. (2003). Leukotriene B4 receptor BLT1 mediates early effector T cell recruitment. *Nat. Immunol.* 4 (10), 982–990. doi:10.1038/ni970

Tager, A. M., Dufour, J. H., Goodarzi, K., Bercury, S. D., von Andrian, U. H., and Luster, A. D. (2000). BLTR mediates leukotriene B(4)-induced chemotaxis and adhesion and plays a dominant role in eosinophil accumulation in a murine model of peritonitis. *J. Exp. Med.* 192 (3), 439–446. doi:10.1084/jem.192.3.439

Takata, S., Matsubara, M., Allen, P. G., Janmey, P. A., Serhan, C. N., and Brady, H. R. (1994). Remodeling of neutrophil phospholipids with 15(S)-hydroxyeicosatetraenoic acid inhibits leukotriene B4-induced neutrophil migration across endothelium. *J. Clin. Invest* 93 (2), 499–508. doi:10.1172/JCI116999

Ternowitz, T., Fogh, K., and Kragballe, K. (1988). 15-Hydroxyeicosatetraenoic acid (15-HETE) specifically inhibits LTB4-induced chemotaxis of human neutrophils. *Skin. Pharmacol.* 1 (2), 93–99. doi:10.1159/000210754

Toda, A., Terawaki, K., Yamazaki, S., Saeki, K., Shimizu, T., and Yokomizo, T. (2010). Attenuated Th1 induction by dendritic cells from mice deficient in the leukotriene B4 receptor 1. *Biochimie* 92 (6), 682–691. doi:10.1016/j.biochi.2009.12.002

Toda, A., Yokomizo, T., and Shimizu, T. (2002). Leukotriene B4 receptors. *Prostagl. Other Lipid Mediat* 68-69, 575–585. doi:10.1016/s0090-6980(02)00056-4

Tourdot, B. E., Adili, R., Isingizwe, Z. R., Ebrahem, M., Freedman, J. C., Holman, T. R., et al. (2017). 12-HETrE inhibits platelet reactivity and thrombosis in part through the prostacyclin receptor. *Blood Adv.* 1 (15), 1124–1131. doi:10.1182/bloodadvances.2017006155

Tourdot, B. E., and Holinstat, M. (2017). Targeting 12-lipoxygenase as a potential novel antiplatelet therapy. *Trends Pharmacol. Sci.* 38 (11), 1006–1015. doi:10.1016/j.tips.2017.08.001

Tull, S. P., Yates, C. M., Maskrey, B. H., O'Donnell, V. B., Madden, J., Grimble, R. F., et al. (2009). Omega-3 fatty acids and inflammation: Novel interactions reveal a new step in neutrophil recruitment. *PLoS Biol.* 7 (8), e1000177. doi:10.1371/journal.pbio.1000177

Van Doren, L., Nguyen, N., Garzia, C., Fletcher, E., Stevenson, R., Jaramillo, D., et al. (2019). Blockade of lipid receptor GPR31 suppresses platelet reactivity and thrombosis with minimal effect on hemostasis. *Blood* 134, 1064. doi:10.1182/blood-2019-126111

Van Doren, L., Nguyen, N., Garzia, C., Fletcher, E. K., Stevenson, R., Jaramillo, D., et al. (2021). Lipid receptor GPR31 (G-Protein-Coupled receptor 31) regulates platelet reactivity and thrombosis without affecting hemostasis. *Arterioscler. Thromb. Vasc. Biol.* 41 (1), e33–e45. doi:10.1161/ATVBAHA.120.315154

Vanderhoek, J. Y., Schoene, N. W., and Pham, P. P. (1991). Inhibitory potencies of fish oil hydroxy fatty acids on cellular lipoxygenases and platelet aggregation. *Biochem. Pharmacol.* 42 (4), 959–962. doi:10.1016/0006-2952(91)90062-a

Vane, J., Bakhle, Y., and Botting, R. (1998). Cyclooxygenases 1 and 2. *Annu. Rev. Pharmacol. Toxicol.* 38 (1), 97–120. doi:10.1146/annurev.pharmtox.38.1.97

Vijil, C., Hermansson, C., Jeppsson, A., Bergström, G., and Hultén, L. M. (2014). Arachidonate 15-lipoxygenase enzyme products increase platelet aggregation and thrombin generation. *PLoS One* 9 (2), e88546. doi:10.1371/journal.pone.0088546

Wang, D., and Dubois, R. N. (2010). Eicosanoids and cancer. *Nat. Rev. Cancer* 10 (3), 181–193. doi:10.1038/nrc2809

Werz, O., Gerstmeier, J., Libreros, S., De la Rosa, X., Werner, M., Norris, P. C., et al. (2018). Human macrophages differentially produce specific resolvin or leukotriene signals that depend on bacterial pathogenicity. *Nat. Commun.* 9 (1), 59. doi:10.1038/s41467-017-02538-5

Whatling, C., McPheat, W., and Herslöf, M. (2007). The potential link between atherosclerosis and the 5-lipoxygenase pathway: Investigational agents with new implications for the cardiovascular field. *Expert Opin. Investig. Drugs* 16 (12), 1879–1893. doi:10.1517/13543784.16.12.1879

Whitaker, M. O., Wyche, A., Fitzpatrick, F., Sprecher, H., and Needleman, P. (1979). Triene prostaglandins: Prostaglandin D3 and icosapentaenoic acid as potential antithrombotic substances. *Proc. Natl. Acad. Sci. U. S. A.* 76 (11), 5919–5923. doi:10.1073/pnas.76.11.5919

Woszczek, G., Chen, L-Y., Nagineni, S., Alsaaty, S., Harry, A., Logun, C., et al. (2007). IFN-gamma induces cysteinyl leukotriene receptor 2 expression and enhances the responsiveness of human endothelial cells to cysteinyl leukotrienes. *J. Immunol.* 178 (8), 5262–5270. doi:10.4049/jimmunol.178.8.5262

Yamaguchi, A., Stanger, L., Freedman, C., Prieur, A., Thav, R., Tena, J., et al. (2022). Supplementation with omega-3 or omega-6 fatty acids attenuates platelet reactivity in postmenopausal women. *Clin. Transl. Sci.* 1, 1.

Yeung, J., Adili, R., Yamaguchi, A., Freedman, C. J., Chen, A., Shami, R., et al. (2020). Omega-6 DPA and its 12-lipoxygenase-oxidized lipids regulate platelet reactivity in a nongenomic PPARα-dependent manner. *Blood Adv.* 4 (18), 4522–4537. doi:10.1182/bloodadvances.2020002493

Yeung, J., Hawley, M., and Holinstat, M. (2017). The expansive role of oxylipins on platelet biology. *J. Mol. Med. Berl.* 95 (6), 575–588. doi:10.1007/s00109-017-1542-4

Yeung, J., and Holinstat, M. (2011). 12-lipoxygenase: A potential target for novel anti-platelet therapeutics. *Cardiovasc Hematol. Agents Med. Chem.* 9 (3), 154–164. doi:10.2174/187152511797037619

Yeung, J., and Holinstat, M. (2017). Who is the real 12-HETrE? *Prostagl. Other Lipid Mediat* 132, 25–30. doi:10.1016/j.prostaglandins.2017.02.005

Yeung, J., Tourdot, B. E., Adili, R., Green, A. R., Freedman, C. J., Fernandez-Perez, P., et al. (2016). 12(S)-HETrE, a 12-lipoxygenase oxylipin of dihomo-γ-linolenic acid, inhibits thrombosis via Gαs signaling in platelets. *Arterioscler. Thromb. Vasc. Biol.* 36 (10), 2068–2077. doi:10.1161/ATVBAHA.116.308050

Yokomizo, T., Izumi, T., Chang, K., Takuwa, Y., and Shimizu, T. (1997). A G-protein-coupled receptor for leukotriene B4 that mediates chemotaxis. *Nature* 387 (6633), 620–624. doi:10.1038/42506

Yokomizo, T., Kato, K., Terawaki, K., Izumi, T., and Shimizu, T. (2000). A second leukotriene B(4) receptor, BLT2. A new therapeutic target in inflammation and immunological disorders. *J. Exp. Med.* 192 (3), 421–432. doi:10.1084/jem.192.3.421

Yokomizo, T., Nakamura, M., and Shimizu, T. (2018). Leukotriene receptors as potential therapeutic targets. *J. Clin. Invest* 128 (7), 2691–2701. doi:10.1172/JCI97946

Zhao, M., Ma, J., Li, M., Zhang, Y., Jiang, B., Zhao, X., et al. (2021). Cytochrome P450 enzymes and drug metabolism in humans. *Int. J. Mol. Sci.* 22 (23), 12808. doi:10.3390/ijms222312808

Zhou, W., Blackwell, T. S., Goleniewska, K., O'Neal, J. F., Fitzgerald, G. A., Lucitt, M., et al. (2007). Prostaglandin I2 analogs inhibit Th1 and Th2 effector cytokine production by CD4 T cells. *J. Leukoc. Biol.* 81 (3), 809–817. doi:10.1189/jlb.0606375

Zhou, W., Hashimoto, K., Goleniewska, K., O'Neal, J. F., Ji, S., Blackwell, T. S., et al. (2007). Prostaglandin I2 analogs inhibit proinflammatory cytokine production and T cell stimulatory function of dendritic cells. *J. Immunol.* 178 (2), 702–710. doi:10.4049/jimmunol.178.2.702

Zu, L., Guo, G., Zhou, B., and Gao, W. (2016). Relationship between metabolites of arachidonic acid and prognosis in patients with acute coronary syndrome. *Thromb. Res.* 144, 192–201. doi:10.1016/j.thromres.2016.06.031

frontiers | Frontiers in Pharmacology

TYPE Original Research
PUBLISHED 12 October 2022
DOI 10.3389/fphar.2022.995459

OPEN ACCESS

EDITED BY
Pallavi R. Devchand,
University of Calgary, Canada

REVIEWED BY
Ren Jun Guo,
Xiyuan Hospital, China
Frank Lammert,
Saarland University, Germany

*CORRESPONDENCE
Arjun Krishnan,
arjun.krishnan@cuanschutz.edu

†These authors have contributed equally to this work and share first authorship

SPECIALTY SECTION
This article was submitted to Inflammation Pharmacology, a section of the journal Frontiers in Pharmacology

RECEIVED 15 July 2022
ACCEPTED 19 August 2022
PUBLISHED 12 October 2022

CITATION
Hickey SL, McKim A, Mancuso CA and Krishnan A (2022), A network-based approach for isolating the chronic inflammation gene signatures underlying complex diseases towards finding new treatment opportunities. *Front. Pharmacol.* 13:995459. doi: 10.3389/fphar.2022.995459

A network-based approach for isolating the chronic inflammation gene signatures underlying complex diseases towards finding new treatment opportunities

Stephanie L. Hickey[1†], Alexander McKim[2,3†], Christopher A. Mancuso[2,4] and Arjun Krishnan[1,2,5*]

[1]Department of Biochemistry and Molecular Biology, Michigan State University, East Lansing, MI, United States, [2]Department of Computational Mathematics, Science and Engineering, Michigan State University, East Lansing, MI, United States, [3]Genetics and Genome Sciences Program, Michigan State University, East Lansing, MI, United States, [4]Department of Biostatistics and Informatics, Colorado School of Public Health, University of Colorado-Denver Anschutz Medical Campus, Aurora, CO, United States, [5]Department of Biomedical Informatics, University of Colorado Anschutz Medical Campus, Aurora, CO, United States

Complex diseases are associated with a wide range of cellular, physiological, and clinical phenotypes. To advance our understanding of disease mechanisms and our ability to treat these diseases, it is critical to delineate the molecular basis and therapeutic avenues of specific disease phenotypes, especially those that are associated with multiple diseases. Inflammatory processes constitute one such prominent phenotype, being involved in a wide range of health problems including ischemic heart disease, stroke, cancer, diabetes mellitus, chronic kidney disease, non-alcoholic fatty liver disease, and autoimmune and neurodegenerative conditions. While hundreds of genes might play a role in the etiology of each of these diseases, isolating the genes involved in the specific phenotype (e.g., inflammation "component") could help us understand the genes and pathways underlying this phenotype across diseases and predict potential drugs to target the phenotype. Here, we present a computational approach that integrates gene interaction networks, disease-/trait-gene associations, and drug-target information to accomplish this goal. We apply this approach to isolate gene signatures of complex diseases that correspond to chronic inflammation and use SAveRUNNER to prioritize drugs to reveal new therapeutic opportunities.

KEYWORDS

complex disease, inflammation, endophenotype, drug repurposing, network analysis, functional modules, disease modules

1 Introduction

Acute inflammation is an organism's healthy response to invasion by pathogens or to cellular damage caused by injury (Rock and Kono 2008). Systemic chronic inflammation (CI) occurs when these inflammatory responses do not resolve, resulting in persistent, low-grade immune activation that causes collateral damage to the affected tissue over time (Furman et al., 2019). While the direct connection of CI to autoimmune diseases has been well known for some time, only recently has the medical community uncovered the prevalence of CI in a multitude of complex diseases and disorders (Furman et al., 2019; Vos et al., 2020). Therefore, it is imperative to better understand the different molecular mechanisms of CI manifestation across diseases.

Network-based methods are powerful collection of tools for both elucidating specific pathways and processes that may underlie a complex phenotype (Ghiassian et al., 2015; Leiserson et al., 2015; Ghiassian et al., 2016) and for drug repurposing (Chen et al., 2015; Cheng et al., 2018; Fiscon and Paci 2021). For instance, HotNet2 is a pan-cancer network analysis tool that identifes active network modules in a genome-wide molecular network by guiding the module detection algorithm with thousands of genes scored by how prevalent they are across 12 cancers in TCGA (Leiserson et al., 2015). HotNet2 is then able to determine if any module is enriched for a given cancer type, pathway, or process. In a similar vein, another approach, DIAMOnD, starts with a genome-wide network, and then creates a disease-specific network using an expanded set of known disease-gene annotations (Ghiassian et al., 2015). This disease-specific network is then analyzed and compared to other disease-specific networks generated using the same technique. Both approaches find regions of a genome-wide network that are enriched for disease-related genes.

Inflammation is an example of an endophenotype, or intermediate phenotype, of a complex disease. Ghiassian *et al.* studied endophenotype network models by starting with a genome-wide network and constructing modules for sets of seed genes related to three endophenotypes: inflammation, thrombosis, and fibrosis (Ghiassian et al., 2016). The authors showed that the network modules derived from the three endophenotypes have strong overlap in the network and that these modules are enriched for genes differentially expressed in various complex diseases. While the above methods provide invaluable insight in disease mechanisms using a disease-focused and a phenotype-focused approach, respectively, they raise the critical question of identifying phenotypic signatures specific to individual diseases. For instance, can we identify the CI-signature that is specific to a given disease and use that to find avenues for therapeutic intervention?

In this work, we address this question using a network-based approach. We first generate a network consisting of only genes associated with a single disease (Figure 1A, steps 1–2) Here, like in DIAMOnD (Ghiassian et al., 2015), we expand our original disease-gene annotations to build more robust networks and glean insight into unstudied genes. We use a network-based supervised machine learning model, shown to systematically outperform label propagation methods like DIAMOnD, to expand our gene sets (Liu et al., 2020). We then cluster the disease-specific network, find clusters that are significantly enriched for known CI genes, and compare these CI signatures across diseases (Figures 1A,B steps 12). We then use the SAveRUNNER (Fiscon and Paci 2021) method on these enriched clusters to predict drugs that might help treat the CI-component specific to a given disease (Figure 1B, step 3).

2 Methods

2.1 Disease selection and disease-associated seed genes

2.1.1 Complex and autoimmune diseases

We searched the literature (Furman et al., 2019; Dregan et al., 2014; Armstrong et al., 2013; Yashiro 2014; Chou et al., 2016; Autoimmune Diseases: Causes, 2022) and curated examples of 17 complex diseases associated with chronic inflammation (CI) and nine common autoimmune diseases. Some of these diseases are quite broad (i.e "Malignant neoplasm of lung"), and to add more narrowly defined diseases to our list, we used the Human Disease Ontology (Schriml et al., 2019) to identify child terms of these diseases. The chosen diseases were not meant to be comprehensive, but examples of autoimmune diseases and complex diseases thought to have immune components. We then identified genes annotated to each disease by the DisGeNet database, which is a database that stores a collection of disease-gene annotations from expert curated repositories, GWAS catalogs, animal models and the scientific literature (Piñero et al., 2020). To ensure that our disease gene sets were largely non-overlapping, we created a network such that nodes were diseases, and an edge was created between two diseases if the two gene sets had ≥ 0.6 overlap ($|A \cap B| / \min(|A|, |B|)$). We then chose the most representative disease from each connected component. This resulted in 10 autoimmune diseases and 37 complex diseases (Supplementary Table S1).

2.1.2 Non-disease traits

Two lab members manually curated 113 non-disease-traits that are unlikely to be associated with CI (i.e. handedness, coffee intake, and average household income) from the list of traits with GWAS results from the UK Biobank (Sudlow et al., 2015) to be used as negative controls. Based on GWAS summary statistics

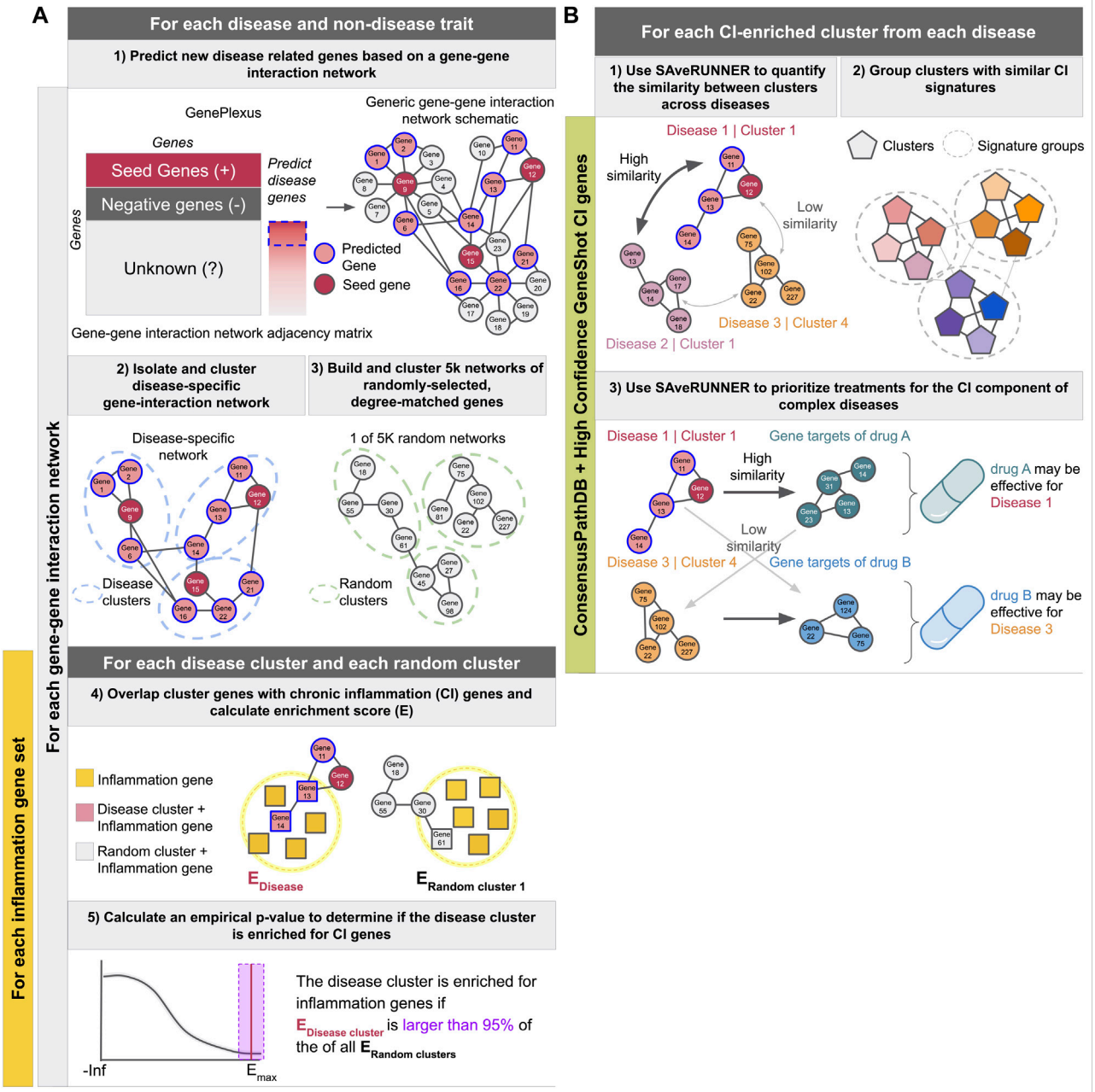

FIGURE 1
Schematics describing the experimental pipeline. **(A)** Describes predicting new disease related genes (step 1), clustering the disease-specific interaction network (step 2) as well as 5,000 networks made from randomly-selected degree-matched genes for each disease (step3), identifying CI-enriched clusters (steps 4 and 5), and calculating the proportion of diseases with at least one CI-enriched cluster. These steps were performed for each gene-gene interaction network in combination with each inflammation gene set described in the methods. **(B)** Describes using SAveRUNNER to find groups of CI-enriched clusters from all diseases with similar CI-signatures (steps 1 and 2), and prioritize treatments for the CI component of complex diseases (step 3). Using ConsensusPathDB with the high-confidence GeneShot derived CI gene set resulted in the highest proportion of autoimmune diseases and the lowest proportion of non-disease traits with at least one CI-enriched cluster. Therefore, steps one to three were performed with clusters from that network-CI gene set combination only.

from the Neale group (Abbot et al., 2021), we used Pascal (Lamparter et al., 2016) (upstream and downstream windows of 50 KB with the sum-of-chi-squared statistics method; only autosomal variants) to associate genes with the non-disease traits. Genes with $p < 0.001$ were included as seed genes for that trait.

2.2 GenePlexus

To predict new genes associated with a set of input seed genes, we used GenePlexus, a tool that builds an L2-regularized logistic regression model using features from a gene interaction network (Liu et al., 2020). As input features, we used the adjacency matrices from STRING, STRING with only experimentally derived edges (STRING-EXP) (Szklarczyk et al., 2017), BioGRID (Stark et al., 2006), and ConsensusPathDB (Kamburov et al., 2013). For predicting disease genes, positive examples were disease/trait seed genes and negative example genes were generated by: (i) finding the union of all genes annotated to all diseases in DisGeNET (Piñero et al., 2020), (ii) removing genes annotated to the given seed genes, and (iii) removing genes annotated to any disease in the collection that significantly overlapped with the given seed genes ($p < 0.05$ based on the one-sided Fisher's exact test) (Liu et al., 2020). We tested the performance of the above features for predicting new genes associated with our diseases and traits of interest using three-fold cross validation and only included diseases in subsequent analyses if the diseases/traits had ≥ 15 associated genes and median $log_2(auPRC/prior) \geq 1$ (i.e. the area under the precision-recall curve 'auPRC' is at least twice as much as expected by random chance 'prior' (Liu et al., 2020)). See Figure 1A, step 1 and Supplementary Table S1.

2.3 Identifying clusters of interacting genes within a disease-specific network

One list of disease-associated genes was formed for each of the four biological networks used as features in GenePlexus. Specifically, we added genes with a GenePlexus prediction probability of ≥ 0.80 on the network of interest to the original disease or trait seed gene list to create our final set of associated genes for each disease or trait for that network. We formed disease-/trait-specific networks by subsetting a given network to include only the disease-/trait-associated genes and any edges directly connecting those genes (Figure 1A, step 2). We tested five prediction-network—cluster-network combinations: Genes predicted on each of the four networks were clustered on the same network. Genes predicted on STRING were also clustered on both STRING and STRING-EXP to test if using the full network for novel gene prediction but only experimentally derived gene-gene associations for clustering would improve performance. We then used the Leiden algorithm (Traag et al., 2019) to partition the disease-/trait-specific networks into clusters (Figure 1A, step 2). Specifically, we used the *leiden_find_partition* function from the leidenbase R package (v 0.1.3) (https://github.com/cole-trapnell-lab/leidenbase) with 100 iterations and *ModularityVertexPartition* as the partition type. We retained clusters containing ≥ 5 genes.

2.4 Cluster GOBP enrichment analysis

We used the R package topGO with the "weight01" algorithm and Fisher testing (Alexa and Rahnenfuhrer 2022) (v 2.44.0) to find enrichment of genes annotated to GO biological processes (min size = 5, max size = 100) among disease gene clusters. The annotations were taken from the Genome wide annotation for Human bioconductor annotation package, org.Hs.eg.db (Carlson 2019) (v 3.13.0). The background gene set included all human genes present in the network of interest. This was performed for every prediction/clustering method combination.

2.5 Isolating CI-associated disease clusters

2.5.1 Defining CI-associated genes

We tested several different sets of chronic inflammation associated genes for this study including the GO biological process (GOBP) terms GO:0002544 ("chronic inflammatory response") and GO:0006954 ("inflammatory response"). These were collected from the *Genome wide annotation for Human* bioconductor annotation package, org. Hs.eg.db (Carlson 2019) (v 3.13.0) with and without propagation of gene-term relationships from the descendent terms (org.Hs.egGO2ALLEGS and org.Hs.egGO2EG, respectively). GO:0006954 was also filtered to retain gene-term relationships inferred from experiments (evidence codes EXP, IDA, IPI, IMP, IGI, IEP, HTP, HDA, HMP, HGI, and HEP). As GO:0002544 without propagation contained < 15 genes, this list was ultimately not included in the study. We also identified genes associated with chronic inflammation using Geneshot which, given the search term "chronic inflammation", searches Pubmed using manually collected GeneRif gene-term associations to return a ranked list containing genes that have been previously published in association with the search term (Lachmann et al., 2019). We tested both the entire Geneshot generated list, and the subset of genes with > 10 associated publications ("High-confidence GeneShot"). As with the disease genes, we predicted additional chronic-inflammation-associated genes using GenePlexus with features from each network. Negative examples for GenePlexus were derived from non-overlapping GOBP terms. We added genes with a prediction probability of ≥ 0.80 to the seed gene list to create our final sets of CI-associated genes.

2.5.2 Creating random traits

After running GenePlexus to predict new genes for each trait, the gene lists for each trait were used to generate 5,000 random gene lists that have matching node degree distributions to the original traits (Figure 1A, step 3). That is, a random gene list was generated for a given trait by replacing each of its genes in the network of interest with a (randomly chosen) gene that has the

same node degree, or a gene that has a close node degree if there are a small number of genes with the exact node degree (Leiserson et al., 2015; Fiscon and Paci 2021). We clustered the random traits as described in Section 2.3. Only clusters with at least five genes were included. Real traits with no corresponding permuted traits with clusters containing at least five genes were excluded from the analysis.

2.5.3 Finding CI-gene enriched disease clusters

For each prediction-network—cluster-network pair and each CI gene list expanded on the prediction network of interest, for each disease and random trait cluster containing ≥ 5 genes, we calculated an enrichment score:

$$E = log_2\left(\frac{(CG \cap CI)/CG}{CI/background}\right)$$

where CG are the genes in a disease cluster, CI are the CI genes, and background is all the genes present in the clustering network (Figure 1A, step 4). For each real disease or trait cluster, we used the matching random trait clusters to calculate a p-value:

$$p = \frac{\sum_{i=1}^{n} x_i}{n+1}$$

where n is the number of random trait clusters from all 5k matching random traits, and

$$x_i = \begin{cases} 1, & E_{random\ cluster\ i} \geq E_{disease\ cluster} \\ 0, & E_{random\ cluster\ i} < E_{disease\ cluster} \end{cases}$$

We corrected for multiple comparisons across clusters within a disease using the Benjamini–Hochberg procedure (Benjamini and Yosef 1995) (Figure 1A, step 5). Clusters with an $FDR < 0.05$ and $E > 0$ were considered chronic-inflammation-associated disease clusters and were deemed to represent the 'CI signature' of the disease.

2.5.4 Identifying the optimal prediction-network/cluster-network/CI gene source combination

We chose the network/inflammation gene set combination that resulted in the highest proportion of autoimmune diseases and lowest proportion of non-disease traits with at least one CI-enriched cluster of any network/CI-gene set combination, ConsensusPathDB and the high-confidence Geneshot generated list.

2.5.5 Comparing CI-signatures across diseases

For CI-enriched clusters identified using ConsensusPathDB and the high-confidence Geneshot CI genes, we used the SAveRUNNER R package to quantify the similarity between each pair of CI-enriched clusters using ConsensusPathDB as the base network (Fiscon and Paci 2021) (Figure 1B, step 1). For each pair, SAveRUNNER computes the average shortest path between each gene in cluster A and the closest gene in cluster B and uses this value to calculate an adjusted similarity score. Then, a p-value is estimated based on a null distribution of adjusted similarity scores between randomly generated clusters with the same node degree distributions as clusters A and B. Because the similarity scores and p-values are not symmetric (i.e., $A \rightarrow B \neq B \rightarrow A$) we used Stouffer's method to combine p-values for the same pair of clusters and averaged the adjusted similarities. We then used the Leiden algorithm as described in Section 2.3 to group related clusters (Figure 1B, step 2). For each group, we took the union of the genes belonging to the resident CI-enriched clusters. Using genes unique to each group, with all the ConsensusPathDB genes as background, we used TopGO as in Section 2.4 to identify enriched GOBPs.

2.6 Predicting novel treatment opportunities

2.6.1 Identifying expert-curated drug-target associations

The known drug-gene interactions used in this study are the subset of the interactions present in the DrugCentral database (Avram et al., 2021) that are also among the expert curated interactions in the Drug-Gene Interaction database (DGIdb) (Freshour et al., 2021). Specifically, we used the DGIdb API to retrieve only drug-gene interactions that were marked "*Expert curated*" (based on the source trust levels endpoint). Intersecting these interactions with those in DrugCentral (through a list of drug synonyms from DrugCentral) resulted in the final list of expert-curated drug-gene pairs.

2.6.2 Treatment prediction and scoring

We predicted treatment opportunities for the inflammatory component of complex diseases by using the SAveRUNNER R package (Fiscon and Paci 2021) (Figure 1B, step 3). SAveRUNNER builds a bipartite drug-disease network by utilizing the previously determined expert-curated drug targets, the CI-associated cluster disease genes, and the ConsensusPathDB network as a human interactome. Network similarity scores returned by SAveRUNNER represent the proximity between disease and drug modules, where a high similarity score means that the disease and drug modules have high proximity in ConsensusPathDB. SAveRUNNER calculates a p-value where a significant value suggest that the disease genes and drug targets closer in the network than expected by chance (based on an empirical null distribution built using 200 pairs of randomly selected groups of genes with the same size and degree distribution of the original sets of disease genes and drug targets). Using the list of final predicted associations after normalization of network similarity, the p-values were corrected for multiple comparisons within each disease using the Benjamini–Hochberg

procedure. Drugs were associated to diseases based on the disease cluster with the lowest FDR. Predicted treatments are disease-drug pairs with an $FDR < 0.01$.

2.6.3 Evaluating SAveRUNNER prediction performance

We calculated $log_2(auPRC/prior)$ by ranking disease-drug pairs by $-log_{10}(SAveRUNNER\,FDR)$ and using either previously indicated drug-disease pairs (both approved and off-label) or drug-disease pairs tested in a clinical trial as positive labels. Approved and off-label drug-disease pairs were collected from DrugCental (Avram et al., 2021). Only drugs with expert curated target genes were included (see Section 2.6.1). The Unified Medical Language System (UMLS) Concept Unique Identifiers (CUI) were limited to diseases (T047) and neoplastic processes (T191), and our diseases were matched to diseases in DrugCentral using UMLS CUIs. Drug-disease pairs tested in a clinical trial were collected from the database for Aggregate Analysis of Clinical Trials (AACT) (AACT Database, 2022). AACT reports the Medical Subject Headings (MeSH) vocabulary names for diseases. We used disease vocabulary mapping provided by DisGeNET to translate UMLS CUIs for our diseases to MeSH vocabulary names, further restricted to only those that were present in AACT. We filtered AACT for trials with "Active, not recruiting", "Enrolling by invitation", "Recruiting", or "Completed" status.

2.6.4 Enrichment of predicted drug-disease pairs among previously indicated drug-disease pairs

To test for an enrichment of predicted drug-disease pairs among previously indicated drug-disease pairs for each disease, we tallied the total number of unique drugs previously indicated to any disease, the number of those drugs indicated to the disease of interest, the number of drugs predicted to treat the disease by our method, and the number of drugs predicted to treat the disease by our method that were also previously indicated for that disease. We calculated a p-value using a one tailed Fisher's exact test and corrected for multiple comparisons within each disease across drugs using the Benjamini–Hochberg procedure.

2.6.5 Enrichment of anti-inflammatory drugs and immunosuppressants among predicted treatments

We searched the DrugBank database for the ATC codes for anti-inflammatory drugs and immunosuppressants including Immunosuppressants (L04), Corticosteroids for systemic use (H02), Anti-inflammatory and antirheumatic products (M01), and Antihistamines (R06) (Wishart et al., 2018). We used these codes to pull all the drugs in these categories from our expert curated drug to target gene database. For each disease we ranked predicted drugs by $-log_{10}(SAveRUNNER\,FDR)$ and used the fgsea R package (v 1.20.0) to perform gene set enrichment analysis for drugs belonging to each of the four classes (Subramanian et al., 2005; Korotkevich et al., 2021).

3 Results

3.1 Expanding lists of disease-related genes and identifying disease-specific gene subnetworks

Our first goal was to establish a comprehensive list of genes associated with the complex diseases of interest and resolve the genes linked to each disease into subsets of tightly connected genes in an underlying molecular network. Towards this goal, we selected 37 complex diseases associated with underlying systemic inflammation (see *Methods*). To ensure that we correctly isolate chronic inflammation (CI) signatures, we devised a set of positive and negative controls. We selected 10 autoimmune disorders as positive controls because autoimmune disorders are characterized by CI and should have an easily identifiable CI gene signature. For negative controls, we selected 113 traits from UK Biobank (Sudlow et al., 2015) that are unlikely to be associated with CI (i.e. Right handedness, filtered coffee intake, and distance between home and workplace). Supplementary Table S2 contains the full list of diseases and traits used in this analysis along with their original associated genes.

While thousands of genes may play a role in the etiology of a chronic disease, it is unlikely that all of these genes have been cataloged in available databases such as DisGeNET or identified by GWAS. Hence, we expanded the lists of disease-or-trait-associated genes using GenePlexus (Liu et al., 2020) (Figure 1A, step 1). Briefly, GenePlexus performs supervised machine learning using network-based features to predict novel genes related to a set of input seed genes. Here, we built one GenePlexus model per disease using disease-associated genes from DisGeNET or trait-associated genes from the UK Biobank GWAS as seed genes (positive examples). To test the robustness of this method for identifying CI enriched clusters, we tested four different biological interaction networks of varying sizes and edge densities—STRING, STRING with only experimentally derived edges (STRING-EXP) (Szklarczyk et al., 2017), BioGRID (Stark et al., 2006), and ConsensusPathDB (Kamburov et al., 2013) (Figure 1A, step 1, see Methods Section 2.2). Genes predicted by the GenePlexus model with a probability ≥ 0.80 were added to the seed gene list to create an expanded list of disease- or trait-associated genes.

Figure 2 shows results for ConsensusPathDB. The proportion of genes predicted by GenePlexus for the non-disease traits is lower than those for the autoimmune and complex diseases (Figure 2B). This observation indicates that genes associated with a specific autoimmune/complex disease tend to have more similar network neighborhoods than genes associated with non-disease traits. All

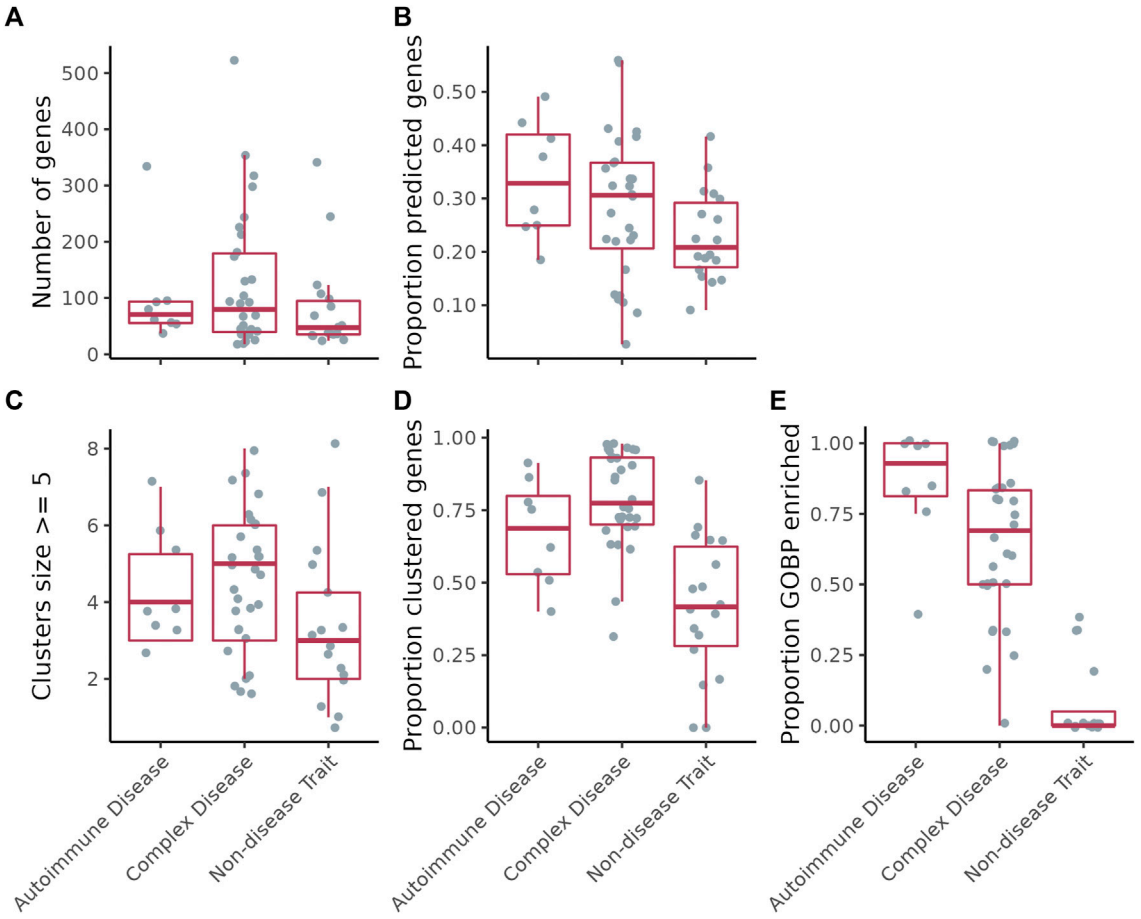

FIGURE 2
(A) Number of genes per disease/trait. **(B)** Proportion of the genes per disease/trait that were predicted by GenePlexus. **(C)** Number of clusters per disease/trait containing at least five genes. **(D)** Proportion of total genes assigned to a cluster containing at least five genes. **(E)** Proportion of clusters per disease/trait enriched with genes from at least one GO biological process.

disease-associated genes after GenePlexus prediction are listed in Supplementary Table S3.

Next, for each disease/trait, we clustered the expanded lists of genes based on their interactions in the gene-gene interaction network (Figure 1A step 2 and Figure 2C; Supplementary Table S3). On ConsensusPathDB, the complex diseases had the highest proportion of genes grouped into clusters of ≥5 genes, followed by autoimmune diseases and non-disease traits (Figure 2D). To assess whether clusters are biologically meaningful, we performed an enrichment analysis between every cluster and hundreds of GO Biological Process (GOBP) gene sets. We theorize that significant enrichment of a cluster with a GOBP means the genes in the cluster likely function together to carry out a specific cellular process or pathway. On ConsensusPathDB, for autoimmune and complex diseases, the median proportion of GOBP enriched clusters are >0.75 and >0.60, respectively, suggesting most clusters are biologically relevant (Figure 2E). In contrast, most clusters in non-disease traits are not enriched for a GOBP (Figure 2E).

3.2 Isolating CI-enriched disease clusters

Clusters of related, disease-associated genes on functional gene interaction networks are likely to correspond to the pathways and biological processes disrupted during disease progression. For complex disorders, multiple pathways are likely to be affected. Our next goal was to identify which cluster(s) within a set of disease-associated genes corresponds to the CI component of the disease. For this analysis, similar to the expansion of disease- or trait-associated genes, we used GenePlexus to predict novel inflammation genes for each of the five sets of inflammation-related seed genes procured from different sources (see Methods Section 2.5.1, Supplementary Table S4). We then scored the enrichment of CI genes in each disease cluster and performed a permutation test using 5,000 random gene sets for each disease to determine the significance of the enrichment score (see Methods Section 2.5.2 and Section 2.5.3 and Figure 1A steps 3–5, Supplementary Table S5).

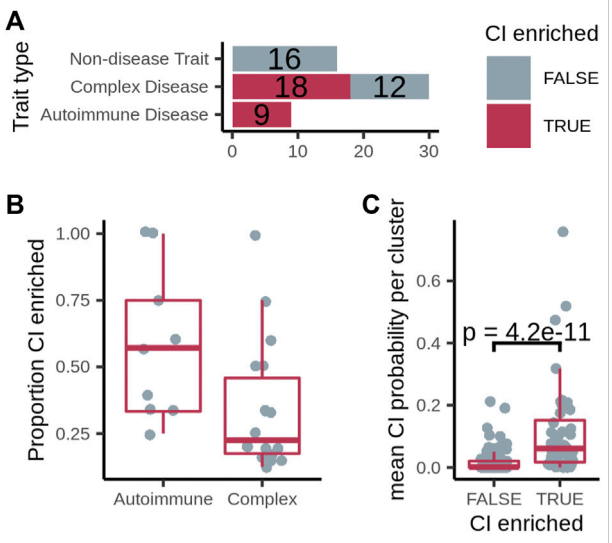

FIGURE 3
(A) Number of diseases/traits with at least one cluster overlapping the expanded chronic inflammation (CI) geneset (dark pink), out of the total number of diseases/traits. **(B)** The proportion of CI-enriched disease clusters among all disease clusters per disease. **(C)** Mean probability that genes with no known relationship with chronic inflammation residing in a CI-enriched cluster or non-CI-enriched cluster are associated with CI. *p*-value calculated using a one-sided Fisher's Exact test.

With various base networks and CI gene sources, we tested all network–CI-geneset combinations and chose the one that resulted in the highest proportion of autoimmune diseases and lowest proportion of non-disease traits with at least one CI-enriched cluster. Based on this test, we picked ConsensusPathDB as the base network and "high-confidence Geneshot" as the source of CI genes (Supplementary Figure S2). We were able to identify clusters enriched for CI genes in all of the autoimmune disorders surveyed (9/9), while finding no CI-enriched clusters among the non-disease traits (Figure 3A). We identified at least one CI-enriched cluster in 18 of 30 of the complex diseases (Figure 3A). Twelve out of the 27 diseases with at least one CI-enriched cluster had two or more CI-enriched clusters, and the median proportion of CI-enriched clusters out of the total clusters is higher for autoimmune diseases than complex diseases (Figure 3B). The number of diseases with at least one CI-enriched cluster varied with different combinations of prediction network, cluster network, and inflammation gene set (Supplementary Table S6). In every case, however, the proportion of autoimmune diseases with at least one CI-enriched cluster was higher than that for non-disease traits suggesting that our method is robust to changes in base-network and inflammation gene set (Supplementary Figure S2).

We hypothesized that, through guilt-by-association, even the genes with no known relationship with chronic inflammation residing in a CI-enriched cluster should have a higher probability of being CI-associated than those in non-CI-enriched clusters. To test this hypothesis, we used GenePlexus with features from each gene-gene interaction network to calculate the probability that every gene is associated with each inflammation gene set. Then, focusing on the genes in disease clusters that were not present in the inflammation gene set, we found that the mean CI probability of these genes in CI-enriched clusters is significantly higher for CI-enriched clusters than non-enriched clusters in 24 out of 25 network/CI-gene set combinations (Supplementary Figure S3-S7), including ConsensusPathDB with the high-confidence Geneshot CI gene set (Figure 3C). This observation suggests that the CI-enriched clusters as a whole, and not just the genes in the high-confidence Geneshot CI gene set residing within them, are CI-associated in the disease of interest. Knocking out putative inflammation associated genes in animal models of the appropriate disease and testing for an increase in known inflammation markers would confirm this result.

3.3 Comparing CI gene signatures across diseases

To determine if related diseases have similar chronic inflammation signatures, we used a network-based approach to quantify the similarity between each pair of ConsensusPathDB/high-confidence GeneShot CI-enriched disease clusters across diseases and grouped similar clusters together using the Leiden algorithm (Traag et al., 2019; Fiscon et al., 2021) (Figure 1B, steps 1–2). Several diseases have more than one CI-enriched cluster and none of these diseases have clusters belonging only to one group (Figure 4A, Supplementary Table S7). Moreover, diseases belonging to the same broad category—i.e. autoimmune, cancer, or cardiovascular disease—do not have a larger proportion of clusters belonging to a particular group than expected by chance (one-sided Fisher's exact test, Figure 4A). This suggests that one disease can harbor more than one type of chronic-inflammation signature, and that the same signatures can be found in very different diseases. For example, rheumatoid arthritis, myocardial ischemia, atherosclerosis, and chronic obstructive airway disease all have CI-enriched clusters belonging to each of the three signature groups.

To determine the biological significance of these signature groups, we performed enrichment analyses for genes unique to each group among GO biological processes (Figure 4B, Supplementary Table S8). The top 10 significantly enriched terms for each group are largely distinct, with group 1 being enriched for immune relevant signaling pathways, group 2 for regulation of immune cell proliferation, and group 3 for regulation of immune cell chemotaxis (Figure 4B).

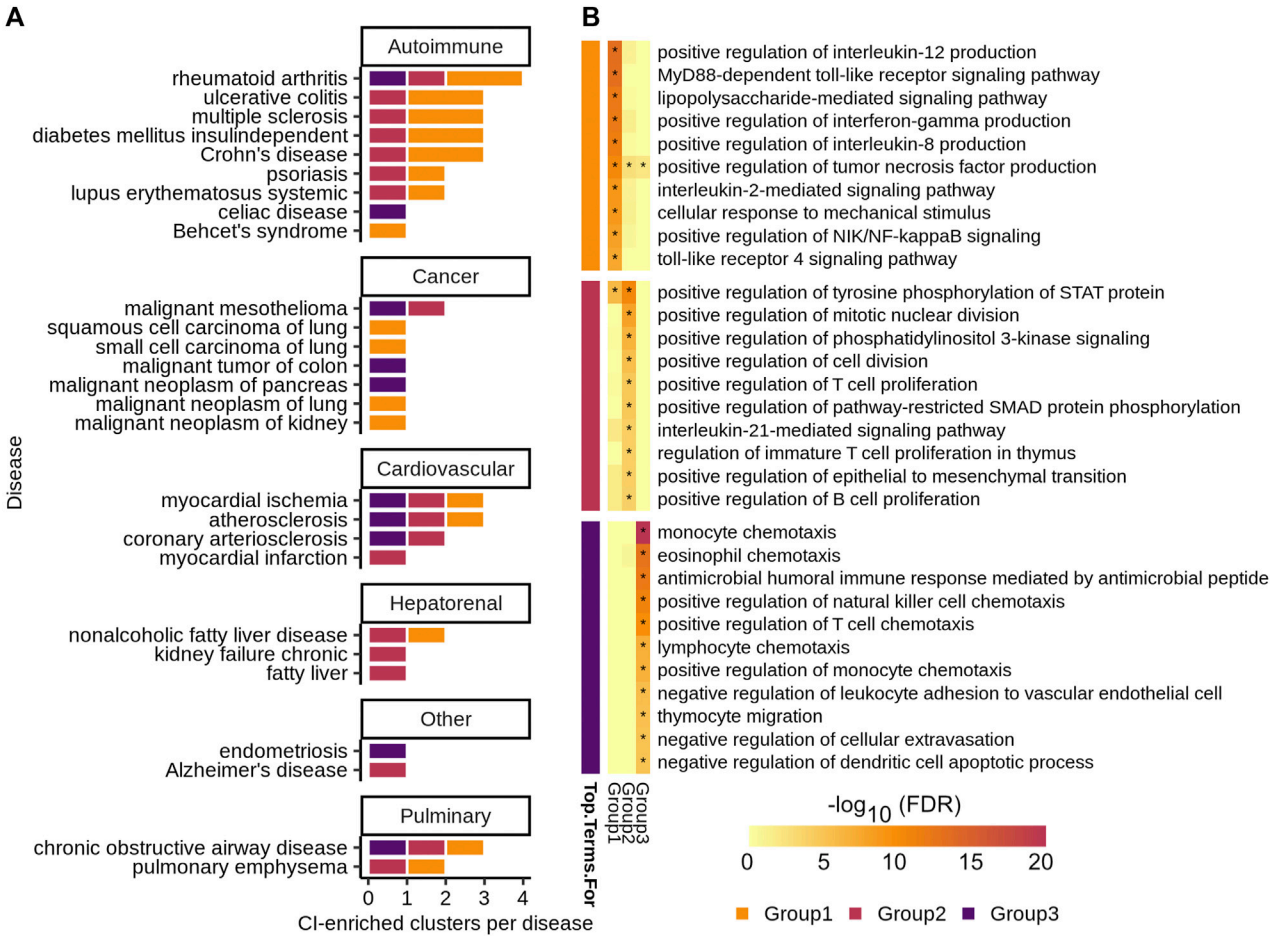

FIGURE 4
(A) Number of CI-enriched clusters per disease colored by CI-signature group. **(B)** Top ten enriched GOBP categories by Benjamini–Hochberg procedure corrected FDR for each CI-signature group—the group is denoted by the colored blocks to the left of the heatmap. The heatmap shows the $-log_{10}(FDR)$ of the enrichment for each CI-signature group — * denotes $p < 0.05$.

3.4 Predicting novel treatment opportunities

Our final goal was to leverage the ConsensusPathDB/high confidence GeneShot CI-enriched disease clusters we discovered to find potential avenues for repurposing approved drugs to therapeutically target systemic inflammation underlying complex diseases (Figure 1B, step 3). Towards this goal, we used SAveRUNNER to find associations between CI-enriched clusters and FDA approved drugs through each drug's target genes (Fiscon et al., 2021). We found that SAveRUNNER predictions for known treatments were better than random chance — $log_2(auPRC/prior) > 0$— for diseases with at least five known treatments (Figure 5A). Moreover, with the exception of myocardial ischemia, SAveRUNNER predicted drugs in Phase IV clinical trials better than random chance (Figure 5A) (AACT Database, 2022). Drugs in Phase IV are those that have already been proved effective for treating a disease (in Phase III) and are being monitored for long-term safety and efficacy.

SAveRUNNER predicted between 3 and 178 high-confidence ($FDR < 0.01$) treatments for each disease and identified previously indicated drugs for five of the nine autoimmune disorders (Figure 5B, Supplementary Table S9), with significant enrichment among drug predictions for celiac disease (one-sided Fisher's exact test, BH corrected $FDR < 0.001$). SAveRUNNER found previously indicated treatments for only three of the 18 complex diseases (Figure 5B, Supplementary Table S9). This result is expected given that, unlike for autoimmune disorders, most known treatments for these complex disorders are not likely to target the immune system. Treatments previously

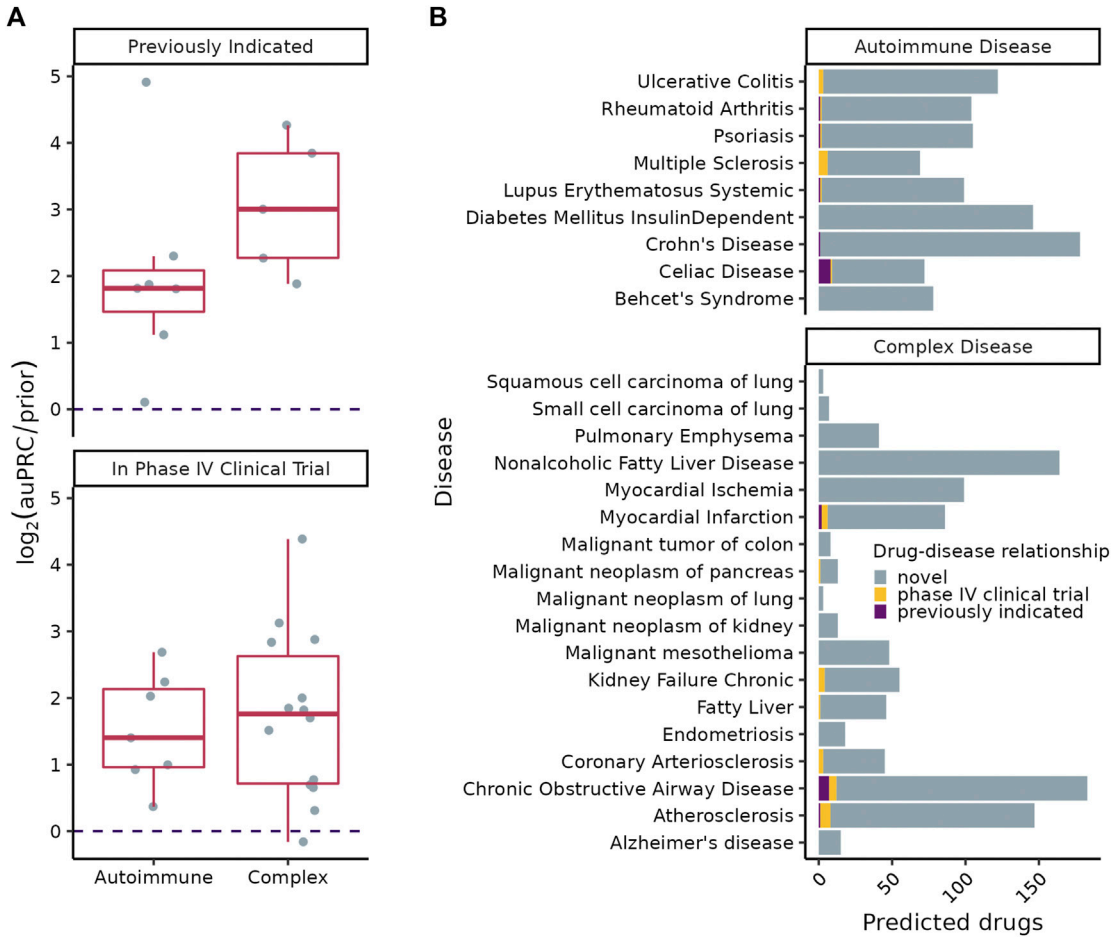

FIGURE 5
(A) $log_2(auPRC/prior)$of SAveRUNNER predictions using drugs previously indicated for the disease (top) or drugs ever in Phase IV clinical trials for a disease (bottom) as positive examples. The dotted line is at$log_2(auPRC/prior) = 0$. $log_2(auPRC/prior) > 0$ denotes predictions better than random chance. **(B)** Number of SAveRUNNER predicted genes (Benjamini–Hochberg procedure corrected $FDR < 0.01$) per disease.

tested in a clinical trial were predicted for six autoimmune disorders and seven of the complex disorders (Figure 5B).

We tested for enrichment of drugs belonging to four immune-related drug classes among treatment predictions highly ranked by SAveRUNNER for each complex disorder (Figure 6A). SAveRUNNER allows for drug prioritization based both on the *p*-value and on the adjusted similarity score between drug target genes and CI-enriched cluster genes. Highly scoring drug-cluster pairs have genes that are closely related in the gene interaction network, which increases the likelihood that the drug will be on-target for the paired disease (Fiscon et al., 2021). We found that antihistamines as a whole are enriched for six of the 18 complex disorders (Figure 6A). Antihistamines that specifically target histamine receptor H1 (*HRH1*) have the highest adjusted similarity score for six of the seven complex disorders with any antihistamine among their high-confidence targets (Figure 6B). SAveRUNNER predicted that cyproheptadine, which targets both *HRH1* and the serotonin 2A receptor, *HTR2A*, instead of *HRH1* alone would be the best antihistamine for treating non-alcoholic fatty liver disease (Figure 6B). While cyproheptadine is also a high-confidence predicted treatment for atherosclerosis, myocardial ischemia, and chronic obstructive airway disease, it is unlikely to be an effective treatment for myocardial infarction or malignant mesothelioma (Figure 6B). Interestingly, of the eight diseases, only myocardial infarction and malignant mesothelioma do not have a CI-enriched cluster belonging to CI-signature group 2 (Figure 4A). This finding suggests that, even among drugs in the same class, we can predict disease-specific treatments for the chronic inflammation component of the disease etiology.

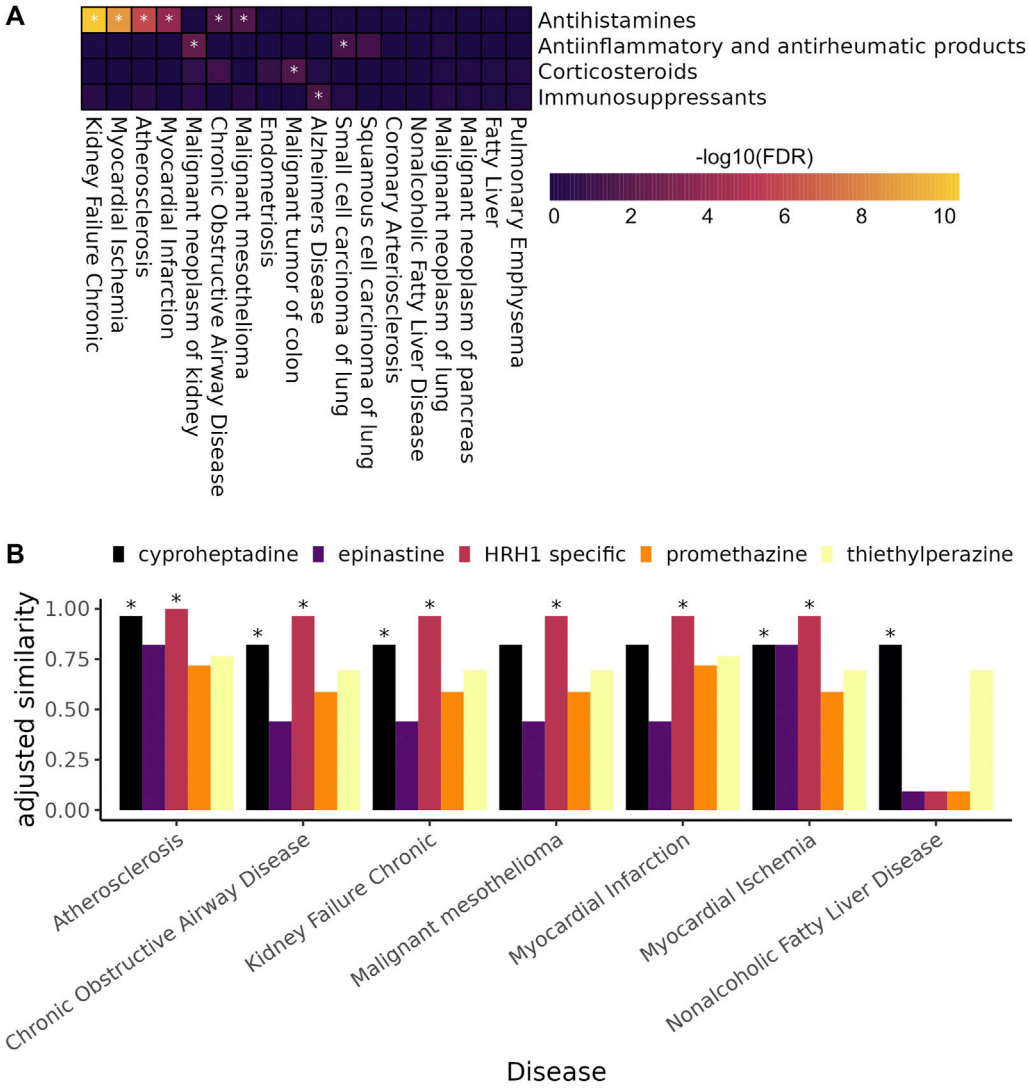

FIGURE 6
(A) Heat map showing the enrichment of anti-inflammatory and immunomodulating drugs among highly ranked SAveRUNNER predicted drugs (gene set enrichment analysis, * denotes *adjusted p – value* < *0.05*). **(B)** Bar plot showing the adjusted similarity scores of antihistamines for complex diseases with at least one antihistamine among drugs predicted by SAveRUUNER to treat the disease — * denotes *FDR* < *0.01*. HRH1 specific antihistamines are those listed in our high-confidence drug target database as only targeting *HRH1*.

4 Discussion

Complex diseases exhibit a staggering amount of heterogeneity, being associated with hundreds of genes and with a range of phenotypes. Therefore, to continue advancing our understanding of disease mechanisms and our ability to treat these diseases, it is critical to deconvolve disease heterogeneity by: a) resolving subsets of disease genes (and cellular processes/pathways) that underlie specific disease-associated phenotypes, and b) identifying avenues to diagnostically and/or therapeutically target those specific phenotypes.

Here, we present a computational data-driven approach to address this critical need (Figure 1). We used our approach to study chronic inflammation (CI) — a phenotype present across many complex diseases. We generated comprehensive lists of (known and predicted) disease-associated genes and identified and classified the CI signal among these genes. We used these signatures to predict novel treatment options to target the inflammatory components of 18 complex diseases.

A key aspect of our approach is ensuring its sensitivity to detect CI disease signatures using autoimmune diseases as positive controls. In autoimmune diseases, the immune system mistakenly attacks healthy tissue causing long-term systemic

inflammation. Thus, we expect that the underlying CI disease signatures would be easily identifiable by a valid approach. Indeed, in each of the nine autoimmune diseases analyzed, our approach isolated gene clusters enriched for CI genes (Figure 1A), and identified drugs already used to treat a number of these disorders (Figure 5B). This finding is encouraging given that we conservatively matched drugs to diseases only based on expert-curated drug-target data from DGIDb (Freshour et al., 2021) rather than using all drug-target information in DrugCentral (Avram et al., 2021).

To show that our method was not erroneously uncovering CI signals where there were none, we identified UK Biobank traits not patently associated with CI (along with their genes) to use as negative controls. Following this analysis, we found that the median fraction of trait-associated genes predicted by GenePlexus and the median fraction of genes assigned to sizable clusters were lower for these traits than for autoimmune and complex diseases (Figures 2C,D). Given that GenePlexus is a method that leverages network connectivity for predicting new genes belonging to a set, these results suggest that the genes associated with non-disease traits may not be as highly connected to one another in ConsensusPathDB as the autoimmune and complex disease genes. Moreover, most of the non-disease trait clusters were not enriched with genes annotated to GO biological processes, suggesting that these clusters are diffuse and that the member genes are unlikely to work together to support a coherent biological task. While non-disease traits like coffee intake and handedness have been associated with inflammation (Searleman and Fugagli 1987; Paiva et al., 2019), this analysis (using GWAS-based trait-associated genes) suggests it is unlikely that SNPs in a coordinated inflammation pathway influence non-disease traits and more likely that any association with inflammation is environmental, not genetic. Taken together, these results suggest that these chosen traits serve as reasonable negative controls and offer a way to meaningfully contrast the results from complex diseases. Ideally, diseases or traits with no underlying inflammatory component but with associated genes that cluster in a network (as well as the autoimmune and complex disease) will serve as better negative controls. Given how common inflammatory processes are in disease, however, such diseases are difficult to definitively identify.

Complex disorders like cardiovascular diseases, diabetes, cancer, and Alzheimer's disease are among the leading causes of death and disability among adults over 50 years of age, and all are associated with underlying systemic inflammation (Furman et al., 2019; Vos et al., 2020). Patients with systemic inflammation caused by autoimmune disorders are more likely to have another CI disorder like cardiovascular disease, type 2 diabetes mellitus, and certain types of cancer (Armstrong et al., 2013; Dregan et al., 2014; Yashiro 2014). Further, treating one chronic-inflammatory disease can reduce the risk of contracting another, suggesting a common underlying pathway (Fullerton and Gilroy 2016). For example, treating rheumatoid arthritis with tumor necrosis factor (TNF) antagonists lowers the incidence of Alzheimer's disease and type II diabetes (Antohe et al., 2012; Chou et al., 2016).

To better understand how CI-associated disorders relate to one another, we used a network-based approach to quantify the similarity between their CI-enriched clusters. We hypothesized, for example, that Crohn's disease and "malignant tumor of colon" would have similar CI-signatures, given that patients with inflammatory bowel disease are at increased risk for developing colorectal cancer (Shah and Itzkowitz 2022). However, Crohn's disease CI-enriched clusters are members of signature groups 1 and 2, while the "malignant tumor of colon" CI-enriched cluster belongs to group 3 (Figure 4A). Instead of sharing CI-signatures, related CI diseases may, instead, have complementary signatures. Indeed, the group 1 signature, which characterizes two of the three Crohn's disease CI-enriched clusters, is enriched for genes that positively regulate proinflammatory cytokines TNF and in interferon-gamma (IFNɣ) (Figure 4B). When these cytokines bind to their respective receptors, reactive oxygen species are generated causing oxidative stress (Chatterjee 2016). Oxidative stress, in turn, induces DNA-damage that can lead to tumor formation. Colorectal tumors are infiltrated with lymphocytes, which mediate the recruitment of immune cells that suppress tumor growth (Idos et al., 2020). Immune cell infiltration likely leads to our ability to detect the group 3 CI-signature among genes associated with "malignant tumor of colon", given that group 3 is enriched for immune cell migration and chemotaxis (Figures 4A,B). Alternatively, there is a possibility that every CI-associated disease actually exhibits all three CI-signatures, and our method is only sensitive enough to detect these in a handful of diseases.

Common treatments for systemic inflammation, including non-steroidal anti-inflammatory drugs (NSAIDs), corticosteroids, and biologics like TNF antagonists, can cause adverse effects when used long term. For instance, patients treated with corticosteroids or TNF antagonists have increased risk of infection (Rosenblum and Howard 2011; Murdaca et al., 2015; Shah and Itzkowitz 2022), and corticosteroid use increases both the risk of fracture (Kanis et al., 2004; Mitra 2011) and the risk of developing type II diabetes (Blackburn et al., 2002). NSAIDs present a unique set of side effects, particularly in elderly patients, including gastrointestinal problems ranging from indigestion to gastric bleeding, and kidney damage (Griffin 1998; Griffin et al., 2000; Marcum and Hanlon 2010). Therefore, the search for better treatment options for CI is ongoing.

Here, we leverage the CI-signatures to identify novel treatment opportunities for the CI-component of 18 complex diseases (Figure 5B). Interestingly, antihistamines were among the top drug associations for

six of 18 complex diseases (Figure 6A), including atherosclerosis. Atherosclerosis is characterized by the deposition of cholesterol plaques on the inner artery walls. Mast cells, immune cells best known for their response to allergens, are recruited to arteries during plaque progression, where they release histamines. Histamines then activate the histamine H_1-receptor, increasing vascular permeability, which allows cholesterol easier access to arteries promoting plaque buildup (Rozenberg et al., 2010). Mepyramine, one of the HRH1-specific antihistamines highly associated with atherosclerosis, has already been shown to decrease the formation of atherogenic plaques in a mouse model of the disease (Rozenberg et al., 2010). Interestingly, it is not predicted as a treatment for myocardial ischemia, which occurs when plaque buildup obstructs blood flow to a coronary artery, suggesting disease-specific antihistamine efficacy even among related diseases. Cetirizine and fexofenadine are also HRH1-specific antihistamines highly associated with atherosclerosis but neither prevented or reduced atherosclerosis progression in a mouse model of atherosclerosis, and both increased atherosclerotic lesions at low doses (Raveendran et al., 2014). In the expert-curated drug-target database used in this study, the histamine H_1-receptor is the only target listed for all three drugs; however, the contradictory results from Rosenberg *et al.* and Raveendran *et al.* suggests that drug-specific off-target effects are mediating atherosclerosis treatment outcomes. A more complete understanding of drug-gene targets would allow for better predictions of novel disease treatments.

For example, unlike the other diseases with antihistamines as predicted treatments, only cyproheptadine, and not the HRH1-specific drugs, is likely to be an effective treatment for non-alcoholic fatty liver disease (NAFLD) (Figure 6B). Cyproheptadine is an antagonist for both histamine receptor H1 and the serotonin 2A receptor (*HTR2A*), suggesting that blocking the serotonin 2A receptor could be specifically helpful for ameliorating symptoms of NAFLD. Indeed, liver-specific *Htr2a* knockout mice are resistant to high-fat diet induced hepatic steatosis and increased fat in the liver (Choi et al., 2018). Moreover, increased serum serotonin levels were correlated with increased disease severity in patients with NAFLD (Wang and Fan. 2020).

Overall, we have shown that our method is capable of isolating the chronic inflammation gene signature of a complex disease using a network-based strategy and, by integrating information across multiple complementary sources of data, it can predict and prioritize potential therapies for the systemic inflammation involved in that specific disease. Importantly, our approach provides a blueprint for identifying and prioritizing therapeutic opportunities for any disease endophenotype.

Data availability statement

The code and data used to generate the results can be found on github repository https://github.com/krishnanlab/chronic-inflammation and Zenodo record https://zenodo.org/record/6858073 (doi: 10.5281/zenodo.6858073), respectively.

Author contributions

SH, AM, CM, and AK conceived and designed the approach and experiments and wrote the manuscript. SH and AM implemented the approach and performed the experiments. CM wrote the GenePlexus code used in the experiments. All authors read, edited, and approved the final manuscript.

Funding

This work was supported by the US National Institutes of Health (NIH) grant R35 GM128765 to AK and NIH Fellowship F32 GM134595 to CM and a 2021 NARSAD Young Investigator Grant from the Brain and Behavior Research Foundation (29956) to SH.

Acknowledgments

We thank the members of the Krishnan Lab for helpful discussions.

Conflict of interest

The authors declare that the research was conducted in the absence of any commercial or financial relationships that could be construed as a potential conflict of interest.

Publisher's note

Supplementary material

The Supplementary Material for this article can be found online at: https://www.frontiersin.org/articles/10.3389/fphar.2022.995459/full#supplementary-material

References

AACT Database (2022). Clinical trials transformation initiative. AvaliableAt: https://aact.ctti-clinicaltrials.org/.

Abbot, L., Bryant, S., Churchhouse, C., Ganna, A., Howrigan, D., Palmer, D., et al. (2021). UK Biobank GWAS nealelab. AvaliableAt: http://www.nealelab.is/uk-biobank/(Accessed November 17, 2021).

Alexa, A., and Rahnenfuhrer, J. (2022). TopGO: Enrichment analysis for gene Ontology. *Bioconductor* 3, 14. doi:10.18129/B9.bioc.topGO

Antohe, J., Bili, A., Jennifer, A., Sartorius, H., Kirchner, L., Morris, S. J., et al. (2012). Diabetes mellitus risk in rheumatoid arthritis: Reduced incidence with anti–tumor necrosis factor α therapy. *Arthritis Care Res.* 64 (2), 215–221. doi:10.1002/acr.20657

Armstrong, A. W., Harskamp, C. T., and Armstrong, E. J. (2013). Psoriasis and the risk of diabetes mellitus: A systematic review and meta-analysis. *JAMA Dermatol.* 149 (1), 84–91. doi:10.1001/2013.jamadermatol.406

Autoimmune Diseases: Causes (2022). Symptoms, what is it & treatment cleveland clinic. AvaliableAt: https://my.clevelandclinic.org/health/diseases/21624-autoimmune-diseases.

Avram, S., Bologa, C., Holmes, J., Bocci, G., Wilson, T., Curpan, R., et al. (2021). DrugCentral 2021 supports drug discovery and repositioning. *Nucleic Acids Res.* 49 (D1), 1160–1169. doi:10.1093/nar/gkaa997

Benjamini, Y., and Yosef, H. (1995). Controlling the false discovery rate: A practical and powerful approach to multiple testing. *J. R. Stat. Soc. Ser. B Methodol.* 57 (1), 289–300. doi:10.1111/j.2517-6161.1995.tb02031.x

Blackburn, D., Hux, J., and Mamdani, M. (2002). Quantification of the risk of corticosteroid-induced diabetes mellitus among the elderly. *J. Gen. Intern. Med.* 17 (9), 717–720. doi:10.1046/j.1525-1497.2002.10649.x

Carlson, M. (2019). Org.Hs.Eg.Db: Genome wide annotation for human. R. AvaliableAt: https://bioconductor.org/packages/release/data/annotation/html/org.Hs.eg.db.html.

Chatterjee, S. (2016). "Chapter two - oxidative stress, inflammation, and disease," in *Oxidative stress and biomaterials*. Editors T. Dziubla and D. Allan Butterfield (Academic Press), 35–58. doi:10.1016/B978-0-12-803269-5.00002-4

Chen, H., Zhang, H., Zhang, Z., Cao, Y., and Tang, W. (2015). Network-based inference methods for drug repositioning. *Comput. Math. Methods Med.* 2015, e130620. doi:10.1155/2015/130620

Cheng, F., Desai, R. J., Handy, D. E., Wang, R., Schneeweiss, S., Barabási, A-L., et al. (2018). Network-based approach to prediction and population-based validation of *in silico* drug repurposing. *Nat. Commun.* 9, 2691. doi:10.1038/s41467-018-05116-5

Choi, W., Namkung, J., Hwang, I., Kim, H., Lim, A., Jung Park, H., et al. (2018). Serotonin signals through a gut-liver Axis to regulate hepatic steatosis. *Nat. Commun.* 9 (1), 4824. doi:10.1038/s41467-018-07287-7

Chou, R. C., Kane, M., Ghimire, S., Gautam, S., and Jiang, G. (2016). Treatment for rheumatoid arthritis and risk of Alzheimer's disease: A nested case-control analysis. *CNS Drugs* 30 (11), 1111–1120. doi:10.1007/s40263-016-0374-z

Dregan, A., Charlton, J., Chowienczyk, P., and Gulliford, M. C. (2014). Chronic inflammatory disorders and risk of type 2 diabetes mellitus, coronary heart disease, and stroke: A population-based cohort study. *Circulation* 130 (10), 837–844. doi:10.1161/CIRCULATIONAHA.114.009990

Fiscon, G., Conte, F., Farina, L., and Paci, P. (2021). SAveRUNNER: A network-based algorithm for drug repurposing and its application to COVID-19. *PLoS Comput. Biol.* 17 (2), e1008686. doi:10.1371/journal.pcbi.1008686

Fiscon, G., and Paci, P. (2021). SAveRUNNER: An R-based tool for drug repurposing. *BMC Bioinforma.* 22 (1), 150. doi:10.1186/s12859-021-04076-w

Freshour, S., Kiwala, S., Cotto, K., Adam, C., McMichael, J., Song, J., et al. (2021). Integration of the drug-gene interaction database (DGIdb 4.0) with open crowdsource efforts. *Nucleic Acids Res.* 49 (D1), 1144–1151. doi:10.1093/nar/gkaa1084

Fullerton, J. N., and Gilroy, D. W. (2016). Resolution of inflammation: A new therapeutic frontier. *Nat. Rev. Drug Discov.* 15 (8), 551–567. doi:10.1038/nrd.2016.39

Furman, D., Campisi, J., Verdin, E., Carrera-Bastos, P., Targ, S., Franceschi, C., et al. (2019). Chronic inflammation in the etiology of disease across the life span. *Nat. Med.* 25 (12), 1822–1832. doi:10.1038/s41591-019-0675-0

Ghiassian, S. D., Menche, J., and Barabási, A. L. (2015). A DIseAse MOdule detection (DIAMOnD) algorithm derived from a systematic analysis of connectivity patterns of disease proteins in the human interactome. *PLoS Comput. Biol.* 11 (4), e1004120. doi:10.1371/journal.pcbi.1004120

Ghiassian, S. D., Menche, J., Chasman, D. I., Giulianini, F., Wang, R., Ricchiuto, P., et al. (2016). Endophenotype network models: Common core of complex diseases. *Sci. Rep.* 6 (1), 27414. doi:10.1038/srep27414

Griffin, M. R. (1998). Epidemiology of nonsteroidal anti-inflammatory drug–associated gastrointestinal injury. *Am. J. Med.* 104 (3), 23S–29S. doi:10.1016/S0002-9343(97)00207-6

Griffin, M. R., Yared, A., and Ray, W. A. (2000). Nonsteroidal antiinflammatory drugs and acute renal failure in elderly persons. *Am. J. Epidemiol.* 151 (5), 488–496. doi:10.1093/oxfordjournals.aje.a010234

Idos, G. E., Kwok, J., Bonthala, N., Lynn, K., Gruber, S. B., and Qu, C. (2020). The prognostic implications of tumor infiltrating lymphocytes in colorectal cancer: A systematic review and meta-analysis. *Sci. Rep.* 10 (1), 3360. doi:10.1038/s41598-020-60255-4

Kamburov, A., Ulrich, S., Lehrach, H., and Herwig, R. (2013). The ConsensusPathDB interaction database: 2013 update. *Nucleic Acids Res.* 41 (D1), D793–D800. doi:10.1093/nar/gks1055

Kanis, J. A., Johansson, H., Anders, O., Johnell, O., de Laet, C., Joseph Melton, L., et al. (2004). A meta-analysis of prior corticosteroid use and fracture risk. *J. Bone Min. Res.* 19 (6), 893–899. doi:10.1359/JBMR.040134

Korotkevich, G., Sukhov, V., Budin, N., Shpak, B., Artyomov, M. N., and Sergushichev, A. (2021). Fast gene set enrichment analysis. bioRxiv. doi:10.1101/060012

Lachmann, A., Schilder, B. M., Wojciechowicz, M. L., Torre, D., Maxim, V., Keenan, A. B., et al. (2019). Geneshot: Search engine for ranking genes from arbitrary text queries. *Nucleic Acids Res.* 47 (W1), W571–W577. doi:10.1093/nar/gkz393

Lamparter, D., Marbach, D., Rueedi, R., Kutalik, Z., and Bergmann, S. (2016). Fast and rigorous computation of gene and pathway scores from SNP-based summary statistics. *PLoS Comput. Biol.* 12 (1), e1004714. doi:10.1371/journal.pcbi.1004714

Leiserson, M., Vandin, F., Wu, H-T., Dobson, J., Eldridge, J., Jacob, T., et al. (2015). Pan-cancer network analysis identifies combinations of rare somatic mutations across pathways and protein complexes. *Nat. Genet.* 47, 106–114. doi:10.1038/ng.3168

Liu, R., Mancuso, C. A., Anna, Y., Johnson, K. A., and Krishnan, A. (2020). Supervised-learning is an accurate method for network-based gene classification. *Bioinformatics* 36, 3457–3465. doi:10.1093/bioinformatics/btaa150

Marcum, Z. A., and Hanlon, J. T. (2010). Recognizing the risks of chronic nonsteroidal anti-inflammatory drug use in older adults. *Ann. Longterm. Care.* 18 (9), 24–27.

Mitra, R. (2011). Adverse effects of corticosteroids on bone metabolism: A review. *PM&R* 3 (5), 466–471. doi:10.1016/j.pmrj.2011.02.017

Murdaca, G., Spanò, F., Contatore, M., Guastalla, A., Elena, P., Magnani, O., et al. (2015). Infection risk associated with anti-TNF-α agents: A review. *Expert Opin. Drug Saf.* 14 (4), 571–582. doi:10.1517/14740338.2015.1009036

Paiva, C., Beserra, B., Reis, C., Dorea, J. G., Da Costa, T., and Amato, A. A. (2019). Consumption of coffee or caffeine and serum concentration of inflammatory markers: A systematic review. *Crit. Rev. Food Sci. Nutr.* 59 (4), 652–663. doi:10.1080/10408398.2017.1386159

Piñero, J., Saüch-Pitarch, J., Ronzano, F., Centeno, E., Sanz, F., and Laura, I. F. (2020). The DisGeNET knowledge platform for disease genomics: 2019 update. *Nucleic Acids Res.* 48 (D1), D845–D855. doi:10.1093/nar/gkz1021

Raveendran, V. V., Smith, D. D., Tan, X., Sweeney, M. E., Flynn, C. A., Tawfik, O. W., et al. (2014). Chronic ingestion of H1-antihistamines increase progression of atherosclerosis in apolipoprotein E-/- mice. *PLoS ONE* 9 (7), e102165. doi:10.1371/journal.pone.0102165

Rock, K. L., and Kono., H. (2008). The inflammatory response to cell death. *Annu. Rev. Pathol.* 3, 99–126. doi:10.1146/annurev.pathmechdis.3.121806.151456

Rosenblum, H., and Howard, A. (2011). Anti-TNF therapy: Safety aspects of taking the risk. *Autoimmun. Rev.* 10 (9), 563–568. doi:10.1016/j.autrev.2011.04.010

Rozenberg, I., Sluka, S. H. M., Rohrer, L., Hofmann, J., Becher, B., Alexander, A., et al. (2010). Histamine H1 receptor promotes atherosclerotic lesion formation by increasing vascular permeability for low-density lipoproteins. *Arterioscler. Thromb. Vasc. Biol.* 30 (5), 923–930. doi:10.1161/ATVBAHA.109.201079

Schriml, L. M., Mitraka, E., Munro, J., Tauber, B., Schor, M., Nickle, L., et al. (2019). Human disease Ontology 2018 update: Classification, content and workflow expansion. *Nucleic Acids Res.* 47, D955–D962. doi:10.1093/nar/gky1032

Searleman, A., and Fugagli, A. K. (1987). Suspected autoimmune disorders and left-handedness: Evidence from individuals with diabetes, Crohn's disease and

ulcerative colitis. *Neuropsychologia* 25 (2), 367–374. doi:10.1016/0028-3932(87)90025-X

Shah, S. C., and Itzkowitz, S. H. (2022). Colorectal cancer in inflammatory bowel disease: Mechanisms and management. *Gastroenterology* 162 (3), 715–730.e3. e3. doi:10.1053/j.gastro.2021.10.035

Stark, C., Reguly, T., Boucher, L., Ashton, B., and Tyers, M. (2006). BioGRID: A general repository for interaction datasets. *Nucleic Acids Res.* 34 (1), D535–D539. doi:10.1093/nar/gkj109

Subramanian, A., Tamayo, P., Mootha, V. K., Mukherjee, S., Ebert, B. L., Gillette, M. A., et al. (2005). Gene set enrichment analysis: A knowledge-based approach for interpreting genome-wide expression profiles. *Proc. Natl. Acad. Sci. U. S. A.* 102 (43), 15545–15550. doi:10.1073/pnas.0506580102

Sudlow, C., Gallacher, J., Allen, N., Beral, V., Burton, P., Danesh, J., et al. (2015). UK Biobank: An open access resource for identifying the causes of a wide range of complex diseases of middle and old age. *PLoS Med.* 12 (3), e1001779. doi:10.1371/journal.pmed.1001779

Szklarczyk, D., Morris, J. H., Cook, H., Kuhn, M., Wyder, S., Simonovic, M., et al. (2017). The STRING database in 2017: Quality-controlled protein–protein association networks, made broadly accessible. *Nucleic Acids Res.* 45 (D1), D362–D368. doi:10.1093/nar/gkw937

Traag, V. A., Waltman, L., and van Eck, N. J. (2019). From louvain to leiden: Guaranteeing well-connected communities. *Sci. Rep.* 9 (1), 5233. doi:10.1038/s41598-019-41695-z

Vos, T., Lim, S. S., Abbafati, C., Abbas, K. M., Abbasi, M., Mitra, A., et al. (2020). Global burden of 369 diseases and injuries in 204 countries and territories, 1990–2019: A systematic analysis for the global burden of disease study 2019. *Lancet* 396 (10258), 1204–1222. doi:10.1016/S0140-6736(20)30925-9

Wang, L., Fan, X., Han, J., Cai, M., Wang, X., Wang, Y., et al. (2020). Jichun han, minxuan cai, xiaozhong wang, yan wang, and jing ShangGut-derived serotonin contributes to the progression of non-alcoholic steatohepatitis via the liver htr2a/pparγ2 pathway. *Front. Pharmacol.* 11, 553. doi:10.3389/fphar.2020.00553

Wishart, D. S., Yannick, D. F., Guo, A. C., Elvis, J., Marcu, A., Grant, J. R., et al. (2018). DrugBank 5.0: A major update to the DrugBank database for 2018. *Nucleic Acids Res.* 46 (D1), D1074–D1082. doi:10.1093/nar/gkx1037

Yashiro, M. (2014). Ulcerative colitis-associated colorectal cancer. *World J. Gastroenterol.* 20 (44), 16389–16397. doi:10.3748/wjg.v20.i44.16389

frontiers | Frontiers in Pharmacology

TYPE Original Research
PUBLISHED 14 October 2022
DOI 10.3389/fphar.2022.1002550

OPEN ACCESS

EDITED BY
Pallavi R. Devchand,
University of Calgary, Canada

REVIEWED BY
Hatice Hasturk,
The Forsyth Institute, United States
Uzma Saqib,
Indian Institute of Technology Indore, India

*CORRESPONDENCE
Amiram Ariel,
amiram.ariel@research.haifa.ac.il

†These authors share first authorship

‡These authors have contributed equally to this work

SPECIALTY SECTION
This article was submitted to Inflammation Pharmacology, a section of the journal Frontiers in Pharmacology

RECEIVED 25 July 2022
ACCEPTED 30 September 2022
PUBLISHED 14 October 2022

CITATION
Kalkar P, Cohen G, Tamari T, Schif-Zuck S, Zigdon-Giladi H and Ariel A (2022), IFN-β mediates the anti-osteoclastic effect of bisphosphonates and dexamethasone.
Front. Pharmacol. 13:1002550.
doi: 10.3389/fphar.2022.1002550

IFN-β mediates the anti-osteoclastic effect of bisphosphonates and dexamethasone

Prajakta Kalkar[1†], Gal Cohen[1,2†], Tal Tamari[2,3], Sagie Schif-Zuck[1], Hadar Zigdon-Giladi[2,3‡] and Amiram Ariel[1*‡]

[1]Departments of Biology and Human Biology, University of Haifa, Haifa, Israel, [2]Laboratory for Bone Repair, Rambam Health Care Campus, Haifa, Israel, [3]The Ruth and Bruce Rappaport Faculty of Medicine, Technion—Israel Institute of Technology, Haifa, Israel

Zoledronic acid (Zol) is a potent bisphosphonate that inhibits the differentiation of monocytes into osteoclasts. It is often used in combination with dexamethasone (Dex), a glucocorticoid that promotes the resolution of inflammation, to treat malignant diseases, such as multiple myeloma. This treatment can result in bone pathologies, namely medication related osteonecrosis of the jaw, with a poor understanding of the molecular mechanism on monocyte differentiation. IFN-β is a pro-resolving cytokine well-known as an osteoclast differentiation inhibitor. Here, we explored whether Zol and/or Dex regulate macrophage osteoclastic differentiation *via* IFN-β. RAW 264.7 and peritoneal macrophages were treated with Zol and/or Dex for 4–24 h, and IFN-β secretion was examined by ELISA, while the IFN stimulated gene (ISG) 15 expression was evaluated by Western blotting. RANKL-induced osteoclastogenesis of RAW 264.7 cells was determined by TRAP staining following treatment with Zol+Dex or IFN-β and anti-IFN-β antibodies. We found only the combination of Zol and Dex increased IFN-β secretion by RAW 264.7 macrophages at 4 h and, correspondingly, ISG15 expression in these cells at 24 h. Moreover, Zol+Dex blocked osteoclast differentiation to a similar extent as recombinant IFN-β. Neutralizing anti-IFN-β antibodies reversed the effect of Zol+Dex on ISG15 expression and partially recovered osteoclastic differentiation induced by each drug alone or in combination. Finally, we found Zol+Dex also induced IFN-β expression in peritoneal resolution phase macrophages, suggesting these drugs might be used to enhance the resolution of acute inflammation. Altogether, our findings suggest Zol+Dex block the differentiation of osteoclasts through the expression of IFN-β. Revealing the molecular pathway behind this regulation may lead to the development of IFN-β-based therapy to inhibit osteoclastogenesis in multiple myeloma patients.

KEYWORDS

IFN-β, resolution of inflammation, macrophages, osteoclast differentiation, dexamethasone, zoledronic acid, multiple myeloma

1 Introduction

Immune cells and cytokines are critical effectors in bone remodeling during inflammation and its resolution, as well as in cancer-associated osteopathologies (Tai et al., 2018; Alvarez et al., 2019; Plemmenos et al., 2020). Zoledronic acid (Zol), a nitrogen-containing bisphosphonate (BP), together with the glucocorticoid dexamethasone (Dex), is commonly used for the treatment of MM (Ishikawa et al., 1990). The beneficial action of Zol in MM is mostly attributed to the induction of osteoclast death that limits the formation of lytic lesions (Takayanagi et al., 2002; Lee and Kim, 2011; Schett, 2011). At the cellular level, Zol is taken up by ostoclasts and inhibits the enzyme farnesyl diphosphate synthase. As a result, there is a reduction in cholesterol synthesis, which is required for cytoskeletal reorganization and vesicular trafficking in the osteoclast, leading to osteoclast inactivation (Reszka and Rodan, 2003). The mechanism of action of Dex in MM is not completely elucidated. Dex reduces IL-6 mRNA levels in myeloma cells and induces plasma cell apoptosis by blocking IL-6 (Alexanian et al., 1992). The combined effect of Zol and Dex on osteoclast formation has not been extensively studied. Nevertheless, clinical evidence showed this drug combination increase the risk for a severe side effect called medication-related osteonecrosis of the jaw (MRONJ) (Hüni and Fryar, 1981). MRONJ is characterized by formation of a necrotic jawbone usually after tooth extraction, in patients taking antiresorptive drugs, like BPs, or anti-receptor activator of nuclear factor kappa-B ligand (RANK-L) antibodies alone or in combination with immune modulators or anti-angiogenic medications (Ruggiero et al., 2022).

The interplay between immune cells and osteoclasts was previously reported. Immune cells secrete pro and anti-inflammatory cytokines that balance bone resorption and apposition (Roodman, 1993; Van Dyke et al., 2015). Cytokines that stimulate bone resorption include IL-1, TNF-α, IL-6, IL-11, IL-15, and IL-17. Inhibitors of resorption include IL-4, IL-10, IL-13, IL-18, GM-CSF, and IFN-γ. TGF-β and prostaglandins can have either stimulatory or inhibitory effects on resorption, depending on the experimental setting (Martin et al., 1998). The role of cytokines in hematological malignancies, including MM, revealed dysregulation of various cytokines that uncouple the balance between bone resorption and bone apposition, leading to the development of lytic bone lesions (Guise and Mundy, 1998).

Interferon β (IFN-β) belongs to the type 1 interferon (IFN) family, representing the first line of endogenous defense mechanisms in response to viruses and bacterial infections. These cytokines are secreted by many cell types, including lymphocytes, macrophages, and endothelial cells (Pertsovskaya et al., 2013). IFN-β promotes bacterial clearance, neutrophil apoptosis, and efferocytosis, as well as macrophage reprogramming to resolution-promoting phenotypes (Kumaran Satyanarayanan et al., 2019). IFN-β is produced in response to M-CSF stimulation of macrophage progenitors as part of the osteogenic process (Yamashita et al., 2012). Similarly, RANKL induces the production of IFN-β in macrophages during osteoclast differentiation. Interestingly, recombinant mouse IFN-β strongly inhibits osteoclastogenesis from bone marrow macrophages stimulated by RANKL in the presence of M-CSF. These results suggest that IFN-β interferes with RANKL signaling, thereby inhibiting osteoclastogenesis (Stark et al., 1998).

The combined therapy of Zol+Dex delays the progression or occurrence of bone lesions in MM patients (Tosi et al., 2006). We hypothesized that this drug combination increases IFN-β expression and secretion in macrophages, thereby reducing osteoclastogenesis. The current study aimed to improve our understanding of the molecular mechanism executed by Zol and Dex in the blocking of osteoclastogenesis, focusing on IFN-β. Revealing the aforementioned molecular pathway may perpetuate the development of new biological treatments to inhibit osteoclastogenesis and prevent the worsening of osteolytic lesions following chemotherapy.

2 Methods

2.1 Cell culture

RAW 264.7 macrophage cells (ATCC, TIB-71, Virginia) were cultured in Minimum Essential Medium-α (MEM-alpha, Biological Industries, Israel) containing 10% fetal bovine serum (FBS, Biological Industries, Israel), 100 μg/ml penicillin and streptomycin (Biological Industries, Israel) at 37°C in a humidified atmosphere of 5% CO_2. The culture medium was changed every 3 days. Cells (1.5×10^6 cells) were seeded in a small flask (25 cm^2, Corning, Israel) for expansion for 3 days, and transferred to a big flask (175 cm^2, Corning, Israel) with culture medium.

2.1.1 Isolation of peritoneal macrophages

Male C57BL/6 mice were injected intraperitoneally with freshly prepared zymosan A in PBS (1 mg/ml/mouse). After 66 h, the peritoneal exudates were collected. Macrophages were labeled with PE-conjugated rat anti-F4/80 and isolated using EasySep PE selection magnetic beads following the manufacturer's instructions (Stem-Cell Technology). All animal experiments were approved by the ethics committee for animal experimentation at the University of Haifa (no 597/18).

2.2 RT-PCR

Peritoneal macrophages ($1*10^6$ cells per ml per treatment) were treated with Zol and/or Dex (5–10 μM and 1–10 μM, respectively, as in (Ural et al., 2003) in RPMI, respectively, for

4 h or 24 h. RNA extraction and cDNA synthesis were performed (Applied BioSystem, California). Then, qPCR was performed in triplicates using specific primers for IFN-β. IFN-γ and IFN-α were analyzed as reference genes and HPRT as a housekeeping gene. The reactions were normalized to mHPRT using the ΔΔ threshold cycle (Ct) method. Mouse primer sequences were as follows: mHPRT- Forward 5′- TTGCTCGAGATGTCATGA AGGA -3′, and Reverse 5′- AGCAGGTCAGCAAA GAACTTATAGC -3′, m-IFN-γ: Forward:5′-GCGTCATTGAATCACACCTG-3′ and Reverse:5′-TGAGCTCATTGAATG CTTGG-3′, m-IFN-α-Forward:5′-CCTGAGAGA GAAGAAACACAGCC-3′ and Reverse: 5′-TCTGCT CTGACCACTCCCAG -3′, mIFN-β-Forward:5′-AACCTCACAGGGCGGACTT-3′ and Reverse: TCCCACGTC AATCTTTCCTCTTG-3′ (Sigma Aldrich, Israel). Quantitative RT-PCR analysis was performed using a SyberGreen system on a Step One Plus (Thermo Fisher, Israel).

2.3 Western blotting

The expression of IFN-β, ISG15, or GAPDH proteins by macrophages (peritoneal or RAW 264.7) treated with vehicle, Zol, Dex, or Zol+Dex ($1.5*10^6$ cells per ml per treatment, 4 or 24 h) was determined. To this end, the protein content of lysed cells was extracted and run using 10% SDS-PAGE (40 μg/lane). Next, separated proteins were transferred to nitrocellulose or PVDF membranes and immunoblotted with rabbit anti-IFNβ, mouse anti-ISG15, or rabbit anti-GAPDH, respectively (Santa-Cruz Biotechnology). The membranes were washed and incubated with appropriate HRP-conjugated secondary antibodies. Then, the membranes were washed, developed using WesternBright ECL (Advansta, CA), and analyzed using Amersham Imager 600. Our analysis focused on the high molecular weight isoforms of IFN-β that are non-secreted intracellular proteins (higher molecular weight than 33 kDa), while the secreted forms (25–33 kDa) were excluded. Densitometry analysis was performed using the ImageJ software.

2.4IFN-β ELISA

Culture media from macrophages treated with Zol and/or Dex or vehicle for 4 h were collected and evaluated for their IFN-β content by custom-made ELISA as in. Briefly, MaxiSorp plates were coated with purified anti-mouse IFNβ capture antibody (1 mg/ml) (BioLegend 519202) and incubated overnight at 4°C. Plates were washed 4 times with 0.05% PBS-Tween-20 and blocked at room temperature for 1 h with 1% B.S.A. in PBS. Plates were washed 4 times before 100 μl of standard (BioLegend 581309), or culture supernatants were plated in duplicate and incubated overnight at 4°C. Plates were washed 4 times and incubated with biotinylated anti-IFN-β detection antibody (BioLegend 508105) at 1 mg/ml at room temperature for 1 h. Plates were washed 5 times and incubated with HRP-Avidin for 30 min at room temperature and then developed using TMB substrate and stopped using 2 N sulfuric acid. Plates were read using BioTek PowerWave Plate reader at 450 nm and 540 nm. Results were calculated using a 4-parameter curve-fitting with Gen5 software (BioTek).

2.5 *In vitro* differentiation of macrophages to osteoclasts

Osteoclastogenesis assay was performed with RAW 264.7 cells ($1.5*10^4$ cells per well in a 24-well plate) that were incubated with 30 ng/ml RANKL (Peprotech, Israel) for 5 days. RANKL-treated cells were also treated with Zol and/or Dex, recombinant mouse IFN-β (0.25 or 2.5 ng/ml, Biolegend), or anti-IFN-β antibodies (2 μg/ml, Abcam, United Kingdom) for the first 2 days of incubation and then washed. RANKL was supplemented after washing.

2.6 TRAP and CD11b staining

To characterize RAW 264.7 cells after differentiation, TRAP and immune-staining were performed. The cells were fixed with 4% paraformaldehyde (PFA)/PBS for 10 min at R.T. Immunocytology was used to detect cells that differentiated into osteoclasts ($TRAP^+CD11b^-$ cells). The cells were stained with a TRAP kit (387A-1KT, Sigma, United States) for 1 h at 37°C. Then, cells displaying deep purple staining (indicating high TRAP staining) were enumerated as cells that differentiated into osteoclasts. In addition, the cells were stained with anti-CD11b (ab52478, Abcam, United Kingdom) to indicate non-differentiated macrophages. The staining was performed as follows: After fixation, the cells were blocked with 1% BSA for 1 h, washed 3 times with PBS, and stained with Rabbit anti-CD11b for 1 h at R.T. After 3 washes with PBS, the cells were stained with a secondary antibody, HRP-conjugatedanti-Rabbit IgG (ZytoChem Plus HRP Polymer anti Rabbit, Zytomed, Berlin, Germany), then incubated with DAB (SuperPicture™ Polymer Detection Kit, DAB, rabbit, Thermo Fisher Scientific, MA, United States) for 15 min and then washed with distilled water. The cell cultures from both staining methods were captured by a digital camera (Olympus DP70, Olympus, Tokyo, Japan) with a calibration scale, 10 fields from each treatment by ×40 magnification were analyzed by shade using ImageJ software (NIH., Bethesda, MD, United States). The percentage of osteoclasts in the culture was calculated.

2.7 Statistical analysis

Statistical Packages for the Social Sciences (SPSS) or GraphPad Prism were used to analyze all experiments.

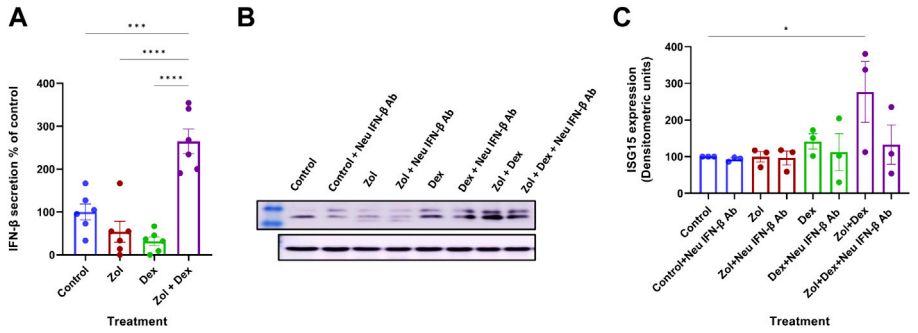

FIGURE 1
Zol+Dex promotes IFN-β secretion and ISG15 expression in RAW 264.7 macrophages. RAW 264.7 macrophages were incubated with Zol (10 μM) and/or Dex (1 μM) for 4 **(A)** or 24 h **(B,C)**. Then, culture medium was collected, and IFN-β levels were determined by standard ELISA (A,% C.V. were: Control = 45.73%, Zol = 110.6%, Dex = 76.80%, Zol+Dex = 26.41%), or cells were collected and analyzed by Western blotting for ISG15 and GAPDH **(B–C)**. Results are averages from 3 experiments **(A,C)** or representative images **(B)**. Statistical significance by one way ANOVA is indicated between the indicated treatments. *$p < 0.05$, ***$p < 0.001$, ****$p < 0.0001$.

Descriptive statistics, including means and standard deviation (SD), are shown for each data point. Comparisons between 2 groups were done using unpaired *t*-test and for more than 2 groups, using one-way ANOVA or mixed-designed ANOVA analysis. The level of statistical significance was set at 5%, and *p* values are indicated between treatments that showed statistically significant differences.

3 Results

3.1 Zoledronic acid and dexamethasone stimulate IFN-β production in macrophages

Combined therapy using Zol+Dex has shown activity in MM. However, the synergy between the drugs leads to reduced skeletal-related events with unclear mechanisms (Tosi et al., 2006). We hypothesized that Zol+Dex treatment blocks osteoclast differentiation *via* changes in IFN-β levels. Therefore, we analyzed changes in IFN-β secretion from RAW 264.7 macrophages following treatment with Zol (10 μM), Dex (1 μM), and Zol+Dex or vehicle. After 4 h of incubation, IFN-β levels were evaluated by ELISA. The results showed the combined treatment with Zol and Dex for 4 h, but not with each drug alone, induced an increase in IFN-β secretion (Figure 1A). This regulation was specific for IFN-β as neither IFN-α nor IFN-γ transcription was upregulated by Zol+Dex (Supplementary Figure S1). Notably, the increase in IFN-β secretion was associated with a corresponding increase in the expression of ISG15 by macrophages exclusively following Zol+Dex treatment (Figures 1B,C). Thus, the combined treatment with Zol and Dex seems to induce the secretion of biologically-active IFN-β by macrophages.

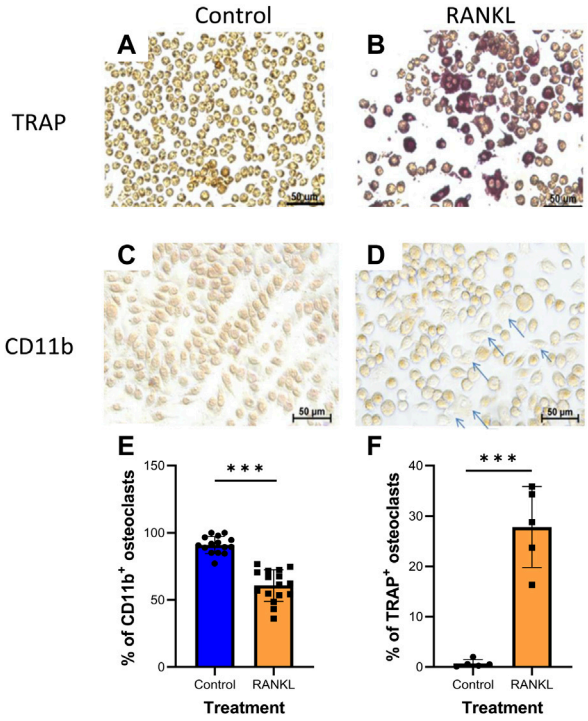

FIGURE 2
RANKL induces osteoclastogenesis in RAW 264.7 macrophages. RAW 264.7 cells were stained for TRAP **(A,B)**; $n = 5$ or CD11b **(C,D)**; $n = 3$ (arrows indicate unstained differentiated cells). **(E–F)** Averages of quantification of osteoclasts ($TRAP^+$, $CD11b^-$cells) using the ImageJ program. Statistical significance by Student's *t*-test between control and RANKL treatments is indicated. ***$p < 0.001$.

3.2 RANKL induces osteoclastic differentiation of RAW 264.7 macrophages

Next, we determined the effect of Zol and/or Dex on osteoclastic differentiation of RAW 264.7 macrophages. To this end, we first determined whether RAW 264.7 macrophages differentiate into osteoclasts upon exposure to the osteoclastogenic cytokine RANKL as in (Kats et al., 2016). Two staining methods were used to identify the cells in the culture: 1) TRAP staining, which stains osteoclasts, and 2) CD11b staining, which identifies undifferentiated macrophages. Our results showed that treatment with RANKL (30 ng/ml) for 5 days resulted in macrophage differentiation to osteoclasts manifested by an increase in the $TRAP^+$ cells (from 1.02 ± 0.67% to 30.7 ± 4.81% of the cells) and a concomitant decrease in $CD11b^+$ cells (from 92.03 ± 5.1% to 60.1 ± 11.47% of cells). Overall, these results suggest that ~30.7% of the macrophages differentiated into osteoclasts when cultured with RANKL. The differences between RANKL and control treatments were significant for both staining methods (P^{***} = 0.0001, Figure 2). Since these results indicate that both staining methods provide similar levels of osteoclastic differentiation, we exclusively used TRAP staining in the following experiments.

3.3 Zoledronic acid+dexamethasone and IFN-β reduce osteoclastic differentiation of macrophages and increase intracellular IFN-β

Our previous findings showed osteoclastic differentiation of 30.7% of macrophages when cultured with RANKL. Next, we determined the effect of Zol and/or Dex or IFN-β on osteoclastic differentiation. To this end, macrophages were cultured with RANKL for 5 days. In the first 48 h, the cells were supplemented with RANKL and Zol, and/or Dex (10 μM each) or IFN-β (0.25–2.5 ng/ml). After 5 days, the percentage of $TRAP^+$ cells was quantified. As previously, 30.7% ± 4.81 of macrophages underwent osteoclastic differentiation ($n = 5$) when cultured with RANKL compared to 1.02 ± 0.67% in the control treatment ($p < 0.0001$). Treatment with Zol+Dex decreased osteoclastic differentiation to 7.12 ± 2.31% ($n = 5$, P^{**} = 0.002 compared to RANKL + group). Moreover, treatment with Zol or Dex alone gave similar results (6.3 ± 4.1% and 7.8 ± 2.5% of cells, respectively; $^{**}p = 0.005$ and $^{*}p = 0.04$, respectively) to the Zol+Dex treatment. As expected, treatment with 2.5 ng/ml of IFN-β antibodies reduced osteoclastic differentiation to 13.5% and was statistically significant compared to RANKL alone or with 0.25 ng/ml IFN-β ($^{***}p = 0.007$, $^{**}p = 0.006$, respectively). Notably, Zol+Dex treatment decreased osteoclastic differentiation to a similar extent as IFN-β (Figure 3, $n = 4$). Next, we determined whether RANKL affects Zol+Dex-induced IFN-β production. Our results show IFN-β levels were reduced following RANKL exposure compared to control treatment. However, higher levels of IFN-β were found when macrophages were treated with Zol+Dex or IFN-β, and RANKL (2.13 ± 0.12 and 2.4 ± 0.42 DU, respectively; $p < 0.05$). In addition, Zol+Dex treatment without RANKL (3.32 ± 0.36 DU) resulted in the highest intracellular levels of IFN-β compared to controls (1.67 ± 0.16 DU). Overall, these results suggest that treatment of macrophages cultured with RANKL with Zol+Dex or IFN-β reduced osteoclastic differentiation and increased intracellular IFN-β levels.

3.4 IFN-β neutralization rescues osteoclastic differentiation of macrophages following Zoledronic acid+dexamethasone treatment

Since Zol+Dex elevated IFN-β levels in RANKL-treated macrophages and IFN-β reduce osteoclastogenesis in these cells, we examined the role of IFN-β in Zol+Dex induced blockade of osteoclastic differentiation of macrophages. To this end, macrophages were treated with RANKL and Zol+Dex or IFN-β (2.5 ng/ml, as control) as well as anti-IFN-β neutralizing antibodies for 48 h. Then, the medium was replaced and resupplemented with RANKL. After additional 3 days, osteoclastic differentiation was measured by TRAP staining. Our results in Figure 4A indicate that Zol and Zol+Dex reduced macrophage numbers, whereas Dex did not. Notably, IFN-β neutralization did not affect Zol-induced cell death but did promote it in Dex-treated macrophages. Importantly, IFN-β neutralization also significantly restored osteoclastic differentiation following Dex or Zol+Dex treatment ($^{***}p < 0.001$) but not following Zol alone (Figure 4B). As expected, treatment with anti-IFN-β antibodies did not affect RANKL-induced osteoclastogenesis (data not shown). Notably, neither STAT1 nor STAT3 inhibition reversed the anti-osteoclastogenic actions of IFN-β or Zol+Dex (Supplementary Figure S2), suggesting that other STAT family members mediate the activity of the Zol+Dex-IFN-β axis. Thus, the abrogation of osteoclast differentiation from macrophages induced by Zol+Dex is mediated, at least in part, by early production of IFN-β.

3.5 Zoledronic acid and dexamethasone induce IFN-β expression by resolution phase macrophages

Dex was previously shown to promote macrophages conversion to the pro-resolving satiated/$CD11b^{low}$ phenotype and enhance IL-10 production by these cells (Schif-Zuck et al., 2011), whereas IFN-β was shown to promote the same events (Kumaran Satyanarayanan et al.,

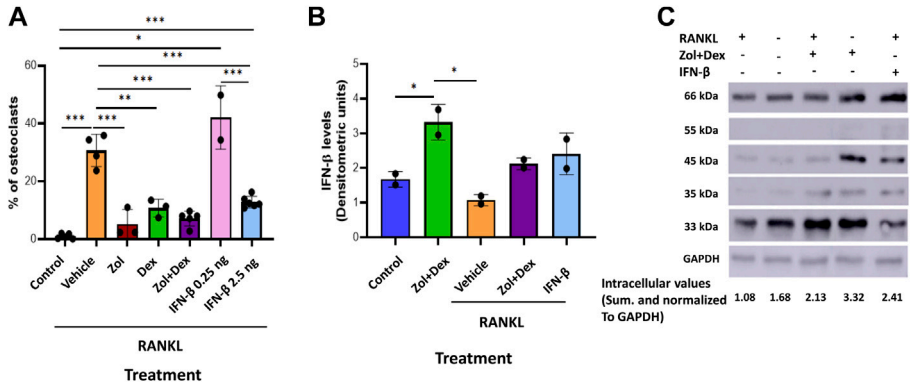

FIGURE 3
Zol+Dex and IFN-β inhibit RANKL-induced osteoclastogenesis. **(A)** Macrophages were treated with RANKL and Zol and/or Dex (10 μM each), or 0.25–2.5 ng/ml IFN-β for 48 h to induce osteoclast differentiation (after 5 days). Then, cells were fixed, stained for TRAP, and image analysis was performed using the ImageJ software. **(B)** Quantitative analysis of macrophages treated with or without RANKL, Zol+Dex, or IFN-β for 24 h. The cells were harvested, and W.B. for IFN-β was performed. The high molecular weight (more than 33 kDa) species of IFN-β underwent densitometric analysis, and the obtained values for each treatment were summed and normalized to GAPDH. **(C)** Representative IFN-β blotting image. Statistical significance by one-way ANOVA between matched treatments is indicated **(A–B)**. *$p < 0.05$, **$p < 0.01$, ***$p < 0.001$, ****$p < 0.0001$ ($n = 2–5$).

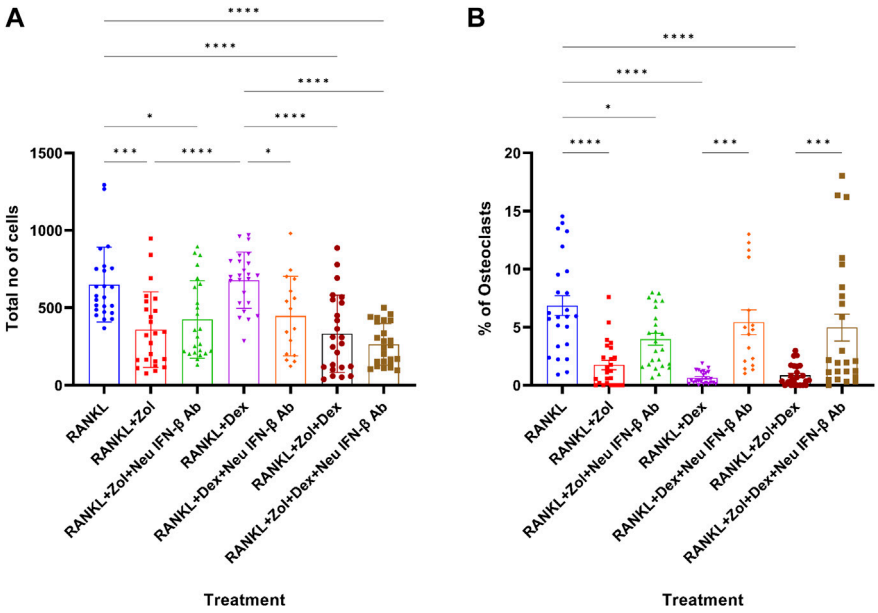

FIGURE 4
Drug-induced inhibition of osteoclastogenesis is mediated by IFN-β. Macrophages were treated for 48 h with RANKL and Zol, Dex or Zol+Dex, and anti-IFN-β neutralizing antibodies (2 μg/ml). Then, culture media was replaced and resupplemented with RANKL for additional 3 days. Next, the cells were stained for TRAP and enumerated, and analysis was performed by the ImageJ software for total cell number **(A)** and % of osteoclasts **(B)**. Statistical significance by one-way ANOVA is indicted ($n = 3$, 8 fields counted). *$p < 0.05$, **$p < 0.01$, ***$p < 0.001$, ****$p < 0.0001$.

2019). Therefore, we sought to determine whether Dex and/or Zol can promote IFN-β expression in resolution phase macrophages. To this end, we recovered macrophages 66 h post zymosan A-induced peritonitis and cultured them for 4–24 h with the indicated drugs. Our results in Figure 5 show a robust increase in IFN-β expression in vehicle and Zol treatments that significantly declined at 24 h. Dex and, to a higher degree, the Zol+Dex treatment induced a much lesser

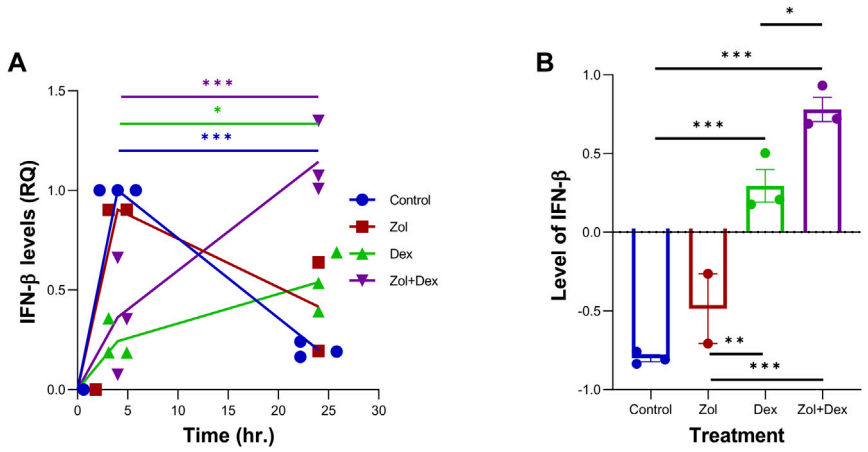

FIGURE 5
Zol+Dex increases IFN-β transcripts in peritoneal macrophages at 24 h. Male C57BL/6 mice were injected intraperitoneally with zymosan A (1 mg/mouse). After 66 h, the peritoneal exudates were collected, and peritoneal macrophages were isolated. Resolution phase peritoneal macrophages were collected and used immediately (time 0) or incubated for 4 or 24 h with Zol, Dex, or Zol+Dex, 10 μM each. R.N.A. was isolated from the samples, and RT-PCR for IFN-β was performed **(A)** Quantitative analysis of RT-PCR assay of IFN-β transcripts, comparison between 4 and 24 h **(B)** Differences between 24 and 4 h of each treatment. Statistical significance by one-way ANOVA (n = 9). *p < 0.05, **p < 0.01, ***p < 0.001.

induction of IFN-β at 4 h, but this response ascended at 24 h. Thus, Dex seems to induce IFN-β production by resolution phase macrophages, which is enhanced by treatment with Zol.

4 Discussion

Skeletal-related events are a common complication of hematological malignancies and cause severe pain, increased risk of death, and reduced quality of life. The impact of zoledronic acid in the prevention of pain and bone fractures in MM was confirmed in a meta-analysis that evaluated 20 randomized clinical trials with nearly 7,000 patients (Alegre et al., 2014). The direct suppression of osteoclast function by BPs and its consequences on bone remodeling has been reported in a few *in vivo* studies (Sharma et al., 2013; Alvarez et al., 2019). These effects are perceived to be caused by the inhibition of the intracellular mevalonate (Mev) pathway and the loss of farnesyl pyrophosphate (FPP) and geranygeranyl pyrophosphate (GGPP) synthesis (Gibbs and Oliff, 1997). Glucocorticoids, such as dexamethasone, play an important role in MM treatment. While glucocorticoids have single-agent activity in MM, their combination with other drugs induces higher clinical responses (Burwick and Sharma, 2019). Here, we investigated a potentially new mechanism of action for combined therapy with BPs and Dex in limiting bone resorption, a likely basis for medication-related osteonecrosis of the jaw. Our results showed that the combination of Zol and Dex increased IFN-β secretion as well as the expression of ISG15. We also found that treatment with Dex, Zol+Dex, or IFN-β alone limited osteoclastogenesis in an IFN-β-dependent manner, irrespective of STAT1 or STAT3 activation.

Dex has been previously shown to limit inflammation and promote its resolution by limiting neutrophil accumulation (Perretti et al., 2002) and enhancing apoptosis of inflammatory (M1) macrophages while promoting the survival of anti-inflammatory macrophages through the adenosine A3 receptor (Barczyk et al., 2010; Achuthan et al., 2018). Dex was also found to enhance the ability of macrophages to engulf apoptotic cells, a key event in the resolution of inflammation (Maderna et al., 2005). In murine peritonitis, Dex was found to promote the uptake of apoptotic cells and limit inflammatory cytokine production while enhancing IL-10 secretion (Schif-Zuck et al., 2011). Notably, we have recently shown elevated levels of IFN-β in peritoneal exudates during the resolution phase of peritonitis and pneumonia in mice, particularly following the uptake of apoptotic cells by resolution-phase macrophages (Kumaran Satyanarayanan et al., 2019). IFN-β, in turn, promotes macrophage efferocytosis and reprogramming to anti-inflammatory phenotypes (Kumaran Satyanarayanan et al., 2019). Thus, we hypothesized that Dex alone or combined with Zol would induce IFN-β expression and secretion from macrophages. Unexpectedly, our results (Figure 1A) showed that only the combination of Zol+Dex, and not each drug alone, induced a rapid secretion of IFN-β. This secretion did not sustain through 24 h (data not shown). However, it was sufficient to result in a significant increase in

the expression of the IFN-β triggered gene ISG15 in Zol+Dex treated macrophages (Figures 1B,C). The fast secretion of IFN-β upon treatment with both drugs suggests that this response does not involve the uptake of apoptotic macrophages but rather the rapid release of internal stores of IFN-β, and could be a result of drug interaction. Thus, Zol and Dex induce a biologically active form of IFN-β from RAW 264.7 macrophages.

Recent publications have shown that type I IFNs decreased Mev lipid synthesis during inflammation (York et al., 2015) and inhibited osteoclast differentiation (Takayanagi et al., 2002). Notably, it was previously shown that BPs induce high levels of IFN-β in osteoclasts, which in turn promotes osteoblast maturation and bone formation (Ma et al., 2018). Moreover, Type I IFN signaling was recently found to limit age-related bone loss and osteoclastogenesis through the induction of guanylate-binding protein (GBP) 5 (Ho and Ivashkiv, 2006; Place et al., 2021). In the current study we have shown only the combined treatment with Zol + Dex, but not with each compound alone, increased IFN-β secretion and the expression of ISG15 in an IFN-β dependent manner in RAW 264.7 macrophages. Moreover, IFN-β, at low concentrations (2.5 ng/ml) inhibited macrophage differentiation to osteoclasts, and IFN-β blockage significantly abrogated either Dex or Zol+Dex inhibition of osteoclastogenesis but did not affect the control treatment. Altogether, these results support our hypothesis that Zol+Dex block macrophage osteoclastogenesis through the secretion of IFN-β and its action on macrophages that might also involve attenuation of Mev synthesis.

In macrophages, IFN-β activates signal transducers and activators of transcription (STAT) 1 and STAT3, mediating the antiviral and inflammatory effects of IFN-β (Ho and Ivashkiv, 2006; Kumaran Satyanarayanan et al., 2019). To detect whether STAT1 or STAT3 mediates the inhibitory effect of Zol+Dex or IFN-β on osteoclastogenesis, specific inhibitors of these transcription factors were used in the aforementioned differentiation assay. Our results indicate that neither the STAT1 nor the STAT3 inhibitor restored the differentiation of osteoclasts upon inhibition by Zol+Dex (Supplementary Figure S2). Nevertheless, the STAT1, but not the STAT3 inhibitor, restored osteoclastogenesis (47.18% recovery) upon inhibition by IFN-β. Notably, this recovery did not reach statistical significance, probably due to the low concentration of fludarabine. Recent publications have shown that STAT3 inhibitors down-regulate the expression of T-bet, GATA3, IL12Rb2, and IFN-γ, as well as the formation of osteoclasts (Holland et al., 2007; Li, 2013). On the other hand, another report has shown that STAT3 deficiency causes skeletal and connective tissue disorders. Notably, Zol treatment increases bone density in these patients by inhibiting the protein suppressor of cytokine signaling 3 (SOCS3), which results in a switch from IL-6 to IL-10 production in macrophages and a decrease in bone loss. The transcription of SOCS3 is regulated by nuclear accumulation of phosphorylated STAT3, and STAT3 is downregulated by SOCS3 (Staines Boone et al., 2016). These results support our conclusion that inhibition of STAT3 does not promote osteoclast differentiation.

STAT1 is essential for gene activation in response to interferon stimulation. Recent publications showed high levels of osteoclasts in bone marrow macrophages from STAT1-deficient mice treated with IFN-β and RANKL (Takayanagi et al., 2002). This manuscript has suggested a signaling cross-talk between RANKL and IFN-β *via* ISGF3, which is composed of STAT1, 2, and IRF-9, and that inhibition of STAT1 impairs the osteogenesis processes by enhancing osteoclast differentiation. Another publication showed that STAT1 protein levels decreased over time after Zol treatment (Muratsu et al., 2013). Our results have shown that STAT1 inhibition did not affect the drug treatment but partially restored osteoclastogenesis upon treatment with IFN-β, albeit without statistical significance. These results suggest STAT1 is not involved in drug-induced IFN-β expression. However, the inhibitory effect of IFN-β on osteoclastogenesis might be dependent, at least in part, on STAT1 activity.

The bone destruction in MM is mediated by osteoclasts, specialized bone-resorbing cells engaged in normal bone remodeling. Myeloma cells and marrow stromal cells produce factors that induce osteoclast formation and activation, thus changing the balance between bone apposition and bone resorption (Muratsu et al., 2013). Combinational therapy of Zol+Dex is clinically effective in preventing and managing myeloma-induced bone disease (Mhaskar et al., 2012). Additional osteoclasts targeting drugs such as: Cyclosporin A (Orcel et al., 1991), Revoremycin A, RANKL antibodies (Ding et al., 2021), Idelalisib (Yeon et al., 2019) and Compactin (Woo et al., 2000) were found to inhibit different satges in osteoclastogenesis and may be usefull to treat MM.

Our findings suggest a new pathway for suppressing bone resorption that involves IFN-β. Within the limits of this study, it can be concluded that Zol+Dex promotes IFN-β secretion. Consequently, IFN-β limits macrophage differentiation into osteoclasts downstream of the Zol+Dex treatment. Notably, IFN-β based therapies are used to treat multiple sclerosis patients with no evidence of MRONJ (Jongen et al., 2011). Thus, IFN-β therapy might be used to inhibit osteoclastogenesis in MM patients, with minimal risk to develop osteonecrosis of the jaw.

Data availability statement

The original contributions presented in the study are included in the article/Supplementary Material, further inquiries can be directed to the corresponding author.

Author contributions

PK performed experiments, analyzed the data, assisted in designing the study, and wrote the manuscript. GC performed experiments, assisted in designing the study, and wrote the manuscript draft. TT and SS-Z assisted in performing the experiments and data analysis. HZ-G and AA designed the study, assisted in data analysis, and wrote the manuscript.

Funding

The study was supported by grants from the Israel Science Foundation (Grant No. 678/13), the Rosetrees Trust (Grant No. M535), and the Wolfson Family Charitable Trust.

Conflict of interest

The authors declare that the research was conducted in the absence of any commercial or financial relationships that could be construed as a potential conflict of interest.

Publisher's note

All claims expressed in this article are solely those of the authors and do not necessarily represent those of their affiliated organizations, or those of the publisher, the editors and the reviewers. Any product that may be evaluated in this article, or claim that may be made by its manufacturer, is not guaranteed or endorsed by the publisher.

Supplementary material

The Supplementary Material for this article can be found online at: https://www.frontiersin.org/articles/10.3389/fphar.2022.1002550/full#supplementary-material

References

Achuthan, A., Aslam, A. S. M., Nguyen, Q., Lam, P. Y., Fleetwood, A. J., Frye, A. T., et al. (2018). Glucocorticoids promote apoptosis of proinflammatory monocytes by inhibiting ERK activity. *Cell. Death Dis.* 9, 267. doi:10.1038/s41419-018-0332-4

Alegre, A., Gironella, M., Bailén, A., and Giraldo, P. (2014). Zoledronic acid in the management of bone disease as a consequence of multiple myeloma: A review. *Eur. J. Haematol.* 92, 181–188. doi:10.1111/ejh.12239

Alexanian, R., Dimopoulos, M. A., Delasalle, K., and Barlogie, B. (1992). Primary dexamethasone treatment of multiple myeloma. *Blood* 80, 887–890. doi:10.1182/blood.v80.4.887.bloodjournal804887

Alvarez, C., Monasterio, G., Cavalla, F., Córdova, L. A., Hernández, M., Heymann, D., et al. (2019). Osteoimmunology of oral and maxillofacial diseases: Translational applications based on biological mechanisms. *Front. Immunol.* 10, 1664. doi:10.3389/fimmu.2019.01664

Barczyk, K., Ehrchen, J., Tenbrock, K., Ahlmann, M., Kneidl, J., Viemann, D., et al. (2010). Glucocorticoids promote survival of anti-inflammatory macrophages via stimulation of adenosine receptor A3. *Blood* 116, 446–455. doi:10.1182/blood-2009-10-247106

Burwick, N., and Sharma, S. (2019). Glucocorticoids in multiple myeloma: Past, present, and future. *Ann. Hematol.* 98, 19–28. doi:10.1007/S00277-018-3465-8

Ding, Y., Cui, Y., Yang, X., Wang, X., Tian, G., Peng, J., et al. (2021). Anti-RANKL monoclonal antibody and bortezomib prevent mechanical unloading-induced bone loss. *J. Bone Min. Metab.* 39, 974–983. doi:10.1007/s00774-021-01246-x

Gibbs, J. B., and Oliff, A. (1997). The potential of farnesyltransferase inhibitors as cancer chemotherapeutics. *Annu. Rev. Pharmacol. Toxicol.* 37, 143–166. doi:10.1146/annurev.pharmtox.37.1.143

Guise, T. A., and Mundy, G. R. (1998). Cancer and bone. *Endocr. Rev.* 19, 18–54. doi:10.1210/edrv.19.1.0323

Ho, H. H., and Ivashkiv, L. B. (2006). Role of STAT3 in type I interferon responses: Negative regulation of STAT1-dependent inflammatory gene activation. *J. Biol. Chem.* 281, 14111–14118. doi:10.1074/jbc.M511797200

Holland, S. M., DeLeo, F. R., Elloumi, H. Z., Hsu, A. P., Uzel, G., Brodsky, N., et al. (2007). STAT3 mutations in the hyper-IgE syndrome. *N. Engl. J. Med.* 357, 1608–1619. doi:10.1056/NEJMOA073687

Hüni, A., and Fryar, J. (1981). Letters to the editor. *World Pat. Inf.* 3, 90–91. doi:10.1016/0172-2190(81)90011-9

Ishikawa, H., Tanaka, H., Iwato, K., Tanabe, O., and Asaoku, H. (1990). Effect of glucocorticoids on the biologic activities of myeloma cells: Inhibition of interleukin-1 beta osteoclast activating factor-induced bone resorption. Available at: https://ashpublications.org/blood/article-abstract/75/3/715/167796 (Accessed July 9, 2022).

Jongen, P. J., Sindic, C., Sanders, E., Hawkins, S., Linssen, W., van Munster, E., et al. (2011). Adverse events of interferon beta-1a: A prospective multi-centre international ich-gcp-based cro-supported external validation study in daily practice. *PLoS One* 6, e26568. doi:10.1371/journal.pone.0026568

Kats, A., Norg Ard, B, M., Wondimu, Z., Koro, C., An, H., Quezada, C., et al. (2016). Aminothiazoles inhibit RANKL- and LPS-mediated osteoclastogenesis and PGE2 production in RAW 264.7 cells. *J. Cell.. Mol. Med.* 20, 1128–1138. doi:10.1111/jcmm.12814

Kumaran Satyanarayanan, S., El Kebir, D., Soboh, S., Butenko, S., Sekheri, M., Saadi, J., et al. (2019). IFN-β is a macrophage-derived effector cytokine facilitating the resolution of bacterial inflammation. *Nat. Commun.* 10, 3471. doi:10.1038/s41467-019-10903-9

Lee, Y., and Kim, H. H. (2011). The role of Jak/STAT pathways in osteoclast differentiation. *Biomol. Ther. Seoul.* 19, 141–148. doi:10.4062/biomolther.2011.19.2.141

Li, J. (2013). JAK-STAT and bone metabolism. *JAK-STAT* 2, e23930. doi:10.4161/jkst.23930

Ma, X., Xu, Z., Ding, S., Yi, G., and Wang, Q. (2018). Alendronate promotes osteoblast differentiation and bone formation in ovariectomy-induced osteoporosis through interferon-β/signal transducer and activator of transcription 1 pathway. *Exp. Ther. Med.* 15, 182–190. doi:10.3892/ETM.2017.5381

Maderna, P., Yona, S., Perretti, M., and Godson, C. (2005). Modulation of phagocytosis of apoptotic neutrophils by supernatant from dexamethasone-treated macrophages and annexin-derived peptide Ac 2–26. *J. Immunol.* 174, 3727–3733. doi:10.4049/jimmunol.174.6.3727

Martin, T. J., Romas, E., and Gillespie, M. T. (1998). Interleukins in the control of osteoclast differentiation. *Crit. Rev. Eukaryot. Gene Expr.* 8, 107–123. doi:10.1615/CritRevEukarGeneExpr.v8.i2.10

Mhaskar, R., Redzepovic, J., Wheatley, K., Clark, O. A. C., Miladinovic, B., Glasmacher, A., et al. (2012). Bisphosphonates in multiple myeloma: A network meta-analysis. *Cochrane Database Syst. Rev.* 16, CD003188. doi:10.1002/14651858.CD003188.pub3

Muratsu, D., Yoshiga, D., Taketomi, T., Onimura, T., Seki, Y., Matsumoto, A., et al. (2013). Zoledronic acid enhances lipopolysaccharide-stimulated proinflammatory reactions through controlled expression of SOCS1 in macrophages. *PLoS One* 8, e67906. doi:10.1371/JOURNAL.PONE.0067906

Orcel, P., Annick Denne, M., and Christine De Vernejoul, M. (1991). Cyclosporin-a *in vitro* decreases bone resorption, osteoclast formation, and the fusion of cells of the monocyte-macrophage lineage. *Endocrinology* 128, 1638–1646. doi:10.1210/endo-128-3-1638

Perretti, M., Chiang, N., La, M., Fierro, I. M., Marullo, S., Getting, S. J., et al. (2002). Endogenous lipid- and peptide-derived anti-inflammatory pathways generated with glucocorticoid and aspirin treatment activate the lipoxin A4 receptor. *Nat. Med.* 8, 1296–1302. doi:10.1038/nm786

Pertsovskaya, I., Abad, E., Domedel-Puig, N., Garcia-Ojalvo, J., and Villoslada, P. (2013). Transient oscillatory dynamics of interferon beta signaling in macrophages. *BMC Syst. Biol.* 7, 59. doi:10.1186/1752-0509-7-59

Place, D. E., Malireddi, R. K. S., Kim, J., Vogel, P., Yamamoto, M., and Kanneganti, T. D. (2021). Osteoclast fusion and bone loss are restricted by interferon inducible guanylate binding proteins. *Nat. Commun.* 12, 496. doi:10.1038/s41467-020-20807-8

Plemmenos, G., Evangeliou, E., Polizogopoulos, N., Chalazias, A., Deligianni, M., and Piperi, C. (2020). Central regulatory role of cytokines in periodontitis and targeting options. *Curr. Med. Chem.* 28, 3032–3058. doi:10.2174/0929867327666200824112732

Reszka, A. A., and Rodan, G. A. (2003). Bisphosphonate mechanism of action. *Curr. Rheumatol. Rep.* 5, 65–74. doi:10.1007/s11926-003-0085-6

Roodman, G. D. (1993). Role of cytokines in the regulation of bone resorption. *Calcif. Tissue Int.* 53, S94–S98. doi:10.1007/BF01673412

Ruggiero, S. L., Dodson, T. B., Aghaloo, T., Carlson, E. R., Ward, B. B., and Kademani, D. (2022). American association of oral and maxillofacial surgeons' position paper on medication-related osteonecrosis of the jaws—2022 update. *J. Oral Maxillofac. Surg.* 80, 920–943. doi:10.1016/j.joms.2022.02.008

Schett, G. (2011). Effects of inflammatory and anti-inflammatory cytokines on the bone. *Eur. J. Clin. Invest.*. 41, 1361–1366. doi:10.1111/j.1365-2362.2011.02545.x

Schif-Zuck, S., Gross, N., Assi, S., Rostoker, R., Serhan, C. N., and Ariel, A. (2011). Saturated-efferocytosis generates pro-resolving CD11blow macrophages: Modulation by resolvins and glucocorticoids. *Eur. J. Immunol.* 41, 366–379. doi:10.1002/eji.201040801

Sharma, D., Ivanovski, S., Slevin, M., Hamlet, S., Pop, T. S., Brinzaniuc, K., et al. (2013). Bisphosphonate-related osteonecrosis of jaw (BRONJ): Diagnostic criteria and possible pathogenic mechanisms of an unexpected anti-angiogenic side effect. *Vasc. Cell.* 5, 1. doi:10.1186/2045-824X-5-1

Staines Boone, A. T., Alcántara-Montiel, J. C., Sánchez-Sánchez, L. M., Arce-Cano, M., García-Campos, J., and Lugo Reyes, S. O. (2016). Zoledronate as effective treatment for minimal trauma fractures in a child with STAT3 deficiency and osteonecrosis of the hip. *Pediatr. Blood Cancer* 63, 2054–2057. doi:10.1002/PBC.26119

Stark, G. R., Kerr, I. M., Williams, B. R. G., Silverman, R. H., and Schreiber, R. D. (1998). How cells respond to interferons. search.proquest.com. Available at: https://search.proquest.com/openview/9839ef1a780a9b89b2fa235e4ccdf131/1?pq-origsite=gscholar&cbl=190 (Accessed July 9, 2022).

Tai, Y. T., Cho, S. F., and Anderson, K. C. (2018). Osteoclast immunosuppressive effects in multiple myeloma: Role of programmed cell death ligand 1. *Front. Immunol.* 9, 1822. doi:10.3389/fimmu.2018.01822

Takayanagi, H., Kim, S., Matsuo, K., Suzuki, H., Suzuki, T., Sato, K., et al. (2002). RANKL maintains bone homeostasis through c-Fos-dependent induction of interferon-beta. *Nature* 416, 744–749. doi:10.1038/416744a

Tosi, P., Zamagni, E., Cellini, C., Parente, R., Cangini, D., Tacchetti, P., et al. (2006). First-line therapy with thalidomide, dexamethasone and zoledronic acid decreases bone resorption markers in patients with multiple myeloma. *Eur. J. Haematol.* 76, 399–404. doi:10.1111/J.0902-4441.2005.T01-1-EJH2520.X

Ural, A. U., Yilmaz, M. I., Avcu, F., Pekel, A., Zerman, M., Nevruz, O., et al. (2003). The bisphosphonate zoledronic acid induces cytotoxicity in human myeloma cell lines with enhancing effects of dexamethasone and thalidomide. *Int. J. Hematol.* 78, 443–449. doi:10.1007/BF02983818

Van Dyke, T. E., Hasturk, H., Kantarci, A., Freire, M. O., Nguyen, D., Dalli, J., et al. (2015). Proresolving nanomedicines activate bone regeneration in periodontitis. *J. Dent. Res.* 94, 148–156. doi:10.1177/0022034514557331

Woo, J. T., Kasai, S., Stern, P. H., and Nagai, K. (2000). Compactin suppresses bone resorption by inhibiting the fusion of prefusion osteoclasts and disrupting the actin ring in osteoclasts. *J. Bone Min. Res.* 15, 650–662. doi:10.1359/jbmr.2000.15.4.650

Yamashita, T., Takahashi, N., and Udagawa, N. (2012). New roles of osteoblasts involved in osteoclast differentiation. *World J. Orthop.* 3, 175–181. doi:10.5312/wjo.v3.i11.175

Yeon, J. T., Kim, K. J., Son, Y. J., Park, S. J., and Kim, S. H. (2019). Idelalisib inhibits osteoclast differentiation and pre-osteoclast migration by blocking the PI3Kδ-Akt-c-Fos/NFATc1 signaling cascade. *Arch. Pharm. Res.* 42, 712–721. doi:10.1007/s12272-019-01163-8

frontiers | Frontiers in Pharmacology

TYPE Original Research
PUBLISHED 13 February 2023
DOI 10.3389/fphar.2023.1126580

OPEN ACCESS

EDITED BY
Pallavi R. Devchand,
University of Calgary, Canada

REVIEWED BY
Fu Liu,
Affiliated Hospital of North Sichuan Medical College, China
Jessica Cusato,
University of Turin, Italy

*CORRESPONDENCE
Mingjie Yu,
ymjxnyy@163.com
Fengjun Sun,
fengj_sun@163.com

†These authors have contributed equally to this work

SPECIALTY SECTION
This article was submitted to Inflammation Pharmacology, a section of the journal Frontiers in Pharmacology

RECEIVED 18 December 2022
ACCEPTED 03 February 2023
PUBLISHED 13 February 2023

CITATION
Cheng L, Liang Z, Liu F, Lin L, Zhang J, Xie L, Yu M and Sun F (2023), Factors influencing plasma concentration of voriconazole and voriconazole- N-oxide in younger adult and elderly patients. *Front. Pharmacol.* 14:1126580. doi: 10.3389/fphar.2023.1126580

Factors influencing plasma concentration of voriconazole and voriconazole- N-oxide in younger adult and elderly patients

Lin Cheng†, Zaiming Liang†, Fang Liu, Ling Lin, Jiao Zhang, Linli Xie, Mingjie Yu* and Fengjun Sun*

Department of Pharmacy, The First Affiliated Hospital of Army Medical University, Third Military Medical University, Chongqing, China

Background: Voriconazole (VCZ) metabolism is influenced by many factors. Identifying independent influencing factors helps optimize VCZ dosing regimens and maintain its trough concentration (C_0) in the therapeutic window.

Methods: We conducted a prospective study investigating independent factors influencing VCZ C_0 and the VCZ C_0 to VCZ N-oxide concentration ratio (C_0/C_N) in younger adults and elderly patients. A stepwise multivariate linear regression model, including the IL-6 inflammatory marker, was used. The receiver operating characteristic (ROC) curve analysis was used to evaluate the predictive effect of the indicator.

Results: A total of 463 VCZ C_0 were analyzed from 304 patients. In younger adult patients, the independent factors that influenced VCZ C_0 were the levels of total bile acid (TBA) and glutamic-pyruvic transaminase (ALT) and the use of proton-pump inhibitors. The independent factors influencing VCZ C_0/C_N were IL-6, age, direct bilirubin, and TBA. The TBA level was positively associated with VCZ C_0 (ρ = 0.176, p = 0.019). VCZ C_0 increased significantly when the TBA levels were higher than 10 μmol/L (p = 0.027). ROC curve analysis indicated that when the TBA level ≥4.05 μmol/L, the incidence of a VCZ C_0 greater than 5 μg/ml (95% CI = 0.54–0.74) (p = 0.007) increased. In elderly patients, the influencing factors of VCZ C_0 were DBIL, albumin, and estimated glomerular filtration rate (eGFR). The independent factors that affected VCZ C_0/C_N were eGFR, ALT, γ-glutamyl transferase, TBA, and platelet count. TBA levels showed a positive association with VCZ C_0 (ρ = 0.204, p = 0.006) and C_0/C_N (ρ = 0.342, p < 0.001). VCZ C_0/C_N increased significantly when TBA levels were greater than 10 μmol/L (p = 0.025). ROC curve analysis indicated that when the TBA level ≥14.55 μmol/L, the incidence of a VCZ C_0 greater than 5 μg/ml (95% CI = 0.52–0.71) (p = 0.048) increased.

Conclusion: TBA level may serve as a novel marker for VCZ metabolism. eGFR and platelet count should also be considered when using VCZ, especially in elderly patients.

KEYWORDS

voriconazole, voriconazole-N-oxide, total bile acid, platelet count, estimated glomerular filtration rate, IL-6

Introduction

Invasive fungal infections (IFIs) remain a clinical problem with high morbidity and mortality despite recent advances in diagnosis and treatment (Jenks et al., 2020). Common pathogens of IFIs are *Candida*, *Cryptococcus*, *Aspergillus*, and *Mucormycetes*. Except for patients with underlying hematologic malignancies, solid organ transplant recipients, and critically ill patients, high rates of IFIs and mortality are also observed among patients 65 years or older (Vallabhaneni et al., 2017; Matthaiou et al., 2018; Hesstvedt et al., 2019; Tsay et al., 2020). Voriconazole (VCZ) is an essential drug for treating IFIs, especially those caused by *Aspergillus* and *Candida*. It is a first-line therapy for patients with invasive *Aspergillosis* (Ullmann et al., 2018). However, VCZ has a narrow therapeutic range. A trough level of 1–5.5 mg/L is recommended for most European patients on VCZ prophylaxis or treatment (Ullmann et al., 2018), while a range of 0.5–5 mg/L is considered adequate for Chinese patients (Chen et al., 2018). Maintaining VCZ trough concentration (C_0) in the therapeutic range is crucial in enhancing its treatment effect.

VCZ exhibits non-linear pharmacokinetics with large interindividual and intraindividual variabilities (Purkins et al., 2002; Theuretzbacher et al., 2006). Many factors influence VCZ C_0, such as age, sex, VCZ dose and administration route, albumin, total bilirubin (TBIL), glutamic-pyruvic transaminase (ALT), glutamic-oxalacetic transaminase (AST), γ-glutamyl transferase (γ-GT), CYP2C19 gene polymorphisms, and inflammatory state. (Vanstraelen et al., 2014; Niioka et al., 2017; Veringa et al., 2017). However, the specificity of each index has certain limitations. Both clinical symptoms and test results must be considered to diagnose and treat infectious diseases. VCZ dosing regimens also require modification according to patients' conditions.

Our previous study found that VCZ C_0 in elderly patients was significantly higher than in younger adult patients. The proportion of patients with C_0 greater than 5 mg/L was higher in older adults (Cheng et al., 2020). VCZ C_0 in elderly patients was not significantly affected by CYP2C19 polymorphisms (Shang et al., 2020). Inflammation could affect liver function, C_0, and the concentration ratio of VCZ C_0 to VCZ N-oxide (C_0/C_N) in younger and older patients (Liang et al., 2022). Therefore, disease state and patient status could confer significant dynamic markers

TABLE 1 Demographic and clinical chacteristics of patients in the two cohorts.

Variable	Younger adult cohort (n = 161)	Elderly cohort (n = 143)	*p*-value
Sex	—	—	0.001
Male (n [%])	96 (59.6)	110 (76.9)	—
Female (n [%])	65 (40.4)	33 (23.1)	—
Age (y)	43 ± 12	72 ± 8	<0.001
Underlying diseases	—	—	—
Leukemia (no. [%])	44 (27.3)	9 (6.3)	—
Hypertension (no. [%])	40 (24.8)	59 (41.3)	—
Diabetes mellitus (no. [%])	23 (14.3)	44 (30.8)	—
Coronary heart disease (no. [%])	2 (1.2)	18 (12.6)	—
Kidney disease (no. [%])	69 (42.9)	53 (37.1)	—
Pneumonia (no. [%])	97 (60.2)	113 (79.0)	—
Fungus category			—
Aspergillus (no. [%])	29 (18.0)	36 (25.2)	—
Saccharomycetes (no. [%])	14 (8.7)	21 (14.7)	—
Monilia (no. [%])	26 (16.1)	33 (23.1)	—
Unidentified fungi (no. [%])	30 (18.6)	27 (18.9)	—
Others (no. [%])	5 (3.1)	1 (0.7)	—
Negative (no. [%])	58 (36.0)	34 (23.8)	—
Route of administration	—	—	0.115
Intravenous (n [%])	130 (80.7)	125 (87.4)	—
Oral (n [%])	31 (19.3)	18 (12.6)	—
VCZ dose (mg/kg/dose)	3.6 ± 0.9	3.4 ± 0.9	0.023
Use of PPI	84 (52.2)	80 (55.9)	0.510

A patient may have several underlying diseases or fungus categories. Abbreviations: PPI, proton-pump inhibitor.

TABLE 2 Laboratory data of patients in the two cohorts.

Variable	Younger adult cohort (*n* = 229)	Elderly cohort (*n* = 234)	*p*-value
Voriconazole C_0 (0.5–5.0 μg/ml)	3.00 (1.60, 4.81)	3.64 (2.12, 5.50)	0.027
Voriconazole C_0/C_N	1.33 (0.67, 3.11)	1.85 (0.85, 3.23)	0.307
IL-6 (0–7 ng/L)	23.9 (6.1, 75.0)	39.9 (15.9, 106.8)	0.001
Platelet count (125–350 $\times 10^9$/L)	113 (39, 211)	169 (96, 255)	<0.001
Hemoglobin (115–150 g/L)	87.6 ± 19.3	93.8 ± 19.0	0.001
Liver function			
ALP (38–126 U/L)	100.0 (73.5, 147.9)	114.7 (80.0, 159.0)	0.170
ALT (13–69 U/L)	22.0 (10.4, 46.0)	22.0 (12.0, 37.9)	0.542
AST (15–46 U/L)	30.9 (18.3, 57.0)	36.8 (24.1, 54.1)	0.068
γ-GT (12–58 U/L)	69.4 (35.0, 151.2)	86.5 (43.8, 169.6)	0.082
TBA (0–10 μmol/L)	4.4 (2.2, 9.8)	5.6 (3.0, 12.0)	0.015
Albumin (30–50 g/L)	33.0 ± 5.6	33.1 ± 5.1	0.870
TBIL (3–22 μmol/L)	13.0 (8.9, 23.8)	14.1 (9.8, 22.7)	0.333
DBIL (0–6 μmol/L)	3.8 (1.7, 8.7)	4.6 (2.5, 10.2)	0.069
IBIL (3–16 μmol/L)	8.7 (5.9, 14.0)	9.1 (6.8, 12.9)	0.436
Renal Function			
Urea nitrogen (1.7–8.3 mmol/L)	9.2 (6.0, 14.1)	12.6 (5.5, 20.0)	0.032
Creatinine (59–104 μmol/L)	81.2 (52.2, 151.5)	75.2 (53.8, 126.0)	0.555
eGFR (80–120 ml/min)	91.7 (41.0, 119.7)	83.9 (46.1, 109.4)	0.445

Data that do not conform to a normal distribution are represented by the median (interquartile range). Abbreviations: C_0, trough concentrations of voriconazole; C_N, trough concentrations of voriconazole-N-oxide; IL-6, interleukin-6; ALP, alkaline phosphatase; ALT, glutamic-pyruvic transaminase; AST, glutamic-oxalacetic transaminase; γ-GT, γ-glutamyl transferase; TBA, total bile acid; TBIL, total bilirubin; DBIL, direct bilirubin; IBIL, indirect bilirubin; eGFR, estimated glomerular filtration rate.

TABLE 3 Influencing factor of VCZ C_0 and C_0/C_N in younger adult patients.

Factor	VCZ C_0			Factor	VCZ C_0/C_N		
	OR (95% CI)	Standardized coefficients	*p*-Value		OR (95% CI)	Standardized coefficients	*p*-Value
Constant	5.074 (3.582, 6.565)	—	<0.001	Constant	−2.030 (−4.059, 0)	—	0.050
TBA	0.049 (0.029, 0.068)	0.428	<0.001	IL-6	0.002 (0.001, 0.002)	0.304	0.004
ALT	−0.016 (−0.029, −0.004)	−0.216	0.012	Age	0.089 (0.046, 0.132)	0.445	<0.001
PPI	−0.968 (−1.844, −0.092)	−0.180	0.031	DBIL	0.132 (0.067, 0.197)	0.684	<0.001
—	—	—	—	TBA	−0.057 (−0.108, −0.006)	−0.361	0.030

Abbreviations: TBA, total bile acid; ALT, glutamic-pyruvic transaminase; PPI, proton-pump inhibitor; DBIL, direct bilirubin.

that contribute to the fluctuation of VCZ concentrations (Chantharit et al., 2020).

According to the US Food and Drug Administration Adverse Event Reporting System (2004–2021 data), the VCZ-induced liver injury ratio is 32.45% (Zhou et al., 2022). Intrinsic and idiosyncratic drug-induced hepatotoxicity causes alterations in bile acid homeostasis (Mosedale and Watkins, 2017). Thus, the total bile acid (TBA) level can influence VCZ metabolism. Platelets are key effector cells for inflammatory responses and have particular advantages (Jenne et al., 2013). Platelet count was one of the determinants of VCZ C_0 in kidney transplant recipients (Zhao Y. C. et al., 2021). VCZ clearance was also significantly associated with platelet count in patients with liver dysfunction (Tang et al., 2019; Tang et al., 2021). The worsening of renal function was significantly associated with a cumulative dose of intravenous VCZ (≥400 mg/kg) (Yasu et al., 2018). Elderly patients often have impaired liver function, renal function, and chronic inflammation induced by chronic disease conditions. Therefore, we hypothesized that platelet count and renal function might affect VCZ metabolism in elderly patients.

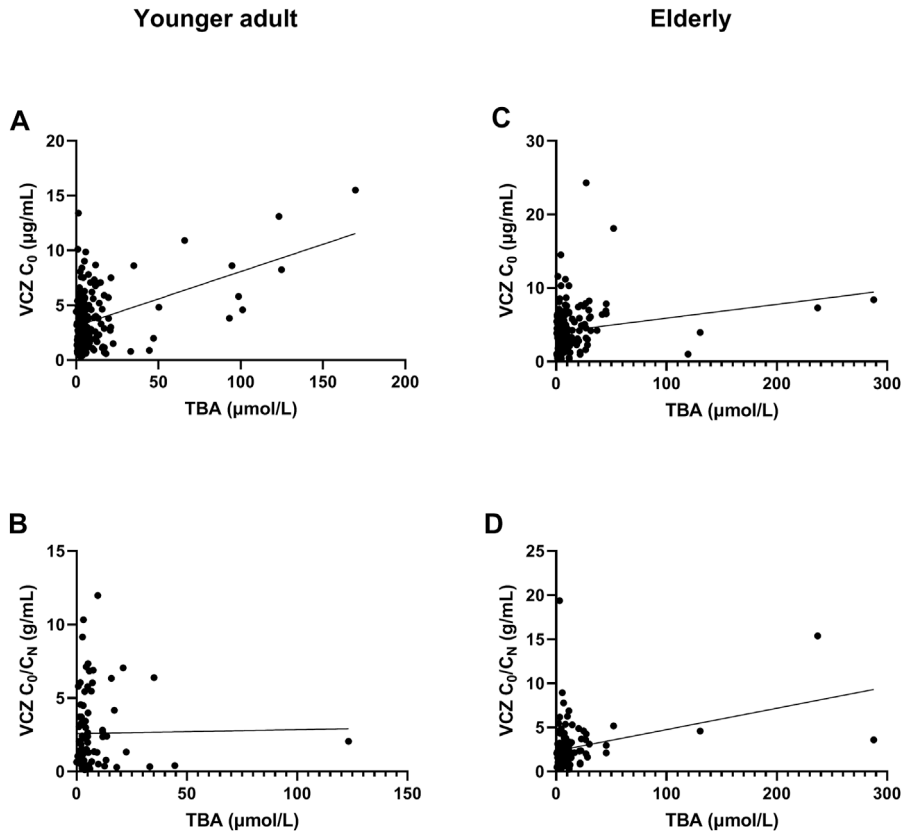

FIGURE 1
Association of total bile acid (TBA) level with voriconazole (VCZ) trough concentration (C_0) and VCZ-to-VCZ N-oxide concentration ratio (C_0/C_N). **(A)**. The TBA level was positively associated with VCZ C_0 in younger adult patients; **(B)**. There was no association between TBA level and VCZ C_0/C_N in younger adult patients; **(C)**. There was a positive association between TBA level and VCZ C_0 in elderly patients; **(D)**. The TBA level was positively associated with VCZ C_0/C_N in elderly patients.

This study aimed to identify the factors affecting VCZ C_0 and C_0/C_N in younger adults and elderly patients using the stepwise multivariate linear regression model. In addition to the influencing factors reported in the literature, the TBA, IL-6, platelet count, hemoglobin, and renal function indexes were also included in the study.

Materials and methods

Patients and study design

A single-center prospective study was conducted from January 2018 to June 2022. The study analyzed patients who received both VCZ prophylaxis and treatment. The inclusion criteria were patients who: (a) received VCZ therapeutic drug monitoring (TDM); (b) aged ≥18 years; (c) with steady-state VCZ $C_0 \geq 0.4$ μg/ml; (d) with available IL-6 concentration data measured on the same day of VCZ C_0 measurement (IL-6 level was routinely detected in our hospital); (e) with available routine blood, liver function, and renal function results measured on the same day of VCZ C_0 measurement; and (f) agreed to the use of their blood samples for VCZ C_N determination and signed informed consent forms.

This study was approved by the Ethics Committee of the First Affiliated Hospital of the Army Medical University. Patients were divided into two cohorts according to age: the elderly cohort (≥60 years) and the younger adult cohort (<60 years).

Data collection

The following data were collected from the medical chart: (a) demographic and clinical characteristics, including age, sex, weight, underlying diseases, fungal infection, VCZ dose and administration route, and combined use of proton-pump inhibitors (PPIs); (b) inflammation marker IL-6 levels; (c) routine blood examination indices, including hemoglobin levels and platelet count; (d) liver function indices, including alkaline phosphatase (ALP), ALT, AST, γ-GT, TBA, albumin, TBIL, direct bilirubin (DBIL), and indirect bilirubin (IBIL) levels; and (e) renal function indices, including urea nitrogen, creatinine levels, and estimated glomerular filtration rate (eGFR). VCZ dosing was adjusted according to the TDM result at the VCZ C_0 measurement.

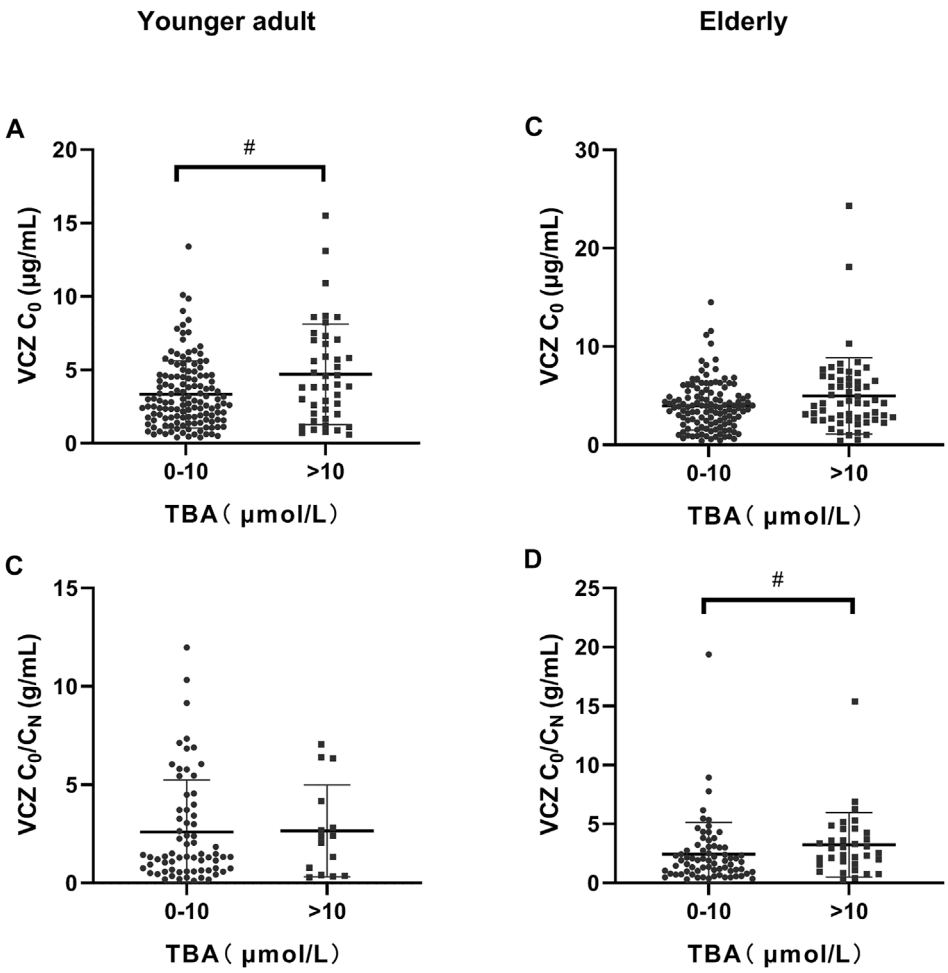

FIGURE 2
Distribution of voriconazole (VCZ) trough concentration (C_0) and the VCZ-to-VCZ N-oxide concentration ratio (C_0/C_N) according to total bile acid (TBA) level. **(A)**. VCZ C_0 in younger adult patients was significantly increased when TBA levels were higher than 10 μmol/L; **(B)**. VCZ C_0/C_N in younger adult patients was similar when TBA levels were between 0 and 10 μmol/L and higher than 10 μmol/L; **(C)**. VCZ C_0 in elderly patients was similar when TBA levels were between 0 and 10 μmol/L and greater than 10 μmol/L; **(D)**. VCZ C_0/C_N in elderly patients increased significantly when TBA levels were higher than 10 μmol/L. $^{\#}p < 0.05$.

VCZ C_0 and VCZ C_N determination

VCZ C_0 was measured routinely in the clinic. The steady state of VCZ C_0 was defined as the concentration obtained after 3 days of intravenous VCZ therapy (a loading dose of 6 mg/kg) or oral VCZ therapy (a loading dose of 400 mg) or the concentration obtained after 5 days of VCZ therapy without a loading dose. VCZ N-oxide is the primary metabolite in plasma, accounting for 72% of circulating VCZ metabolites (Geist et al., 2013). The plasma VCZ C_0/C_N ratio may provide information about VCZ clearance. Therefore, the VCZ C_N was detected. VCZ C_N was measured together with VCZ C_0 using liquid chromatography-tandem mass spectrometry (LC-MS/MS) as previously described (Shang et al., 2020). The limit of detection (LOD) of VCZ and VCZ N-oxide was 8 ng/ml and 10 ng/ml, respectively. The lower limit of quantification (LLOQ) of VCZ and VCZ N-oxide were both 400 ng/ml.

Statistical analysis

IBM SPSS 19.0 (IBM Corp., Armonk, NY, USA) was used to perform the analysis. Categorical data were compared with the chi-square test. Data that do not conform to a normal distribution are represented by the median and interquartile range (IQR). Data from the two cohorts were compared using independent sample t-tests and Mann-Whitney U tests. A stepwise multivariate linear regression model was used to identify the factors influencing the VCZ C_0 and C_0/C_N ratios.

A total of 20 factors were used in the analysis, including sex, age, route of administration of VCZ, VCZ dose, combined use of PPIs, platelet count, and levels of hemoglobin, ALP, ALT, AST, γ-GT, TBA, albumin, TBIL, DBIL, IBIL, urea nitrogen, creatinine, eGFR, and IL-6. Additionally, the Spearman correlation test was performed to assess the association of the TBA level with VCZ C_0 and VCZ C_0/C_N. The receiver operating characteristic (ROC) curve analysis was used to evaluate the predictive effect of

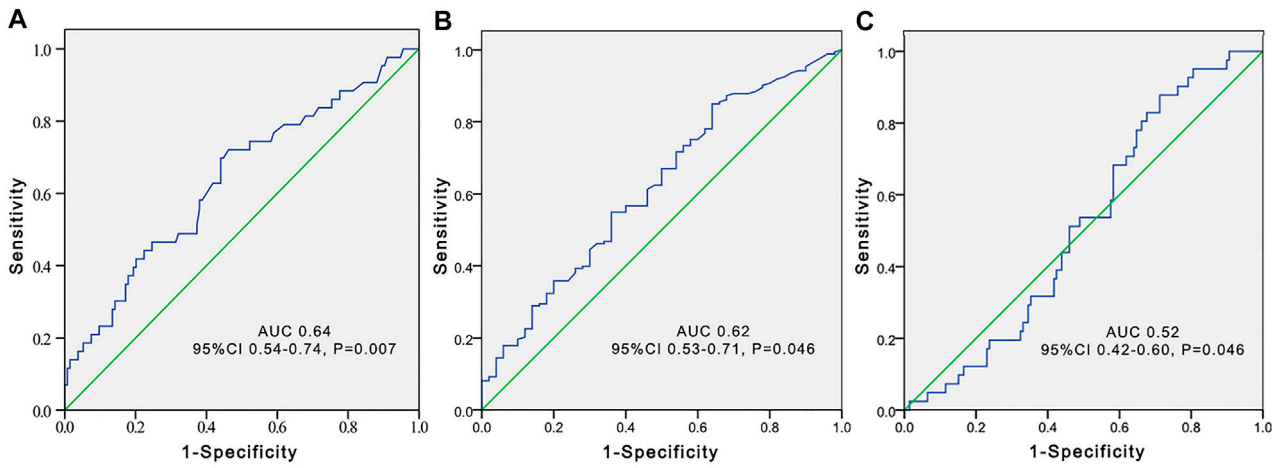

FIGURE 3
Receiver operating characteristic (ROC) curve to predict voriconazole trough concentrations greater than 5 μg/ml according to the total bile acid level **(A)**, platelet count **(B)**, and estimated glomerular filtration rate **(C)** in younger adult patients.

indicators. Covariates with a p-value < 0.1 in the univariate analysis were entered into the multivariate analysis. A p-value < 0.05 was considered statistically significant.

Results

Younger adult patients

A total of 161 younger adult patients were included, with 229 VCZ C_0 and 102 VCZ C_0/C_N. The primary baseline diseases were pneumonia, kidney disease, and leukemia. Almost a third of the patients had negative fungus detection results. Most patients received VCZ intravenously, with a dose of 3.6 ± 0.9 mg/kg, twice daily. Almost half of the patients received PPIs when taking VCZ (Table 1). The percentages of ALP, ALT, AST, TBA, albumin, TBIL, and DBIL within the normal range were 58.3%, 53.4%, 50.0%, 75.7%, 69.3%, 71.9%, and 61.6%, respectively (Table 2).

The independent influencing factors of VCZ C_0 were levels of TBA and ALT and the use of PPIs. The independent influencing factors of VCZ C_0/C_N were IL-6, age, DBIL, and TBA levels (Table 3). TBA values showed a positive association with VCZ C_0 (ρ = 0.176, p = 0.019) but not with VCZ C_0/C_N (ρ = 0.114, p = 0.305) (Figure 1). As shown in Figure 2, VCZ C_0 increased significantly when TBA levels were higher than 10 μmol/L (p = 0.027). The analysis of the ROC curve indicated that TBA levels of ≥4.05 μmol/L, as well as the platelet count less than 31, increased the incidence of VCZ C_0 greater than 5 μg/ml (95% CI = 0.54–0.74) (p = 0.007) (Figure 3). The ROC curve was not used for C_0/C_N due to the lack of a clinically significant threshold.

Elderly patients

A total of 143 elderly patients were included, with 234 VCZ C_0 and 131 VCZ C_0/C_N. The primary baseline diseases were pneumonia, hypertension, and kidney disease. Thirty-four patients (23.8%) had negative fungi detection results. The proportion of men in the elderly cohort was higher than that in the younger adult cohort (p = 0.001). The route of VCZ administration in patients in the two cohorts was similar (p > 0.05). In contrast, the dose of VCZ in the elderly cohort was significantly lower than that in the younger adult cohort (p < 0.001) (Table 1).

VCZ C_0 in the elderly cohort was significantly higher than that in the younger adult cohort (p < 0.05), while the VCZ C_0/C_N ratio in the two cohorts was similar (p > 0.05). The percentages of ALP, ALT, AST, TBA, albumin, TBIL, and DBIL within the normal range were 57.9%, 67.5%, 58.4%, 67.8%, 73.4%, 71.6%, and 59.5%, respectively. The levels of IL-6, platelet count, hemoglobin, TBA, and urea nitrogen in the elderly cohort were significantly higher than those of the younger adult cohort (p < 0.05) (Table 2).

The independent influencing factors of VCZ C_0 were the levels of DBIL, albumin, and eGFR. The independent influencing factors of VCZ C_0/C_N were eGFR, ALT, γ-GT, TBA, and platelet count (Table 4). The TBA level showed a positive association with VCZ C_0 (ρ = 0.204, p = 0.006) and C_0/C_N (ρ = 0.342, p < 0.001), respectively (Figure 1). VCZ C_0/C_N significantly increased when TBA levels were higher than 10 μmol/L (p = 0.025) (Figure 2). ROC curve analysis indicated that when the TBA level ≥14.55 μmol/L, the incidence of a VCZ C_0 greater than 5 μg/ml (95% CI = 0.52–0.71) (p = 0.048) increased (Figure 4).

Discussion

VCZ-induced adverse reactions are generally considered the main reason for drug discontinuation and treatment failure associated with C_0 (Jin et al., 2016; Hamada et al., 2020). Our previous study also showed a considerable number of VCZ C_0 greater than 5 μg/ml, with a ratio of 23.4% in the younger adult cohort and 31.3% in the elderly cohort (Cheng et al., 2020). Therefore, it is crucial to investigate factors affecting VCZ

10.3389/fphar.2023.1126580

TABLE 4 Influencing factor of VCZ C_0 and C_0/C_N in elderly patients.

VCZ C_0				VCZ C_0/C_N			
Factor	OR (95% CI)	Standardized coefficients	*p*-Value	Factor	OR (95% CI)	Standardized coefficients	*p*-Value
Constant	10.112 (5.497, 14.726)	—	<0.001	Constant	3.736 (2.789, 4.683)	—	<0.001
DBIL	0.071 (0.027, 0.115)	0.307	0.002	eGFR	−0.014 (−0.022, −0.007)	−0.382	<0.001
Albumin	−0.160 (−0.288, −0.031)	−0.233	0.016	ALT	0.044 (0.026, 0.061)	0.462	<0.001
eGFR	−0.018 (−0.032, −0.003)	−0.235	0.016	γ-GT	−0.006 (−0.008, −0.003)	−0.398	<0.001
—	—	—	—	TBA	0.022 (0.004, 0.041)	0.230	0.019
—	—	—	—	Platelet count	−0.003 (−0.006, 0)	−0.224	0.026

Abbreviations: DBIL, direct bilirubin; eGFR, estimated glomerular filtration rate; ALT, glutamic-pyruvic transaminase; γ-GT, γ-glutamyl transferase; TBA, total bile acid.

metabolism. A significant correlation was found between VCZ C_0 and age (Allegra et al., 2020; Bolcato et al., 2021). Niioka et al. found that older Japanese patients had higher VCZ C_0/C_N ratios (Niioka et al., 2017). Age was also a predictor of VCZ trough levels >5 μg/ml (Chen et al., 2022). Therefore, we investigated the factors affecting VCZ C_0 and C_0/C_N in younger and elderly patients.

Our previous study found that IL-6 levels were associated with the VCZ C_0/C_N ratio in both younger and elderly patients (r = 0.355, p = 0.003; r = 0.386, p = 0.001). Therefore, this study included IL-6 as an inflammatory marker. IL-6 can directly target liver cells and down-regulate CYP2C19 and CYP3A4 gene expression during inflammation (Li et al., 2014; Klein et al., 2015), affecting VCZ metabolism. Our results showed that IL-6 level was an independent influencing factor of VCZ C_0/C_N in younger adults, which further confirmed the results of our previous study (Cheng et al., 2020; Liang et al., 2022).

Data on the effect of TBA on VCZ metabolism are limited. In the current study, TBA level was the independent influencing factor of VCZ C_0 and C_0/C_N in younger adult patients and the independent influencing factor of C_0/C_N in older patients. TBA can effectively reflect the liver cell injury and the secretion and synthesis function of liver cells. TBA levels rise before the increase of bilirubin, which may partially explain our findings. Furthermore, the ROC curve identified the good predictive effects of TBA for VCZ C_0 greater than 5 μg/ml. Our results indicate that TBA could be a good predictor of VCZ C_0 in younger adult patients.

Platelets emerge as key players in inflammation and are key elements in the early phases of the inflammatory response (Nicolai and Massberg, 2020; Portier and Campbell, 2021). Accumulating evidence demonstrates that platelets contribute to the initiation and propagation of both local and systemic inflammatory processes (Manne et al., 2017). Since platelet count is routinely measured at our hospital, it was chosen as a key element in the inflammatory response. C-reactive protein (CRP) is an inflammatory marker commonly investigated in association with VCZ C_0 and VCZ C_0/C_N in IFI patients (Dote et al., 2016; Encalada Ventura et al., 2016; Veringa et al., 2017; Vreugdenhil et al., 2018). We did not include CRP in this study due to the limited CRP data in the elderly. We also omitted procalcitonin because its association with VCZ C_0/C_N was insignificant in our previous study (Liang et al., 2022). Our results showed that platelet count was an independent influencing factor of VCZ C_0/C_N in elderly individuals. Therefore, platelet count could be considered in patients on VCZ therapies.

Liver function is generally considered to influence VCZ metabolism. VCZ is bound to albumin. Decreased albumin levels increase the unbound fraction of VCZ (Vanstraelen et al., 2014). Serum albumin and γ-GT levels were significantly correlated with the VCZ clearance rate (Chantharit et al., 2020). This study found that albumin level was an independent influencing factor of VCZ C_0, and the γ-GT level was an independent influencing factor of VCZ C_0/C_N in elderly patients. Plasma TBIL concentration significantly influenced VCZ protein-protein binding (Vanstraelen et al., 2014). The TBIL level was associated with VCZ clearance in IFI patients with liver dysfunction (Tang et al., 2021). TBIL level was also considered an independent factor influencing VCZ C_0 (Cheng et al., 2020; Zeng et al., 2020; Zhao Y. et al., 2021). However, our results showed that levels of DBIL but not TBIL influenced VCZ C_0 and C_0/C_N. The liver is rich in a smooth endoplasmic reticulum (ER) equipped with enzymes that metabolize several drugs, including VCZ. DBIL is bioconverted to IBIL in the ER. DBIL

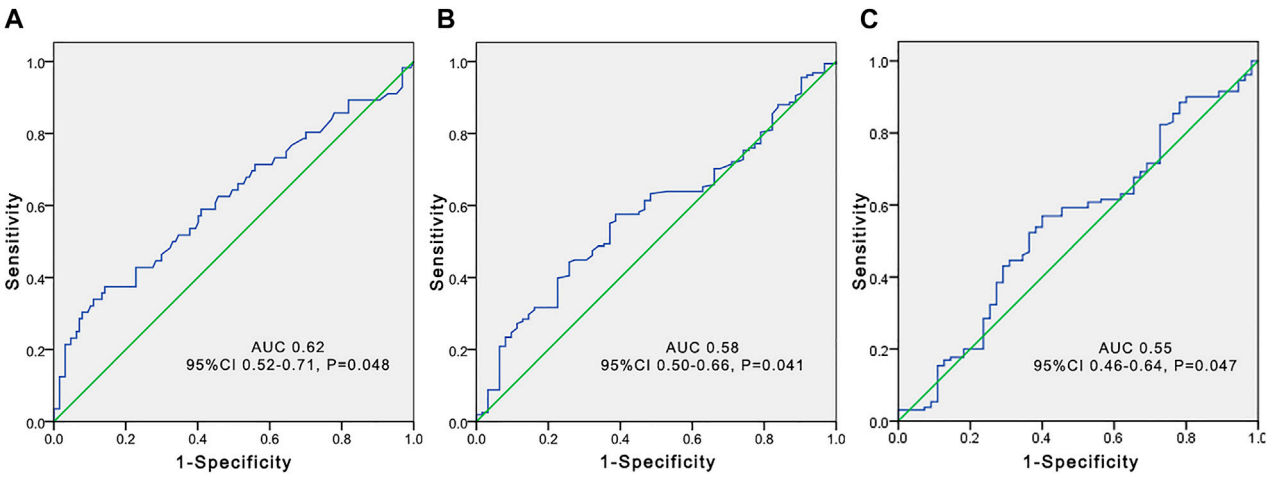

FIGURE 4
Receiver operating characteristic (ROC) curve to predict voriconazole trough concentrations greater than 5 μg/ml according to the total bile acid level **(A)**, platelet count **(B)**, and estimated glomerular filtration rate **(C)** in elderly patients.

levels may reflect the state of the ER and then exhibit an association with the metabolism of VCZ.

We found that eGFR was an independent influencing factor of VCZ C_0 and VCZ C_0/C_N in elderly individuals. Our results showed that the eGFR in the elderly cohort was lower than that in the younger adult cohort, indicating an impaired renal function in the elderly cohort. Although VCZ dose adjustment is not recommended for patients with renal impairment, we should still pay attention to its use in the elderly based on our results. Furthermore, the degree of inflammation in the elderly cohort was more severe than in the younger adult cohort, with impaired liver and kidney function. Therefore, the use of VCZ in elderly patients should be monitored.

CYP2C19, CYP3A4, and CYP2C9 enzymes metabolize PPIs. The combined use of PPIs with VCZ can affect VCZ concentration (Yan et al., 2018). PPIs also significantly affected VCZ C_0 in younger adult patients in our study.

This study has several limitations. First, we did not include samples with VCZ C_0 lower than 0.4 mg/L because the LLOQ of VCZ and VCZ N-oxide were both 400 ng/ml. Second, although the polymorphisms of CYP2C19*2 and *3 are critical for examining the pharmacokinetics of VCZ (Moriyama et al., 2017), the CYP2C19 genotypes were not assessed since testing is not routinely performed. Finally, this study had a relatively small sample size. A large multicenter, prospective study is needed to confirm our results.

In conclusion, we report for the first time that TBA, eGFR, and platelet count were associated with VCZ C_0 and C_0/C_N. Furthermore, the TBA level had a good predictive effect on VCZ C_0 in younger adult patients and may serve as a novel marker of VCZ metabolism. eGFR and platelet count should also be considered when using VCZ, especially in elderly patients.

Data availability statement

The raw data supporting the conclusions of this article will be made available by the authors, without undue reservation.

Ethics statement

The studies involving human participants were reviewed and approved by Ethics Committee of the First Affiliated Hospital of Army Medical University. The patients/participants provided their written informed consent to participate in this study.

Author contributions

LC and FS designed the study, performed the data analysis, and drafted the manuscript. ZL searched the data and performed the data analysis. MY performed the detection. FL, LL, JZ, and LX searched the data. All authors approved the final version of the manuscript.

Funding

This study was supported by the Medical Research Project of Science and Health of Chongqing (2021MSXM218).

Conflict of interest

The authors declare that the research was conducted in the absence of any commercial or financial relationships that could be construed as a potential conflict of interest.

Publisher's note

References

Allegra, S., De Francia, S., De Nicolo, A., Cusato, J., Avataneo, V., Manca, A., et al. (2020). Effect of gender and age on voriconazole trough concentrations in Italian adult patients. *Eur. J. Drug Metab. Pharmacokinet.* 45 (3), 405–412. doi:10.1007/s13318-019-00603-6

Bolcato, L., Khouri, C., Veringa, A., Alffenaar, J. W. C., Yamada, T., Naito, T., et al. (2021). Combined impact of inflammation and pharmacogenomic variants on voriconazole trough concentrations: A meta-analysis of individual data. *J. Clin. Med.* 10 (10), 2089. doi:10.3390/jcm10102089

Chantharit, P., Tantasawat, M., Kasai, H., and Tanigawara, Y. (2020). Population pharmacokinetics of voriconazole in patients with invasive aspergillosis: Serum albumin level as a novel marker for clearance and dosage optimization. *Ther. Drug Monit.* 42 (6), 872–879. doi:10.1097/FTD.0000000000000799

Chen, C., Xu, T., Zhou, K., and Zhu, S. (2022). Factors affecting voriconazole concentration to dose ratio changes according to route of administration. *Eur. J. Hosp. Pharm.* ejhpharm-2021-003173. doi:10.1136/ejhpharm-2021-003173

Chen, K., Zhang, X., Ke, X., Du, G., Yang, K., and Zhai, S. (2018). Individualized medication of voriconazole: A practice guideline of the division of therapeutic drug monitoring, Chinese pharmacological society. *Ther. Drug Monit.* 40 (6), 663–674. doi:10.1097/FTD.0000000000000561

Cheng, L., Xiang, R., Liu, F., Li, Y., Chen, H., Yao, P., et al. (2020). Therapeutic drug monitoring and safety of voriconazole in elderly patients. *Int. Immunopharmacol.* 78, 106078. doi:10.1016/j.intimp.2019.106078

Dote, S., Sawai, M., Nozaki, A., Naruhashi, K., Kobayashi, Y., and Nakanishi, H. (2016). A retrospective analysis of patient-specific factors on voriconazole clearance. *J. Pharm. Health Care Sci.* 2, 10. doi:10.1186/s40780-016-0044-9

Encalada Ventura, M. A., van Wanrooy, M. J., Span, L. F., Rodgers, M. G., van den Heuvel, E. R., Uges, D. R., et al. (2016). Longitudinal analysis of the effect of inflammation on voriconazole trough concentrations. *Antimicrob. Agents Chemother.* 60 (5), 2727–2731. doi:10.1128/AAC.02830-15

Geist, M. J., Egerer, G., Burhenne, J., Riedel, K. D., Weiss, J., and Mikus, G. (2013). Steady-state pharmacokinetics and metabolism of voriconazole in patients. *J. Antimicrob. Chemother.* 68 (11), 2592–2599. doi:10.1093/jac/dkt229

Hamada, Y., Ueda, T., Miyazaki, Y., Nakajima, K., Fukunaga, K., Miyazaki, T., et al. (2020). Effects of antifungal stewardship using therapeutic drug monitoring in voriconazole therapy on the prevention and control of hepatotoxicity and visual symptoms: A multicentre study conducted in Japan. *Mycoses* 63 (8), 779–786. doi:10.1111/myc.13129

Hesstvedt, L., Gaustad, P., Muller, F., Torp Andersen, C., Brunborg, C., Mylvaganam, H., et al. (2019). The impact of age on risk assessment, therapeutic practice and outcome in candidemia. *Infect. Dis. (Lond)* 51 (6), 425–434. doi:10.1080/23744235.2019.1595709

Jenks, J. D., Cornely, O. A., Chen, S. C., Thompson, G. R., 3rd, and Hoenigl, M. (2020). Breakthrough invasive fungal infections: Who is at risk? *Mycoses* 63 (10), 1021–1032. doi:10.1111/myc.13148

Jenne, C. N., Urrutia, R., and Kubes, P. (2013). Platelets: Bridging hemostasis, inflammation, and immunity. *Int. J. Lab. Hematol.* 35 (3), 254–261. doi:10.1111/ijlh.12084

Jin, H., Wang, T., Falcione, B. A., Olsen, K. M., Chen, K., Tang, H., et al. (2016). trough concentration of voriconazole and its relationship with efficacy and safety: A systematic review and meta-analysis. *J. Antimicrob. Chemother.* 71 (7), 1772–1785. doi:10.1093/jac/dkw045

Klein, M., Thomas, M., Hofmann, U., Seehofer, D., Damm, G., and Zanger, U. M. (2015). A systematic comparison of the impact of inflammatory signaling on absorption, distribution, metabolism, and excretion gene expression and activity in primary human hepatocytes and HepaRG cells. *Drug Metab. Dispos.* 43 (2), 273–283. doi:10.1124/dmd.114.060962

Li, A. P., Yang, Q., Vermet, H., Raoust, N., Klieber, S., and Fabre, G. (2014). Evaluation of human hepatocytes under prolonged culture in a novel medium for the maintenance of hepatic differentiation: Results with the model pro-inflammatory cytokine interleukin 6. *Drug Metab. Lett.* 8 (1), 12–18. doi:10.2174/1872312808011409291553 51

Liang, Z., Yu, M., Liu, Z., Liu, F., Jia, C., Xiong, L., et al. (2022). Inflammation affects liver function and the metabolism of voriconazole to voriconazole-N-oxide in adult and elderly patients. *Front. Pharmacol.* 13, 835871. doi:10.3389/fphar.2022.835871

Manne, B. K., Xiang, S. C., and Rondina, M. T. (2017). Platelet secretion in inflammatory and infectious diseases. *Platelets* 28 (2), 155–164. doi:10.1080/09537104.2016.1240766

Matthaiou, D. K., Dimopoulos, G., Taccone, F. S., Bulpa, P., Van den Abeele, A. M., Misset, B., et al. (2018). Elderly versus nonelderly patients with invasive aspergillosis in the ICU: A comparison and risk factor analysis for mortality from the aspICU cohort. *Med. Mycol.* 56 (6), 668–678. doi:10.1093/mmy/myx117

Moriyama, B., Obeng, A. O., Barbarino, J., Penzak, S. R., Henning, S. A., Scott, S. A., et al. (2017). Clinical pharmacogenetics implementation consortium (CPIC) guidelines for CYP2C19 and voriconazole therapy. *Clin. Pharmacol. Ther.* 102 (1), 45–51. doi:10.1002/cpt.583

Mosedale, M., and Watkins, P. B. (2017). Drug-induced liver injury: Advances in mechanistic understanding that will inform risk management. *Clin. Pharmacol. Ther.* 101 (4), 469–480. doi:10.1002/cpt.564

Nicolai, L., and Massberg, S. (2020). Platelets as key players in inflammation and infection. *Curr. Opin. Hematol.* 27 (1), 34–40. doi:10.1097/MOH.0000000000000551

Niioka, T., Fujishima, N., Abumiya, M., Yamashita, T., Ubukawa, K., Nara, M., et al. (2017). Relationship between the CYP2C19 phenotype using the voriconazole-to-voriconazole N-oxide plasma concentration ratio and demographic and clinical characteristics of Japanese patients with different CYP2C19 genotypes. *Ther. Drug Monit.* 39 (5), 514–521. doi:10.1097/FTD.0000000000000441

Portier, I., and Campbell, R. A. (2021). Role of platelets in detection and regulation of infection. *Arterioscler. Thromb. Vasc. Biol.* 41 (1), 70–78. doi:10.1161/ATVBAHA.120.314645

Purkins, L., Wood, N., Ghahramani, P., Greenhalgh, K., Allen, M. J., and Kleinermans, D. (2002). Pharmacokinetics and safety of voriconazole following intravenous-to oral-dose escalation regimens. *Antimicrob. Agents Chemother.* 46 (8), 2546–2553. doi:10.1128/AAC.46.8.2546-2553.2002

Shang, S., Cheng, L., Li, X., Xiang, R., Yu, M., Xiong, L., et al. (2020). Effect of CYP2C19 polymorphism on the plasma voriconazole concentration and voriconazole-to-voriconazole-N-oxide concentration ratio in elderly patients. *Mycoses* 63 (11), 1181–1190. doi:10.1111/myc.13105

Tang, D., Song, B. L., Yan, M., Zou, J. J., Zhang, M., Zhou, H. Y., et al. (2019). Identifying factors affecting the pharmacokinetics of voriconazole in patients with liver dysfunction: A population pharmacokinetic approach. *Basic Clin. Pharmacol. Toxicol.* 125 (1), 34–43. doi:10.1111/bcpt.13208

Tang, D., Yan, M., Song, B. L., Zhao, Y. C., Xiao, Y. W., Wang, F., et al. (2021). Population pharmacokinetics, safety and dosing optimization of voriconazole in patients with liver dysfunction: A prospective observational study. *Br. J. Clin. Pharmacol.* 87 (4), 1890–1902. doi:10.1111/bcp.14578

Theuretzbacher, U., Ihle, F., and Derendorf, H. (2006). Pharmacokinetic/pharmacodynamic profile of voriconazole. *Clin. Pharmacokinet.* 45 (7), 649–663. doi:10.2165/00003088-200645070-00002

Tsay, S. V., Mu, Y., Williams, S., Epson, E., Nadle, J., Bamberg, W. M., et al. (2020). Burden of candidemia in the United States, 2017. *Clin. Infect. Dis.* 71 (9), e449–e453. doi:10.1093/cid/ciaa193

Ullmann, A. J., Aguado, J. M., Arikan-Akdagli, S., Denning, D. W., Groll, A. H., Lagrou, K., et al. (2018). Diagnosis and management of Aspergillus diseases: Executive summary of the 2017 ESCMID-ECMM-ERS guideline. *Clin. Microbiol. Infect.* 24 (1), e1–e38. doi:10.1016/j.cmi.2018.01.002

Vallabhaneni, S., Benedict, K., Derado, G., and Mody, R. K. (2017). Trends in hospitalizations related to invasive aspergillosis and mucormycosis in the United States, 2000-2013. *Open Forum Infect. Dis.* 4 (1), ofw268. doi:10.1093/ofid/ofw268

Vanstraelen, K., Wauters, J., Vercammen, I., de Loor, H., Maertens, J., Lagrou, K., et al. (2014). Impact of hypoalbuminemia on voriconazole pharmacokinetics in critically ill adult patients. *Antimicrob. Agents Chemother.* 58 (11), 6782–6789. doi:10.1128/AAC.03641-14

Veringa, A., Ter Avest, M., Span, L. F., van den Heuvel, E. R., Touw, D. J., Zijlstra, J. G., et al. (2017). Voriconazole metabolism is influenced by severe inflammation: A prospective study. *J. Antimicrob. Chemother.* 72 (1), 261–267. doi:10.1093/jac/dkw349

Vreugdenhil, B., van der Velden, W., Feuth, T., Kox, M., Pickkers, P., van de Veerdonk, F. L., et al. (2018). Moderate correlation between systemic IL-6 responses and CRP with trough concentrations of voriconazole. *Br. J. Clin. Pharmacol.* 84 (9), 1980–1988. doi:10.1111/bcp.13627

Yan, M., Wu, Z. F., Tang, D., Wang, F., Xiao, Y. W., Xu, P., et al. (2018). The impact of proton pump inhibitors on the pharmacokinetics of voriconazole *in vitro* and *in vivo*. *Biomed. Pharmacother.* 108, 60–64. doi:10.1016/j.biopha.2018.08.121

Yasu, T., Konuma, T., Kuroda, S., Takahashi, S., and Tojo, A. (2018). Effect of cumulative intravenous voriconazole dose on renal function in hematological patients. *Antimicrob. Agents Chemother.* 62 (9), e00507–e00518. doi:10.1128/AAC.00507-18

Zeng, G., Wang, L., Shi, L., Li, H., Zhu, M., Luo, J., et al. (2020). Variability of voriconazole concentrations in patients with hematopoietic stem cell transplantation and hematological malignancies: Influence of loading dose, procalcitonin, and pregnane X receptor polymorphisms. *Eur. J. Clin. Pharmacol.* 76 (4), 515–523. doi:10.1007/s00228-020-02831-1

Zhao, Y. C., Lin, X. B., Zhang, B. K., Xiao, Y. W., Xu, P., Wang, F., et al. (2021b). Predictors of adverse events and determinants of the voriconazole trough concentration in kidney transplantation recipients. *Clin. Transl. Sci.* 14 (2), 702–711. doi:10.1111/cts.12932

Zhao, Y., Xiao, C., Hou, J., Wu, J., Xiao, Y., Zhang, B., et al. (2021a). A large sample retrospective study on the distinction of voriconazole concentration in asian patients from different clinical departments. *Pharm. (Basel)* 14 (12), 1239. doi:10.3390/ph14121239

Zhou, Z. X., Yin, X. D., Zhang, Y., Shao, Q. H., Mao, X. Y., Hu, W. J., et al. (2022). Antifungal drugs and drug-induced liver injury: A real-world study leveraging the fda adverse event reporting System database. *Front. Pharmacol.* 13, 891336. doi:10.3389/fphar.2022.891336

frontiers | Frontiers in Pharmacology

TYPE Review
PUBLISHED 21 February 2023
DOI 10.3389/fphar.2023.1109576

OPEN ACCESS

EDITED BY
Pallavi R. Devchand,
University of Calgary, Canada

REVIEWED BY
Wei Zhou,
China Pharmaceutical University, China
Shen Xiang-chun,
Guizhou Medical University, China

*CORRESPONDENCE
Cong Chen,
706427081@qq.com

SPECIALTY SECTION
This article was submitted to Inflammation Pharmacology, a section of the journal Frontiers in Pharmacology

RECEIVED 29 November 2022
ACCEPTED 27 January 2023
PUBLISHED 21 February 2023

CITATION
Wang J, Liu Y-M, Hu J and Chen C (2023), Trained immunity in monocyte/macrophage: Novel mechanism of phytochemicals in the treatment of atherosclerotic cardiovascular disease. *Front. Pharmacol.* 14:1109576. doi: 10.3389/fphar.2023.1109576

Trained immunity in monocyte/macrophage: Novel mechanism of phytochemicals in the treatment of atherosclerotic cardiovascular disease

Jie Wang, Yong-Mei Liu, Jun Hu and Cong Chen*

Guang'anmen Hospital, China Academy of Chinese Medicine Sciences, Beijing, China

Atherosclerosis (AS) is the pathology of atherosclerotic cardiovascular diseases (ASCVD), characterized by persistent chronic inflammation in the vessel wall, in which monocytes/macrophages play a key role. It has been reported that innate immune system cells can assume a persistent proinflammatory state after short stimulation with endogenous atherogenic stimuli. The pathogenesis of AS can be influenced by this persistent hyperactivation of the innate immune system, which is termed trained immunity. Trained immunity has also been implicated as a key pathological mechanism, leading to persistent chronic inflammation in AS. Trained immunity is mediated *via* epigenetic and metabolic reprogramming and occurs in mature innate immune cells and their bone marrow progenitors. Natural products are promising candidates for novel pharmacological agents that can be used to prevent or treat cardiovascular diseases (CVD). A variety of natural products and agents exhibiting antiatherosclerotic abilities have been reported to potentially interfere with the pharmacological targets of trained immunity. This review describes in as much detail as possible the mechanisms involved in trained immunity and how phytochemicals of this process inhibit AS by affecting trained monocytes/macrophages.

KEYWORDS

trained immunity, monocyte/macrophage, atherosclerosis, natural products, epigenetic reprogramming, metabolic reprogramming

1 Introduction

Atherosclerotic cardiovascular diseases (ASCVD) have emerged as the most common burden of disease as a result of the aging and expanding global population (Mensah et al., 2019). As the pathology of ASCVD, atherosclerosis (AS) generates a continuous buildup of vessel-occluding plaques in the subendothelial intimal layer of coronary arteries, eventually leading to considerable blood flow restriction and essential tissue hypoxia (Libby, 2002; Gallino et al., 2014). Most cardiovascular events are caused by the rupture of atherosclerotic plaques in the arterial artery wall and the subsequent formation of an occluding thrombus.

In addition to the deposition and retention of modified lipoproteins and the buildup of immune cells in the walls of major arteries, AS is characterized by a low-grade, persistent, chronic inflammation of the arterial wall (Edgar et al., 2021). All phases of AS are mostly attributed to monocytes and monocyte-derived macrophages, which are also thought to be responsible for persistent chronic inflammation (Moore et al., 2013). The traditional view is

that innate immune cells, such as macrophages, can only eliminate pathogens non-specifically through biological processes such as phagocytes (Bonilla and Oettgen, 2010). However, a growing body of research suggests that monocytes/macrophages may also develop memory capabilities similar to those of the adaptive immune system after exposure to pathogens (Arts et al., 2018). Myeloid cells of the innate immune system become more sensitive after activation with the same or different stimuli to produce a persistent inflammatory monocyte/macrophage phenotype, a phenomenon known as "trained immunity" or "innate immunological memory" (Netea et al., 2020). This persistent overactivation of the innate immune system could contribute to the incessant vascular wall inflammation that is characteristic of AS (Moore et al., 2013).

For thousands of years, herbal medicines have been widely utilized alone or as a supplementary strategy to treat various disorders in East Asia because of their reduced toxicity, fewer side effects, and cheaper cost (Wang et al., 2018). Along with the development of these natural therapies, herbal medicine is becoming more widely accepted as a supplement and alternative therapy in many countries (Liang et al., 2021). According to the most recent statistics on US-FDA (United States Food and Drug Administration) authorized drugs, herbal remedies have been a vital source of novel medications (Newman and Cragg, 2020). A growing body of scientific evidence has revealed that natural medicines and phytochemicals from natural herbal medicines exhibit promising anti-AS properties (Zhang et al., 2021a). Based on the regulation of targeting trained immunity in monocyte and macrophage, natural compounds generated from herbal remedies are surely excellent resources for selecting potential therapeutics to treat AS.

This review aims to provide more information on the role of trained immunity in the pathophysiology of AS, which might be a potential pharmacological target of natural products.

2 Trained immunity in AS

Conventional wisdom generally considers the adaptive immune system as a specific protective mechanism that can form more specialized lines of defense against re-infection with the same pathogens (Domínguez-Andrés et al., 2019). However, innate immune cells (e.g., macrophages/monocytes) have been reported to display similar immune memory, referred to as trained immunity (Conrath et al., 2015; Milutinović and Kurtz, 2016; Gourbal et al., 2018). Studies of gene-specific chromatin changes brought about by lipopolysaccharide (LPS) have first shown trained immunity characteristics of monocytes/macrophages (Foster et al., 2007). Subsequently, infectious stimuli, such as β-glucan and Bacille Calmette–Guérin (BCG), improved their reactivity to stimulation with unrelated infections or molecular patterns linked with those pathogens (Quintin et al., 2012; Saeed et al., 2014). Factors that contribute to the development of AS, such as uric acid and oxidized low-density lipoprotein (oxLDL), and other endogenous ligands can activate trained immunity (Bekkering et al., 2014; Crișan et al., 2017). Freshly isolated monocytes from patients who had symptoms of coronary artery disease (CAD) had a higher capacity to produce cytokines than those from healthy controls, and this capacity was maintained following *ex vivo* conversion to macrophages for 5 days (Shirai et al., 2016). The atherogenic factors are characterized by increased production of proatherogenic cytokines and chemokines like tumor necrosis factor-α (TNF-α), IL-6, monocyte chemoattractant protein-1 (MCP-1), matrix metalloproteinases 2 (MMP-2), and MMP-9 and increased foam cell formation is indeed demonstrated by large-scale phenotyping of trained macrophages *in vitro* (Bekkering et al., 2014).

After short activation with endogenous ligands, a persistent proinflammatory phenotype can emerge in AS monocytes/macrophages (Leentjens et al., 2018). The three key components of trained immunity are metabolic reprogramming, epigenetic reprogramming, and the promotion of myelopoiesis progenitors (Fanucchi et al., 2021) (Figure 1). First, metabolic reprogramming is responsible for the induction, maintenance, and regulation of trained immunity. Different metabolic pathways supply the required substrates for altering the structure of the respective sections of the chromatin and genome, in addition to acting as a source of energy and building components for the dynamic remodeling of the epigenetic landscape. Second, epigenetic reprogramming ultimately links metabolic changes to a cell's gene expression and inflammatory phenotype. Finally, trained immunity in bone marrow by hematopoietic stem cells (HSCs) maintains long-term effects on circulating monocytes through differentiation into progenitor and mature cells (Mitroulis et al., 2018). In addition to atherosclerotic triggers, such as lipoproteins, glucose, diet, and microbiota-derived substances, proinflammatory cytokines secreted by monocytes/macrophages with an inflammatory phenotype may alter the tissue microenvironment by altering macrophages, the functional state of cells, leading to a vicious circle (Groh et al., 2018).

2.1 Metabolic reprogramming of trained immunity in AS

The trained immune activation has to quickly access a supply of substrates to initiate the numerous metabolic processes associated with the immune response. Intracellular metabolic pathways of glucose, amino acids, lipids, and nucleic acids are altered in response to trained immune activation (Fanucchi et al., 2021). When normal cells are at rest, they obtain enough energy *via* metabolic processes that are extremely effective but rather slow, such as oxidative phosphorylation (OXPHOS) and fatty acid oxidation (FAO) (Augert et al., 2020). In contrast, trained immune cells continue to opt for "aerobic glycolysis," which uses glycolysis instead of OXPHOS to generate energy under normoxic conditions, similar to the "Warburg effect" in cancer (Mills et al., 2016; Renner et al., 2017). In addition to glucose metabolism, trained immune cells exhibit altered lipid and amino acid metabolic patterns. For instance, the Krebs cycle's anabolic redefinition to synthesize cholesterol and phospholipids from citrate and acetyl coenzyme A (CoA) is a crucial metabolic event in trained monocytes (Arts et al., 2016a). When exposed to β-glucan, cholesterol synthesis is increased, but fluvastatin, an inhibitor of the enzyme 3-hydroxy-3-methylglutaryl-coenzyme A (HMG-CoA) reductase, inhibits trained immunity by downregulating histone H3 lysine 4 trimethylation (H3K4me3) and limiting the production of proinflammatory

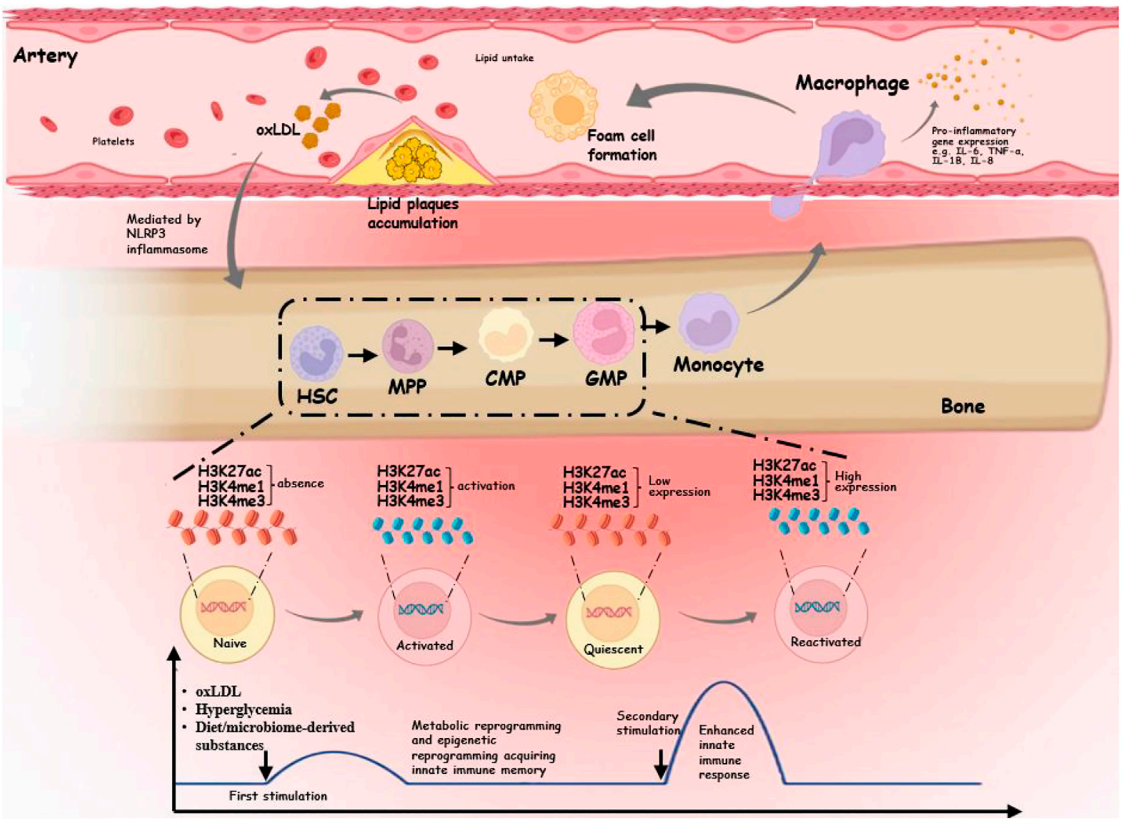

FIGURE 1
Schematic diagram of the trained immunity mechanism in atherosclerotic cardiovascular disease. In the hematopoietic system, myeloid cells exposed to endogenous triggers undergo epigenetic and metabolic reprogramming, resulting in acquiring innate immune memory. The initial gene activation is accompanied by the accumulation of H3K4me3 on the gene promoter, and the persistence of H3K4me1 or H3K27ac in secondary stimulation leads to an enhanced innate immune response. These trained myeloid cells differentiate into monocytes, which travel further into the intima to become macrophages. Trained macrophages produce high levels of proinflammatory cytokines such as TNF-α, IL-6, IL-8, and IL-18 and uptake of lipids to form foam cells. When plaques form, endogenous stimuli may be further released to form trained immunity mediated by the NLRP3 inflammasome.

cytokines (Bekkering et al., 2018). For the progression of AS, the control of cholesterol import and efflux is critical. Similar to glutamine, arginine, and glycine, several particular amino acids are overexpressed in atherosclerotic plaques and have AS-promoting effects (Mallat et al., 1999; Sheehan et al., 2011). The intermediate metabolites from many metabolic pathways, such as aerobic glycolysis, glutaminolysis, cholesterol metabolism, and fatty acid synthesis, not only are a source of energy for the cell but also play several significant biological roles (Groh et al., 2018). Additionally, some chemo drugs made from natural herbal products, such as resveratrol and epigallocatechin gallate, can prevent cells from reprogramming their metabolism in response to AS.

2.1.1 Glucose metabolism and AS

Although OXPHOS produces ATP more efficiently than other cellular processes (approximately 30 ATP molecules can be produced per glucose molecule during OXPHOS, whereas glycolysis can only produce two ATP molecules per glucose molecule) (Tabas and Bornfeldt, 2020). However, glycolysis produces ATP faster than OXPHOS, allowing immune cells to respond quickly to stimuli (Tabas and Bornfeldt, 2020). A clinical trial found an enhanced capacity for cytokine production in circulating monocytes obtained from ASCVD patients, which was associated with the upregulation of glycolytic enzymes (Bekkering et al., 2016; Shirai et al., 2016). This phenotype continued even after *in vitro* macrophage differentiation, displaying a greater glycolytic flux and a higher oxygen consumption rate (Shirai et al., 2016). Furthermore, the inhibition of specific tricarboxylic acid (TCA) cycle steps that support inflammatory processes is associated with increased glycolysis in inflammatory macrophages that primarily produce and release proinflammatory mediators, such as interleukin-1 (IL-1), TNF-α, chemokine C–C motif ligand 2 (CCL2), IL-12, and nitric oxide (NO), through inducible nitric oxide synthase (iNOS). The key proteins involved in glycolysis are introduced in the following sections.

2.1.1.1 GLUT1

Glucose transporter 1 (GLUT1; gene name SLC2A1) on the cell membrane initiates glucose uptake by monocytes/macrophages (Fukuzumi et al., 1996). LPS and oxLDL, which cause inflammation, can boost GLUT1 expression and thereby increase

glucose influx. Hexokinase phosphorylates glucose inside the cell to produce glucose-6-phosphate, which is then utilized in the pentose phosphate pathway (PPP), fatty acid synthase (FAS), or glycolysis. When glucose is processed in the cytosol by glycolysis, two ATPs and pyruvates are produced. Pyruvate produced during glycolysis either enters the mitochondrial TCA cycle or is transformed to lactate by lactate dehydrogenase (Christofk et al., 2008). In plaque macrophages, GLUT1 can promote antiatherosclerotic activities. The efferocytosis procedure increases the expression of GLUT1, which promotes an increase in glucose absorption and a transition from OXPHOS to improved aerobic glycolysis, both of which are required for the effective clearance of apoptotic cells (Morioka et al., 2018). When myeloid-targeted LysM-Cre Slc2a1$^{fl/fl}$ animals were transplanted into Ldlr$^{-/-}$ mice on a Western-style diet (WTD), the amount of necrotic core in the aorta increased (Morioka et al., 2018). Another study revealed that GLUT1 deletion in hematopoietic cells inhibited myelopoiesis, monocyte recruitment to lesions, and the progression of AS in ApoE$^{-/-}$ mice, indicating that the main role of GLUT1 in this model was to encourage the proliferation of bone marrow HSCs and multi-potential progenitors, as well as the commitment of these cells to the bone marrow (Sarrazy et al., 2016).

2.1.1.2 HIF-1α

Hyperoxia-inducible substance 1α (HIF-1α) is activated in hypoxic circumstances, allowing cells to switch to glycolysis and create ATP when oxygen is limited. Low oxygen levels trigger the HIF-1α transcription factor to initiate glycolytic metabolism, which decreases the need for OXPHOS and increases the expression of the key glycolysis proteins GLUT1, hexokinase II (HK-II), and 6-phosphofructo-2-kinase/fructo-2, 6-bisphosphatase (PFKFB3), which increases glycolytic flux (Tawakol et al., 2015). The activated macrophages will emit a lot of cytokines and absorb a lot of glucose. Indeed, hypoxia, HIF-1α expression, and FDG (fluorodeoxyglucose) uptake in macrophages are associated with atherosclerotic plaques in animal models of AS (Folco et al., 2011; Tawakol et al., 2015; Aarup et al., 2016).

2.1.2 Lipid metabolism and AS

In homeostasis, lipoproteins taken up by macrophages are transported to lysosomes for the hydrolysis of cholesteryl esters. Free cholesterol is transported to the cytoplasm, where it is transported to the cell membrane for export or transported to the ER for re-esterification and storage in lipid droplets (LDs). Macrophages in advanced plaques provide signs of huge accumulations of free cholesterol, which suggests a breakdown in the mechanisms that keep cholesterol levels in balance. Membrane damage and metabolic dysregulation in the ER and mitochondria are required to maintain macrophage cholesterol homeostasis and reduce inflammation, which results from excessive accumulation of free cholesterol. Furthermore, high levels of modified cholesterol, oxLDL, are taken up by macrophages to form foam cells and promote plaque by secreting numerous proinflammatory cytokines and chemokines and producing MMPs that degrade plaque extracellular matrix pathogenesis (Khokha et al., 2013; Tall and Yvan-Charvet, 2015). It is reported that the induction of trained immunity in monocytes required stimulation of the cholesterol biosynthesis pathway but not cholesterol synthesis itself. oxLDL is an endogenous ligand that triggers trained immunity to activate monocytes/macrophages (Bekkering et al., 2014; Crişan et al., 2017). Another crucial characteristic of monocytes trained on β-glucan is increased cholesterol production (Netea et al., 2020). In primary human monocytes, fluvastatin, an inhibitor of HMG-CoA reductase, inhibits trained immunity (Arts et al., 2016a). Notably, β-glucan-induced training of mature myeloid cells and their progenitors requires enhanced cholesterol production. The accumulation of cholesterol esters and lipids with more saturated acyl chains is associated with the long-term myelopoiesis bias that β-glucan induced training imparts to HSCs (Mitroulis et al., 2018). The HSC population increase and myelopoiesis caused by β-glucan are reduced by HMG-CoA reductase inhibitor (Mitroulis et al., 2018).

2.1.3 Amino acid metabolism and AS

Under AS pathological conditions, amino acid metabolites play an important role in supporting the induction, maintenance, and regulation mechanisms of trained immunity (Napoli et al., 2006). Therefore, it is necessary to decipher the role of specific amino acid metabolites in the induction of trained immunity.

2.1.3.1 Glutamine

Glutamate is one of the amino acids that has been well-studied for its role in controlling inflammation (Wallace and Keast, 1992). By directly converting into glutamate, α-ketoglutarate, and succinate semialdehyde, glutamine contributes to the TCA cycle (Jha et al., 2015). Additionally, glutamate can be employed as a source of citrate for the FAS-catalyzed production of fatty acids. Recent research has demonstrated that glutaminolysis is increased in trained macrophages and is essential for the establishment of a trained macrophage phenotype in response to β-glucan (Arts et al., 2016a). In a different research study, oxidized phospholipids made of 1-palmitoyl-2-arachidonoyl-sn-glycero-3-phosphorylcholine (oxPAPC) were exposed to macrophages, which led to the development of AS, glutaminolysis, and IL-1 [48]. This study demonstrated that in contrast to macrophages activated with LPS alone, those exposed to oxPAPC and LPS together had a metabolic change (Di Gioia et al., 2020). This metabolic shift was characterized by increased mitochondrial respiration, glutaminolysis, and accumulation of oxaloacetate, which stabilized HIF-1α and increased IL-1β production. IL-1β immunoreactivity in CD68^{+} lesional cells decreased in mice with systemic suppression of this pathway, which also reduced early AS (Di Gioia et al., 2020). Furthermore, the TCA cycle's glutamine replenishment causes fumarate to accumulate, which integrates immunological and metabolic circuits to cause monocyte epigenetic reprogramming by inhibiting KDM5 activity and boosting the methylation of histone lysine 4 residues (Arts et al., 2016a). An epigenetic program identical to trained immunity-mediated by β-glucan was induced by fumarate. To support this, glutaminolysis inhibition and cholesterol production suppression in mice decreased the induction of trained immunity by β-glucan (Arts et al., 2016a).

2.1.3.2 Arginine

In the context of AS pathology, arginine metabolism and its by-product NO are critical for the early stages of the disease (Lv et al., 2021). iNOS is ubiquitously expressed in activated and developing macrophages. NO creation by arginine is probably a factor in the

metabolic transition. NO has been reported to inhibit OXPHOS in activated dendritic cells and inflammatory macrophages downstream of iNOS (Everts et al., 2012; Van den Bossche et al., 2016). Conversely, in alternatively activated macrophages and in the macrophages of atherosclerotic lesions that are regressing, Arg1 converts arginine to putrescine (Willecke et al., 2015). Under specific conditions, these two arginine metabolic routes can inhibit one another. As a result, NO inhibits ornithine decarboxylase's ability to catalyze the conversion of ornithine to putrescine by S-nitrosylation a cysteine that is essential for the enzyme's ability to function (Bauer et al., 2001). Conversely, ornithine decarboxylase prevents macrophages from becoming activated in an inflammatory response (Hardbower et al., 2017). Arginine metabolism has been reprogrammed, which promotes proinflammatory and healing processes.

2.1.3.3 Serine

Recent research has demonstrated that LPS-activated macrophages promote serine synthesis, PPP, and one-carbon metabolism, which synergistically drive epigenetic reprogramming of IL-1β expression. The production of S-adenosylmethionine (SAM) during LPS-induced inflammation is fueled by the synergistic integration of glucose-derived ribose and one-carbon units supplied by glucose and serine metabolism into the methionine cycle through *de novo* ATP synthesis. Impairment of these metabolic pathways that feed SAM generation leads to anti-inflammatory outcomes (Yu et al., 2019). According to a different research study, serine is necessary for the synthesis of glutathione and IL-1β through the action of glycine (Rodriguez et al., 2019).

2.2 Epigenetic reprogramming of trained immunity in AS

Regulating gene expression without changing the DNA sequence itself is referred to as epigenetic reprogramming. Epigenetic reprogramming enables innate immune cells to react to future stimuli with a stronger, quicker, or qualitatively different transcriptional response (Zarzour et al., 2019). Epigenetic regulatory mechanisms encompass diverse molecular processes, including histone post-translational modifications, DNA methylation, and long non-coding RNAs (lncRNAs).

2.2.1 Histone modifications

Epigenetic reprogramming occurs primarily through histone changes at the level of the chromatin structure to promote a sustained enhanced functional state of trained innate immune cells (Saeed et al., 2014). Neutralization of the positive charge of lysine residues in histones by histone acetylation increases the binding of transcription factors activating gene transcription (Bannister and Kouzarides, 2011). The specific lysine residue implicated and the sum of the additional methyl groups determine the effect of histone methylation on gene transcription. Two important epigenetic marks for trained immunity are as follows: the H3K4me3 accumulation at the gene promoter and the histone 3 lysine 27 acetylation (H3K27ac) acquisition at the gene's distal enhancer (generated by histone 3 lysine acid 4 methylation (H3K4me1)) (Netea et al., 2020).

2.2.2 DNA methylation

DNA methylation is involved in the regulation of patterns of gene expression. DNA methyltransferases (DNMTs) use CpG-rich regions as recognition cues to methylate cytosines (m5C), which suppresses transcription. Proteins with histone-binding domains that can "read," "write," or "erase" histone marks may detect the tails that protrude from histone octamers (Fanucchi et al., 2021). In addition to methylation, acetylation, phosphorylation, and ubiquitination, these enzymes can catalyze the addition or removal of a broad and diverse range of other histone modifications. Different DNA methylation patterns discriminate between "responders" (those who can experience taught immunity) and "non-responders" to stimuli, such as BCG, that produce trained immunity (Verma et al., 2017). Forty-three genes had distinct methylation patterns in BCG-naive responders as opposed to non-responders in a follow-up investigation, which may be utilized to predict sensitivity to triggers of trained immunity (Das et al., 2019). Numerous studies have shown that various DNA and histone modification combinations affect whether DNA is kept in an accessible or "open" state or an inaccessible or "closed" one (Fanucchi et al., 2021). To enable quick and effective transcriptional activation, highly accessible DNA is quickly bound by the transcriptional machinery and transcription factors. This establishes a clear connection between the transcriptional state of protein-coding genes and the "openness" of DNA.

2.2.3 lncRNAs

During trained immunity, lncRNA-dependent regulation has a significant impact on the epigenetic reprogramming of immune genes (Fanucchi et al., 2021). Several lncRNAs known as immune-gene priming lncRNAs (IPLs) were found by the application of a bioinformatic pipeline that comprised 3D nuclear architecture, lncRNA and enhancer expression data, and the epigenetic status of immune genes at the genome scale (Fanucchi et al., 2019). The WD repeat-containing protein 5 (WDR5)-mixed lineage leukemia protein 1 complex is directed across the chemokine promoters by UMLILO (upstream master lncRNA of the inflammatory chemokine locus), allowing H3K4me3 epigenetic priming, according to careful analysis of a prototypical IPL known as UMLILO (Fanucchi et al., 2019). Several trained immune genes share this mechanism. Training mediated by β-glucan upregulates IPLs in a way that depends on the nuclear factor of activated T cells, which epigenetically reprograms immune genes. The Cxcl genes are not trained, and the murine chemokine topologically associating domain is devoid of an IPL. Cxcl genes are trained as a result of the insertion of UMLILO into the chemokine topologically associating domain in murine macrophages (Fanucchi et al., 2019). This offers compelling evidence that the development of trained immunity depends on lncRNA-mediated control. Further research is required to examine these pathways in various experimental contexts, as recent studies have only examined the function of IPLs in β-glucan-induced trained immune characteristics.

TABLE 1 Endogenous triggers of trained immunity.

Ligand	Model	Receptor	Trained immunity signaling	Metabolic reprogramming	Epigenetic reprogramming	Atherogenic factor	Reference
oxLDL	Monocytes/ macrophages	TLR IL-1	mTOR/HIF1-α	Glycolysis Mevalonate synthesis	H3K4me3	IL-6, TNF-α, SR-A, CD36, and MCP1	Bekkering et al. (2014); Sohrabi et al. (2018); Keating et al. (2020)
Lipoprotein(a)	Monocytes/ macrophages	Oxidized phospholipids	—	—	—	IL-6 and TNF-α	van der Valk et al. (2016); Stiekema et al. (2020)
Hyperglycemia	BMHSCs	Runx1	IFN-γ	Glycolysis	H3K4me3 and H3K27ac	IL-6 and IL-1β	Edgar et al. (2021)
Catecholamines	BMHSCs	—	β-Adrenergic receptor 1 and 2 cAMP-protein kinase A	Glycolysis and oxidative phosphorylation	H3K4me3	IL-6, IL-8, and TNF-α	van der Heijden et al. (2020a)
Aldosterone	Monocytes/ macrophages	Mineralocorticoid	Fatty acid synthesis pathway	Fatty acid synthesis	H3K4me3	Arterial wall inflammation	van der Heijden et al. (2020b); van der Heijden et al. (2020c)
Hyperlipidemia	BMHSCs	—	NLRP3 IL-1	Cholesterol biosynthesis pathway	Chromatin landscape	—	Christ et al. (2018)

Abbreviation: BMHSCs, bone marrow hematopoietic stem cells; Runx1, Runt-related transcription factor 1; HIF1α, hypoxia-inducible factor 1-alpha; oxLDL, oxidized low-density lipoprotein; IFN-γ, interferon-gamma; TLR, Toll-like receptor; mTOR, mammalian target of rapamycin; NLRP3, NLR family pyrin domain-containing 3; H3K4m3, histone 3 lysine 4 tri-methylation; H3K27ac, histone 3 lysine 27 acetylation; SR-A, type A scavenger receptor; CD36, cluster of differentiation 36; MCP1, monocyte chemoattractant protein 1; TNF-α, tumor necrosis factor-α; IL, interleukin.

2.3 Modulation of myelopoiesis progenitors

The observation of trained circulating monocytes months after BCG vaccination suggests that adaptive processes induced by trained immunity involve alterations in hematopoietic progenitors at the bone marrow level (Kleinnijenhuis et al., 2012). Evidence shows that trained immunity plays a role at the bone marrow level in the context of AS. In mice, the administration of β-glucan leads to long-term transcriptional and metabolic alterations in hematopoietic stem and progenitor cells, resulting in their expansion and bias toward myelopoiesis. This enhances their ability to respond to secondary LPS stimulation and protects them from chemotherapy-induced myelosuppression (Mitroulis et al., 2018). The shared β-subunit of the IL-3/GM-CSF receptor, CD131, is linked with enhanced surface expression in this long-term reprogramming. In a mouse model of predisposition to AS, a similar process occurs when hypercholesterolemia induces enhanced myeloid proliferation and inflammation, suggesting a possible role for trained immunity in the context of traditional cardiovascular risk factors (Wang et al., 2014). Existing evidence also supports a link between enhanced glycolysis in myeloid cells and AS. In hypercholesterolemic ApoE$^{-/-}$ mice, leucocytes and HSPCs show enhanced GLUT1-dependent glucose absorption, which is linked to an elevated mitochondrial potential, providing evidence for a role for myeloid cell glycolysis in myelopoiesis and atherogenesis. This suggests that the mitochondria in these cells are fed by the inflow of glycolytic metabolites for OXPHOS and ATP synthesis (Sarrazy et al., 2016).

3 Endogenous triggers of trained immunity

In addition to microbial sources, endogenous molecules, such as cellular metabolites oxLDL, lipoprotein(a), and hyperglycemia, can induce trained immunity (Bekkering et al., 2014; van der Valk et al., 2016; Braza et al., 2018; Edgar et al., 2021). These endogenous triggers play a role in the development of ASCVD (Flores-Gomez et al., 2021). We will discuss the link between these endogenous triggers of trained immunity and atherosclerotic plaque formation in activated monocyte–macrophages (Table 1).

3.1 oxLDL

oxLDL is a modified lipoprotein and is one of the key atherogenic molecules within plaques that activates immune cells (Moore and Tabas, 2011). oxLDL-trained macrophages exhibit significant metabolic and epigenetic rewiring, similar to BCG and β-glucan. The mammalian target of the rapamycin (mTOR)/HIF1-α signaling pathway is necessary for the upregulation of glycolysis and OXPHOS in oxLDL-induced cells (Keating et al., 2020). The increase in glycolysis and the proinflammatory phenotype in

macrophages were avoided by pharmacological suppression of the mTOR pathway and the signaling molecules involved and by inhibiting glycolysis with 2-deoxyglucose (Sohrabi et al., 2018). Epigenetic reprogramming is another characteristic of oxLDL-trained macrophages. OxLDL interacts with the myeloid cell surface receptor cluster of differentiation 36 (CD36) as a damage-associated molecular pattern (DAMP) (Moore et al., 2013). The internalization and release of oxLDL into the cytoplasm may create cholesterol crystals, which activates the NOD-, LRR-, and pyrin domain-containing protein 3 (NLRP3) inflammasome and releases IL-1β and other proinflammatory cytokines, as well as a protracted inflammatory response (Sheedy et al., 2013). Promoters of genes encoding proinflammatory and proatherogenic cytokines and chemokines, such as IL-6, TNF-α, type A scavenger receptor (SR-A), and CD36, are more likely to have the activating histone modification H3K4me3 [20]. OxLDL training was fully blocked by pharmacologically inhibiting histone methyltransferases, demonstrating that epigenetic alterations are what actually trained immunity by oxLDL (Bekkering et al., 2014).

3.2 Lipoprotein(a)

Lipoprotein(a) is the main circulating carrier of oxidized phospholipids, which plays an important role in atherogenesis (Boffa and Koschinsky, 2019). Monocytes from healthy donors exposed for 24 h to high lipoprotein(a) extracted from hyperlipidemic patients produced more proinflammatory cytokines during the subsequent 6 days compared to controls. Anti-oxidized phospholipid antibodies reduced the training of monocyte-derived macrophages, demonstrating that oxidized phospholipids are the mediating factor in this process (van der Valk et al., 2016). After Pam3Cys and LPS *ex vivo* stimulation, monocytes showed an increased ability to generate proinflammatory cytokines, including IL-6 and TNF-α (van der Valk et al., 2016). A recent study has shown that individuals with cardiovascular diseases (CVD) may have their proinflammatory monocyte activation reversed by significantly reducing their lipoprotein(a) levels, demonstrating that at least some of this proinflammatory impact is reversible (Stiekema et al., 2020).

3.3 Hyperglycemia

Hyperglycemia, a cardinal feature of diabetes, exacerbates AS progression, delays plaque regression (Parathath et al., 2011), and increases proinflammatory gene expression and resistance to induction of M2-related gene expression (American Diabetes Association, 2015). Evidence suggests that hyperglycemia induces trained immunity in HSCs and macrophages, significantly exacerbating AS (Edgar et al., 2021). High extracellular glucose stimulated the production of proinflammatory genes and the functional properties that are proatherogenic in macrophages through pathways that depend on glycolysis. These traits were sustained by diabetic mouse bone marrow-derived macrophages even when they were cultivated in physiological glucose, showing hyperglycemia-induced trained immunity. A disease-relevant and enduring kind of trained innate immunity was demonstrated by an increase in aortic root AS following bone marrow transplantation from diabetic mice into (normoglycemic) $Ldlr^{-/-}$ mice. HSCs and macrophages generated from the bone marrow showed a proinflammatory priming effect in diabetes, according to integrated tests for transposase-accessible chromatin, chromatin immunoprecipitation, and RNA sequencing analysis (Edgar et al., 2021). Transcription factors, notably runt-related transcription factor 1 (Runx1), are implicated as mediators of trained immunity (Himes et al., 2005). These *in vitro* signs of trained immunity brought on by hyperglycemia were eliminated by pharmacological suppression of Runx1.

3.4 Catecholamines

Increased sympathetic nervous system activity leads to proinflammatory leukocytosis in models of chronic psychological stress, stroke, and myocardial infarction (Dutta et al., 2012; Heidt et al., 2014; Courties et al., 2015). The pathways causing inflammatory alterations in disorders with high catecholamine levels can be explained by the fact that catecholamines cause long-lasting proinflammatory modifications in monocytes *in vitro* and *in vivo*, indicating well-trained immunity (van der Heijden et al., 2020a). After being restimulated with LPS 6 days later, monocyte-derived macrophages exposed to a relevant quantity of epinephrine/norepinephrine had higher levels of TNF-α and IL-6. Similar to oxLDL, this trained immune phenotype is connected to a higher glycolytic capability and OXPHOS. Studies using pharmacological inhibition demonstrated that the cAMP-protein kinase A pathway and the β-adrenergic receptors 1 and 2 are crucial for catecholamine-induced training (van der Heijden et al., 2020a). Patients who have pheochromocytoma and are regularly exposed to brief bursts of catecholamine production have this proinflammatory monocyte characteristic (Neumann and Young, 2019). Systemic inflammatory symptoms and an increased *ex vivo* cytokine response in activated monocytes were present in these individuals (Neumann and Young, 2019).

3.5 Aldosterone

Human macrophages deriving from monocytes have a long-lasting proinflammatory phenotype *in vitro* in response to transiently elevated aldosterone concentrations, which may be a factor in the atherosclerotic condition AS chronic inflammation of the artery wall (van der Heijden et al., 2020d). Aldosterone affects intracellular metabolism by increasing fatty acid synthesis, but it does not influence glycolysis and OXPHOS, as found in oxLDL training (van der Heijden et al., 2020c). Additionally, training by aldosterone is linked to the enrichment of H3K4me3 at the promoters of proinflammatory cytokines, including TNF-α and IL-6, demonstrating that aldosterone trains monocyte-derived macrophages *in vitro*. However, circulating monocytes are not more capable of producing cytokines in individuals with primary hyperaldosteronism. The macrophages of individuals with primary hyperaldosteronism only express more TNF-α following *ex vivo* differentiation into macrophages in autologous serum (van der Heijden et al., 2020b). These findings imply that aldosterone

differs from the trained immune systems that have been well-established and elaborated by other stimuli.

3.6 Hyperlipidemia

Recent research examined the possibility that a WTD, which is high in fats, sweets, and salt and lacks fiber, might lead to trained immunity (Christ et al., 2018). Circulating monocytes and their myeloid progenitors in AS-prone Ldlr$^{-/-}$ mice were significantly affected by proinflammatory transcriptional and epigenetic reprogramming from this WTD over 4 weeks. Increased inflammatory responses to subsequent innate immunological stimulation were brought on by the food intervention. Even when the mice were shifted to a typical chow diet for an additional 4 weeks, this trained immune phenotype was maintained despite circulating cholesterol levels and systemic inflammatory indicators reverting to normal (Christ et al., 2018).

4 Inhibitors of targeting trained immunity

Pharmacological inhibitors of histone methyltransferases and inhibitors of glycolysis, glutaminolysis, and the mevalonate pathway could restrain trained immunity. Following intraperitoneal injection of β-glucan, the effects of pharmacologically suppressing glutaminolysis and the pathway that produces mevalonate on the formation of trained immunity have been established in mouse models *in vivo* (Arts et al., 2016a). As a result, it would allow the development of innovative pharmaceutical methods to lower the risk of ASCVD and maybe lessen its negative consequences. In this section, we systematically summarize all reported drugs that suppress trained immunity based on multiple publications.

4.1 Agents that modulate metabolic reprogramming

4.1.1 Wortmannin

The fungus metabolite wortmannin was demonstrated to function as a selective inhibitor of AKT/phosphoinositide 3-kinase (PI3K) (Ui et al., 1995). The intermediate stimulation of the Akt/PI3K pathway is what causes mTOR to become active (Kelley et al., 1999). As stimulation with β-glucan caused a high phosphorylation of Akt, β-glucan was responsible for inducing this signal pathway in monocytes. Additionally, mTOR activation was inhibited as a result of Akt phosphorylation inhibition. Monocyte-trained immunity by β-glucan was suppressed by the Akt inhibitor wortmannin in a dose-dependent manner (Cheng et al., 2014).

4.1.2 Rapamycin

Accumulated mevalonate enhances the AKT-mTOR pathway during the establishment of trained immunity, which then triggers HIF1-α activation and a switch from OXPHOS to glycolysis. This response results in circulating monocytes with a trained immunity phenotype (Bekkering et al., 2018). The inhibition of mTOR with rapamycin prevents mevalonate-induced trained immunity. Additionally, BCG-induced trained immunity and β-glucan-induced trained immunity depend on the development of the histone marks H3K4me3 and H3K9me3, which are inhibited by the pharmacological regulation of rate-limiting glycolysis enzymes with rapamycin [30] [88]. Although rapamycins potently suppress trained immunity *in vitro* and T-cell proliferation *in vivo*, they exert little effect on innate immune cells (Braza et al., 2018).

4.1.3 AICAr

One of the most widely utilized pharmacological AMP-activated protein kinase (AMPK) activity modulators is the nucleoside 5-aminoimidazole-4-carboxamide (AICAr). Early research on AMPK's function in the physiological control of metabolism and the etiology of cancer was mostly centered on the use of AICAr as an AMPK activator (Višnjić et al., 2021). AICAr produces dose-dependent inhibition of β-glucan-induced trained immunity by indirectly inhibiting mTOR (Cheng et al., 2014).

4.1.4 Metformin

Metformin is extensively used as a first-line therapy for type 2 diabetes and has a high safety profile (McCreight et al., 2016). Metformin acts through AMPK activation and subsequent mTOR inhibition. Metformin completely inhibits the protective effects of mice receiving metformin during and after primary infection with low-inoculum *C. albicans*, which increases survival during disseminated candidiasis brought on by a primary *C. albicans* injection. *In vitro*, metformin suppresses trained immunity induced by β-glucan (Cheng et al., 2014). Metformin also inhibits trained immunity by inhibiting the formation of histone marks, H3K4me3 and H3K9me3, by regulating the rate-limiting enzymes of glycolysis [30] [88].

4.1.5 Ascorbate

Ascorbate (vitamin C) is an essential micronutrient in primates and serves as an antioxidant and a cofactor for various enzymatic activities represented by prolyl hydroxylases (Fujii et al., 2022). Because the induction of glycolysis by mTOR is mediated by the activation of HIF1-α and stimulation of glycolytic enzymes and ascorbate inhibits HIF-1α expression, it inhibits training immune in a dose-dependent manner (Cheng et al., 2014).

4.1.6 ZVAD-fmk

Western diet feeding of Ldlr$^{-/-}$ mice induces systemic inflammation, which induces long-lasting trained immunity in myeloid cells (Christ et al., 2018). NLRP3 is a key pathway mediating Western diet-induced trained immunity, and the use of small-molecule inhibitors that block NLRP3 signaling can mitigate its potentially deleterious effects in inflammatory diseases (Christ et al., 2018). ZVAD-fmk (benzyloxycarbonyl-Val-Ala-Asp-fluoromethylketone), a pan-caspase inhibitor, inhibits NLRP3 inflammasome activation in atherosclerotic mice, reducing the accumulation of serum IL-1β and plaque cholesterol crystals (Sheedy et al., 2013).

4.1.7 2-DG

A d-glucose mimic, 2-deoxy-d-glucose (2-DG), inhibits glycolysis by producing and accumulating intracellularly 2-deoxy-d-glucose-6-phosphate (2-DG6P), which then inhibits the activity of

hexokinase and glucose-6-phosphate isomerase and results in cell death (Pajak et al., 2019). BCG immunization causes immunometabolic activation and epigenetic reprogramming, whereas 2-DG's restriction of glycolysis during BCG-induced training cancels out the enhanced cytokine production (Arts et al., 2016b). In addition, the inhibitory effect of 2-DG on glycolysis also inhibits histone methylation and prevents mevalonate-induced trained immunity (Arts et al., 2016b).

4.1.8 3PO

3-(3-Pyridinyl)-1-(4-pyridinyl)-2-propen-1-one (3PO), a small-molecule inhibitor of PFKFB3, inhibits glycolytic flow and is cytostatic to malignant cells (Clem et al., 2008). In cells trained with oxLDL, PFKFB3, a critical rate-limiting enzyme in glycolysis, is increased. The *in vitro* training protocol's dose-dependent attenuation of the oxLDL-augmented production of TNF-α and IL-6 upon subsequent stimulation with LPS was achieved by co-incubating 3PO with oxLDL for the first 24 h (Clem et al., 2008).

4.1.9 Fluvastatin

Fluvastatin, the first fully synthetic HMG-CoA reductase (HMGCR) inhibitor, is reported to prevent the growth and spread of certain malignancies (Cai and Zhao, 2021). Fluvastatin prevents trained immunity by downregulating H3K4me3 and blocking the production of proinflammatory cytokines (Arts et al., 2016a). Fluvastatin also prevents the enhanced foam cell production brought on by training with oxLDL and stops the epigenetic reprogramming of BCG, β-glucan, and oxLDL-induced trained immunity (Arts et al., 2016a). Additionally, following OxLDL-induced trained immunity, scavenger receptor CD36 and SR-A mRNA expression increase, whereas cholesterol efflux transporter ATP binding cassette transporter A1 (ABCA1) and ATP binding cassette transporter G1 (ABCG1) decrease. These effects may be reversed by adding fluvastatin (Bekkering et al., 2018).

4.1.10 Cerulenin

Cerulenin is a potent and specific inhibitor of type II FAS found in various bacteria and mammalian tissues (Tomoda et al., 1984). It is an antifungal antibiotic discovered in a culture filtrate of *Cephalosporium caerulens* (Porrini et al., 2014). Aldosterone levels above normal are linked to a higher risk of CVD in people and the induction of trained immunity in primary human monocytes (van der Heijden et al., 2019). Aldosterone's trained immunity was reduced when cells were pre-incubated with the fatty acid synthesis inhibitor cerulenin for 1 h before re-stimulating with P3C (van der Heijden et al., 2019).

4.2 Agents that modulate epigenetic reprogramming

4.2.1 Ro5-3335

Extracellular glucose promotes macrophage-trained immunity and induces a pro-atherogenic phenotype through a glycolysis-dependent pathway. Runx1, which mediates trained immunity produced by hyperglycemia, is implicated by the pattern of open chromatin (Edgar et al., 2021). A benzodiazepine identified from the screen, Ro5-3335, has a direct interaction with Runx1 (Cunningham et al., 2012). *In vitro* hyperglycemia-induced trained immunity was reversed by pharmacological suppression of Runx1 with Ro5-3335 [4].

4.2.2 MTA

The histone methyltransferase inhibitor 5′-deoxy-5′-methylthioadenosine (MTA) is a non-selective methyltransferase inhibitor. OxLDL causes monocytes to develop a proinflammatory phenotype that persists over time and speeds up AS. MTA completely reverses the methylation of histones, which is required for the change in chromatin architecture that results in increased gene transcription, and thus completely reverses the trained immunity phenotype induced by oxLDL (Bekkering et al., 2014).

4.2.3 Resveratrol

Sirtuin 1 is a nicotinamide adenine dinucleotide (NAD^+)-dependent protein deacetylase and master metabolic regulator (Deng et al., 2019). Phytochemical resveratrol, which is abundant in the skin of red grapes and wine, has been studied extensively for its ability to stimulate Sirtuin 1 activity (Lee et al., 2019). Given that histone acetylation is necessary for β-glucan-induced trained immunity, trained immunity in the presence of the histone deacetylase activator resveratrol prevented trained SHIP-1-deficient macrophages from producing more TNF-α (Saz-Leal et al., 2018).

4.2.4 EGCG

The compound epigallocatechin-3-gallate (EGCG) has been discovered to be a new histone acetyltransferase inhibitor (HATi) with broad specificity for the majority of HAT enzymes (Choi et al., 2009). EGCG can also inhibit trained immunity that relies on β-glucan-induced epigenetic reprogramming (Ifrim et al., 2014).

5 Antiatherosclerotic herbal medicine potentially targeting trained immunity

The notion that trained monocytes/macrophages exhibit a broad range of pro-atherogenic phenotypes, including increased production of cytokines/chemokines and foam cells, has recently been extensively supported experimentally (Leentjens et al., 2018). Trained immunity occurs not only in circulating monocytes but also in myeloid progenitors, ensuring a long-term state of hyperactivation of innate immune cells. Trained immunity is mediated by metabolic and epigenetic reprogramming at the level of histone methylation. Theoretically, these processes are amenable to pharmacological intervention. In the past few decades, more studies have shown that various naturally occurring anti-atherogenic natural products, such as flavonoids, phenols, terpenoids, carotenoids, phenylpropanoids, and alkaloids, may be involved in the regulation of pharmacological targets of trained immunity (Supplementary Table S2). We systematically summarize all relevant literature to investigate all potential natural products against trained immunity in ASCVD.

5.1 Flavonoids

Flavonoids are a group of secondary plant metabolites often employed by vegetables for growth and microbial defense (Izzo et al., 2020). Flavonoids can be further classified as flavones, flavonols, flavanones, isoflavonoids, anthocyanins, flavanols, or catechins based on structural distinctions (Kumar and Pandey, 2013). Due to their antioxidant, anti-inflammatory, anti-mutagenic, anti-aging, cardioprotective, antiviral/bacterial, and anticarcinogenic qualities and their ability to influence enzyme performance, they are linked to a variety of positive health impacts. Flavonoids are thought to mediate epigenetic changes, including DNA methylation, histone modifications, and non-coding RNAs (Fatima et al., 2021). We examine some significant natural products that may target monocyte/macrophage and trained immunity in AS in this section.

5.1.1 Alpinetin

Alpinetin (7-hydroxy-5-methoxyflavanone), a flavonoid, is the main active component of *Alpinia katsumadai* Hayata, a traditional medicinal plant. It engages in various biological processes that affect the NF-κB, MAPK, and PI3K signaling pathways, such as antibacterial, anti-ROS, anticancer, and anti-inflammatory actions (Huo et al., 2012; Wu et al., 2020a; Zhang et al., 2020). The inhibition of the NLRP3 inflammasome may be one way of suppressing trained immunity (Christ et al., 2018). Mechanistically, alpinetin inhibits NLRP3-mediated anti-inflammatory activity and reduces mitochondrial ROS production and HIF-1α transcription, thereby inhibiting HIF-1α signaling (Zhang et al., 2020; Zhu et al., 2021). The expression of the toll-like receptor 4 (TLR4) stimulated by LPS may be dramatically downregulated by alpinetin; alpinetin was reported to have had an anti-inflammatory impact by preventing the production of TNF-α, IL-6, and IL-1β in LPS-stimulated human macrophages (Hu et al., 2013).

5.1.2 Anthocyanins

Anthocyanins are water-soluble glycosides of polyhydroxyl and polymethoxyl derivatives of 2-phenylbenzopyrylium or flavylium salts and are partially responsible for the pigmentation of berries (Azzini et al., 2017). The major anthocyanins in plant foods are glycoside forms of anthocyanidins, including pelargonidin, cyanidin, delphinidin, peonidin, petunidin, and malvidin (Khoo et al., 2017). The bioavailability of anthocyanins is higher than previously thought because the parent compounds are immediately absorbed and converted to bioactive metabolites that remain in circulation (Scalbert et al., 2005; Czank et al., 2013). Anthocyanins increase total antioxidant capacity, antioxidant defense enzymes, and high-density lipoprotein (HDL) antioxidant properties in preclinical and clinical populations through multiple measures, thereby reducing CVD risk factors and mortality in patients with coronary heart disease (Garcia and Blesso, 2021). An essential mediator of trained immunity, the NLRP3-caspase-1 inflammasome, is directly activated upstream by ROS, which is an important mediator of trained immunity (Sun et al., 2020). Preclinical research suggests that anthocyanidins regulate cellular cholesterol efflux from macrophages, hepatic paraoxonase 1 expression, and activity to affect reverse cholesterol transport (RCT) and HDL function beyond simple HDL cholesterol content (Millar et al., 2017). In human populations (such as those who are hyperlipidemic, hypertensive, or diabetic), dietary anthocyanin intake is linked to positive changes in serum biomarkers related to HDL function. These changes include an increase in HDL cholesterol concentration and HDL antioxidant and cholesterol efflux capacities (Millar et al., 2017).

The powdered wild blueberry (*Vaccinium angustifolium*) component high in anthocyanins also reduced lipid buildup in macrophages generated from THP-1 (Del Bo et al., 2016). In accordance with additional studies, the black rice anthocyanin-rich extract blocked the generation of oxLDL and decreased total cholesterol (TC) and LDL-cholesterol (LDL-C) while boosting the amount of HDL-cholesterol (HDL-C) in serum from rats and $ApoE^{-/-}$ mice. In order to lower the risk of an embolism, it also decreased the area of atherosclerotic plaque and improved the stability of the plaque (Xia et al., 2006). In hypercholesterolemic rabbits, fatty streak development and lipid metabolism were slightly influenced by pomegranate peel extract containing anthocyanins (Sharifiyan et al., 2016). This evidence suggests that the potential of anthocyanins to regulate inflammation, lipid buildup, and macrophage may play a role in how an anthocyanin-rich diet lowers the risk of developing CVD.

5.1.2.1 Cyanidin-3-O-β-glucoside

Cyanidin-3-O-glucoside (C3G) is the anthocyanin with the greatest abundance. C3G is abundantly found in fresh fruits, including grapes, berries, blood oranges, peaches, and apples, and in beverages and colored cereals, such as purple rice and maize (Fang, 2015). One investigation found that methylated proteins, particularly H3K4, lose mono- or dimethyl groups when exposed to C3G or its metabolites, which block the enzyme lysine-specific demethylase 1, which controls histone methylation (Abdulla et al., 2013), thereby directly affecting histone-modifying enzymes (Persico et al., 2021). The results reported here show how dietary C3G intake may effectively control H3K4me3 in the mouse liver, especially in promoter areas (Persico et al., 2021). Recent research in a rat model of high-fat diet (HFD)-induced AS examined the antiatherosclerotic potential of C3G. The findings demonstrated that adding 150 mg/kg of C3G to the diet significantly reduced body weight, visceral adiposity, TG, TC, free fatty acids, and AS index (Um et al., 2013). C3G protected $ApoE^{-/-}$ mice against endothelial dysfunction and AS brought on by hypercholesterolemia by preventing the buildup of cholesterol and 7-oxysterol in the aorta (Wang et al., 2012).

5.1.3 Baicalin

Baicalin is a flavonoid active ingredient extracted from the roots of *Scutellaria baicalensis* Georgi, a plant used for many years in Chinese traditional medicine to treat various inflammatory illnesses (Liu and Liu, 2017; Riham et al., 2019). One study showed that baicalin could control metabolic diseases *in vivo*. The therapy with baicalin in HFD rats markedly improved fasting blood glucose levels (Guo et al., 2009). Furthermore, baicalin is reported to inactivate succinate dehydrogenase (SDH) to inhibit ROS production and protect glutamine synthetase (GS) protein stability from oxidative stress to improve glutamate handling and reduce excitotoxicity (Song et al., 2020a).

5.1.4 Chrysin

Chrysin (5,7-dihydroxyflavone) is a flavonoid that naturally occurs in food and is frequently found in honey and propolis, among other plant extracts (Song et al., 2020b). Chrysin possesses various biological qualities, including anti-inflammatory, anti-bacterial, antidiabetic, anticancer, antioxidant, and anti-allergenic actions (Kasala et al., 2015; Mani and Natesan, 2018). One study showed that chrysin has a good expansion effect on human HSCs due to its antioxidant properties by delaying HSC differentiation, inhibiting ROS-activated apoptosis, and regulating cyclin-dependent kinase inhibitors, which can maintain the self-renewal and multilineage differentiation potential of human HSCs (Litviňuková et al., 2020). Chrysin is an emerging histone deacetylase inhibitor for epigenetic regulation in cancer studies (Ganai et al., 2021).

Chrysin may reduce inflammation by modulating M1/M2 status. It promotes the anti-inflammatory M2 phenotype and suppresses the M1 phenotype in peritoneal and cultured macrophages *in vitro* by activating PPAR-γ (Feng et al., 2014). One study showed that chrysin inhibited NLRP3 inflammasome activation and increased IL-1β levels to reduce synovitis (Liao et al., 2020). Another study showed that chrysin inhibits ROS-mediated Akt/mTOR signaling in cells and induces autophagy (He et al., 2021). The study showed that the overexpression of PPARγ, liver X receptor (LXR)α, ABCA1, and ABCG1 expression led to a considerable increase in HDL-mediated RAW264.7 macrophage cholesterol efflux following chrysin treatment (Lin et al., 2015b).

5.1.5 Daidzein

Daidzein, a substance mostly present in soy foods and plants such as red clover, is one of the most studied and potent phytoestrogens (Yang et al., 2012). Studies in non-human primates have shown that dietary intake of soy protein can interfere with related epigenetic changes that may influence the etiology of complex diseases (Howard et al., 2011). By stimulating the PPARγ-LXRα-ABCA1 pathway, daidzein protected low-density lipoprotein (LDL) from oxidation and increased paraoxonase-1 (PON-1) activity in Huh7 cells, which may control cholesterol efflux (Schrader et al., 2012; Ikhlef et al., 2016). Furthermore, daidzein therapy decreased blood cholesterol and increased TG levels in middle-aged male rats given HFD designed to induce AS (Sosić-Jurjević et al., 2007). These suggest that daidzein has antiatherosclerotic potential.

5.1.6 Ellagic acid

Ellagic acid (EA) is a dilactone of hexahydroxydiphenic acid that may be found in various nuts, fruits, and vegetables, such as pomegranates, walnuts, black raspberries, raspberries, almonds, and strawberries (Galano et al., 2014). According to *in vitro*, *in vivo*, and clinical investigations, it has a wide range of physiological actions, including anti-inflammatory, antioxidant, antibacterial, anticarcinogenic, antiplasmodial, antiviral, hepatoprotective, antifibrotic, immunomodulatory, and neuroprotective activities (Gupta et al., 2021). A study showed that EA promotes hematopoietic progenitor cell proliferation and megakaryocyte differentiation (Gao et al., 2014). Other studies have shown that EA interrupts the sequential histone remodeling steps of adipocyte differentiation by reducing the coactivator-associated arginine methyltransferase 1 (CARM1) activity, including histone acetylation and dissociation of HDAC9 from chromatin (Kang et al., 2014). Pomegranate peel polyphenols, in particular pomegranate ellagic acid (PEA), also boosted ApoA1-mediated macrophage cholesterol efflux by upregulating ABCA1 and LXRα and inhibited macrophage lipid buildup by lowering the expression of CD36 (Zhao et al., 2016).

5.1.7 EGCG

EGCG, a typical polyphenol flavonoid molecule with eight free hydroxyl groups, is the most common (Chakrawarti et al., 2016). Research has revealed that EGCG has antibacterial, antiviral, antioxidant, anti-arteriosclerosis, anti-thrombosis, anti-vascular proliferation, anti-inflammatory, and anti-tumor activities (Liu and Yan, 2019). As a histone acetyltransferase inhibitor, EGCG can significantly inhibit the training of monocytes (Ifrim et al., 2014). In different research, EGCG-loaded nanoparticles targeted macrophages *via* their CD36 receptor, reduced the release of inflammatory factors by mouse peritoneal macrophages, and reduced the lesion surface area of arterial plaques in $LDLr^{-/-}$ mice (Zhang et al., 2019). EGCG also inhibited the oxLDL-induced overexpression of SR-A in the same cell line, reducing oxLDL absorption and the formation of foam cells (Chen et al., 2017). EGCG regulated macrophage polarization toward the M2 state. EGCG decreased the expression of proinflammatory M1 mediators, iNOS, TNF-α, IL-1β, and IL-6, in the LPS-administered lung microenvironment and increased the expression of KLF4, Arg1, and ym1, which enhanced the M2 phenotype of macrophages (Almatroodi et al., 2020).

5.1.8 Hesperidin

Hesperidin (3′,5,7,-trihydroxy-4′-methoxyflavanone), a flavanone family of flavonoids, is a derivative of hesperetin, which is present in citrus fruits, such as oranges and grapefruit (Muhammad et al., 2019). Hesperidin has several pharmacological effects, with the main ones being the stimulation of antioxidation, the inhibition of the generation of proinflammatory cytokines, and the inhibition of the proliferation of cancer cells (Li and Schluesener, 2017). A study using metabolic tracing studies showed that TLR signaling in mouse and human macrophages redirects metabolic flux to increase acetyl-CoA for glucose production, thereby enhancing histone acetylation (Christ and Latz, 2019). According to a preclinical study, hesperetin provided neuroprotection by controlling the TLR4/NF-κB signaling pathway in response to the harmful effects of LPS (Muhammad et al., 2019). Hesperetin decreased the generation of foam cells produced from THP-1 by promoting ABCA1 expression by boosting the activities of the ABCA1 promoter and LXR enhancer, upregulating the ApoA1-mediated cholesterol efflux (Iio et al., 2012).

5.1.9 Icariin

Icariin, one of the primary ingredients in epimedium, is an 8-isopentane flavonoside that has several pharmacological benefits, including enhancement of cardiovascular function, promotion of hematological function, prevention of neuronal damage, and

anti-osteoporosis properties (El-Shitany and Eid, 2019). Icariin decreased RAW264.7 macrophage infiltration at atherosclerotic lesions by reducing the CX3CR1–CX3CL1 interaction, which is directly related to monocyte adhesion and migration (Wang et al., 2016a).

5.1.10 Pratensein

Pratensein is a compound extracted from Radix Polygala roots. It has anti-inflammatory, anti-apoptotic, and antioxidant effects (Liu et al., 2016b). Pratensein increases the expression of the ABCA1 protein and HDL levels in HepG2 cells (Gao et al., 2008). AS is brought on by passive LDL transport across damaged endothelial cells. Recent research has revealed a novel therapeutic target in the fight against AS: scavenger receptor class B type I (SR-BI)-mediated endothelial LDL transcytosis. This process increases LDL entry into the arterial wall and the development of AS (Huang et al., 2019). Further investigation found that pratensein increased the expression of CLA-1, a human homolog of SR-BI, indicating that it may have some bearing on the *in vitro* process of cholesterol efflux (Yang et al., 2009).

5.1.11 Puerarin

Puerarin, an isoflavone component extracted from the herb Radix Puerariae, is often employed in China to treat inflammatory and immunological disorders (Yang et al., 2021). Its powerful pharmacological effects are a result of the compounds' many bioactivities. Puerarin's anti-inflammatory processes, which include the control of important signals, including TLR, Nrf2, HDAC, and PPARα, and the enhancement of organelle function (Ni et al., 2020; Niu et al., 2020; Chen et al., 2021), have been thoroughly investigated in recent years (Chang et al., 2021). An earlier study investigated the epigenetic mechanism through which puerarin suppresses MCP-1 production using high-glucose circumstances. It was shown that puerarin dramatically reduced high glucose's ability to upregulate H3K4 di- and tri-methylation (H3K4me2/3) on the MCP-1 gene promoter, suggesting that it may be useful in treating diabetes-related vascular damage (Han et al., 2015). Puerarin promoted ABCA1-mediated cholesterol efflux *via* pathways involving miRNA-7, serine/threonine kinase 11 (STK11), and the AMPK-PPARγ-LXRα-ABCA1 cascade, therefore reducing cellular lipid buildup in THP-1 macrophages (Li et al., 2017a).

5.1.12 Quercetin

Quercetin (3,3′,4′,5,7-pentahydroxyflavone) is one of the most prevalent plant flavonoids and a key dietary antioxidant in the human diet (Boots et al., 2008). It can be found in various traditional Chinese herbal medicines, tea, fruit, and other vegetables and has also been proven effective in clinical studies (Ferry et al., 1996). The antioxidant, anti-inflammatory, antiviral, anticancer, and antifibrotic effects of quercetin should be preserved (Russo et al., 2012). Moreover, quercetin stimulates autophagy in the hematopoietic stem/progenitor cell compartment of myelodysplastic bone marrow (Daw and Law, 2021). Qu also promotes apoptosis through DNA demethylation activity, HDAC inhibition, and enrichment of H3ac and H4ac in the promoter regions of genes that enhance apoptotic pathways (Alvarez et al., 2018).

In vitro studies have shown that quercetin can inhibit two stages of macrophage differentiation and polarization: macrophage infiltration (from monocytes to macrophages) and macrophage subtype conversion (from M2 to M1 subtypes). Quercetin downregulated the expression of M1 macrophage markers and proinflammatory cytokines and upregulated the expression of M2 macrophage markers and anti-inflammatory cytokines in BMDM under both basal and LPS-stimulated conditions (Dong et al., 2014b). Jia et al. (2019) demonstrated that in apoE$^{-/-}$ mice fed with HFD, quercetin protects against AS by regulating the expression of proprotein convertase subtilisin/kexin type 9 (PCSK9), CD36, PPARγ, LXRα, and ABCA1. In THP-1-derived foam cells, quercetin increased ApoA1-mediated cholesterol efflux and promoted ABCA1 and PPARγ expression by activating PPARγ signaling (Sun et al., 2015). Quercetin has also been linked to reduced AS in ApoE$^{-/-}$ mice by enhancing RCT, which depends on ABCA1 and ABCG1 (Cui et al., 2017).

5.1.13 Silymarin

Silymarin is extracted from the seeds of *Silybum marianum* L. Gaertn. (also known as milk thistle). Silymarin is a blend of flavonoids, primarily silybin, silydianin, silychristin, and other active components (Rašković et al., 2011). In addition to protecting the liver and lowering enzymes and lipids, this combination has antioxidant, anti-inflammatory, and anticancer properties (Zhao et al., 2021). Studies have shown that silibinin may interfere with epigenetic cellular mechanisms, including increasing the total DNMT activity, while reducing histone deacetylase (HDAC) expression levels (Anestopoulos et al., 2016). The silymarin compounds, isosilybin A, isosilybin B, silychristin, and isosilychristin, increased ABCA1 protein expression in THP-1 cells. Due to its PPARγ activating qualities, isosilybin A, in particular, enhanced cholesterol efflux from THP-1 macrophages (Wang et al., 2015b).

5.2 Phenols

Phenolic chemicals are found all over the plant world and have more than 8,000 distinct known structures. Phenols can be classified as monophenols, binary phenols, or polyphenols, depending on the number of phenolic hydroxyl groups in the chemical structure (Xiao et al., 2012). Through various mechanisms, phenolic compounds have various pharmacological and biological actions. These activities include the control of various cell signaling pathways, gene expression, and antioxidation.

5.2.1 Curcumin

Curcumin ((1E, 6E)-1,7-bis(4-hydroxy-3-methoxyphenyl)-1,6-heptadiene-3,5-dione) is a polyphenolic derivative produced from turmeric (*Curcuma longa*) (Wu et al., 2020b). Curcumin can control inflammation in *in vitro* and *in vivo* studies. This property makes curcumin an effective treatment for various inflammatory disorders, including obesity, diabetes, CVD, bronchial asthma, and rheumatoid arthritis (Chen et al., 2019a). Studies have demonstrated a direct inhibitory effect of curcumin on NLRP3 inflammasome activation in macrophages, which can prevent HFD-induced insulin resistance and inhibit LPS-priming

and NLRP3 inflammasome activation pathways in macrophages (Yin et al., 2018). Curcumin may also act as an epigenetic regulator, including the inhibition of DNMTs, regulation of histone modifications *via* the regulation of histone acetyltransferases (HATs) and HDACs, regulation of miRNA, action as a DNA-binding agent, and interaction with transcription factors (Hassan et al., 2019). Additionally, c-Jun N-terminal kinases (JNK), histone methyltransferase p300, and transcriptional factor activating protein-1 (AP-1) were all inhibited by curcumin (Huwait et al., 2011).

In terms of regulating M1/M2 macrophages, curcumin can enhance the secretion of M2 macrophage markers, such as macrophage mannose receptor (MMR), Arg-1, PPAR-γ, IL-4, and/or IL-13. These effects have been observed in experimental autoimmune myocarditis (EAM) models and hyaline membrane disease, where curcumin polarizes M0 and M1 macrophages to an M2 phenotype (Saqib et al., 2018). A previous study indicated that without having a sizable impact on other cholesterol transporters, curcumin dramatically reduced the oxLDL-induced lipid buildup in J774.A1 macrophages by reducing the SR-A-dependent oxLDL uptake and enhancing the ABCA1-dependent cholesterol efflux (Zhao et al., 2012). The evidence suggests that curcumin inhibits the production of SR-A through a ubiquitin/proteasome mechanism. Additionally, through LXRα-dependent transcriptional regulation, curcumin increased ABCA1 expression (Zhao et al., 2012).

5.2.2 Paeonol

Paeonol is an active component of the Chinese herbal remedy Moutan Cortex (Pae, 2-hydroxy-4-methoxyacetophenone), which is obtained from the root bark (Chen et al., 2019b). Pae has several physiologic benefits, including anti-inflammatory and antioxidant properties (Mei et al., 2019). LncRNAs are RNA molecules longer than 200 nucleotides interacting with target genes at the transcriptional level. They function as competing endogenous RNA (ceRNA) sponges to control mRNA expression and promote cisplatin-induced nephrotoxicity by regulating AKT/TSC/mTOR-mediated autophagy (Jing et al., 2021). Pae can inhibit the expression of lnc-MEG3 to alleviate renal injury in mice (Jing et al., 2021).

In ApoE$^{-/-}$ mice, Pae therapy decreased the development of atherosclerotic lesions, slowed systemic inflammation, and enhanced ABCA1 expression (Zhao et al., 2013b).

5.2.3 Polydatin

The main active ingredient of *Polygonum cuspidatum* Sieb. et Zucc. (Polygonaceae), a plant widely used in traditional medicine worldwide, particularly in China and Japan, is polydatin (Du et al., 2013). Polydatin clearly possesses hypoglycemic, antiatherosclerotic, hypolipidemic, hypouricemic, and anti-inflammatory effects, according to the findings of the literature review (Luo et al., 2022). In oxLDL-stimulated ApoE$^{-/-}$ mouse macrophages, a 48 h polydatin therapy decreased TC, FC, and CE levels and TNF-α and IL-1β production. The mechanism generating these effects is linked to the stimulation of PPARγ-dependent ABCA1 overexpression and the decrease in CD36 expression (Wu et al., 2015a).

5.2.4 Protocatechuic acid

In vegetables, fruits, and rice, protocatechuic acid (PCA, 3,4-dihydroxybenzoic acid) has been demonstrated to enhance vasodilation in apolipoprotein E-deficient rats with AS *via* the eNOS-mediated endothelium-dependent pathway (Bai et al., 2021). PCA may also control lipid metabolism by inhibiting the expression of HMG-CoA reductase (Liu et al., 2010). PCA also prevent ED intercellular adhesion molecule 1 (ICAM-1) and vascular cell adhesion molecule 1 (VCAM-1)-dependent monocyte adherence to activated HUVECs as well as CCL2-mediated monocyte transmigration, inhibiting the effects of cholesterol metabolism in addition to decreasing the progression of AS in ApoE$^{-/-}$ mice (Wang et al., 2010b; Stumpf et al., 2013).

5.2.5 Resveratrol

Resveratrol (RV), the most studied stilbene structure, is present in typical food sources such as grapes, berries, peanuts, and red wine, and, in some herbs, it is regarded as a strong antioxidant, among other properties (Sarubbo et al., 2017). In fact, research has identified several RV advantageous properties, making it possible for it to play crucial roles in the treatment of diseases including cancer, CVD, and AD, as well as other degenerative brain illnesses (Choi et al., 2012). Recent evidence suggests that the beneficial effects of RV may be related to altered epigenetic mechanisms. After being taken orally, RV can cause several chemical modifications, including oxidation, dehydroxylation, and demethylation, which can either directly inhibit the activity of epigenetic enzymes such as DNMTs, HDACs, or HATs or change the amount of substrate that is available for those enzymatic reactions (Griñán-Ferré et al., 2021). Since β-glucan-induced trained immunity depends on histone acetylation, under the action of the histone deacetylase activator RV (a sirtuin 1 activator), trained immunity is significantly inhibited and partially suppressed enhancement of IL-6 production (Cheng et al., 2014).

Regarding the effect on macrophages, RV can reverse the oxysterol-induced M2/M1 phenotypic switch (Buttari et al., 2014). RV regulates microglial M1/M2 polarization through PGC-1α under neuroinflammatory injury. Similar studies have shown that malibatol A (MA), an oligomer of RV, inhibits the expression of proinflammatory cytokines and M1 markers (CD16, CD32, and CD86) while increasing M2 in LPS-stimulated microglia markers (CD206 and YM-1) (Pan et al., 2015). RV has the atherosclerotic protective mechanism by regulating monocyte/macrophage differentiation, among other mechanisms, including inhibition of LDL oxidation, enhanced endothelial protection, reduction of trimethylamine N-oxide (TMAO) by gut flora, and inhibition of vascular smooth muscle cell (VSMC) proliferation and migration (Vasamsetti et al., 2016). RV suppressed LPS-induced RAW264.7 foam cell development by lowering ROS production and MCP1 expression through the Akt/Foxo3a and AMPK/Sirt1 pathways, which rely on NADPH oxidase 1 (Nox1) (Park et al., 2009; Dong et al., 2014a). According to clinical research, RV decreases the amount of TC and TG in individuals with dyslipidemia (Simental-Mendía and Guerrero-Romero, 2019).

5.2.6 Salicylic acid

Radix *Salvia miltiorrhiza* (Danshen), which produces salvianolic acid B (SalB), has several medicinal actions, including antioxidant,

anticancer, anti-inflammatory, and antiatherosclerotic qualities (Tang et al., 2022). Research showed that SalB induced the production of ABCA1 in differentiated THP-1 macrophages, which helped the HDL and ApoA-1-mediated cholesterol export. Additional mechanism experiments revealed that PPARγ and LXRα inhibitors might decrease the overexpression of ABCA1 triggered by SalB, which suggested that SalB promoted cholesterol efflux through a PPARγ/LXRα/ABCA1-dependent mechanism in THP-1 macrophages to minimize lipid buildup (Yue et al., 2015). Salvianolic acid B was discovered using a high-throughput screening experiment to be a powerful CD36 antagonist that prevents oxLDL absorption in RAW264.7 macrophages (Wang et al., 2010c).

5.3 Terpenoids

Terpenoids, also known as isoprenoids, are isoprene-based natural compounds having critical functions in every organism's metabolism (Bergman et al., 2019). The terpenoid family of natural compounds, which includes several plant terpenoids, has been a valuable source of medicinal discoveries.

5.3.1 Betulinic acid

Betulinic acid (BA), a natural pentacyclic triterpenoid, is an active compound in the bark of the birch tree *Betula* spp. (Betulaceae). BA has many biological effects, including anti-inflammatory, antiviral, antioxidant, and anticancer properties (Appiah et al., 2018). Research found that betulinic acid reduced atherosclerotic lesions, TG, TC, and LDL-C levels in ApoE$^{-/-}$ mice by blocking the NF-κB signaling pathway and miR-33 expression (Zhao et al., 2013c). In RAW264.7 and THP-1 cells, betulin (a derivative of betulinic acid) consistently improved ABCA1/ABCG1-mediated cholesterol efflux by preventing the synthesis of SREBPs, which bound to E-box motifs in the ABCA1 promoter (Gui et al., 2016).

5.3.2 Ginsenosides

The main active compounds in ginseng are called ginsenosides, which are triterpene glycosides of the dammarane type (Nah et al., 2007). Ginsenosides are expressed by the formula Rx, where x represents the separation from the thin-layer chromatography origin (Kim et al., 2017). The segments are labeled A for the most polar and H for the least polar (Kim et al., 2017). Protopanaxadiols, protopanaxatriols, and oleanane are the three main families of ginsenosides (ginsenoside Ro). Ginsenosides Rb1, Rb2, Rb3, Rc, Rd, Rg3, and Rh3 are examples of protopanaxadiols, which include sugar moieties on the C-3 position of dammarane-type triterpenes. Ginsenosides Re, Rf, Rg1, Rg2, and Rh1 are examples of the sugar moieties on the C-6 position dammarane-type triterpenes that make up protopanaxatriol (Lü et al., 2009; Kim et al., 2018). Ginseng is a well-liked supplement due to its wide range of pharmacological and therapeutic effects on aging, cancer, the cardiovascular system, diabetes, immune-regulatory function, and inflammation (Im, 2020). Ginsenoside Rg1 exerts positive effects on mesenchymal stem cells (MSCs). Ginsenoside Rg1 can influence HSC proliferation and migration, control HSCs/hematopoietic progenitor cell (HPC) differentiation, and slow down HSC aging. These findings may offer new approaches for increasing the homing rate of HSCs during HSC transplantation and for the treatment of graft-versus-host disease (GVHD) and other diseases caused by HSCs/HPC dysplasia (He and Yao, 2021).

Regarding the effect on macrophage polarization, ginsenoside Rg3 showed a positive effect on M2 polarization. After treatment with LPS, isolated mouse peritoneal macrophages significantly expressed several M1 marker genes, such as COX-2 (cyclooxygenase), iNOS, IL-1β, and TNFα. Pretreatment with Rg3 successfully restored a representative M2 marker (arginase-1), which was reduced after treatment with LPS (Koh et al., 2018). Ginsenoside Rg3 significantly reduced ox-LDL-induced atherosclerotic pathological changes in ApoE$^{-/-}$ mice fed with HFD, upregulated PPARγ, and inhibited the activation of focal adhesion kinase (FAK) in the aorta, thus inhibiting the expression of VCAM-1 and ICAM-1 in the intima (Geng et al., 2020). Another crucial component of ginseng is ginsenoside Rd. Data from a RAW264.7 cell model showed that Rd inhibited the expression of the SR-A protein, followed by a decrease in the uptake of oxLDL and in the amount of cholesterol inside the cell (Li et al., 2011). An *in vivo* investigation revealed that Rd administration decreased the atherosclerotic plaque areas and oxLDL absorption in ApoE$^{-/-}$ mice.

5.3.3 Tanshinone IIA

Extracted from *Salvia miltiorrhiza* Bunge, tanshinone IIA (Tan IIA) is a significant lipophilic diterpene (Ono, 2018). Tan IIA can prevent or decrease the advancement of several illnesses, including cardiovascular diseases, cancers, cerebrovascular diseases, and Alzheimer's disease, according to several experimental and clinical studies (Ding et al., 2020). One study demonstrated that TIIA treatment attenuated high glucose-induced kidney damage by modulating the DNA methylation of related genes Nmu, Fgl2, Glo, and Kcnip2 (Li et al., 2019). Tanshinone IIA consistently boosted ERK/Nrf2/HO-1 loop-mediated ABCA1- and ABCG1-mediated cholesterol efflux and decreased SR-A-mediated oxLDL absorption by inhibiting AP-1, which reduced cholesterol buildup in cells (Liu et al., 2014a). Another investigation using peritoneal macrophages from rats and macrophages generated from THP-1 revealed that tanshinone IIA treatment greatly raised ABCA1 mRNA and protein expression while considerably reducing CD36, suggesting simultaneous effects on cholesterol intake and efflux (Jia et al., 2016). In addition, a clinical trial has demonstrated that tanshinone IIA lowers hs-CRP in CAD patients (Li et al., 2017c).

5.3.4 Ursolic acid

Ursolic acid (3B-hydroxy-12-urc-12-en-28-oic acid) is a pentacyclic triterpenoid produced from plants that have antioxidant, anti-inflammatory, and neuroprotective properties (Rong et al., 2022). A study on skin cancer reported that ursolic acid therapy reduces hypermethylated CpG islands of the Nrf2 gene promoter region in mouse epidermal cells, restoring Nrf2 expression, accomplished by lowering the production of epigenetic-modifying enzymes such as DNA methyltransferases (Kim et al., 2016). A recent study found that ursolic acid improved the transport of cholesterol from LDL-loaded macrophages to ApoA-1 through autophagy without changing the levels of ABCA1 and ABCG1 mRNA or protein in MPMs

(Leng et al., 2016). *In vivo*, UA therapy dramatically decreased the size of the atherosclerotic lesion and increased macrophage autophagy in $LDLR^{-/-}$ mice (Leng et al., 2016).

5.3.5 Zerumbone

A naturally occurring substance called zerumbone is derived from pinecone or shampoo ginger, *Zingiber zerumbet* L. Smith, and contains several pharmacological properties, including antiulcer, antioxidant, anticancer, and antibacterial (Rosa et al., 2019). Earlier research found that zerumbone significantly reduced the inflammatory response caused by LPS in *in vitro* and *ex vivo* trials using the macrophages employed in this investigation by inhibiting the activation of the ERK-MAPK and NF-κB signaling pathways and the NLRP3 inflammasome (Su et al., 2021). Studies in a rabbit model fed cholesterol show that zerumbone can stop the development of atherosclerotic lesions (Hemn et al., 2015). Zerumbone reduced the expression of SR-A and CD36 mRNA in vitro studies by controlling AP-1 and NF-κB suppression, which blocked the absorption of acLDL by THP-1 macrophages (Eguchi et al., 2007). Additionally, zerumbone treatment of THP-1 macrophages resulted in a considerable decrease in cholesterol levels through increasing the mRNA and protein levels of ABCA1, but not ABCG1, and ERK1/2 phosphorylation (Zhu and Liu, 2015).

5.4 Carotenoids

Carotenoids represent a class of pigmented terpenoids. The human diet contains around 50 of more than 700 carotenoids identified in nature, with about half present in human blood and tissues (Krinsky and Johnson, 2005). Lycopene, lutein, zeaxanthin, β-cryptoxanthin, α-carotene, and β-carotene are the main carotenoids in human serum (Krinsky and Johnson, 2005). According to epidemiologic research, it may be linked to better cognitive and visual abilities and a lower chance of developing chronic conditions, including cancer, CVD, and age-related macular degeneration (AMD) (Moran et al., 2018).

5.4.1 Astaxanthin

A natural xanthophyll carotenoid called astaxanthin (3,3′-dihydroxy-β,β′-carotene-4,4′-dione) is present in various marine species, such as *Haematococcus pluvialis*, *Chlorella zofingiensis*, *Chlorococcum*, and *Phaffia rhodozyma* (Hussein et al., 2006). It has been suggested that it has anti-inflammatory, antioxidant, and neuroprotective properties, and research from different experimental models has demonstrated that these properties are linked to a decreased expression of proinflammatory cytokines and a decreased production of ROS and free radicals (Kim et al., 2020). Xue et al. (2017) reported that astaxanthin prevents oxidative stress and apoptosis, which reduces the hematopoietic damage caused by whole-body radiation in mice. Yang et al. (2017) stated that astaxanthin could demethylate certain promoters of particular genes, which may help increase the stability of the total chromatin structure. Only at high dosages does astaxanthin enhance the expression of ABCA1/G1 (up to 2.0- and 3.2-fold at the protein level), which promotes ApoA-1/HDL-mediated cholesterol efflux (Iizuka et al., 2012).

5.4.2 β-Carotene

β-Carotene (BC), a precursor to vitamin A, is present in a greater variety of fruits and vegetables. It is frequently used in foods as an antioxidant and natural colorant (Zhao et al., 2020). Lower overall, CVD, heart disease, stroke, cancer, and other causes of death are linked to a higher β-carotene biochemical state (Huang et al., 2018). Kim et al. (2019) suggested that BC can regulate epigenetic modifications for its anticancer effects in colon cancer stem cells. Furthermore, endogenous β-carotene 15,15′-monooxygenase 1 may convert 9-cis-c into 9-cis retinoic acid or other retinoids, activate the retinoid X receptor (RXR), and stop foam cell formation and the development of AS (Zolberg Relevy et al., 2015).

5.4.3 Lycopene

Lycopene, a member of the carotenoid family, is mostly found in foods such as tomatoes (particularly the red kind), watermelons, and red pomelo (Zhan et al., 2021). Lycopene is widely recognized for its anti-inflammatory and antioxidant properties and ability to affect important bodily metabolic processes (Han et al., 2016). Napolitano et al. (2007) demonstrated that lycopene reduced cholesterol buildup by upregulating IL-10 secretion in human peripheral blood monocyte-derived macrophages (HMDMs) and THP-1 macrophages and downregulating SR-A mRNA expression and lipid synthesis. Furthermore, HMG-CoA reductase inhibition, RhoA inactivation, an increase in PPARγ and LXRα activation, and ultimately an improvement in ABCA1 and caveolin 1 expression may all contribute to the potential cascade impact of lycopene in lowering foam cell formation (Palozza et al., 2011).

5.4.4 Retinoids

Retinol, generally known as vitamin A1, and its natural derivatives, 9-cis retinoic acid (9-cis-RA) and all-trans retinoic acid (ATRA), are thought to be prospective therapeutic agents for the prevention of AS development because they can promote macrophage cholesterol efflux. Retinoids reportedly cause epigenetic alterations that cause stem cell differentiation (Gudas, 2013). Through binding to the RARs, ATRA modifies how the retinoic acid receptors (RARs) interact with various protein elements of the transcription complex at multiple genes in stem cells. The epigenetic marks on histones or DNA are added to or removed by some of these protein components of the transcription complex, altering the chromatin structure and leading to the departure from the self-renewing, pluripotent stem cell state (Gudas, 2013). According to research, 9-cis-RA and ATRA can significantly increase the expression of ABCA1, ABCG1, and ApoE in THP-1 macrophages and the efflux of cholesterol to ApoA-1 in RAW264.7 macrophages (Langmann et al., 2005). Additionally, 9-cis-RA has been connected to the ABCA1-mediated cholesterol efflux from J774 macrophages, THP-1-derived macrophages, and RAW264.7 macrophages (Schwartz et al., 2000; Kiss et al., 2005).

5.5 Phenylpropanoids

5.5.1 Ferulic acid

Ferulic acid (FA) ((E)-3-(4-hydroxy-3-methoxy-phenyl) prop-2-enoic acid), a caffeic acid derivative, can be isolated from several Chinese herbal medicines, including *Cimicifuga racemosa*, *Angelica*

sinensis, and Rhizoma Ligustici Chuanxiong, as well as from plants that are commonly found in our diet, including *Oryza sativa*, *Glycine max*, and *Zea mays* (Li et al., 2022). FA has free radical scavenging and antioxidant properties that have a wide range of potential applications in the prevention and treatment of CVD and the management of cancer, as well as hepatoprotective, antimicrobial, and anti-inflammatory therapies (Li et al., 2022). FA, a metabolite of chlorogenic acid, has an improving effect on HDL-mediated cholesterol efflux from macrophages by increasing the expression of ABCG1 and SR-BI (Uto-Kondo et al., 2010).

5.5.2 Chlorogenic acid

Chlorogenic acid (CA) is a phenolic molecule from the hydroxycinnamic family found in drinks made from herbs, fruits, and vegetables. It is recognized for its antioxidant capabilities against free radicals (Santana-Gálvez et al., 2017). In ApoE$^{-/-}$ mice fed a diet high in cholesterol, CA decreased the percentage and total atherosclerotic lesion area, as well as the aortic dilatation and serum levels of TC, LDL-C, and TG (Wu et al., 2014). Through the upregulation of the transcription of PPARγ, LXRα, ABCA1, and ABCG1 in *in vitro* mechanistic studies, CA repressed foam cell growth and decreased the oxLDL-induced neutral lipid and cholesterol accumulation in RAW264.7 macrophages (Wu et al., 2014). In HepG2 cells, chlorogenic acid enhanced mRNA expression of ABCA1, CYP7A1, and AMPKα2 and facilitated the efflux of TC and triacylglycerol (Hao et al., 2016).

5.5.3 Lignans

The largest concentration of lignans, which are bioactive, non-nutritive, non-caloric phenolic plant chemicals, is found in flax and sesame seeds (Peterson et al., 2010). Dietary lignans demonstrate strong antiviral, antioxidant, anticancer, and antiatherosclerotic properties *via* functioning as phytoestrogens (Peterson et al., 2010).

5.5.3.1 Arctigenin

Across hundreds of years, people all over the world have used the roots of *Arctium lappa*, also known as larger burdock, as food and traditional herbal medicine. The seeds of the *Arctium lappa* plant contain arctigenin, a phenylpropanoid dibenzylbutyrolactone lignin (Nam and Nam, 2020). The antibacterial, antiviral, antioxidant, anti-inflammatory, and anticancer properties of arctigenin have been demonstrated (Maxwell et al., 2018). Arctigenin boosted the expression of ApoE, ABCA1, and ABCG1 in oxLDL-loaded THP-1 macrophages, increasing cholesterol efflux (Xu et al., 2013).

5.5.3.2 Honokiol

Honokiol (HKL) [2-(4-hydroxy-3-prop-2-enyl-phenyl)-4-prop-2-enyl-phenol] is a naturally occurring biphenolic chemical with a low molecular weight, which is obtained from the bark of magnolia trees and is utilized in traditional Chinese medicine (Fried and Arbiser, 2009). It possesses analgesic, anti-inflammatory, antioxidant, anti-tumor, and neuroprotective activities as a pharmaceutical (Pillai et al., 2015). Honokiol could activate the RXR/LXR heterodimer, inducing the ABCA1 expression and improving cholesterol efflux from MPMs (Kotani et al., 2010). According to another study, honokiol boosted ABCA1 expression by interacting with RXRβ. Additionally, it boosted the expression of ABCG1 and ApoE (Jung et al., 2010).

5.5.3.3 Sesamin

Sesamin, a naturally occurring lignin compound, is isolated from sesame seeds and has many positive health effects, including anti-inflammatory, anticancer, anti-hypertension, anti-thrombotic, antidiabetic, anti-atherogenic, anti-obesity, and lipolytic effects (Dalibalta et al., 2020). It also can reduce damage to the intestine, kidneys, heart, brain, and liver (Wang et al., 2021b). Studies have shown that sesamin inhibits LPS-induced macrophage-derived chemokine expression through ER, PPAR-α, MAPK-p38 pathway, NFκB-p65 pathway, and epigenetic regulation (Hsieh et al., 2014). Sesamin boosted cholesterol efflux from RAW264.7 macrophages and decreased the oxLDL-induced accumulation of cholesterol, most likely by activating PPARγ, LXRα, and ABCG1 (Liu et al., 2014b). Sesamin reduced AS in ApoE$^{-/-}$ mice by stifling vascular inflammation, according to *in vivo* research (Wu et al., 2010).

5.6 Alkaloids

5.6.1 Berberine

Berberine (BBR) is a naturally occurring substance extracted from herbs, including *Coptis chinensis* and *Berberis vulgaris*. BBR has been identified as a safe and effective treatment for type 2 diabetes and hyperlipidemia with new mechanisms since 2004 (Kong et al., 2004). Over the past 10 years, several studies have demonstrated the clinical effectiveness of BBR in decreasing lipids and glucose (Wang et al., 2021c). The investigation results demonstrated that BBR administration mostly impacted enzymes involved in histone acetylation and methylation (Zhang et al., 2016). The expression of the proteins H3K4me3, H3K27me3, and H3K36me3 reduced after BBR administration, according to Western blotting tests conducted concurrently (Zhang et al., 2016). By encouraging LXRα/ABCA1-dependent cholesterol efflux, BBR reduced the development of foam cells in THP-1 macrophages (Lee et al., 2010). Nevertheless, ABCG1, SR-BI, CD36, and SR-A were unaffected by berberine. The impact of BBR on macrophages is also mediated by other pathways, including AMPK/Sirt1 activation, autophagy induction, and adipocyte enhancer-binding protein 1 suppression (Huang et al., 2012; Chi et al., 2014; Kou et al., 2017). Moreover, in a rat model of adjuvant arthritis, BBR treatment restrained the phagocytic function of macrophages and restored the balance of M1/M2 by reducing the levels of M1 cytokines (TNF-α, IL-1β, and IL-6), increasing the levels of M2 cytokines (IL-10 and TGF-β1), increasing the expression of arginase 1(Arg1) (M2 marker), and decreasing the expression of iNOS (M1 marker) (Zhou et al., 2019).

5.6.2 Piperine

Long and black peppers contain piperine (Srinivasan, 2007). Previous research has demonstrated that piperine has a variety of pharmacological properties. In terms of pharmaceuticals, piperine decreases depressive disorders, prevents hepatotoxicity, and reduces obesity and diabetes (Nogara et al., 2016). According to studies, piperine suppresses the

development of adipocytes by dynamically controlling histone modifications and regulating the expression of genes involved in adipogenesis and lipolysis (Park et al., 2019). In THP-1-differentiated human macrophages, piperine was likewise observed to increase ABCA1 protein expression. However, it did not affect ABCG1 or SR-BI expression (Wang et al., 2017a).

5.6.3 Rutaecarpine

Rutaecarpine (8,13-dihydro-7H-indolo-[2′,3′:3.4]-pyrido [2,1-b]-quinazolin-5-one) is an alkaloid first isolated from *E. rutaecarpa*. Earlier studies demonstrated that rutaecarpine possesses many biological and pharmacological features, including the ability to cause diuresis, sweating, uterotonic action, brain function improvement, antinociception, and anti-obesity (Jayakumar et al., 2021). Studies showed that rutaecarpine increased cholesterol efflux by upregulating the expression of ABCA1 and SR-BI *in vitro* (RAW264.7 macrophages and HepG2 cells) and *in vivo* (ApoE$^{-/-}$ mice) (without changing ABCG1 and CD36) (Xu et al., 2014). This reduced the lipid buildup and foam cell formation. Through this method, rutaecarpine decreased the growth of atherosclerotic plaque in ApoE$^{-/-}$ mice (Xu et al., 2014).

5.7 Others

5.7.1 Astragalus polysaccharides

The primary active ingredient of *Astragalus membranaceus*, *Astragalus* polysaccharides (APS), is widely used in clinical applications as an immunomodulator (Li et al., 2012). It has several bio-activities, including anti-inflammatory, proliferative, and immune-regulating effects, and a molecular weight of 3.6×10^4 Da (Sun et al., 2021a). Studies have demonstrated that APS significantly abrogates LPS-induced IL-6 levels in THP-1 macrophages (Long et al., 2022). ABCA1 expression in foam cells exposed to TNF-α increases in response to APS (Wang et al., 2010a). As a result, APS increases the outflow of cholesterol and reduces fat accumulation. According to further research, TNF-α-induced NF-κB activation in foam cells generated from THP-1 was reversed by APS (Wang et al., 2010a).

5.7.2 Diosgenin

Diosgenin has gained more attention recently due to its efficacy in treating several metabolic diseases, including diabetes, CVD, neurological conditions, osteoporosis, and hyperlipidemia, as well as its anticancer effects, which are mediated *via* multiple targets and regulate a variety of signals (Sun et al., 2021b). By preventing the nuclear translocation of the Notch intracellular domain in THP-1 cells, diosgenin prevented AS (Binesh et al., 2018). By preventing the induction of ICAM1, VCAM1, and endothelial lipase, it also prevented the adherence of TNF-α-induced leukocytes to activated endothelium cells (Wu et al., 2015b). Diosgenin is a naturally occurring compound capable of modulating M1 polarization (Saqib et al., 2018). Additionally, dioscin prevented systemic inflammation and the LOX-1/NF-κB pathway in MPMs from rats with atherosclerotic arteries, inhibiting the absorption of oxLDL (Wang et al., 2017b).

5.7.3 *Panax notoginseng* saponins

The primary bioactive components of *Panax notoginseng* (*P. notoginseng*) are known as *Panax notoginseng* saponins (PNS), which include several saponins of the dammarane type (Xu et al., 2019). PNS have several cardiovascular preventive properties, including avoiding endothelial dysfunction, boosting blood flow, inhibiting the production of foam cells, antioxidation, anti-inflammation, and antithrombosis (Yuan et al., 2011). According to Duan et al. (2022), PNS regulate the miR-194 promoter, miR-194, and MAPK methylation using cellular assays and blinded, controlled trials. PNS increased ABCA1 expression in macrophages, which reduced the buildup of cholesterol esters (Jia et al., 2010). PNS, at a dosage of 100 mg/kg per day, reduced foam cell development in rats with AS caused by zymosan A, according to *in vivo* research (Yuan et al., 2011).

5.7.4 Emodin

Emodin is an anthraquinone derivative isolated from *Polygonum multiflorum* (Ma et al., 2015). It has various therapeutic actions, including anti-tumor, anti-inflammatory, antioxidant, and anti-virus properties (Zheng et al., 2019). Studies have shown that emodin can bidirectionally regulate macrophage polarization and epigenetic regulation of macrophage memory (Iwanowycz et al., 2016). Emodin prevented H3K27 trimethylation (H3K27m3) marks from being removed from, and H3K27ac marks from being added to, genes needed for M1 or M2 polarization of macrophages (Iwanowycz et al., 2016). By activating the PPARγ/LXRα/ABCA1 signaling pathway, emodin boosted ApoA-1-mediated cholesterol efflux from THP-1 macrophages. Emodin also reduced diet-induced AS in rabbits (Hei et al., 2006; Fu et al., 2014).

6 Summary and perspectives

Evidence suggests that low-grade inflammation, predominantly driven by the immune system, plays a critical role in the development of AS (Leentjens et al., 2018). Although anti-inflammatory medications, such as canakinumab and colchicine, have been recently proven to lower the risk of CVD, there are still significant side effects and a high residual risk (Ridker et al., 2017; Tardif et al., 2019). Therefore, innovative therapies are urgently needed, and trained immunity provides interesting new pharmacological targets for new drug therapies. With enhanced production of pro-atherosclerotic cytokines/chemokines and higher foam cell generation, trained monocytes and macrophages showed a strong pro-atherosclerotic character. This is accomplished by epigenetic reprogramming of histone methylation levels and metabolic rewiring. These processes occur not only in circulating monocytes but also in myeloid progenitor cells, which ensure a long-term state of hyperactivation of innate immune cells. This review describes the aforementioned mechanisms in detail.

Although trained immunity is an immunological memory that is not disease-specific, different trained immune programs have different levels of disease specificity (Mulder et al., 2019). Natural products serve as a desirable resource in the search for novel therapies due to their high structural variety and biodiversity. Many natural products have been potential candidates for regulating immune training through different mechanisms, such as RV and EGCG. This paper provides an overview of anti-ASCVD natural products, such as flavonoids, phenols, terpenoids, carotenoids, phenylpropanoids, and alkaloids, that

potentially modulate trained immunity. Although *in vivo* studies of AS models already exist for these natural compounds, making these compounds more promising, there is currently less evidence that these natural compounds can directly modulate training immunity. Further studies are needed to reveal possible pathways by which natural products act on trained immunity.

Data availability statement

The original contributions presented in the study are included in the article/Supplementary Material, further inquiries can be directed to the corresponding author.

Author contributions

The research project was designed by JW and CC, organized by JW and JH, and reviewed and critiqued by Y-ML. The first draft of the manuscript was written by JW, CC, and JH and reviewed and critiqued by CC. All authors contributed to the graphical analysis, drafting, and critical revision of the paper and agreed to take responsibility for all aspects of the work.

Funding

This work was supported by grants from the Programs Foundation for Leading Talents in National Administration of Traditional Chinese Medicine of China "Qihuang scholars" Project (no. 0201000401), the National Natural Science Foundation of China (no. 81974556), and the National Key Research and Development Program of China (no. 2020YFC2002701).

Conflict of interest

The authors declare that the research was conducted in the absence of any commercial or financial relationships that could be construed as a potential conflict of interest.

Publisher's note

All claims expressed in this article are solely those of the authors and do not necessarily represent those of their affiliated organizations or those of the publisher, the editors, and the reviewers. Any product that may be evaluated in this article, or claim that may be made by its manufacturer, is not guaranteed or endorsed by the publisher.

Supplementary material

The Supplementary Material for this article can be found online at: https://www.frontiersin.org/articles/10.3389/fphar.2023.1109576/full#supplementary-material

References

Aarup, A., Pedersen, T. X., Junker, N., Christoffersen, C., Bartels, E. D., Madsen, M., et al. (2016). Hypoxia-inducible factor-1α expression in macrophages promotes development of atherosclerosis. *Arterioscler. Thromb. Vasc. Biol.* 36 (9), 1782–1790. doi:10.1161/atvbaha.116.307830

Abdulla, A., Zhao, X., and Yang, F. (2013). Natural polyphenols inhibit lysine-specific demethylase-1 *in vitro*. *J. Biochem. Pharmacol. Res.* 1 (1), 56–63.

Almatroodi, S. A., Almatroudi, A., Alsahli, M. A., Aljasir, M. A., Syed, M. A., and Rahmani, A. H. (2020). Epigallocatechin-3-Gallate (EGCG), an active compound of green tea attenuates acute lung injury regulating macrophage polarization and krüpple-like-factor 4 (KLF4) expression. *Molecules* 25 (12), 2853. doi:10.3390/molecules25122853

Alvarez, M. C., Maso, V., Torello, C. O., Ferro, K. P., and Saad, S. T. O. (2018). The polyphenol quercetin induces cell death in leukemia by targeting epigenetic regulators of pro-apoptotic genes. *Clin. Epigenetics* 10 (1), 139. doi:10.1186/s13148-018-0563-3

American Diabetes Association (2015). Cardiovascular disease and risk management. *Diabetes Care* 38 (1), S49–S57. doi:10.2337/dc15-S011

Anestopoulos, I., Sfakianos, A. P., Franco, R., Chlichlia, K., Panayiotidis, M. I., Kroll, D. J., et al. (2016). A novel role of silibinin as a putative epigenetic modulator in human prostate carcinoma. *Molecules* 22 (1), 62. doi:10.3390/molecules22010062

Anukunwithaya, T., Poo, P., Hunsakunachai, N., Rodsiri, R., Malaivijitnond, S., and Khemawoot, P. (2018). Absolute oral bioavailability and disposition kinetics of puerarin in female rats. *BMC Pharmacol. Toxicol.* 19 (1), 25. doi:10.1186/s40360-018-0216-3

Appiah, B., Amponsah, I. K., Poudyal, A., and Mensah, M. L. K. (2018). Identifying strengths and weaknesses of the integration of biomedical and herbal medicine units in Ghana using the WHO health systems framework: A qualitative study. *BMC Complement. Altern. Med.* 18 (1), 286. doi:10.1186/s12906-018-2334-2

Arts, R. J., Novakovic, B., Ter Horst, R., Carvalho, A., Bekkering, S., Lachmandas, E., et al. (2016). Glutaminolysis and fumarate accumulation integrate immunometabolic and epigenetic programs in trained immunity. *Cell. Metab.* 24 (6), 807–819. doi:10.1016/j.cmet.2016.10.008

Arts, R. J. W., Carvalho, A., La Rocca, C., Palma, C., Rodrigues, F., Silvestre, R., et al. (2016). Immunometabolic pathways in BCG-induced trained immunity. *Cell. Rep.* 17 (10), 2562–2571. doi:10.1016/j.celrep.2016.11.011

Arts, R. J. W., Moorlag, S., Novakovic, B., Li, Y., Wang, S. Y., Oosting, M., et al. (2018). BCG vaccination protects against experimental viral infection in humans through the induction of cytokines associated with trained immunity. *Cell. Host Microbe* 23 (1), 89–100. doi:10.1016/j.chom.2017.12.010

Augert, A., Mathsyaraja, H., Ibrahim, A. H., Freie, B., Geuenich, M. J., Cheng, P. F., et al. (2020). MAX functions as a tumor suppressor and rewires metabolism in small cell lung cancer. *Cancer Cell.* 38 (1), 97–114. doi:10.1016/j.ccell.2020.04.016

Azzini, E., Giacometti, J., and Russo, G. L. (2017). Antiobesity effects of anthocyanins in preclinical and clinical studies. *Oxid. Med. Cell. Longev.* 2017, 2740364. doi:10.1155/2017/2740364

Bai, L., Kee, H. J., Han, X., Zhao, T., Kee, S. J., and Jeong, M. H. (2021). Protocatechuic acid attenuates isoproterenol-induced cardiac hypertrophy via downregulation of ROCK1-Sp1-PKCγ axis. *Sci. Rep.* 11 (1), 17343. doi:10.1038/s41598-021-96761-2

Bannister, A. J., and Kouzarides, T. (2011). Regulation of chromatin by histone modifications. *Cell. Res.* 21 (3), 381–395. doi:10.1038/cr.2011.22

Bao, L., Zhang, Y., Wei, G., Wang, Y., Ma, R., Cheng, R., et al. (2015). The anti-atherosclerotic effects of puerarin on induced-atherosclerosis in rabbits. *Biomed. Pap. Med. Fac. Univ. Palacky. Olomouc Czech Repub.* 159 (1), 53–59. doi:10.5507/bp.2013.096

Bauer, P. M., Buga, G. M., Fukuto, J. M., Pegg, A. E., and Ignarro, L. J. (2001). Nitric oxide inhibits ornithine decarboxylase via S-nitrosylation of cysteine 360 in the active site of the enzyme. *J. Biol. Chem.* 276 (37), 34458–34464. doi:10.1074/jbc.M105219200

Bechor, S., Zolberg Relevy, N., Harari, A., Almog, T., Kamari, Y., Ben-Amotz, A., et al. (2016). 9-cis β-carotene increased cholesterol efflux to HDL in macrophages. *Nutrients* 8 (7), 435. doi:10.3390/nu8070435

Bekkering, S., Arts, R. J. W., Novakovic, B., Kourtzelis, I., van der Heijden, C. D. C. C., Li, Y., et al. (2018). Metabolic induction of trained immunity through the mevalonate pathway. *Cell.* 172 (1-2), 135–146. doi:10.1016/j.cell.2017.11.025

Bekkering, S., Quintin, J., Joosten, L. A., van der Meer, J. W. M., Netea, M. G., and Riksen, N. P. (2014). Oxidized low-density lipoprotein induces long-term proinflammatory cytokine production and foam cell formation via epigenetic reprogramming of monocytes. *Arterioscler. Thromb. Vasc. Biol.* 34 (8), 1731–1738. doi:10.1161/atvbaha.114.303887

Bekkering, S., van den Munckhof, I., Nielen, T., Lamfers, E., Dinarello, C., Rutten, J., et al. (2016). Innate immune cell activation and epigenetic remodeling in symptomatic and asymptomatic atherosclerosis in humans *in vivo*. *Atherosclerosis* 254, 228–236. doi:10.1016/j.atherosclerosis.2016.10.019

Bergman, M. E., Davis, B., and Phillips, M. A. (2019). Medically useful plant terpenoids: Biosynthesis, occurrence, and mechanism of action. *Molecules* 24 (21), 3961. doi:10.3390/molecules24213961

Binesh, A., Devaraj, S. N., and Devaraj, H. (2018). Inhibition of nuclear translocation of notch intracellular domain (NICD) by diosgenin prevented atherosclerotic disease progression. *Biochimie* 148, 63–71. doi:10.1016/j.biochi.2018.02.011

Biswas, S., Kar, A., Sharma, N., Haldar, P. K., and Mukherjee, P. K. (2021). Synergistic effect of ursolic acid and piperine in CCl(4) induced hepatotoxicity. *Ann. Med.* 53 (1), 2009–2017. doi:10.1080/07853890.2021.1995625

Boffa, M. B., and Koschinsky, M. L. (2019). Oxidized phospholipids as a unifying theory for lipoprotein(a) and cardiovascular disease. *Nat. Rev. Cardiol.* 16 (5), 305–318. doi:10.1038/s41569-018-0153-2

Bonilla, F. A., and Oettgen, H. C. (2010). Adaptive immunity. *J. Allergy Clin. Immunol.* 125 (2), S33–S40. doi:10.1016/j.jaci.2009.09.017

Boots, A. W., Haenen, G. R., and Bast, A. (2008). Health effects of quercetin: From antioxidant to nutraceutical. *Eur. J. Pharmacol.* 585 (2-3), 325–337. doi:10.1016/j.ejphar.2008.03.008

Braza, M. S., van Leent, M. M. T., Lameijer, M., Sanchez-Gaytan, B. L., Arts, R. J. W., Perez-Medina, C., et al. (2018). Inhibiting inflammation with myeloid cell-specific nanobiologics promotes organ transplant acceptance. *Immunity* 49 (5), 819–828. doi:10.1016/j.immuni.2018.09.008

Buttari, B., Profumo, E., Segoni, L., D'Arcangelo, D., Rossi, S., Facchiano, F., et al. (2014). Resveratrol counteracts inflammation in human M1 and M2 macrophages upon challenge with 7-oxo-cholesterol: Potential therapeutic implications in atherosclerosis. *Oxid. Med. Cell. Longev.* 2014, 257543. doi:10.1155/2014/257543

Cai, Y., and Zhao, F. (2021). Fluvastatin suppresses the proliferation, invasion, and migration and promotes the apoptosis of endometrial cancer cells by upregulating Sirtuin 6 (SIRT6). *Bioengineered* 12 (2), 12509–12520. doi:10.1080/21655979.2021.2009415

Cao, R., Zhao, Y., Zhou, Z., and Zhao, X. (2018). Enhancement of the water solubility and antioxidant activity of hesperidin by chitooligosaccharide. *J. Sci. Food Agric.* 98 (6), 2422–2427. doi:10.1002/jsfa.8734

Chakrawarti, L., Agrawal, R., Dang, S., Gupta, S., and Gabrani, R. (2016). Therapeutic effects of EGCG: A patent review. *Expert Opin. Ther. Pat.* 26 (8), 907–916. doi:10.1080/13543776.2016.1203419

Chang, X., Zhang, T., Liu, D., Meng, Q., Yan, P., Luo, D., et al. (2021). Puerarin attenuates LPS-induced inflammatory responses and oxidative stress injury in human umbilical vein endothelial cells through mitochondrial quality control. *Oxid. Med. Cell. Longev.* 2021, 6659240. doi:10.1155/2021/6659240

Chen, B., Li, H., Ou, G., Ren, L., Yang, X., and Zeng, M. (2019). Curcumin attenuates MSU crystal-induced inflammation by inhibiting the degradation of IκBα and blocking mitochondrial damage. *Arthritis Res. Ther.* 21 (1), 193. doi:10.1186/s13075-019-1974-z

Chen, G., Jia, P., Yin, Z. Y., Kong, S. Z., Xiang, Z. B., and Zheng, X. X. (2019). Paeonol ameliorates monosodium urate-induced arthritis in rats through inhibiting nuclear factor-κB-mediated proinflammatory cytokine production. *Phytother. Res.* 33 (11), 2971–2978. doi:10.1002/ptr.6472

Chen, S. J., Kao, Y. H., Jing, L., Chuang, Y. P., Wu, W. L., Liu, S. T., et al. (2017). Epigallocatechin-3-gallate reduces scavenger receptor A expression and foam cell formation in human macrophages. *J. Agric. Food Chem.* 65 (15), 3141–3150. doi:10.1021/acs.jafc.6b05832

Chen, X., Huang, C., Sun, H., Hong, H., Jin, J., Bei, C., et al. (2021). Puerarin suppresses inflammation and ECM degradation through Nrf2/HO-1 axis in chondrocytes and alleviates pain symptom in osteoarthritic mice. *Food Funct.* 12 (5), 2075–2089. doi:10.1039/d0fo03076g

Cheng, S. C., Quintin, J., Cramer, R. A., Shepardson, K. M., Saeed, S., Kumar, V., et al. (2014). mTOR- and HIF-1α-mediated aerobic glycolysis as metabolic basis for trained immunity. *Science* 345 (6204), 1250684. doi:10.1126/science.1250684

Chi, L., Peng, L., Pan, N., Hu, X., and Zhang, Y. (2014). The anti-atherogenic effects of berberine on foam cell formation are mediated through the upregulation of sirtuin 1. *Int. J. Mol. Med.* 34 (4), 1087–1093. doi:10.3892/ijmm.2014.1868

Choi, D. Y., Lee, Y. J., Hong, J. T., and Lee, H. J. (2012). Antioxidant properties of natural polyphenols and their therapeutic potentials for Alzheimer's disease. *Brain Res. Bull.* 87 (2-3), 144–153. doi:10.1016/j.brainresbull.2011.11.014

Choi, K. C., Jung, M. G., Lee, Y. H., Yoon, J. C., Kwon, S. H., Kang, H. B., et al. (2009). Epigallocatechin-3-gallate, a histone acetyltransferase inhibitor, inhibits EBV-induced B lymphocyte transformation via suppression of RelA acetylation. *Cancer Res.* 69 (2), 583–592. doi:10.1158/0008-5472.Can-08-2442

Christ, A., Günther, P., Lauterbach, M. A. R., Duewell, P., Biswas, D., Pelka, K., et al. (2018). Western diet triggers NLRP3-dependent innate immune reprogramming. *Cell.* 172 (1-2), 162–175. doi:10.1016/j.cell.2017.12.013

Christ, A., and Latz, E. (2019). The Western lifestyle has lasting effects on metaflammation. *Nat. Rev. Immunol.* 19 (5), 267–268. doi:10.1038/s41577-019-0156-1

Christofk, H. R., Vander Heiden, M. G., Harris, M. H., Ramanathan, A., Gerszten, R. E., Wei, R., et al. (2008). The M2 splice isoform of pyruvate kinase is important for cancer metabolism and tumour growth. *Nature* 452 (7184), 230–233. doi:10.1038/nature06734

Clem, B., Telang, S., Clem, A., Yalcin, A., Meier, J., Simmons, A., et al. (2008). Small-molecule inhibition of 6-phosphofructo-2-kinase activity suppresses glycolytic flux and tumor growth. *Mol. Cancer Ther.* 7 (1), 110–120. doi:10.1158/1535-7163.Mct-07-0482

Conrath, U., Beckers, G. J., Langenbach, C. J., and Jaskiewicz, M. R. (2015). Priming for enhanced defense. *Annu. Rev. Phytopathol.* 53, 97–119. doi:10.1146/annurev-phyto-080614-120132

Cotler, S., Buggé, C. J., and Colburn, W. A. (1983). Role of gut contents, intestinal wall, and liver on the first pass metabolism and absolute bioavailability of isotretinoin in the dog. *Drug Metab. Dispos.* 11 (5), 458–462.

Courties, G., Herisson, F., Sager, H. B., Heidt, T., Ye, Y., Wei, Y., et al. (2015). Ischemic stroke activates hematopoietic bone marrow stem cells. *Circ. Res.* 116 (3), 407–417. doi:10.1161/circresaha.116.305207

Crişan, T. O., Cleophas, M. C. P., Novakovic, B., Erler, K., van de Veerdonk, F. L., Stunnenberg, H. G., et al. (2017). Uric acid priming in human monocytes is driven by the AKT-PRAS40 autophagy pathway. *Proc. Natl. Acad. Sci. U. S. A.* 114 (21), 5485–5490. doi:10.1073/pnas.1620910114

Cui, Y., Hou, P., Li, F., Liu, Q., Qin, S., Zhou, G., et al. (2017). Quercetin improves macrophage reverse cholesterol transport in apolipoprotein E-deficient mice fed a high-fat diet. *Lipids Health Dis.* 16 (1), 9. doi:10.1186/s12944-016-0393-2

Cunningham, L., Finckbeiner, S., Hyde, R. K., Southall, N., Marugan, J., Yedavalli, V. R. K., et al. (2012). Identification of benzodiazepine Ro5-3335 as an inhibitor of CBF leukemia through quantitative high throughput screen against RUNX1-CBFβ interaction. *Proc. Natl. Acad. Sci. U. S. A.* 109 (36), 14592–14597. doi:10.1073/pnas.1200037109

Czank, C., Cassidy, A., Zhang, Q., Morrison, D. J., Preston, T., Kroon, P. A., et al. (2013). Human metabolism and elimination of the anthocyanin, cyanidin-3-glucoside: A (13)C-tracer study. *Am. J. Clin. Nutr.* 97 (5), 995–1003. doi:10.3945/ajcn.112.049247

Dalibalta, S., Majdalawieh, A. F., and Manjikian, H. (2020). Health benefits of sesamin on cardiovascular disease and its associated risk factors. *Saudi Pharm. J.* 28 (10), 1276–1289. doi:10.1016/j.jsps.2020.08.018

Das, J., Verma, D., Gustafsson, M., and Lerm, M. (2019). Identification of DNA methylation patterns predisposing for an efficient response to BCG vaccination in healthy BCG-naïve subjects. *Epigenetics* 14 (6), 589–601. doi:10.1080/15592294.2019.1603963

Daw, S., and Law, S. (2021). Quercetin induces autophagy in myelodysplastic bone marrow including hematopoietic stem/progenitor compartment. *Environ. Toxicol.* 36 (2), 149–167. doi:10.1002/tox.23020

Del Bo, C., Cao, Y., Roursgaard, M., Riso, P., Porrini, M., Loft, S., et al. (2016). Anthocyanins and phenolic acids from a wild blueberry (Vaccinium angustifolium) powder counteract lipid accumulation in THP-1-derived macrophages. *Eur. J. Nutr.* 55 (1), 171–182. doi:10.1007/s00394-015-0835-z

Del Rio, D., Stalmach, A., Calani, L., and Crozier, A. (2010). Bioavailability of coffee chlorogenic acids and green tea flavan-3-ols. *Nutrients* 2 (8), 820–833. doi:10.3390/nu2080820

Deng, Z., Li, Y., Liu, H., Xiao, S., Li, L., Tian, J., et al. (2019). The role of sirtuin 1 and its activator, resveratrol in osteoarthritis. *Biosci. Rep.* 39 (5). doi:10.1042/bsr20190189

Di Gioia, M., Spreafico, R., Springstead, J. R., Mendelson, M. M., Joehanes, R., Levy, D., et al. (2020). Endogenous oxidized phospholipids reprogram cellular metabolism and boost hyperinflammation. *Nat. Immunol.* 21 (1), 42–53. doi:10.1038/s41590-019-0539-2

Ding, B., Lin, C., Liu, Q., He, Y., Ruganzu, J. B., Jin, H., et al. (2020). Tanshinone IIA attenuates neuroinflammation via inhibiting RAGE/NF-κB signaling pathway *in vivo* and *in vitro*. *J. Neuroinflammation* 17 (1), 302. doi:10.1186/s12974-020-01981-4

Domínguez-Andrés, J., Ferreira, A. V., Jansen, T., Smithers, N., Prinjha, R. K., Furze, R. C., et al. (2019). Bromodomain inhibitor I-BET151 suppresses immune responses during fungal-immune interaction. *Eur. J. Immunol.* 49 (11), 2044–2050. doi:10.1002/eji.201848081

Dong, J., Zhang, X., Zhang, L., Bian, H. X., Xu, N., Bao, B., et al. (2014). Quercetin reduces obesity-associated ATM infiltration and inflammation in mice: A mechanism including ampkα1/SIRT1. *J. Lipid Res.* 55 (3), 363–374. doi:10.1194/jlr.M038786

Dong, W., Wang, X., Bi, S., Pan, Z., Liu, S., Yu, H., et al. (2014). Inhibitory effects of resveratrol on foam cell formation are mediated through monocyte chemotactic protein-1 and lipid metabolism-related proteins. *Int. J. Mol. Med.* 33 (5), 1161–1168. doi:10.3892/ijmm.2014.1680

Du, Q. H., Peng, C., and Zhang, H. (2013). Polydatin: A review of pharmacology and pharmacokinetics. *Pharm. Biol.* 51 (11), 1347–1354. doi:10.3109/13880209.2013.792849

Duan, L., Liu, Y., Li, J., Zhang, Y., Dong, Y., Liu, C., et al. (2022). Panax notoginseng saponins alleviate coronary artery disease through hypermethylation of the miR-194-MAPK pathway. *Front. Pharmacol.* 13, 829416. doi:10.3389/fphar.2022.829416

Dutta, P., Courties, G., Wei, Y., Leuschner, F., Gorbatov, R., Robbins, C. S., et al. (2012). Myocardial infarction accelerates atherosclerosis. *Nature* 487 (7407), 325–329. doi:10.1038/nature11260

Edgar, L., Akbar, N., Braithwaite, A. T., Krausgruber, T., Gallart-Ayala, H., Bailey, J., et al. (2021). Hyperglycemia induces trained immunity in macrophages and their precursors and promotes atherosclerosis. *Circulation* 144 (12), 961–982. doi:10.1161/circulationaha.120.046464

Eguchi, A., Kaneko, Y., Murakami, A., and Ohigashi, H. (2007). Zerumbone suppresses phorbol ester-induced expression of multiple scavenger receptor genes in THP-1 human monocytic cells. *Biosci. Biotechnol. Biochem.* 71 (4), 935–945. doi:10.1271/bbb.60596

El-Shitany, N. A., and Eid, B. G. (2019). Icariin modulates carrageenan-induced acute inflammation through HO-1/Nrf2 and NF-kB signaling pathways. *Biomed. Pharmacother.* 120, 109567. doi:10.1016/j.biopha.2019.109567

Everts, B., Amiel, E., van der Windt, G. J., Freitas, T. C., Chott, R., Yarasheski, K. E., et al. (2012). Commitment to glycolysis sustains survival of NO-producing inflammatory dendritic cells. *Blood* 120 (7), 1422–1431. doi:10.1182/blood-2012-03-419747

Evtyugin, D. D., Magina, S., and Evtuguin, D. V. (2020). Recent advances in the production and applications of ellagic acid and its derivatives. A review. *Molecules* 25 (12), 2745. doi:10.3390/molecules25122745

Faisal, W., O'Driscoll, C. M., and Griffin, B. T. (2010). Bioavailability of lycopene in the rat: The role of intestinal lymphatic transport. *J. Pharm. Pharmacol.* 62 (3), 323–331. doi:10.1211/jpp.62.03.0006

Fang, J. (2015). Classification of fruits based on anthocyanin types and relevance to their health effects. *Nutrition* 31 (11-12), 1301–1306. doi:10.1016/j.nut.2015.04.015

Fanucchi, S., Domínguez-Andrés, J., Joosten, L. A. B., Netea, M. G., and Mhlanga, M. M. (2021). The intersection of epigenetics and metabolism in trained immunity. *Immunity* 54 (1), 32–43. doi:10.1016/j.immuni.2020.10.011

Fanucchi, S., Fok, E. T., Dalla, E., Shibayama, Y., Borner, K., Chang, E. Y., et al. (2019). Immune genes are primed for robust transcription by proximal long noncoding RNAs located in nuclear compartments. *Nat. Genet.* 51 (1), 138–150. doi:10.1038/s41588-018-0298-2

Fatima, N., Baqri, S. S. R., Bhattacharya, A., Koney, N. K. K., Husain, K., Abbas, A., et al. (2021). Role of flavonoids as epigenetic modulators in cancer prevention and therapy. *Front. Genet.* 12, 758733. doi:10.3389/fgene.2021.758733

Felgines, C., Texier, O., Besson, C., Lyan, B., Lamaison, J. L., and Scalbert, A. (2007). Strawberry pelargonidin glycosides are excreted in urine as intact glycosides and glucuronidated pelargonidin derivatives in rats. *Br. J. Nutr.* 98 (6), 1126–1131. doi:10.1017/s0007114507764772

Feng, X., Qin, H., Shi, Q., Zhang, Y., Zhou, F., Wu, H., et al. (2014). Chrysin attenuates inflammation by regulating M1/M2 status via activating PPARγ. *Biochem. Pharmacol.* 89 (4), 503–514. doi:10.1016/j.bcp.2014.03.016

Feng, X., Wang, K., Cao, S., Ding, L., and Qiu, F. (2020). Pharmacokinetics and excretion of berberine and its nine metabolites in rats. *Front. Pharmacol.* 11, 594852. doi:10.3389/fphar.2020.594852

Ferry, D. R., Smith, A., Malkhandi, J., Fyfe, D. W., deTakats, P. G., AnDerson, D., et al. (1996). Phase I clinical trial of the flavonoid quercetin: Pharmacokinetics and evidence for *in vivo* tyrosine kinase inhibition. *Clin. Cancer Res.* 2 (4), 659–668.

Flores-Gomez, D., Bekkering, S., Netea, M. G., and Riksen, N. P. (2021). Trained immunity in atherosclerotic cardiovascular disease. *Arterioscler. Thromb. Vasc. Biol.* 41 (1), 62–69. doi:10.1161/atvbaha.120.314216

Folco, E. J., Sheikine, Y., Rocha, V. Z., Christen, T., Shvartz, E., Sukhova, G. K., et al. (2011). Hypoxia but not inflammation augments glucose uptake in human macrophages: Implications for imaging atherosclerosis with 18fluorine-labeled 2-deoxy-D-glucose positron emission tomography. *J. Am. Coll. Cardiol.* 58 (6), 603–614. doi:10.1016/j.jacc.2011.03.044

Foster, S. L., Hargreaves, D. C., and Medzhitov, R. (2007). Gene-specific control of inflammation by TLR-induced chromatin modifications. *Nature* 447 (7147), 972–978. doi:10.1038/nature05836

Fried, L. E., and Arbiser, J. L. (2009). Honokiol, a multifunctional antiangiogenic and antitumor agent. *Antioxid. Redox Signal* 11 (5), 1139–1148. doi:10.1089/ars.2009.2440

Fu, X., Xu, A. G., Yao, M. Y., Guo, L., and Zhao, L. S. (2014). Emodin enhances cholesterol efflux by activating peroxisome proliferator-activated receptor-γ in oxidized low density lipoprotein-loaded THP1 macrophages. *Clin. Exp. Pharmacol. Physiol.* 41 (9), 679–684. doi:10.1111/1440-1681.12262

Fujii, J., Osaki, T., and Bo, T. (2022). Ascorbate is a primary antioxidant in mammals. *Molecules* 27 (19), 6187. doi:10.3390/molecules27196187

Fukuzumi, M., Shinomiya, H., Shimizu, Y., Ohishi, K., and UtSumi, S. (1996). Endotoxin-induced enhancement of glucose influx into murine peritoneal macrophages via GLUT1. *Infect. Immun.* 64 (1), 108–112. doi:10.1128/iai.64.1.108-112.1996

Fullerton, M. D., Ford, R. J., McGregor, C. P., LeBlond, N. D., Snider, S. A., Stypa, S. A., et al. (2015). Salicylate improves macrophage cholesterol homeostasis via activation of Ampk. *J. Lipid Res.* 56 (5), 1025–1033. doi:10.1194/jlr.M058875

Galano, A., Francisco Marquez, M., and Pérez-González, A. (2014). Ellagic acid: An unusually versatile protector against oxidative stress. *Chem. Res. Toxicol.* 27 (5), 904–918. doi:10.1021/tx500065y

Gallino, A., Aboyans, V., Diehm, C., Cosentino, F., Stricker, H., Falk, E., et al. (2014). Non-coronary atherosclerosis. *Eur. Heart J.* 35 (17), 1112–1119. doi:10.1093/eurheartj/ehu071

Ganai, S. A., Sheikh, F. A., and Baba, Z. A. (2021). Plant flavone Chrysin as an emerging histone deacetylase inhibitor for prosperous epigenetic-based anticancer therapy. *Phytother. Res.* 35 (2), 823–834. doi:10.1002/ptr.6869

Gani, S. A., Muhammad, S. A., Kura, A. U., Barahuie, F., Hussein, M. Z., and Fakurazi, S. (2019). Effect of protocatechuic acid-layered double hydroxide nanoparticles on diethylnitrosamine/phenobarbital-induced hepatocellular carcinoma in mice. *PLoS One* 14 (5), e0217009. doi:10.1371/journal.pone.0217009

Gao, J., Xu, Y., Yang, Y., Yang, Y., Zheng, Z., Jiang, W., et al. (2008). Identification of upregulators of human ATP-binding cassette transporter A1 via high-throughput screening of a synthetic and natural compound library. *J. Biomol. Screen* 13 (7), 648–656. doi:10.1177/1087057108320545

Gao, X., Wu, J., Zou, W., and Dai, Y. (2014). Two ellagic acids isolated from roots of Sanguisorba officinalis L. promote hematopoietic progenitor cell proliferation and megakaryocyte differentiation. *Molecules* 19 (4), 5448–5458. doi:10.3390/molecules19045448

Garcia, C., and Blesso, C. N. (2021). Antioxidant properties of anthocyanins and their mechanism of action in atherosclerosis. *Free Radic. Biol. Med.* 172, 152–166. doi:10.1016/j.freeradbiomed.2021.05.040

Geng, J., Fu, W., Yu, X., Lu, Z., Liu, Y., Sun, M., et al. (2020). Ginsenoside Rg3 alleviates ox-LDL induced endothelial dysfunction and prevents atherosclerosis in ApoE(-/-) mice by regulating PPARγ/FAK signaling pathway. *Front. Pharmacol.* 11, 500. doi:10.3389/fphar.2020.00500

Gobalakrishnan, S., Asirvatham, S. S., and Janarthanam, V. (2016). Effect of silybin on lipid profile in hypercholesterolaemic rats. *J. Clin. Diagn Res.* 10 (4), Ff01–5. doi:10.7860/jcdr/2016/16393.7566

Godugu, C., Patel, A. R., Doddapaneni, R., Somagoni, J., and Singh, M. (2014). Approaches to improve the oral bioavailability and effects of novel anticancer drugs berberine and betulinic acid. *PLoS One* 9 (3), e89919. doi:10.1371/journal.pone.0089919

Gourbal, B., Pinaud, S., Beckers, G. J. M., Van Der Meer, J. W. M., Conrath, U., and Netea, M. G. (2018). Innate immune memory: An evolutionary perspective. *Immunol. Rev.* 283 (1), 21–40. doi:10.1111/imr.12647

Griñán-Ferré, C., Bellver-Sanchis, A., Izquierdo, V., Corpas, R., Roig-Soriano, J., Chillon, M., et al. (2021). The pleiotropic neuroprotective effects of resveratrol in cognitive decline and Alzheimer's disease pathology: From antioxidant to epigenetic therapy. *Ageing Res. Rev.* 67, 101271. doi:10.1016/j.arr.2021.101271

Groh, L., Keating, S. T., Joosten, L. A. B., Netea, M. G., and Riksen, N. P. (2018). Monocyte and macrophage immunometabolism in atherosclerosis. *Semin. Immunopathol.* 40 (2), 203–214. doi:10.1007/s00281-017-0656-7

Gudas, L. J. (2013). Retinoids induce stem cell differentiation via epigenetic changes. *Semin. Cell. Dev. Biol.* 24 (10-12), 701–705. doi:10.1016/j.semcdb.2013.08.002

Gui, Y. Z., Yan, H., Gao, F., Xi, C., Li, H. H., and Wang, Y. P. (2016). Betulin attenuates atherosclerosis in apoE(-/-) mice by up-regulating ABCA1 and ABCG1. *Acta Pharmacol. Sin.* 37 (10), 1337–1348. doi:10.1038/aps.2016.46

Guo, H. X., Liu, D. H., Ma, Y., Liu, J. f., Wang, Y., Du, Z. y., et al. (2009). Long-term baicalin administration ameliorates metabolic disorders and hepatic steatosis in rats given a high-fat diet. *Acta Pharmacol. Sin.* 30 (11), 1505–1512. doi:10.1038/aps.2009.150

Gupta, A., Singh, A. K., Kumar, R., Jamieson, S., Pandey, A. K., and Bishayee, A. (2021). Neuroprotective potential of ellagic acid: A critical review. *Adv. Nutr.* 12 (4), 1211–1238. doi:10.1093/advances/nmab007

Han, G. M., Soliman, G. A., Meza, J. L., Islam, K. M. M., and Watanabe-Galloway, S. (2016). The influence of BMI on the association between serum lycopene and the metabolic syndrome. *Br. J. Nutr.* 115 (7), 1292–1300. doi:10.1017/s0007114516000179

Han, P., Gao, D., Zhang, W., Liu, S., Yang, S., and Li, X. (2015). Puerarin suppresses high glucose-induced MCP-1 expression via modulating histone methylation in cultured endothelial cells. *Life Sci.* 130, 103–107. doi:10.1016/j.lfs.2015.02.022

Hao, H., Wang, G., Cui, N., Li, J., Xie, L., and Ding, Z. (2006). Pharmacokinetics, absorption and tissue distribution of tanshinone IIA solid dispersion. *Planta Med.* 72 (14), 1311–1317. doi:10.1055/s-2006-951698

Hao, S., Xiao, Y., Lin, Y., Mo, Z., Chen, Y., Peng, X., et al. (2016). Chlorogenic acid-enriched extract from Eucommia ulmoides leaves inhibits hepatic lipid accumulation through regulation of cholesterol metabolism in HepG2 cells. *Pharm. Biol.* 54 (2), 251–259. doi:10.3109/13880209.2015.1029054

Hardbower, D. M., Asim, M., Luis, P. B., Singh, K., Barry, D. P., Yang, C., et al. (2017). Ornithine decarboxylase regulates M1 macrophage activation and mucosal inflammation via histone modifications. *Proc. Natl. Acad. Sci. U. S. A.* 114 (5), E751-E760–e60. doi:10.1073/pnas.1614958114

Hassan, F. U., Rehman, M. S., Khan, M. S., Ali, M. A., Javed, A., Nawaz, A., et al. (2019). Curcumin as an alternative epigenetic modulator: Mechanism of action and potential effects. *Front. Genet.* 10, 514. doi:10.3389/fgene.2019.00514

He, F., and Yao, G. (2021). Ginsenoside Rg1 as a potential regulator of hematopoietic stem/progenitor cells. *Stem Cells Int.* 2021, 4633270. doi:10.1155/2021/4633270

He, X. W., Yu, D., Li, W. L., Zheng, Z., Lv, C. L., Li, C., et al. (2016). Anti-atherosclerotic potential of baicalin mediated by promoting cholesterol efflux from macrophages via the PPARγ-LXRα-ABCA1/ABCG1 pathway. *Biomed. Pharmacother.* 83, 257–264. doi:10.1016/j.biopha.2016.06.046

He, Y., Shi, Y., Yang, Y., Huang, H., Feng, Y., Wang, Y., et al. (2021). Chrysin induces autophagy through the inactivation of the ROS-mediated Akt/mTOR signaling pathway in endometrial cancer. *Int. J. Mol. Med.* 48 (3), 172. doi:10.3892/ijmm.2021.5005

Hei, Z. Q., Huang, H. Q., Tan, H. M., Liu, P. q., Zhao, L. z., Chen, S. r., et al. (2006). Emodin inhibits dietary induced atherosclerosis by antioxidation and regulation of the sphingomyelin pathway in rabbits. *Chin. Med. J. Engl.* 119 (10), 868–870. doi:10.1097/00029330-200605020-00012

Heidt, T., Sager, H. B., Courties, G., Dutta, P., Iwamoto, Y., Zaltsman, A., et al. (2014). Chronic variable stress activates hematopoietic stem cells. *Nat. Med.* 20 (7), 754–758. doi:10.1038/nm.3589

Hemn, H. O., Noordin, M. M., Rahman, H. S., Hazilawati, H., Zuki, A., and Chartrand, M. S. (2015). Antihypercholesterolemic and antioxidant efficacies of zerumbone on the formation, development, and establishment of atherosclerosis in cholesterol-fed rabbits. *Drug Des. Devel Ther.* 9, 4173–4208. doi:10.2147/dddt.S76225

Himes, S. R., Cronau, S., Mulford, C., and Hume, D. A. (2005). The Runx1 transcription factor controls CSF-1-dependent and -independent growth and survival of macrophages. *Oncogene* 24 (34), 5278–5286. doi:10.1038/sj.onc.1208657

Howard, T. D., Ho, S. M., Zhang, L., Chen, J., Cui, W., Slager, R., et al. (2011). Epigenetic changes with dietary soy in cynomolgus monkeys. *PLoS One* 6 (10), e26791. doi:10.1371/journal.pone.0026791

Hsieh, C. C., Kuo, C. H., Kuo, H. F., Chen, Y. S., Wang, S. L., Chao, D., et al. (2014). Sesamin suppresses macrophage-derived chemokine expression in human monocytes via epigenetic regulation. *Food Funct.* 5 (10), 2494–2500. doi:10.1039/c4fo00322e

Hu, K., Yang, Y., Tu, Q., and Luo, Y. (2013). Alpinetin inhibits LPS-induced inflammatory mediator response by activating PPAR-γ in THP-1-derived macrophages. *Eur. J. Pharmacol.* 721 (1-3), 96–102. doi:10.1016/j.ejphar.2013.09.049

Hu, Y., Sun, B., Liu, K., Yan, M., Zhang, Y., Miao, C., et al. (2016). Icariin attenuates high-cholesterol diet induced atherosclerosis in rats by inhibition of inflammatory response and p38 MAPK signaling pathway. *Inflammation* 39 (1), 228–236. doi:10.1007/s10753-015-0242-x

Huang, J., Weinstein, S. J., Yu, K., Mannisto, S., and Albanes, D. (2018). Serum beta carotene and overall and cause-specific mortality. *Circ. Res.* 123 (12), 1339–1349. doi:10.1161/circresaha.118.313409

Huang, L., Chambliss, K. L., Gao, X., Yuhanna, I. S., Behling-Kelly, E., Bergaya, S., et al. (2019). SR-B1 drives endothelial cell LDL transcytosis via DOCK4 to promote atherosclerosis. *Nature* 569 (7757), 565–569. doi:10.1038/s41586-019-1140-4

Huang, Z., Dong, F., Li, S., Chu, M., Zhou, H., Lu, Z., et al. (2012). Berberine-induced inhibition of adipocyte enhancer-binding protein 1 attenuates oxidized low-density lipoprotein accumulation and foam cell formation in phorbol 12-myristate 13-acetate-induced macrophages. *Eur. J. Pharmacol.* 690 (1-3), 164–169. doi:10.1016/j.ejphar.2012.07.009

Huo, M., Chen, N., Chi, G., Yuan, X., Guan, S., Li, H., et al. (2012). Traditional medicine alpinetin inhibits the inflammatory response in Raw 264.7 cells and mouse models. *Int. Immunopharmacol.* 12 (1), 241–248. doi:10.1016/j.intimp.2011.11.017

Hussein, G., Sankawa, U., Goto, H., Matsumoto, K., and Watanabe, H. (2006). Astaxanthin, a carotenoid with potential in human health and nutrition. *J. Nat. Prod.* 69 (3), 443–449. doi:10.1021/np050354+

Huwait, E. A., Greenow, K. R., Singh, N. N., and Ramji, D. P. (2011). A novel role for c-Jun N-terminal kinase and phosphoinositide 3-kinase in the liver X receptor-mediated induction of macrophage gene expression. *Cell. Signal* 23 (3), 542–549. doi:10.1016/j.cellsig.2010.11.002

Ifrim, D. C., Quintin, J., Joosten, L. A., Jacobs, C., Jansen, T., Jacobs, L., et al. (2014). Trained immunity or tolerance: Opposing functional programs induced in human monocytes after engagement of various pattern recognition receptors. *Clin. Vaccine Immunol.* 21 (4), 534–545. doi:10.1128/cvi.00688-13

Iio, A., Ohguchi, K., Iinuma, M., Nozawa, Y., and Ito, M. (2012). Hesperetin upregulates ABCA1 expression and promotes cholesterol efflux from THP-1 macrophages. *J. Nat. Prod.* 75 (4), 563–566. doi:10.1021/np200696r

Iizuka, M., Ayaori, M., Uto-Kondo, H., Yakushiji, E., Takiguchi, S., Nakaya, K., et al. (2012). Astaxanthin enhances ATP-binding cassette transporter A1/G1 expressions and cholesterol efflux from macrophages. *J. Nutr. Sci. Vitaminol. (Tokyo)* 58 (2), 96–104. doi:10.3177/jnsv.58.96

Ikhlef, S., Berrougui, H., Kamtchueng Simo, O., and Khalil, A. (2016). Paraoxonase 1-treated oxLDL promotes cholesterol efflux from macrophages by stimulating the PPARγ-LXRα-ABCA1 pathway. *FEBS Lett.* 590 (11), 1614–1629. doi:10.1002/1873-3468.12198

Im, D. S. (2020). Pro-resolving effect of ginsenosides as an anti-inflammatory mechanism of panax ginseng. *Biomolecules* 10 (3), 444. doi:10.3390/biom10030444

Iwanowycz, S., Wang, J., Altomare, D., Hui, Y., and Fan, D. (2016). Emodin bidirectionally modulates macrophage polarization and epigenetically regulates macrophage memory. *J. Biol. Chem.* 291 (22), 11491–11503. doi:10.1074/jbc.M115.702092

Izzo, S., Naponelli, V., and Bettuzzi, S. (2020). Flavonoids as epigenetic modulators for prostate cancer prevention. *Nutrients* 12 (4), 1010. doi:10.3390/nu12041010

Jayakumar, T., Lin, K. C., Chang, C. C., Hsia, C. W., Manubolu, M., Huang, W. C., et al. (2021). Targeting MAPK/NF-κB pathways in anti-inflammatory potential of rutaecarpine: Impact on src/FAK-mediated macrophage migration. *Int. J. Mol. Sci.* 23 (1), 92. doi:10.3390/ijms23010092

Jha, A. K., Huang, S. C., Sergushichev, A., Lampropoulou, V., Ivanova, Y., Loginicheva, E., et al. (2015). Network integration of parallel metabolic and transcriptional data reveals metabolic modules that regulate macrophage polarization. *Immunity* 42 (3), 419–430. doi:10.1016/j.immuni.2015.02.005

Jia, L. Q., Zhang, N., Xu, Y., Chen, W. n., Zhu, M. l., Song, N., et al. (2016). Tanshinone IIA affects the HDL subfractions distribution not serum lipid levels: Involving in intake and efflux of cholesterol. *Arch. Biochem. Biophys.* 592, 50–59. doi:10.1016/j.abb.2016.01.001

Jia, Q., Cao, H., Shen, D., Li, S., Yan, L., Chen, C., et al. (2019). Quercetin protects against atherosclerosis by regulating the expression of PCSK9, CD36, PPARγ, LXRα and ABCA1. *Int. J. Mol. Med.* 44 (3), 893–902. doi:10.3892/ijmm.2019.4263

Jia, Y., Li, Z. Y., Zhang, H. G., Li, H. B., Liu, Y., and Li, X. H. (2010). Panax notoginseng saponins decrease cholesterol ester via up-regulating ATP-binding cassette transporter A1 in foam cells. *J. Ethnopharmacol.* 132 (1), 297–302. doi:10.1016/j.jep.2010.08.033

Jiang, J., Mo, Z. C., Yin, K., Zhao, G. J., Lv, Y. C., Ouyang, X. P., et al. (2012). Epigallocatechin-3-gallate prevents TNF-α-induced NF-κB activation thereby upregulating ABCA1 via the Nrf2/Keap1 pathway in macrophage foam cells. *Int. J. Mol. Med.* 29 (5), 946–956. doi:10.3892/ijmm.2012.924

Jiang, Z., Sang, H., Fu, X., Liang, Y., and Li, L. (2015). Alpinetin enhances cholesterol efflux and inhibits lipid accumulation in oxidized low-density lipoprotein-loaded human macrophages. *Biotechnol. Appl. Biochem.* 62 (6), 840–847. doi:10.1002/bab.1328

Jing, X., Han, J., Zhang, J., Chen, Y., Yuan, J., Wang, J., et al. (2021). Long non-coding RNA MEG3 promotes cisplatin-induced nephrotoxicity through regulating AKT/TSC/mTOR-mediated autophagy. *Int. J. Biol. Sci.* 17 (14), 3968–3980. doi:10.7150/ijbs.58910

Jung, C. G., Horike, H., Cha, B. Y., Uhm, K. O., Yamauchi, R., Yamaguchi, T., et al. (2010). Honokiol increases ABCA1 expression level by activating retinoid X receptor beta. *Biol. Pharm. Bull.* 33 (7), 1105–1111. doi:10.1248/bpb.33.1105

Kang, I., Okla, M., and Chung, S. (2014). Ellagic acid inhibits adipocyte differentiation through coactivator-associated arginine methyltransferase 1-mediated chromatin modification. *J. Nutr. Biochem.* 25 (9), 946–953. doi:10.1016/j.jnutbio.2014.04.008

Kasala, E. R., Bodduluru, L. N., Madana, R. M., V, A. K., Gogoi, R., and Barua, C. C. (2015). Chemopreventive and therapeutic potential of chrysin in cancer: Mechanistic perspectives. *Toxicol. Lett.* 233 (2), 214–225. doi:10.1016/j.toxlet.2015.01.008

Keating, S. T., Groh, L., van der Heijden, C. D. C. C., Rodriguez, H., Dos Santos, D. C., Fanucchi, S., et al. (2020). Rewiring of glucose metabolism defines trained immunity induced by oxidized low-density lipoprotein. *J. Mol. Med. Berl.* 98 (6), 819–831. doi:10.1007/s00109-020-01915-w

Kelley, T. W., Graham, M. M., Doseff, A. I., Pomerantz, R. W., Lau, S. M., Ostrowski, M. C., et al. (1999). Macrophage colony-stimulating factor promotes cell survival through Akt/protein kinase B. *J. Biol. Chem.* 274 (37), 26393–26398. doi:10.1074/jbc.274.37.26393

Kesharwani, S. S., and Bhat, G. J. (2020). Formulation and nanotechnology-based approaches for solubility and bioavailability enhancement of zerumbone. *Med. Kaunas.* 56 (11), 557. doi:10.3390/medicina56110557

Khokha, R., Murthy, A., and Weiss, A. (2013). Metalloproteinases and their natural inhibitors in inflammation and immunity. *Nat. Rev. Immunol.* 13 (9), 649–665. doi:10.1038/nri3499

Khoo, H. E., Azlan, A., Tang, S. T., and Lim, S. M. (2017). Anthocyanidins and anthocyanins: Colored pigments as food, pharmaceutical ingredients, and the potential health benefits. *Food Nutr. Res.* 61 (1), 1361779. doi:10.1080/16546628.2017.1361779

Kim, D., Kim, Y., and Kim, Y. (2019). Effects of β-carotene on expression of selected MicroRNAs, histone acetylation, and DNA methylation in colon cancer stem cells. *J. Cancer Prev.* 24 (4), 224–232. doi:10.15430/jcp.2019.24.4.224

Kim, H., Ramirez, C. N., Su, Z. Y., and Kong, A. N. T. (2016). Epigenetic modifications of triterpenoid ursolic acid in activating Nrf2 and blocking cellular transformation of mouse epidermal cells. *J. Nutr. Biochem.* 33, 54–62. doi:10.1016/j.jnutbio.2015.09.014

Kim, J., Byeon, H., Im, K., and Min, H. (2018). Effects of ginsenosides on regulatory T cell differentiation. *Food Sci. Biotechnol.* 27 (1), 227–232. doi:10.1007/s10068-017-0255-3

Kim, J. H., Yi, Y. S., Kim, M. Y., and Cho, J. Y. (2017). Role of ginsenosides, the main active components of Panax ginseng, in inflammatory responses and diseases. *J. Ginseng Res.* 41 (4), 435–443. doi:10.1016/j.jgr.2016.08.004

Kim, R. E., Shin, C. Y., Han, S. H., and Kwon, K. J. (2020). Astaxanthin suppresses pm2.5-induced neuroinflammation by regulating Akt phosphorylation in BV-2 microglial cells. *Int. J. Mol. Sci.* 21 (19), 7227. doi:10.3390/ijms21197227

Kishimoto, Y., Tani, M., Uto-Kondo, H., Iizuka, M., Saita, E., Sone, H., et al. (2010). Astaxanthin suppresses scavenger receptor expression and matrix metalloproteinase activity in macrophages. *Eur. J. Nutr.* 49 (2), 119–126. doi:10.1007/s00394-009-0056-4

Kiss, R. S., Maric, J., and Marcel, Y. L. (2005). Lipid efflux in human and mouse macrophagic cells: Evidence for differential regulation of phospholipid and cholesterol efflux. *J. Lipid Res.* 46 (9), 1877–1887. doi:10.1194/jlr.M400482-JLR200

Kleinnijenhuis, J., Quintin, J., Preijers, F., Joosten, L. A. B., Ifrim, D. C., Saeed, S., et al. (2012). Bacille Calmette-Guerin induces NOD2-dependent nonspecific protection from reinfection via epigenetic reprogramming of monocytes. *Proc. Natl. Acad. Sci. U. S. A.* 109 (43), 17537–17542. doi:10.1073/pnas.1202870109

Koh, Y. C., Yang, G., Lai, C. S., Weerawatanakorn, M., and Pan, M. H. (2018). Chemopreventive effects of phytochemicals and medicines on M1/M2 polarized macrophage role in inflammation-related diseases. *Int. J. Mol. Sci.* 19 (8), 2208. doi:10.3390/ijms19082208

Kong, W., Wei, J., Abidi, P., Lin, M., Inaba, S., Li, C., et al. (2004). Berberine is a novel cholesterol-lowering drug working through a unique mechanism distinct from statins. *Nat. Med.* 10 (12), 1344–1351. doi:10.1038/nm1135

Kotani, H., Tanabe, H., Mizukami, H., Makishima, M., and Inoue, M. (2010). Identification of a naturally occurring rexinoid, honokiol, that activates the retinoid X receptor. *J. Nat. Prod.* 73 (8), 1332–1336. doi:10.1021/np100120c

Kou, J. Y., Li, Y., Zhong, Z. Y., Jiang, Y. Q., Li, X. S., Han, X. B., et al. (2017). Berberine-sonodynamic therapy induces autophagy and lipid unloading in macrophage. *Cell. Death Dis.* 8 (1), e2558. doi:10.1038/cddis.2016.354

Kou, M. C., Chiou, S. Y., Weng, C. Y., Wang, L., Ho, C. T., and Wu, M. J. (2013). Curcuminoids distinctly exhibit antioxidant activities and regulate expression of scavenger receptors and heme oxygenase-1. *Mol. Nutr. Food Res.* 57 (9), 1598–1610. doi:10.1002/mnfr.201200227

Krinsky, N. I., and Johnson, E. J. (2005). Carotenoid actions and their relation to health and disease. *Mol. Asp. Med.* 26 (6), 459–516. doi:10.1016/j.mam.2005.10.001

Kumar, S., and Pandey, A. K. (2013). Chemistry and biological activities of flavonoids: An overview. *ScientificWorldJournal* 2013, 162750. doi:10.1155/2013/162750

Langmann, T., Liebisch, G., Moehle, C., Schifferer, R., Dayoub, R., Heiduczek, S., et al. (2005). Gene expression profiling identifies retinoids as potent inducers of macrophage lipid efflux. *Biochim. Biophys. Acta* 1740 (2), 155–161. doi:10.1016/j.bbadis.2004.11.016

Lee, S. H., Lee, J. H., Lee, H. Y., and Min, K. J. (2019). Sirtuin signaling in cellular senescence and aging. *BMB Rep.* 52 (1), 24–34. doi:10.5483/BMBRep.2019.52.1.290

Lee, T. S., Pan, C. C., Peng, C. C., Kou, Y. R., Chen, C. Y., Ching, L. C., et al. (2010). Anti-atherogenic effect of berberine on LXRalpha-ABCA1-dependent cholesterol efflux in macrophages. *J. Cell. Biochem.* 111 (1), 104–110. doi:10.1002/jcb.22667

Leentjens, J., Bekkering, S., Joosten, L. A. B., Netea, M. G., Burgner, D. P., and Riksen, N. P. (2018). Trained innate immunity as a novel mechanism linking infection and the development of atherosclerosis. *Circ. Res.* 122 (5), 664–669. doi:10.1161/circresaha.117.312465

Leng, S., Iwanowycz, S., Saaoud, F., Wang, J., Wang, Y., Sergin, I., et al. (2016). Ursolic acid enhances macrophage autophagy and attenuates atherogenesis. *J. Lipid Res.* 57 (6), 1006–1016. doi:10.1194/jlr.M065888

Li, C., and Schluesener, H. (2017). Health-promoting effects of the citrus flavanone hesperidin. *Crit. Rev. Food Sci. Nutr.* 57 (3), 613–631. doi:10.1080/10408398.2014.906382

Li, C., Wang, Q., Ren, T., Zhang, Y., Lam, C. W. K., Chow, M. S. S., et al. (2016). Non-linear pharmacokinetics of piperine and its herb-drug interactions with docetaxel in Sprague-Dawley rats. *J. Pharm. Biomed. Anal.* 128, 286–293. doi:10.1016/j.jpba.2016.05.041

Li, C. H., Gong, D., Chen, L. Y., Zhang, M., Xia, X. D., Cheng, H. P., et al. (2017). Puerarin promotes ABCA1-mediated cholesterol efflux and decreases cellular lipid accumulation in THP-1 macrophages. *Eur. J. Pharmacol.* 811, 74–86. doi:10.1016/j.ejphar.2017.05.055

Li, J., Xie, Z. Z., Tang, Y. B., Zhou, J. G., and Guan, Y. Y. (2011). Ginsenoside-Rd, a purified component from panax notoginseng saponins, prevents atherosclerosis in apoE knockout mice. *Eur. J. Pharmacol.* 652 (1-3), 104–110. doi:10.1016/j.ejphar.2010.11.017

Li, L., Ni, J., Li, M., Chen, J., Han, L., Zhu, Y., et al. (2017). Ginsenoside Rg3 micelles mitigate doxorubicin-induced cardiotoxicity and enhance its anticancer efficacy. *Drug Deliv.* 24 (1), 1617–1630. doi:10.1080/10717544.2017.1391893

Li, Q., Bao, J. M., Li, X. L., Zhang, T., and Shen, X. h. (2012). Inhibiting effect of Astragalus polysaccharides on the functions of CD4+CD25 highTreg cells in the tumor microenvironment of human hepatocellular carcinoma. *Chin. Med. J. Engl.* 125 (5), 786–793.

Li, S., Jiao, Y., Wang, H., Shang, Q., Lu, F., Huang, L., et al. (2017). Sodium tanshinone IIA sulfate adjunct therapy reduces high-sensitivity C-reactive protein level in coronary artery disease patients: A randomized controlled trial. *Sci. Rep.* 7 (1), 17451. doi:10.1038/s41598-017-16980-4

Li, W., Sargsyan, D., Wu, R., Li, S., Wang, L., Cheng, D., et al. (2019). DNA methylome and transcriptome alterations in high glucose-induced diabetic nephropathy cellular model and identification of novel targets for treatment by tanshinone IIA. *Chem. Res. Toxicol.* 32 (10), 1977–1988. doi:10.1021/acs.chemrestox.9b00117

Li, X., Wu, J., Xu, F., Chu, C., Li, X., Shi, X., et al. (2022). Use of ferulic acid in the management of diabetes mellitus and its complications. *Molecules* 27 (18), 6010. doi:10.3390/molecules27186010

Li, X., Zhou, Y., Yu, C., Yang, H., Zhang, C., Ye, Y., et al. (2015). Paeonol suppresses lipid accumulation in macrophages via upregulation of the ATP-binding cassette transporter A1 and downregulation of the cluster of differentiation 36. *Int. J. Oncol.* 46 (2), 764–774. doi:10.3892/ijo.2014.2757

Liang, Z., Currais, A., Soriano-Castell, D., Schubert, D., and Maher, P. (2021). Natural products targeting mitochondria: Emerging therapeutics for age-associated neurological disorders. *Pharmacol. Ther.* 221, 107749. doi:10.1016/j.pharmthera.2020.107749

Liao, T., Ding, L., Wu, P., Zhang, L., Li, X., Xu, B., et al. (2020). Chrysin attenuates the NLRP3 inflammasome cascade to reduce synovitis and pain in KOA rats. *Drug Des. Devel Ther.* 14, 3015–3027. doi:10.2147/dddt.S261216

Libby, P. (2002). Inflammation in atherosclerosis. *Nature* 420 (6917), 868–874. doi:10.1038/nature01323

Lin, H. L., Cheng, W. T., Chen, L. C., Ho, H. O., Lin, S. Y., and Hsieh, C. M. (2021). Honokiol/magnolol-loaded self-assembling lecithin-based mixed polymeric micelles (lbMPMs) for improving solubility to enhance oral bioavailability. *Int. J. Nanomedicine* 16, 651–665. doi:10.2147/ijn.S290444

Lin, M. C., Ou, T. T., Chang, C. H., Chan, K. C., and Wang, C. J. (2015). Protocatechuic acid inhibits oleic acid-induced vascular smooth muscle cell proliferation through activation of AMP-activated protein kinase and cell cycle arrest in G0/G1 phase. *J. Agric. Food Chem.* 63 (1), 235–241. doi:10.1021/jf505303s

Lin, X. L., Liu, M. H., Hu, H. J., Feng, H. r., Fan, X. J., Zou, W. w., et al. (2015). Curcumin enhanced cholesterol efflux by upregulating ABCA1 expression through AMPK-SIRT1-LXRα signaling in THP-1 macrophage-derived foam cells. *DNA Cell. Biol.* 34 (9), 561–572. doi:10.1089/dna.2015.2866

Litviňuková, M., Talavera-López, C., Maatz, H., Reichart, D., Worth, C. L., Lindberg, E. L., et al. (2020). Cells of the adult human heart. *Nature* 588 (7838), 466–472. doi:10.1038/s41586-020-2797-4

Liu, B., and Yan, W. (2019). Lipophilization of EGCG and effects on antioxidant activities. *Food Chem.* 272, 663–669. doi:10.1016/j.foodchem.2018.08.086

Liu, C., Wang, W., Lin, W., Ling, W., and Wang, D. (2016). Established atherosclerosis might be a prerequisite for chicory and its constituent protocatechuic acid to promote endothelium-dependent vasodilation in mice. *Mol. Nutr. Food Res.* 60 (10), 2141–2150. doi:10.1002/mnfr.201600002

Liu, C. H., Zhang, W. D., Wang, J. J., and Feng, S. D. (2016). Senegenin ameliorate acute lung injury through reduction of oxidative stress and inhibition of inflammation in cecal ligation and puncture-induced sepsis rats. *Inflammation* 39 (2), 900–906. doi:10.1007/s10753-016-0322-6

Liu, N., Wu, C., Sun, L., Zheng, J., and Guo, P. (2014). Sesamin enhances cholesterol efflux in RAW264.7 macrophages. *Molecules* 19 (6), 7516–7527. doi:10.3390/molecules19067516

Liu, R., Li, J., Cheng, Y., Huo, T., Xue, J., Liu, Y., et al. (2015). Effects of ellagic acid-rich extract of pomegranates peel on regulation of cholesterol metabolism and its molecular mechanism in hamsters. *Food Funct.* 6 (3), 780–787. doi:10.1039/c4fo00759j

Liu, W. H., Lin, C. C., Wang, Z. H., Mong, M. C., and Yin, M. C. (2010). Effects of protocatechuic acid on trans fat induced hepatic steatosis in mice. *J. Agric. Food Chem.* 58 (18), 10247–10252. doi:10.1021/jf102379n

Liu, X., and Liu, C. (2017). Baicalin ameliorates chronic unpredictable mild stress-induced depressive behavior: Involving the inhibition of NLRP3 inflammasome activation in rat prefrontal cortex. *Int. Immunopharmacol.* 48, 30–34. doi:10.1016/j.intimp.2017.04.019

Liu, Z., Wang, J., Huang, E., Gao, S., Li, H., Lu, J., et al. (2014). Tanshinone IIA suppresses cholesterol accumulation in human macrophages: Role of heme oxygenase-1. *J. Lipid Res.* 55 (2), 201–213. doi:10.1194/jlr.M040394

Long, H., Lin, H., Zheng, P., Hou, L., Zhang, M., Lin, S., et al. (2022). WTAP mediates the anti-inflammatory effect of Astragalus mongholicus polysaccharide on THP-1 macrophages. *Front. Pharmacol.* 13, 1023878. doi:10.3389/fphar.2022.1023878

Lü, J. M., Yao, Q., and Chen, C. (2009). Ginseng compounds: An update on their molecular mechanisms and medical applications. *Curr. Vasc. Pharmacol.* 7 (3), 293–302. doi:10.2174/157016109788340767

Lu, Z., He, B., Chen, J., Wu, L. J., Chen, X. B., Ye, S. Q., et al. (2021). Optimisation of the conversion and extraction of arctigenin from fructus arctii into arctiin using fungi. *Front. Microbiol.* 12, 663116. doi:10.3389/fmicb.2021.663116

Luo, J., Chen, S., Wang, L., Zhao, X., and Piao, C. (2022). Pharmacological effects of polydatin in the treatment of metabolic diseases: A review. *Phytomedicine* 102, 154161. doi:10.1016/j.phymed.2022.154161

Lv, B., Chen, S., Tang, C., Jin, H., Du, J., and Huang, Y. (2021). Hydrogen sulfide and vascular regulation - an update. *J. Adv. Res.* 27, 85–97. doi:10.1016/j.jare.2020.05.007

Ma, J., Zheng, L., He, Y. S., and Li, H. J. (2015). Hepatotoxic assessment of Polygoni Multiflori Radix extract and toxicokinetic study of stilbene glucoside and anthraquinones in rats. *J. Ethnopharmacol.* 162, 61–68. doi:10.1016/j.jep.2014.12.045

Mallat, Z., Heymes, C., Ohan, J., Faggin, E., Leseche, G., and Tedgui, A. (1999). Expression of interleukin-10 in advanced human atherosclerotic plaques: Relation to inducible nitric oxide synthase expression and cell death. *Arterioscler. Thromb. Vasc. Biol.* 19 (3), 611–616. doi:10.1161/01.atv.19.3.611

Mani, R., and Natesan, V. (2018). Chrysin: Sources, beneficial pharmacological activities, and molecular mechanism of action. *Phytochemistry* 145, 187–196. doi:10.1016/j.phytochem.2017.09.016

Maxwell, T., Lee, K. S., Kim, S., and Nam, K. S. (2018). Arctigenin inhibits the activation of the mTOR pathway, resulting in autophagic cell death and decreased ER expression in ER-positive human breast cancer cells. *Int. J. Oncol.* 52 (4), 1339–1349. doi:10.3892/ijo.2018.4271

McCreight, L. J., Bailey, C. J., and Pearson, E. R. (2016). Metformin and the gastrointestinal tract. *Diabetologia* 59 (3), 426–435. doi:10.1007/s00125-015-3844-9

Mei, L., He, M., Zhang, C., Miao, J., Wen, Q., Liu, X., et al. (2019). Paeonol attenuates inflammation by targeting HMGB1 through upregulating miR-339-5p. *Sci. Rep.* 9 (1), 19370. doi:10.1038/s41598-019-55980-4

Mensah, G. A., Roth, G. A., and Fuster, V. (2019). The global burden of cardiovascular diseases and risk factors: 2020 and beyond. *J. Am. Coll. Cardiol.* 74 (20), 2529–2532. doi:10.1016/j.jacc.2019.10.009

Millar, C. L., Duclos, Q., and Blesso, C. N. (2017). Effects of dietary flavonoids on reverse cholesterol transport, HDL metabolism, and HDL function. *Adv. Nutr.* 8 (2), 226–239. doi:10.3945/an.116.014050

Mills, E. L., Kelly, B., Logan, A., Costa, A. S. H., Varma, M., Bryant, C. E., et al. (2016). Succinate dehydrogenase supports metabolic repurposing of mitochondria to drive inflammatory macrophages. *Cell.* 167 (2), 457–470. doi:10.1016/j.cell.2016.08.064

Milutinović, B., and Kurtz, J. (2016). Immune memory in invertebrates. *Semin. Immunol.* 28 (4), 328–342. doi:10.1016/j.smim.2016.05.004

Min, K. J., Um, H. J., Cho, K. H., and Kwon, T. K. (2013). Curcumin inhibits oxLDL-induced CD36 expression and foam cell formation through the inhibition of p38 MAPK phosphorylation. *Food Chem. Toxicol.* 58, 77–85. doi:10.1016/j.fct.2013.04.008

Mitroulis, I., Ruppova, K., Wang, B., Chen, L. S., Grzybek, M., Grinenko, T., et al. (2018). Modulation of myelopoiesis progenitors is an integral component of trained immunity. *Cell.* 172 (1-2), 147–161. doi:10.1016/j.cell.2017.11.034

Moore, K. J., Sheedy, F. J., and Fisher, E. A. (2013). Macrophages in atherosclerosis: A dynamic balance. *Nat. Rev. Immunol.* 13 (10), 709–721. doi:10.1038/nri3520

Moore, K. J., and Tabas, I. (2011). Macrophages in the pathogenesis of atherosclerosis. *Cell.* 145 (3), 341–355. doi:10.1016/j.cell.2011.04.005

Moran, N. E., Mohn, E. S., Hason, N., Erdman, J. W., and Johnson, E. J. (2018). Intrinsic and extrinsic factors impacting absorption, metabolism, and health effects of dietary carotenoids. *Adv. Nutr.* 9 (4), 465–492. doi:10.1093/advances/nmy025

Morioka, S., Perry, J. S. A., Raymond, M. H., Medina, C. B., Zhu, Y., Zhao, L., et al. (2018). Efferocytosis induces a novel SLC program to promote glucose uptake and lactate release. *Nature* 563 (7733), 714–718. doi:10.1038/s41586-018-0735-5

Muhammad, T., Ikram, M., Ullah, R., Rehman, S. U., and Kim, M. O. (2019). Hesperetin, a citrus flavonoid, attenuates LPS-induced neuroinflammation, apoptosis and memory impairments by modulating TLR4/NF-κB signaling. *Nutrients* 11 (3), 648. doi:10.3390/nu11030648

Mulder, W. J. M., Ochando, J., Joosten, L. A. B., Fayad, Z. A., and Netea, M. G. (2019). Therapeutic targeting of trained immunity. *Nat. Rev. Drug Discov.* 18 (7), 553–566. doi:10.1038/s41573-019-0025-4

Nah, S. Y., Kim, D. H., and Rhim, H. (2007). Ginsenosides: Are any of them candidates for drugs acting on the central nervous system? *CNS Drug Rev.* 13 (4), 381–404. doi:10.1111/j.1527-3458.2007.00023.x

Nam, G. S., and Nam, K-S. (2020). Arctigenin attenuates platelet activation and clot retraction by regulation of thromboxane A2 synthesis and cAMP pathway. *Biomed. Pharmacother.* 130, 110535. doi:10.1016/j.biopha.2020.110535

Napoli, C., de Nigris, F., Williams-Ignarro, S., Pignalosa, O., Sica, V., and Ignarro, L. J. (2006). Nitric oxide and atherosclerosis: An update. *Nitric Oxide* 15 (4), 265–279. doi:10.1016/j.niox.2006.03.011

Napolitano, M., De Pascale, C., Wheeler-Jones, C., Botham, K. M., and Bravo, E. (2007). Effects of lycopene on the induction of foam cell formation by modified LDL. *Am. J. Physiol. Endocrinol. Metab.* 293 (6), E1820–E1827. doi:10.1152/ajpendo.00315.2007

Nelson, K. M., Dahlin, J. L., Bisson, J., Graham, J., Pauli, G. F., and Walters, M. A. (2017). The essential medicinal chemistry of curcumin. *J. Med. Chem.* 60 (5), 1620–1637. doi:10.1021/acs.jmedchem.6b00975

Netea, M. G., Domínguez-Andrés, J., Barreiro, L. B., Chavakis, T., Divangahi, M., Fuchs, E., et al. (2020). Defining trained immunity and its role in health and disease. *Nat. Rev. Immunol.* 20 (6), 375–388. doi:10.1038/s41577-020-0285-6

Neumann, H. P. H., and Young, W. F., Jr. (2019). Pheochromocytoma and paraganglioma. *N. Engl. J. Med.* 381 (6), 552–565. doi:10.1056/NEJMra1806651

Newman, D. J., and Cragg, G. M. (2020). Natural products as sources of new drugs over the nearly four decades from 01/1981 to 09/2019. *J. Nat. Prod.* 83 (3), 770–803. doi:10.1021/acs.jnatprod.9b01285

Ni, S. Y., Zhong, X. L., Li, Z. H., Huang, D. J., Xu, W. T., Zhou, Y., et al. (2020). Puerarin alleviates lipopolysaccharide-induced myocardial fibrosis by inhibiting PARP-1 to prevent HMGB1-mediated TLR4-NF-κb signaling pathway. *Cardiovasc Toxicol.* 20 (5), 482–491. doi:10.1007/s12012-020-09571-9

Niu, L., Luo, R., Zou, M., Sun, Y., Fu, Y., Wang, Y., et al. (2020). Puerarin inhibits Mycoplasma gallisepticum (MG-HS)-induced inflammation and apoptosis via suppressing the TLR6/MyD88/NF-κB signal pathway in chicken. *Int. Immunopharmacol.* 88, 106993. doi:10.1016/j.intimp.2020.106993

Nogara, L., Naber, N., Pate, E., Canton, M., Reggiani, C., and Cooke, R. (2016). Piperine's mitigation of obesity and diabetes can be explained by its up-regulation of the metabolic rate of resting muscle. *Proc. Natl. Acad. Sci. U. S. A.* 113 (46), 13009–13014. doi:10.1073/pnas.1607536113

Noh, K., Oh do, G., Nepal, M. R., Jeong, K. S., Choi, Y., Kang, M. J., et al. (2016). Pharmacokinetic interaction of chrysin with caffeine in rats. *Biomol. Ther. Seoul.* 24 (4), 446–452. doi:10.4062/biomolther.2015.197

Ono, K. (2018). Alzheimer's disease as oligomeropathy. *Neurochem. Int.* 119, 57–70. doi:10.1016/j.neuint.2017.08.010

Pajak, B., Siwiak, E., Sołtyka, M., Priebe, A., Zielinski, R., Fokt, I., et al. (2019). 2-Deoxy-d-Glucose and its analogs: From diagnostic to therapeutic agents. *Int. J. Mol. Sci.* 21 (1), 234. doi:10.3390/ijms21010234

Palozza, P., Simone, R., Catalano, A., Parrone, N., Monego, G., and Ranelletti, F. O. (2011). Lycopene regulation of cholesterol synthesis and efflux in human macrophages. *J. Nutr. Biochem.* 22 (10), 971–978. doi:10.1016/j.jnutbio.2010.08.010

Pan, J., Jin, J. L., Ge, H. M., Yin, K. l., Chen, X., Han, L. j., et al. (2015). Malibatol A regulates microglia M1/M2 polarization in experimental stroke in a PPARγ-dependent manner. *J. Neuroinflammation* 12, 51. doi:10.1186/s12974-015-0270-3

Parathath, S., Grauer, L., Huang, L. S., Sanson, M., Distel, E., Goldberg, I. J., et al. (2011). Diabetes adversely affects macrophages during atherosclerotic plaque regression in mice. *Diabetes* 60 (6), 1759–1769. doi:10.2337/db10-0778

Park, D. W., Baek, K., Kim, J. R., Lee, J. J., Ryu, S. H., Chin, B. R., et al. (2009). Resveratrol inhibits foam cell formation via NADPH oxidase 1- mediated reactive oxygen species and monocyte chemotactic protein-1. *Exp. Mol. Med.* 41 (3), 171–179. doi:10.3858/emm.2009.41.3.020

Park, S. H., Kim, J. L., Lee, E. S., Han, S. Y., Gong, J. H., Kang, M. K., et al. (2011). Dietary ellagic acid attenuates oxidized LDL uptake and stimulates cholesterol efflux in murine macrophages. *J. Nutr.* 141 (11), 1931–1937. doi:10.3945/jn.111.144816

Park, U. H., Hwang, J. T., Youn, H., Kim, E. J., and Um, S. J. (2019). Piperine inhibits adipocyte differentiation via dynamic regulation of histone modifications. *Phytother. Res.* 33 (9), 2429–2439. doi:10.1002/ptr.6434

Persico, G., Casciaro, F., Marinelli, A., Tonelli, C., Petroni, K., and Giorgio, M. (2021). Comparative analysis of histone H3K4me3 distribution in mouse liver in different diets reveals the epigenetic efficacy of cyanidin-3-O-glucoside dietary intake. *Int. J. Mol. Sci.* 22 (12), 6503. doi:10.3390/ijms22126503

Peterson, J., Dwyer, J., Adlercreutz, H., Scalbert, A., Jacques, P., and McCullough, M. L. (2010). Dietary lignans: Physiology and potential for cardiovascular disease risk reduction. *Nutr. Rev.* 68 (10), 571–603. doi:10.1111/j.1753-4887.2010.00319.x

Pillai, V. B., Samant, S., Sundaresan, N. R., Raghuraman, H., Kim, G., Bonner, M. Y., et al. (2015). Honokiol blocks and reverses cardiac hypertrophy in mice by activating mitochondrial Sirt3. *Nat. Commun.* 6, 6656. doi:10.1038/ncomms7656

Porrini, L., Cybulski, L. E., Altabe, S. G., Mansilla, M. C., and de Mendoza, D. (2014). Cerulenin inhibits unsaturated fatty acids synthesis in Bacillus subtilis by modifying the input signal of DesK thermosensor. *Microbiologyopen* 3 (2), 213–224. doi:10.1002/mbo3.154

Qiao, L., Zhang, X., Liu, M., Liu, X., Dong, M., Cheng, J., et al. (2017). Ginsenoside Rb1 enhances atherosclerotic plaque stability by improving autophagy and lipid metabolism in macrophage foam cells. *Front. Pharmacol.* 8, 727. doi:10.3389/fphar.2017.00727

Quintin, J., Saeed, S., Martens, J. H. A., Giamarellos-Bourboulis, E. J., Ifrim, D. C., Logie, C., et al. (2012). Candida albicans infection affords protection against reinfection via functional reprogramming of monocytes. *Cell. Host Microbe* 12 (2), 223–232. doi:10.1016/j.chom.2012.06.006

Rašković, A., Stilinović, N., Kolarović, J., Vasovic, V., Vukmirovic, S., and Mikov, M. (2011). The protective effects of silymarin against doxorubicin-induced cardiotoxicity and hepatotoxicity in rats. *Molecules* 16 (10), 8601–8613. doi:10.3390/molecules16108601

Renner, K., Singer, K., Koehl, G. E., Geissler, E. K., Peter, K., Siska, P. J., et al. (2017). Metabolic hallmarks of tumor and immune cells in the tumor microenvironment. *Front. Immunol.* 8, 248. doi:10.3389/fimmu.2017.00248

Ridker, P. M., Everett, B. M., Thuren, T., MacFadyen, J. G., Chang, W. H., Ballantyne, C., et al. (2017). Antiinflammatory therapy with canakinumab for atherosclerotic disease. *N. Engl. J. Med.* 377 (12), 1119–1131. doi:10.1056/NEJMoa1707914

Riham, I. E-G., Gaber, S. A. A., and Nasr, M. (2019). Polymeric nanocapsular baicalin: Chemometric optimization, physicochemical characterization and mechanistic anticancer approaches on breast cancer cell lines. *Sci. Rep.* 9 (1), 11064. doi:10.1038/s41598-019-47586-7

Rodriguez, A. E., Ducker, G. S., Billingham, L. K., Martinez, C. A., Mainolfi, N., Suri, V., et al. (2019). Serine metabolism supports macrophage IL-1β production. *Cell. Metab.* 29 (4), 1003–1011. doi:10.1016/j.cmet.2019.01.014

Rong, Z. J., Cai, H. H., Wang, H., Liu, G. H., Zhang, Z. W., Chen, M., et al. (2022). Ursolic acid ameliorates spinal cord injury in mice by regulating gut microbiota and metabolic changes. *Front. Cell. Neurosci.* 16, 872935. doi:10.3389/fncel.2022.872935

Rosa, A., Caprioglio, D., Isola, R., Appendino, G., and Falchi, A. M. (2019). Dietary zerumbone from shampoo ginger: New insights into its antioxidant and anticancer activity. *Food Funct.* 10 (3), 1629–1642. doi:10.1039/c8fo02395f

Russo, M., Spagnuolo, C., Tedesco, I., Bilotto, S., and Russo, G. L. (2012). The flavonoid quercetin in disease prevention and therapy: Facts and fancies. *Biochem. Pharmacol.* 83 (1), 6–15. doi:10.1016/j.bcp.2011.08.010

Saeed, S., Quintin, J., Kerstens, H. H., Rao, N. A., Aghajanirefah, A., Matarese, F., et al. (2014). Epigenetic programming of monocyte-to-macrophage differentiation and trained innate immunity. *Science* 345 (6204), 1251086. doi:10.1126/science.1251086

Salunkhe, R., Gadgoli, C., Naik, A., and Patil, N. (2021). Pharmacokinetic profile and oral bioavailability of diosgenin, charantin, and hydroxychalcone from a polyherbal formulation. *Front. Pharmacol.* 12, 629272. doi:10.3389/fphar.2021.629272

Santana-Gálvez, J., Cisneros-Zevallos, L., and Jacobo-Velázquez, D. A. (2017). Chlorogenic acid: Recent advances on its dual role as a food additive and a nutraceutical against metabolic syndrome. *Molecules* 22 (3), 358. doi:10.3390/molecules22030358

Saqib, U., Sarkar, S., Suk, K., Mohammad, O., Baig, M. S., and Savai, R. (2018). Phytochemicals as modulators of M1-M2 macrophages in inflammation. *Oncotarget* 9 (25), 17937–17950. doi:10.18632/oncotarget.24788

Sarrazy, V., Viaud, M., Westerterp, M., Ivanov, S., Giorgetti-Peraldi, S., Guinamard, R., et al. (2016). Disruption of Glut1 in hematopoietic stem cells prevents myelopoiesis and enhanced glucose flux in atheromatous plaques of ApoE(-/-) mice. *Circ. Res.* 118 (7), 1062–1077. doi:10.1161/circresaha.115.307599

`Sarubbo, F., Moranta, D., Asensio, V. J., Miralles, A., and Esteban, S. (2017). Effects of resveratrol and other polyphenols on the most common brain age-related diseases. *Curr. Med. Chem.* 24 (38), 4245–4266. doi:10.2174/0929867324666170724102743

Saz-Leal, P., Del Fresno, C., Brandi, P., Martinez-Cano, S., Dungan, O. M., Chisholm, J. D., et al. (2018). Targeting SHIP-1 in myeloid cells enhances trained immunity and boosts response to infection. *Cell. Rep.* 25 (5), 1118–1126. doi:10.1016/j.celrep.2018.09.092

Scalbert, A., Manach, C., Morand, C., Remesy, C., and Jimenez, L. (2005). Dietary polyphenols and the prevention of diseases. *Crit. Rev. Food Sci. Nutr.* 45 (4), 287–306. doi:10.1080/1040869059096

Schrader, C., Ernst, I. M., Sinnecker, H., Soukup, S. T., Kulling, S. E., and Rimbach, G. (2012). Genistein as a potential inducer of the anti-atherogenic enzyme paraoxonase-1: Studies in cultured hepatocytes *in vitro* and in rat liver *in vivo*. *J. Cell. Mol. Med.* 16 (10), 2331–2341. doi:10.1111/j.1582-4934.2012.01542.x

Schwartz, K., Lawn, R. M., and Wade, D. P. (2000). ABC1 gene expression and ApoA-I-mediated cholesterol efflux are regulated by LXR. *Biochem. Biophys. Res. Commun.* 274 (3), 794–802. doi:10.1006/bbrc.2000.3243

Secretan, P. H., Thirion, O., Sadou Yayé, H., Damy, T., Astier, A., Paul, M., et al. (2021). Simple approach to enhance green tea epigallocatechin gallate stability in aqueous solutions and bioavailability: Experimental and theoretical characterizations. *Pharm. (Basel)* 14 (12), 1242. doi:10.3390/ph14121242

Sharifiyan, F., Movahedian-Attar, A., Nili, N., and Asgary, S. (2016). Study of pomegranate (Punica granatum L.) peel extract containing anthocyanins on fatty streak formation in the renal arteries in hypercholesterolemic rabbits. *Adv. Biomed. Res.* 5, 8. doi:10.4103/2277-9175.175241

Sheedy, F. J., Grebe, A., Rayner, K. J., Kalantari, P., Ramkhelawon, B., Carpenter, S. B., et al. (2013). CD36 coordinates NLRP3 inflammasome activation by facilitating intracellular nucleation of soluble ligands into particulate ligands in sterile inflammation. *Nat. Immunol.* 14 (8), 812–820. doi:10.1038/ni.2639

Sheehan, A. L., Carrell, S., Johnson, B., Stanic, B., Banfi, B., and Miller, F. J. (2011). Role for Nox1 NADPH oxidase in atherosclerosis. *Atherosclerosis* 216 (2), 321–326. doi:10.1016/j.atherosclerosis.2011.02.028

Shirai, T., Nazarewicz, R. R., Wallis, B. B., Yanes, R. E., Watanabe, R., Hilhorst, M., et al. (2016). The glycolytic enzyme PKM2 bridges metabolic and inflammatory dysfunction in coronary artery disease. *J. Exp. Med.* 213 (3), 337–354. doi:10.1084/jem.20150900

Simental-Mendía, L. E., and Guerrero-Romero, F. (2019). Effect of resveratrol supplementation on lipid profile in subjects with dyslipidemia: A randomized double-blind, placebo-controlled trial. *Nutrition* 58, 7–10. doi:10.1016/j.nut.2018.06.015

Sohrabi, Y., Lagache, S. M. M., Schnack, L., Godfrey, R., Kahles, F., Bruemmer, D., et al. (2018). mTOR-dependent oxidative stress regulates oxLDL-induced trained innate immunity in human monocytes. *Front. Immunol.* 9, 3155. doi:10.3389/fimmu.2018.03155

Song, I. S., Nam, S. J., Jeon, J. H., Park, S. J., and Choi, M. K. (2021). Enhanced bioavailability and efficacy of silymarin solid dispersion in rats with acetaminophen-induced hepatotoxicity. *Pharmaceutics* 13 (5), 628. doi:10.3390/pharmaceutics13050628

Song, S., Gao, K., Niu, R., Wang, J., Zhang, J., Gao, C., et al. (2020). Inclusion complexes between chrysin and amino-appended β-cyclodextrins (ACDs): Binding behavior, water solubility, *in vitro* antioxidant activity and cytotoxicity. *Mater Sci. Eng. C Mater Biol. Appl.* 106, 110161. doi:10.1016/j.msec.2019.110161

Song, X., Gong, Z., Liu, K., Kou, J., and Liu, B. (2020). Baicalin combats glutamate excitotoxicity via protecting glutamine synthetase from ROS-induced 20S proteasomal degradation. *Redox Biol.* 34, 101559. doi:10.1016/j.redox.2020.101559

Sosić-Jurjević, B., Filipović, B., Ajdzanović, V., Brkic, D., Ristic, N., Stojanoski, M. M., et al. (2007). Subcutaneously administrated genistein and daidzein decrease serum cholesterol and increase triglyceride levels in male middle-aged rats. *Exp. Biol. Med. (Maywood)* 232 (9), 1222–1227. doi:10.3181/0703-bc-82

Srinivasan, K. (2007). Black pepper and its pungent principle-piperine: A review of diverse physiological effects. *Crit. Rev. Food Sci. Nutr.* 47 (8), 735–748. doi:10.1080/10408390601062054

Stiekema, L. C. A., Prange, K. H. M., Hoogeveen, R. M., Verweij, S. L., Kroon, J., Schnitzler, J. G., et al. (2020). Potent lipoprotein(a) lowering following apolipoprotein(a) antisense treatment reduces the pro-inflammatory activation of circulating monocytes in patients with elevated lipoprotein(a). *Eur. Heart J.* 41 (24), 2262–2271. doi:10.1093/eurheartj/ehaa171

Stompor-Gorący, M., and Machaczka, M. (2021). Recent advances in biological activity, new formulations and prodrugs of ferulic acid. *Int. J. Mol. Sci.* 22 (23), 12889. doi:10.3390/ijms222312889

Stumpf, C., Fan, Q., Hintermann, C., Raaz, D., Kurfurst, I., Losert, S., et al. (2013). Anti-inflammatory effects of danshen on human vascular endothelial cells in culture. *Am. J. Chin. Med.* 41 (5), 1065–1077. doi:10.1142/s0192415x13500729

Su, C. C., Wang, S. C., Chen, I. C., Chiu, F. Y., Liu, P. L., Huang, C. H., et al. (2021). Zerumbone suppresses the LPS-induced inflammatory response and represses activation of the NLRP3 inflammasome in macrophages. *Front. Pharmacol.* 12, 652860. doi:10.3389/fphar.2021.652860

Sun, F., Yang, X., Ma, C., Zhang, S., Yu, L., Lu, H., et al. (2021). The effects of diosgenin on hypolipidemia and its underlying mechanism: A review. *Diabetes Metab. Syndr. Obes.* 14, 4015–4030. doi:10.2147/dmso.S326054

Sun, J., Wei, S., Zhang, Y., and Li, J. (2021). Protective effects of Astragalus polysaccharide on sepsis-induced acute kidney injury. *Anal. Cell. Pathol. (Amst)* 2021, 7178253. doi:10.1155/2021/7178253

Sun, L., Li, E., Wang, F., Wang, T., Qin, Z., Niu, S., et al. (2015). Quercetin increases macrophage cholesterol efflux to inhibit foam cell formation through activating PPARγ-ABCA1 pathway. *Int. J. Clin. Exp. Pathol.* 8 (9), 10854–10860.

Sun, Y., Lu, Y., Saredy, J., Wang, X., Drummer Iv, C., Shao, Y., et al. (2020). ROS systems are a new integrated network for sensing homeostasis and alarming stresses in organelle metabolic processes. *Redox Biol.* 37, 101696. doi:10.1016/j.redox.2020.101696

Szabó, R., Rácz, C. P., and Dulf, F. V. (2022). Bioavailability improvement strategies for icariin and its derivates: A review. *Int. J. Mol. Sci.* 23 (14), 7519. doi:10.3390/ijms23147519

Tabas, I., and Bornfeldt, K. E. (2020). Intracellular and intercellular aspects of macrophage immunometabolism in atherosclerosis. *Circ. Res.* 126 (9), 1209–1227. doi:10.1161/circresaha.119.315939

Tall, A. R., and Yvan-Charvet, L. (2015). Cholesterol, inflammation and innate immunity. *Nat. Rev. Immunol.* 15 (2), 104–116. doi:10.1038/nri3793

Tang, F. T., Cao, Y., Wang, T. Q., Wang, L. J., Guo, J., Zhou, X. S., et al. (2011). Tanshinone IIA attenuates atherosclerosis in ApoE(-/-) mice through down-regulation of scavenger receptor expression. *Eur. J. Pharmacol.* 650 (1), 275–284. doi:10.1016/j.ejphar.2010.07.038

Tang, Y., Wa, Q., Peng, L., Zheng, Y., Chen, J., Chen, X., et al. (2022). Salvianolic acid B suppresses ER stress-induced NLRP3 inflammasome and pyroptosis via the AMPK/FoxO4 and syndecan-4/rac1 signaling pathways in human endothelial progenitor cells. *Oxid. Med. Cell. Longev.* 2022, 8332825. doi:10.1155/2022/8332825

Tardif, J. C., Kouz, S., Waters, D. D., Bertrand, O. F., Diaz, R., Maggioni, A. P., et al. (2019). Efficacy and safety of low-dose colchicine after myocardial infarction. *N. Engl. J. Med.* 381 (26), 2497–2505. doi:10.1056/NEJMoa1912388

Tawakol, A., Singh, P., Mojena, M., Pimentel-Santillana, M., Emami, H., MacNabb, M., et al. (2015). HIF-1α and PFKFB3 mediate a tight relationship between proinflammatory activation and anerobic metabolism in atherosclerotic macrophages. *Arterioscler. Thromb. Vasc. Biol.* 35 (6), 1463–1471. doi:10.1161/atvbaha.115.305551

Tomoda, H., Kawaguchi, A., Omura, S., and Okuda, S. (1984). Cerulenin resistance in a cerulenin-producing fungus. II. Characterization of fatty acid synthetase from Cephalosporium caerulens. *J. Biochem.* 95 (6), 1705–1712. doi:10.1093/oxfordjournals.jbchem.a134784

Trichard, L., Fattal, E., Besnard, M., and Bochot, A. (2007). Alpha-cyclodextrin/oil beads as a new carrier for improving the oral bioavailability of lipophilic drugs. *J. Control Release* 122 (1), 47–53. doi:10.1016/j.jconrel.2007.06.004

Ui, M., Okada, T., Hazeki, K., and Hazeki, O. (1995). Wortmannin as a unique probe for an intracellular signalling protein, phosphoinositide 3-kinase. *Trends Biochem. Sci.* 20 (8), 303–307. doi:10.1016/s0968-0004(00)89056-8

Um, M. Y., Ahn, J., and Ha, T. Y. (2013). Hypolipidaemic effects of cyanidin 3-glucoside rich extract from black rice through regulating hepatic lipogenic enzyme activities. *J. Sci. Food Agric.* 93 (12), 3126–3128. doi:10.1002/jsfa.6070

Uto-Kondo, H., Ayaori, M., Ogura, M., Nakaya, K., Ito, M., Suzuki, A., et al. (2010). Coffee consumption enhances high-density lipoprotein-mediated cholesterol efflux in macrophages. *Circ. Res.* 106 (4), 779–787. doi:10.1161/circresaha.109.206615

Van den Bossche, J., Baardman, J., Otto, N. A., van der Velden, S., Neele, A. E., van den Berg, S. M., et al. (2016). Mitochondrial dysfunction prevents repolarization of inflammatory macrophages. *Cell. Rep.* 17 (3), 684–696. doi:10.1016/j.celrep.2016.09.008

van der Heijden, C., Groh, L., Keating, S. T., Kaffa, C., Noz, M. P., Kersten, S., et al. (2020). Catecholamines induce trained immunity in monocytes *in vitro* and *in vivo*. *Circ. Res.* 127 (2), 269–283. doi:10.1161/circresaha.119.315800

van der Heijden, C., Keating, S. T., Groh, L., Joosten, L. A. B., Netea, M. G., and Riksen, N. P. (2020). Aldosterone induces trained immunity: The role of fatty acid synthesis. *Cardiovasc Res.* 116 (2), 317–328. doi:10.1093/cvr/cvz137

van der Heijden, C., Smeets, E. M. M., Aarntzen, E., Noz, M. P., Monajemi, H., Kersten, S., et al. (2020). Arterial wall inflammation and increased hematopoietic activity in patients with primary aldosteronism. *J. Clin. Endocrinol. Metab.* 105 (5), e1967–e1980. doi:10.1210/clinem/dgz306

van der Heijden, C. D. C. C., Keating, S. T., Groh, L., Joosten, L. A. B., Netea, M. G., and Riksen, N. P. (2019). Aldosterone induces trained immunity: The role of fatty acid synthesis. *Cardiovasc. Res.* 116 (2), 317–328. doi:10.1093/cvr/cvz137

van der Heijden, C. D. C. C., Keating, S. T., Groh, L., Joosten, L. A. B., Netea, M. G., and Riksen, N. P. (2020). Aldosterone induces trained immunity: The role of fatty acid synthesis. *Cardiovasc. Res.* 116 (2), 317–328. doi:10.1093/cvr/cvz137

van der Valk, F. M., Bekkering, S., Kroon, J., Yeang, C., Van den Bossche, J., van Buul, J. D., et al. (2016). Oxidized phospholipids on lipoprotein(a) elicit arterial wall inflammation and an inflammatory monocyte response in humans. *Circulation* 134 (8), 611–624. doi:10.1161/circulationaha.116.020838

Vasamsetti, S. B., Karnewar, S., Gopoju, R., Gollavilli, P. N., Narra, S. R., Kumar, J. M., et al. (2016). Resveratrol attenuates monocyte-to-macrophage differentiation and associated inflammation via modulation of intracellular GSH homeostasis: Relevance in atherosclerosis. *Free Radic. Biol. Med.* 96, 392–405. doi:10.1016/j.freeradbiomed.2016.05.003

Verma, D., Parasa, V. R., Raffetseder, J., Martis, M., Mehta, R. B., Netea, M., et al. (2017). Anti-mycobacterial activity correlates with altered DNA methylation pattern in immune cells from BCG-vaccinated subjects. *Sci. Rep.* 7 (1), 12305. doi:10.1038/s41598-017-12110-2

Višnjić, D., Lalić, H., Dembitz, V., Tomić, B., and Smoljo, T. (2021). AICAr, a widely used AMPK activator with important AMPK-independent effects: A systematic review. *Cells* 10 (5), 1095. doi:10.3390/cells10051095

Wallace, C., and Keast, D. (1992). Glutamine and macrophage function. *Metabolism* 41 (9), 1016–1020. doi:10.1016/0026-0495(92)90130-3

Wang, C. Y., Yen, C. C., Hsu, M. C., and Wu, Y. T. (2020). Self-nanoemulsifying drug delivery systems for enhancing solubility, permeability, and bioavailability of sesamin. *Molecules* 25 (14), 3119. doi:10.3390/molecules25143119

Wang, D., Wei, X., Yan, X., Jin, T., and Ling, W. (2010). Protocatechuic acid, a metabolite of anthocyanins, inhibits monocyte adhesion and reduces atherosclerosis in apolipoprotein E-deficient mice. *J. Agric. Food Chem.* 58 (24), 12722–12728. doi:10.1021/jf103427j

Wang, F., Shan, Q., Chang, X., Li, Z., and Gui, S. (2021). Paeonol-loaded PLGA nanoparticles as an oral drug delivery system: Design, optimization and evaluation. *Int. J. Pharm.* 602, 120617. doi:10.1016/j.ijpharm.2021.120617

Wang, L., Bao, Y., Yang, Y., Wu, Y., Chen, X., Si, S., et al. (2010). Discovery of antagonists for human scavenger receptor CD36 via an ELISA-like high-throughput screening assay. *J. Biomol. Screen* 15 (3), 239–250. doi:10.1177/1087057109359686

Wang, L., Palme, V., Rotter, S., Schilcher, N., Cukaj, M., Wang, D., et al. (2017). Piperine inhibits ABCA1 degradation and promotes cholesterol efflux from THP-1-derived macrophages. *Mol. Nutr. Food Res.* 61 (4), 1500960. doi:10.1002/mnfr.201500960

Wang, L., Rotter, S., Ladurner, A., Heiss, E. H., Oberlies, N. H., Dirsch, V. M., et al. (2015). Silymarin constituents enhance ABCA1 expression in THP-1 macrophages. *Molecules* 21 (1), E55. doi:10.3390/molecules21010055

Wang, M., Subramanian, M., Abramowicz, S., Murphy, A. J., Gonen, A., Witztum, J., et al. (2014). Interleukin-3/granulocyte macrophage colony-stimulating factor receptor promotes stem cell expansion, monocytosis, and atheroma macrophage burden in mice with hematopoietic ApoE deficiency. *Arterioscler. Thromb. Vasc. Biol.* 34 (5), 976–984. doi:10.1161/atvbaha.113.303097

Wang, P., He, L. Y., Shen, G. D., and Yang, J. L. (2017). Inhibitory effects of Dioscin on atherosclerosis and foam cell formation in hyperlipidemia rats. *Inflammopharmacology* 25 (6), 633–642. doi:10.1007/s10787-017-0341-4

Wang, S., Zhang, X., Liu, M., Luan, H., Ji, Y., Guo, P., et al. (2015). Chrysin inhibits foam cell formation through promoting cholesterol efflux from RAW264.7 macrophages. *Pharm. Biol.* 53 (10), 1481–1487. doi:10.3109/13880209.2014.986688

Wang, Y., Tong, Q., Ma, S. R., Zhao, Z. X., Pan, L. B., Cong, L., et al. (2021). Oral berberine improves brain dopa/dopamine levels to ameliorate Parkinson's disease by regulating gut microbiota. *Signal Transduct. Target Ther.* 6 (1), 77. doi:10.1038/s41392-020-00456-5

Wang, Y., Wang, Y. S., Song, S. L., Liang, H., and Ji, A. G. (2016). Icariin inhibits atherosclerosis progress in Apoe null mice by downregulating CX3CR1 in macrophage. *Biochem. Biophys. Res. Commun.* 470 (4), 845–850. doi:10.1016/j.bbrc.2016.01.118

Wang, Y., Wen, J., Almoiliqy, M., Wang, Y., Liu, Z., Yang, X., et al. (2021). Sesamin protects against and ameliorates rat intestinal ischemia/reperfusion injury with involvement of activating Nrf2/HO-1/NQO1 signaling pathway. *Oxid. Med. Cell. Longev.* 2021, 5147069. doi:10.1155/2021/5147069

Wang, Y., Zhang, Y., Wang, X., Liu, Y., and Xia, M. (2012). Cyanidin-3-O-β-glucoside induces oxysterol efflux from endothelial cells: Role of liver X receptor alpha. *Atherosclerosis* 223 (2), 299–305. doi:10.1016/j.atherosclerosis.2012.06.004

Wang, Y. F., Yang, X. F., Cheng, B., Mei, C. L., Li, Q. X., Xiao, H., et al. (2010). Protective effect of Astragalus polysaccharides on ATP binding cassette transporter A1 in THP-1 derived foam cells exposed to tumor necrosis factor-alpha. *Phytother. Res.* 24 (3), 393–398. doi:10.1002/ptr.2958

Wang, Z., Liu, Y., Xue, Y., Hu, H., Ye, J., Li, X., et al. (2016). Berberine acts as a putative epigenetic modulator by affecting the histone code. *Toxicol Vitro* 36, 10–17. doi:10.1016/j.tiv.2016.06.004

Wang, Z., Qi, F., Cui, Y., Zhao, L., Sun, X., Tang, W., et al. (2018). An update on Chinese herbal medicines as adjuvant treatment of anticancer therapeutics. *Biosci. Trends* 12 (3), 220–239. doi:10.5582/bst.2018.01144

Wenzel, E., and Somoza, V. (2005). Metabolism and bioavailability of trans-resveratrol. *Mol. Nutr. Food Res.* 49 (5), 472–481. doi:10.1002/mnfr.200500010

Willecke, F., Yuan, C., Oka, K., Chan, L., Hu, Y., Barnhart, S., et al. (2015). Effects of high fat feeding and diabetes on regression of atherosclerosis induced by low-density lipoprotein receptor gene therapy in LDL receptor-deficient mice. *PLoS One* 10 (6), e0128996. doi:10.1371/journal.pone.0128996

Wu, C., Luan, H., Zhang, X., Wang, S., Zhang, X., Sun, X., et al. (2014). Chlorogenic acid protects against atherosclerosis in ApoE-/- mice and promotes cholesterol efflux from RAW264.7 macrophages. *PLoS One* 9 (9), e95452. doi:10.1371/journal.pone.0095452

Wu, D., Li, S., Liu, X., Xu, J., Jiang, A., Zhang, Y., et al. (2020). Alpinetin prevents inflammatory responses in OVA-induced allergic asthma through modulating PI3K/AKT/NF-κB and HO-1 signaling pathways in mice. *Int. Immunopharmacol.* 89 (1), 107073. doi:10.1016/j.intimp.2020.107073

Wu, M., Liu, M., Guo, G., Zhang, W., and Liu, L. (2015). Polydatin inhibits formation of macrophage-derived foam cells. *Evid. Based Complement. Altern. Med.* 2015, 729017. doi:10.1155/2015/729017

Wu, R., Wang, L., Yin, R., Hudlikar, R., Li, S., Kuo, H. D., et al. (2020). Epigenetics/epigenomics and prevention by curcumin of early stages of inflammatory-driven colon cancer. *Mol. Carcinog.* 59 (2), 227–236. doi:10.1002/mc.23146

Wu, S., Xu, H., Peng, J., Wang, C., Jin, Y., Liu, K., et al. (2015). Potent anti-inflammatory effect of dioscin mediated by suppression of TNF-α-induced VCAM-1, ICAM-1and EL expression via the NF-κB pathway. *Biochimie* 110, 62–72. doi:10.1016/j.biochi.2014.12.022

Wu, W. H., Wang, S. H., KuanII, Kao, Y. S., Wu, P. J., Liang, C. J., et al. (2010). Sesamin attenuates intercellular cell adhesion molecule-1 expression *in vitro* in TNF-alpha-treated human aortic endothelial cells and *in vivo* in apolipoprotein-E-deficient mice. *Mol. Nutr. Food Res.* 54 (9), 1340–1350. doi:10.1002/mnfr.200900271

Xia, X., Ling, W., Ma, J., Xia, M., Hou, M., Wang, Q., et al. (2006). An anthocyanin-rich extract from black rice enhances atherosclerotic plaque stabilization in apolipoprotein E-deficient mice. *J. Nutr.* 136 (8), 2220–2225. doi:10.1093/jn/136.8.2220

Xiao, M., Yang, H., Xu, W., Ma, S., Lin, H., Zhu, H., et al. (2012). Inhibition of 03B1-KG-dependent histone and DNA demethylases by fumarate and succinate that are accumulated in mutations of FH and SDH tumor suppressors. *Genes Dev.* 26 (12), 1326–1338. doi:10.1101/gad.191056.112

Xu, C., Wang, W., Wang, B., Zhang, T., Cui, X., Pu, Y., et al. (2019). Analytical methods and biological activities of Panax notoginseng saponins: Recent trends. *J. Ethnopharmacol.* 236, 443–465. doi:10.1016/j.jep.2019.02.035

Xu, X., Li, Q., Pang, L., Huang, G., Huang, J., Shi, M., et al. (2013). Arctigenin promotes cholesterol efflux from THP-1 macrophages through PPAR-γ/LXR-α signaling pathway. *Biochem. Biophys. Res. Commun.* 441 (2), 321–326. doi:10.1016/j.bbrc.2013.10.050

Xu, Y., Liu, Q., Xu, Y., Liu, C., Wang, X., He, X., et al. (2014). Rutaecarpine suppresses atherosclerosis in ApoE-/- mice through upregulating ABCA1 and SR-BI within RCT. *J. Lipid Res.* 55 (8), 1634–1647. doi:10.1194/jlr.M044198

Xue, X. L., Han, X. D., Li, Y., Chu, X. F., Miao, W. M., Zhang, J. L., et al. (2017). Astaxanthin attenuates total body irradiation-induced hematopoietic system injury in

mice via inhibition of oxidative stress and apoptosis. *Stem Cell. Res. Ther.* 8 (1), 7. doi:10.1186/s13287-016-0464-3

Yang, J., Wu, M., Fang, H., Su, Y., Zhang, L., and Zhou, H. (2021). Puerarin prevents acute liver injury via inhibiting inflammatory responses and ZEB2 expression. *Front. Pharmacol.* 12, 727916. doi:10.3389/fphar.2021.727916

Yang, S. H., Liao, C. C., Chen, Y., Syu, J. P., Jeng, C. J., and Wang, S. M. (2012). Daidzein induces neuritogenesis in DRG neuronal cultures. *J. Biomed. Sci.* 19 (1), 80. doi:10.1186/1423-0127-19-80

Yang, Y., Fuentes, F., Shu, L., Wang, C., Pung, D., Li, W., et al. (2017). Epigenetic CpG methylation of the promoter and reactivation of the expression of GSTP1 by astaxanthin in human prostate LNCaP cells. *Aaps J.* 19 (2), 421–430. doi:10.1208/s12248-016-0016-x

Yang, Y., Jiang, W., Wang, L., Zhang, Z. B., Si, S. Y., and Hong, B. (2009). Characterization of the isoflavone pratensein as a novel transcriptional up-regulator of scavenger receptor class B type I in HepG2 cells. *Biol. Pharm. Bull.* 32 (7), 1289–1294. doi:10.1248/bpb.32.1289

Ye, W., Lin, X., Zhang, Y., Xu, Y., Sun, R., Wen, C., et al. (2018). Quantification and pharmacokinetics of alpinetin in rat plasma by UHPLC-MS/MS using protein precipitation coupled with dilution approach to eliminate matrix effects. *J. Pharm. Biomed. Anal.* 152, 242–247. doi:10.1016/j.jpba.2017.12.046

Yin, H., Guo, Q., Li, X., Tang, T., Li, C., Wang, H., et al. (2018). Curcumin suppresses IL-1β secretion and prevents inflammation through inhibition of the NLRP3 inflammasome. *J. Immunol.* 200 (8), 2835–2846. doi:10.4049/jimmunol.1701495

Yu, W., Wang, Z., Zhang, K., Chi, Z., Xu, T., Jiang, D., et al. (2019). One-carbon metabolism supports S-adenosylmethionine and histone methylation to drive inflammatory macrophages. *Mol. Cell.* 75 (6), 1147–1160. doi:10.1016/j.molcel.2019.06.039

Yuan, X., Chen, J., and Dai, M. (2016). Paeonol promotes microRNA-126 expression to inhibit monocyte adhesion to ox-LDL-injured vascular endothelial cells and block the activation of the PI3K/Akt/NF-κB pathway. *Int. J. Mol. Med.* 38 (6), 1871–1878. doi:10.3892/ijmm.2016.2778

Yuan, Z., Liao, Y., Tian, G., Li, H., Jia, Y., Zhang, H., et al. (2011). Panax notoginseng saponins inhibit Zymosan A induced atherosclerosis by suppressing integrin expression, FAK activation and NF-κB translocation. *J. Ethnopharmacol.* 138 (1), 150–155. doi:10.1016/j.jep.2011.08.066

Yue, J., Li, B., Jing, Q., and Guan, Q. (2015). Salvianolic acid B accelerated ABCA1-dependent cholesterol efflux by targeting PPAR-γ and LXRα. *Biochem. Biophys. Res. Commun.* 462 (3), 233–238. doi:10.1016/j.bbrc.2015.04.122

Zaheer, K., and Humayoun Akhtar, M. (2017). An updated review of dietary isoflavones: Nutrition, processing, bioavailability and impacts on human health. *Crit. Rev. Food Sci. Nutr.* 57 (6), 1280–1293. doi:10.1080/10408398.2014.989958

Zarzour, A., Kim, H. W., and Weintraub, N. L. (2019). Epigenetic regulation of vascular diseases. *Arterioscler. Thromb. Vasc. Biol.* 39 (6), 984–990. doi:10.1161/atvbaha.119.312193

Zhan, J., Yan, Z., Kong, X., Liu, J., Lin, Z., Qi, W., et al. (2021). Lycopene inhibits IL-1β-induced inflammation in mouse chondrocytes and mediates murine osteoarthritis. *J. Cell. Mol. Med.* 25 (7), 3573–3584. doi:10.1111/jcmm.16443

Zhang, F., Xia, Y., Yan, W., Zhang, H., Zhou, F., Zhao, S., et al. (2016). Sphingosine 1-phosphate signaling contributes to cardiac inflammation, dysfunction, and remodeling following myocardial infarction. *Am. J. Physiology-Heart Circulatory Physiology* 310 (2), H250–H261. doi:10.1152/ajpheart.00372.2015

Zhang, J., Nie, S., Zu, Y., Abbasi, M., Cao, J., Li, C., et al. (2019). Anti-atherogenic effects of CD36-targeted epigallocatechin gallate-loaded nanoparticles. *J. Control Release* 303, 263–273. doi:10.1016/j.jconrel.2019.04.018

Zhang, Q., Liu, J., Duan, H., Li, R., Peng, W., and Wu, C. (2021). Activation of Nrf2/HO-1 signaling: An important molecular mechanism of herbal medicine in the treatment of atherosclerosis via the protection of vascular endothelial cells from oxidative stress. *J. Adv. Res.* 34, 43–63. doi:10.1016/j.jare.2021.06.023

Zhang, T., Guo, S., Zhu, X., Qiu, J., Deng, G., and Qiu, C. (2020). Alpinetin inhibits breast cancer growth by ROS/NF-κB/HIF-1α axis. *J. Cell. Mol. Med.* 24 (15), 8430–8440. doi:10.1111/jcmm.15371

Zhang, X., Chen, S., Duan, F., Liu, A., Li, S., Zhong, W., et al. (2021). Prebiotics enhance the biotransformation and bioavailability of ginsenosides in rats by modulating gut microbiota. *J. Ginseng Res.* 45 (2), 334–343. doi:10.1016/j.jgr.2020.08.001

Zhao, G., Zhang, X., Wang, H., and Chen, Z. (2020). Beta carotene protects H9c2 cardiomyocytes from advanced glycation end product-induced endoplasmic reticulum stress, apoptosis, and autophagy via the PI3K/Akt/mTOR signaling pathway. *Ann. Transl. Med.* 8 (10), 647. doi:10.21037/atm-20-3768

Zhao, G. J., Tang, S. L., Lv, Y. C., Ouyang, X. P., He, P. P., Yao, F., et al. (2013). Antagonism of betulinic acid on LPS-mediated inhibition of ABCA1 and cholesterol efflux through inhibiting nuclear factor-kappaB signaling pathway and miR-33 expression. *PLoS One* 8 (9), e74782. doi:10.1371/journal.pone.0074782

Zhao, J. F., Ching, L. C., Huang, Y. C., Chen, C. Y., Chiang, A. N., Kou, Y. R., et al. (2012). Molecular mechanism of curcumin on the suppression of cholesterol accumulation in macrophage foam cells and atherosclerosis. *Mol. Nutr. Food Res.* 56 (5), 691–701. doi:10.1002/mnfr.201100735

Zhao, J. F., Jim Leu, S. J., Shyue, S. K., Su, K. H., Wei, J., and Lee, T. S. (2013). Novel effect of paeonol on the formation of foam cells: Promotion of lxrα-ABCA1-dependent cholesterol efflux in macrophages. *Am. J. Chin. Med.* 41 (5), 1079–1096. doi:10.1142/s0192415x13500730

Zhao, L., Wei, Y., Huang, Y., He, B., Zhou, Y., and Fu, J. (2013). Nanoemulsion improves the oral bioavailability of baicalin in rats: *In vitro* and *in vivo* evaluation. *Int. J. Nanomedicine* 8, 3769–3779. doi:10.2147/ijn.S51578

Zhao, S., Li, J., Wang, L., and Wu, X. (2016). Pomegranate peel polyphenols inhibit lipid accumulation and enhance cholesterol efflux in raw264.7 macrophages. *Food Funct.* 7 (7), 3201–3210. doi:10.1039/c6fo00347h

Zhao, X., Wang, H., Yang, Y., Gou, Y., Wang, Z., Yang, D., et al. (2021). Protective effects of silymarin against D-gal/LPS-induced organ damage and inflammation in mice. *Drug Des. Devel Ther.* 15, 1903–1914. doi:10.2147/dddt.S305033

Zhao, Y., Lin, S., Fang, R., Shi, Y., Wu, W., Zhang, W., et al. (2022). Mechanism of enhanced oral absorption of a nano-drug delivery system loaded with trimethyl chitosan derivatives. *Int. J. Nanomedicine* 17, 3313–3324. doi:10.2147/ijn.S358832

Zheng, X. Y., Yang, S. M., Zhang, R., Wang, S. M., Li, G. B., and Zhou, S. W. (2019). Emodin-induced autophagy against cell apoptosis through the PI3K/AKT/mTOR pathway in human hepatocytes. *Drug Des. Devel Ther.* 13, 3171–3180. doi:10.2147/dddt.S204958

Zhou, J., Yu, Y., Yang, X., Wang, Y., Song, Y., Wang, Q., et al. (2019). Berberine attenuates arthritis in adjuvant-induced arthritic rats associated with regulating polarization of macrophages through AMPK/NF-κB pathway. *Eur. J. Pharmacol.* 852, 179–188. doi:10.1016/j.ejphar.2019.02.036

Zhou, L., Hu, X., Han, C., Niu, X., Han, L., Yu, H., et al. (2022). Comprehensive investigation on the metabolism of emodin both *in vivo* and *in vitro*. *J. Pharm. Biomed. Anal.* 223, 115122. doi:10.1016/j.jpba.2022.115122

Zhou, M., Xu, H., Pan, L., Wen, J., Guo, Y., and Chen, K. (2008). Emodin promotes atherosclerotic plaque stability in fat-fed apolipoprotein E-deficient mice. *Tohoku J. Exp. Med.* 215 (1), 61–69. doi:10.1620/tjem.215.61

Zhu, S., and Liu, J. H. (2015). Zerumbone, A natural cyclic sesquiterpene, promotes ABCA1-dependent cholesterol efflux from human THP-1 macrophages. *Pharmacology* 95 (5-6), 258–263. doi:10.1159/000381722

Zhu, Z., Hu, R., Li, J., Xing, X., Chen, J., Zhou, Q., et al. (2021). Alpinetin exerts anti-inflammatory, anti-oxidative and anti-angiogenic effects through activating the Nrf2 pathway and inhibiting NLRP3 pathway in carbon tetrachloride-induced liver fibrosis. *Int. Immunopharmacol.* 96, 107660. doi:10.1016/j.intimp.2021.107660

Zolberg Relevy, N., Bechor, S., Harari, A., Ben-Amotz, A., Kamari, Y., Harats, D., et al. (2015). The inhibition of macrophage foam cell formation by 9-cis β-carotene is driven by BCMO1 activity. *PLoS One* 10 (1), e0115272. doi:10.1371/journal.pone.0115272

Glossary

ASCVD atherosclerotic cardiovascular diseases
AS atherosclerosis
ABCA1 ATP-binding cassette transporter A1
APS *Astragalus* polysaccharides
ATRA all-trans retinoic acid
AMD age-related macular degeneration
ABCG1 ATP-binding cassette transporter G1
ATP adenosine triphosphate
AMPK AMP-activated protein kinase
AP-1 activating protein-1
BCG bacille Calmette–Guérin
BA betulinic acid
BC β-carotene
BBR berberine
CA chlorogenic acid
CD36 cluster of differentiation 36
CAD coronary artery disease
CoA acetyl coenzyme A
CCL2 chemokine C–C motif ligand 2
CVD cardiovascular diseases
C3G Cyanidin-3-O-glucoside
chrysin 5,7-dihydroxyflavone
CARM1 coactivator-associated arginine methyltransferase 1
ceRNA competing endogenous RNA
DAMP damage-associated molecular pattern
DNMTs DNA methyltransferases
EGCG epigallocatechin-3-gallate
EA ellagic acid
FAO fatty acid oxidation
FAS fatty acid synthase
FAK focal adhesion kinase
GM-CSF granulocyte–macrophage colony-stimulating factor
GS glutamine synthetase
GVHD graft-versus-host disease
HATi histone acetyltransferase inhibitor
HATs histone acetyltransferases
HDACs histone deacetylases
HDL-C HDL-cholesterol
HFD high-fat diet
HDL High-density lipoprotein
HSCs hematopoietic stem cells
HMG-CoA 3-hydroxy-3-methylglutaryl-coenzyme A
H3K4me3 histone H3 lysine 4 trimethylation
HIF-1α hyperoxia-inducible substance 1α
HK-II hexokinase II
H3K27ac histone 3 lysine 27 acetylation
H3K4me1 histone 3 lysine 4 methylation
hesperidin 3′,5,7,-trihydroxy-4′-methoxyflavanone
H3K4me2/3 H3K4 di- and tri-methylation
HDAC1–2 histone deacetylase 1–2
HPC hematopoietic progenitor cell
HMDMs human peripheral blood monocyte-derived macrophages
H3K27m3 H3K27 trimethylation
iNOS
inducible nitric oxide synthase
IL interleukin
ICAM-1 intercellular adhesion molecule 1
JNK c-Jun N-terminal kinases
LDL low-density lipoprotein
LDs lipid droplets
LXR liver X receptor
LPS lipopolysaccharide
lncRNAs long non-coding RNAs
LDL-C LDL-cholesterol
MCP-1 monocyte chemoattractant protein-1
MMP-2 matrix metalloproteinases 2
m5C methylate cytosine
mTOR mammalian target of rapamycin
MSCs mesenchymal stem cells
NLRP3
NOD-, LRR-, and pyrin domain-containing protein 3
NO nitric oxide
Nox1 NADPH oxidase 1
oxLDL oxidized LDL
OXPHOS oxidative phosphorylation
oxPAPC oxidized phospholipids made of 1-palmitoyl-2-arachidonoyl-sn-glycero-3-phosphorylcholine
PPARγ peroxisome proliferator-activated receptor γ
PPP pentose phosphate pathway
PFKFB3 6-phosphofructo-2-kinase/fructo-2, 6-bisphosphatase
PDK1 pyruvate dehydrogenase kinase isozyme 1
PI3K phosphoinositide 3-kinase
PON-1 paraoxonase-1
PEA pomegranate ellagic acid
PCSK9 proprotein convertase subtilisin/kexin type 9
PCA protocatechuic acid
PNS *Panax notoginseng* saponins
quercetin
3,3',4',5,7-pentahydroxyflavone
RXR retinoid X receptor

ROS reactive oxygen species
Runx1 Runt-related transcription factor 1
RCT reverse cholesterol transport
RV resveratrol
RARs retinoic acid receptors
SalB salvianolic acid B
SAM S-adenosylmethionine
SR-A type A scavenger receptor
SR-BI scavenger receptor class B type I
SDH succinate dehydrogenase
STK11 serine/threonine kinase 11
TNF-α tumor necrosis factor-α
TCA cycle tricarboxylic acid cycle
TLR4 Toll-like receptor 4
TC total cholesterol
TMAO trimethylamine N-oxide
Tan IIA tanshinone IIA
ursolic acid
3B-hydroxy-12-urc-12-en-28-oic acid
9-cis-RA
9-cis retinoic acid
VCAM-1 vascular cell adhesion molecule 1
VSMCs vascular smooth muscle cells
WTD Western-style diet
WDR5 WD repeat-containing protein 5
2-DG
2-deoxy-d-glucose
2-DG6P
2-deoxy-d-glucose-6-phosphate.

frontiers | Frontiers in Pharmacology

TYPE Original Research
PUBLISHED 01 March 2023
DOI 10.3389/fphar.2023.1092473

OPEN ACCESS

EDITED BY
Pallavi R. Devchand,
University of Calgary, Canada

REVIEWED BY
Emi Dika,
University of Bologna, Italy
Xin Tong,
Northwestern University, United States

*CORRESPONDENCE
Yiya Zhang,
yiya0108@csu.edu.cn
Ji Li,
liji_xy@csu.edu.cn

SPECIALTY SECTION
This article was submitted to Inflammation Pharmacology, a section of the journal Frontiers in Pharmacology

RECEIVED 29 November 2022
ACCEPTED 13 February 2023
PUBLISHED 01 March 2023

CITATION
Zhou L, Zhong Y, Wang Y, Deng Z, Huang Y, Wang Q, Xie H, Zhang Y and Li J (2023), EGCG identified as an autophagy inducer for rosacea therapy. *Front. Pharmacol.* 14:1092473. doi: 10.3389/fphar.2023.1092473

EGCG identified as an autophagy inducer for rosacea therapy

Lei Zhou[1,2], Yun Zhong[1,2], Yaling Wang[1,2], Zhili Deng[1,2,3], Yingxue Huang[1,2], Qian Wang[4], Hongfu Xie[1,2,3], Yiya Zhang[1,2,3]* and Ji Li[1,2,3]*

[1]Department of Dermatology, Xiangya Hospital, Central South University, Changsha, China, [2]Hunan Key Laboratory of Aging Biology, Xiangya Hospital, Central South University, Changsha, China, [3]National Clinical Research Center for Geriatric Disorders, Xiangya Hospital, Central South University, Changsha, China, [4]Hunan Binsis Biotechnology Co, Ltd., Changsha, China

Background: Rosacea is a common facial skin inflammatory disease featured by hyperactivation of mTORC1 signaling in the epidermis. Due to unclear pathogenesis, the effective treatment options for rosacea remain limited.

Methods: Weighted gene co-expression network analysis (WGCNA) analyzed the relationship between epidermis autophagy and mTOR pathways in rosacea, and further demonstrated it through immunofluorescence and qPCR analysis. A potential therapeutic agent for rosacea was predicted based on the key genes of the WGCNA module. *In vivo* and *in vitro* experiments were conducted to verify its therapeutic role. Drug–target prediction (TargetNet, Swiss, and Tcmsp) and molecular docking offered potential pharmacological targets.

Results: WGCNA showed that epidermis autophagy was related to the activation of mTOR pathways in rosacea. Next, autophagy was downregulated in the epidermis of rosacea, which was regulated by mTOR. In addition, the *in vivo* experiment demonstrated that autophagy induction could be an effective treatment strategy for rosacea. Subsequently, based on the key genes of the WGCNA module, epigallocatechin-3-gallate (EGCG) was predicted as a potential therapeutic agent for rosacea. Furthermore, the therapeutic role of EGCG on rosacea was confirmed *in vivo* and *in vitro*. Finally, drug–target prediction and molecular docking revealed that AKT1/MAPK1/MMP9 could be the pharmacological targets of EGCG in rosacea.

Conclusion: Collectively, our findings revealed the vital role of autophagy in rosacea and identified that EGCG, as a therapeutic agent for rosacea, attenuated rosacea-like inflammation *via* inducing autophagy in keratinocytes.

KEYWORDS

rosacea, EGCG, mTOR, autophagy, skin inflammation

Abbreviations: EGCG, epigallocatechin-3-gallate; mTOR, mammalian target of rapamycin; ID, interface dermatitis; AD, atopic dermatitis; GSVA, gene set variation analysis; PFA, paraformaldehyde frozen.

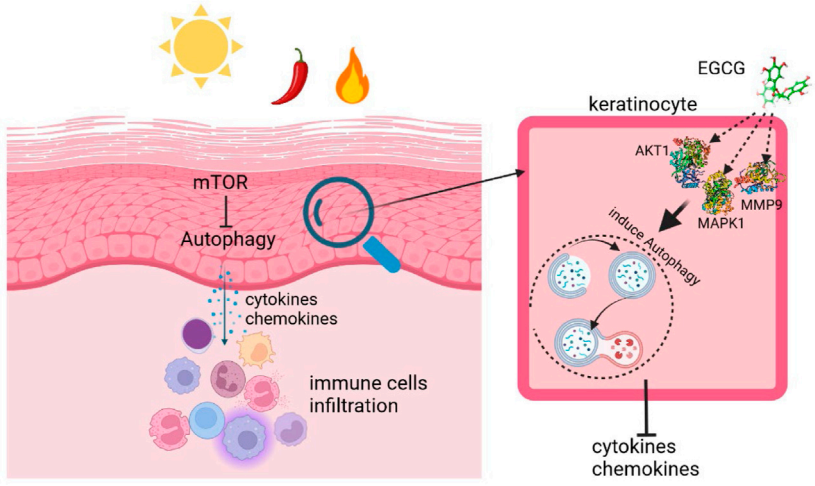

GRAPHICAL ABSTRACT

Background

Rosacea is a common chronic inflammatory skin disorder with a series of features such as facial erythema, telangiectasia, papules, and pustules (Gallo et al., 2018). It significantly impacts the quality of life and affects between 5% and 20% of the population (Gether et al., 2018). The pathogenesis of rosacea is not well understood, but previous studies have shown that the interaction of genetics and a variety of environmental factors may lead to disorders of the skin's immune system, particularly the abnormal production of cathelicidin LL37, leading to chronic inflammation and abnormal vascular responses of rosacea (Steinhoff et al., 2011; Ahn and Huang, 2018; Awosika and Oussedik, 2018). Due to the ambiguous pathophysiological mechanisms, there is still no effective treatment for rosacea.

The mammalian target of the rapamycin (mTOR) pathway is crucial for various biological processes including cell proliferation, apoptosis, metastasis, and angiogenesis (Deng et al., 2015; Fogel et al., 2015). Our previous work verified hyperactivated mTORC1 signaling in rosacea which promotes rosacea skin inflammation (Deng et al., 2021). Meanwhile, topical administration of rapamycin (mTOR inhibitor) ameliorated clinical lesions in rosacea patients (Deng et al., 2021). However, the underlying mechanism of mTOR signaling in rosacea still needs to be elucidated.

Autophagy is a dynamic process that maintains cellular homeostasis during environmental stress stimuli. Dysregulation of autophagy contributes to the pathogenesis of various skin diseases, including allergic contact dermatitis, atopic dermatitis, and psoriasis (Ohsumi, 2014; Cadwell, 2016). It has been reported that autophagy deficiency led to DNA damage and senescence of keratinocytes (Song et al., 2017). A recent study found that autophagy is essential for the activation of keratinocytes in wound healing (Qiang et al., 2021). In addition, autophagy plays a pivotal role in psoriasiform keratinocyte inflammation (Wang Z. et al., 2021). It is well known that mTOR is an important regulator of the autophagy process (Munson and Ganley, 2015). However, little is known about the link between autophagy and rosacea pathogenesis.

Epigallocatechin-3-gallate (EGCG), a natural polyphenol found in green tea, has many biological activities, including anti-inflammatory, antioxidant, cardioprotective, neuroprotective, and anticancer activities (Nan et al., 2019; Yi et al., 2020; Nan et al., 2021). Studies have revealed EGCG as a potential therapeutic agent for various skin inflammation conditions, including psoriasiform dermatitis (Chamcheu et al., 2018), interface dermatitis (ID) (Braegelmann et al., 2022), and atopic dermatitis (AD) (Noh et al., 2008). Although a clinical trial of four healthy volunteers demonstrated the potential anti-angiogenic effect of EGCG cream (Domingo et al., 2010), whether EGCG has a therapeutic effect on rosacea remains unknown.

Here, we revealed that the autophagy of keratinocytes was associated with the aberrant activation of mTOR signals and contributed to the progression of rosacea. Furthermore, we identified EGCG as a therapeutic agent of rosacea and found that it significantly attenuated rosacea inflammation by inducing autophagy in keratinocytes.

Methods

Rosacea transcriptome data

The gene expression array of rosacea (GSE65914) was downloaded from the GEO database. Our previous epidermal transcriptome data (HRA000809) from 18 rosacea tissues and 5 normal skin tissues were downloaded for gene set variation analysis (GSVA).

GSVA

To investigate the activation of mTOR pathways in rosacea, GSVA was performed using "GSVA" R packages.

WGCNA

After removing the low-expressed genes (FPKM<1), the genes with the top 25% largest variance were used for WGCNA with

power (β) = 4 using the "WGCNA" R package as previously described (Li Y. et al., 2021). The genes from modules related to the mTOR pathway with GS > 0.5 were identified as hub genes and used for drug prediction.

Drug prediction

DGIdb (https://dgidb.org/) was used for drug prediction. The predicted drugs with more than two target genes were collected for further analysis (Cotto et al., 2018; Freshour et al., 2021).

Animals

For the experiment, 8-week-old female BALB/c mice were purchased from Shanghai SLAC Laboratory Animal Co., LTD. (Shanghai, China). All studies and experimental procedures were approved by the Animal Ethics Committee of Xiangya Hospital of Central South University (No. 201703211). The rosacea-like mouse model was induced as previously described (Agrahari et al., 2020; Kulkarni et al., 2020). Skin inflammation of the mouse model was evaluated by the severity of erythema and edema as previously described (Deng et al., 2021). For EGCG treatment, BALB/c mice were treated with EGCG at a dose of 80 mg/kg per day for seven constitutive days. For topical bafilomycin A1 (BafA1) treatment, mice were injected intradermally with bafilomycin A1 (100 μM) twice a day for 2 days. The rapamycin treatment was as previously described (Deng et al., 2021).

Cell culture and treatment

HaCaT cells (Biovector Science Lab, Beijing, China) were cultured according to the manufacturer's instructions, and the cells were then treated with different doses of EGCG with or without LL-37 (8 μM). For each experiment, 3-MA (10 μM) or BafA1 (10 nM) was added to HaCaT cells 1 h prior to the EGCG treatment. The cells treated with rapamycin, the mTOR inhibitor, were considered a positive control for this study.

RNA extraction and real-time quantitative PCR (qPCR)

Total RNA was extracted from mouse skin tissue or cells using the Trizol reagent (Invitrogen, United States), and then, cDNA was synthesized using the Maxima H Minus First Strand cDNA Synthesis Kit with dsDNase (Thermo Fisher Scientific, United States). qPCR assay was performed with iTaqTM Universal SYBR® Green Supermix (Bio-Rad, United States) using the CFX Connect Real-Time PCR System (Bio-Rad, United States). qPCR primers are shown in Supplementary Table S1.

Histological analysis

Skin tissues were fixed overnight with 4% formaldehyde, and sections of 4 μm thickness were used for hematoxylin and eosin (H&E) staining as previously described (Xie et al., 2022). All studies and experimental procedures were approved by the Human Ethics Committee of Xiangya Hospital of the Central South University (No. 201703212).

For immunofluorescence, skin tissues were embedded in OCT and sectioned at 8 μm thickness. The sections were washed with PBS, fixed in 4% frozen paraformaldehyde (PFA) for 15 min, and then blocked for 1 h in PBS containing 1% BSA and 0.3% Triton X-100. Primary antibodies were incubated at 4°C overnight. The sections were washed with PBS and incubated with secondary antibodies for 1 h at room temperature. The nuclei were stained with DAPI. All images were taken using a Zeiss fluorescence microscope and analyzed using Zen2 software (Germany). Anti-LC3 (1:200; Sigma-Aldrich, catalog L7543), anti-CD4 (1:100; eBioscience, catalog 12–0043-82), anti-Beclin1 (1:100; Proteintech, catalog 66665-1-Ig), and Alexa Fluor 488-conjugated goat anti-mouse IgG (H + L) cross-adsorbed secondary Ab (1:500; Invitrogen, catalog A-32723) were used.

Cell viability assay

Cell proliferation was evaluated using a Cell Counting Kit-8 assay (Vazyme, Nanjing, China). Briefly, 1×10^3 cells/100 μl/well cells were seeded into 96-well plates. The supernatant was removed 48 h later, and 10 μl of the CCK-8 reagent and 100 μl fresh media were introduced per well and incubated for 2 h at 5% CO_2 and 37°C. Then, the absorbance at 450 nm was measured using the EnSight™ Multimode Plate Reader (PerkinElmer, Waltham, MA).

Immunoblotting

The skin tissues and cells were lysed in RIPA buffer (Thermo Fisher Scientific, United States). Next, the protein was separated by SDS-PAGE and incubated with primary antibodies, including anti-LC3 (1:1,000; Sigma-Aldrich, catalog L7543), anti-GAPDH (1:5,000; Abcam, catalog ab8245), anti-p62 (1:1,000; Cell Signal Technology, catalog 88,588), anti-S6 (1:1,000; Cell Signal Technology, catalog 2317), and anti-pS6 (Ser240/244) (1:1,000; Cell Signal Technology, catalog 5364).

Transmission electron microscopy

Cells were treated and collected by trypsinization and fixed in 2.5% glutaraldehyde for 4 h and then refixed in 1% osmium tetroxide for 2 h. After dehydration using a stepwise ethanol series, the cells were embedded in an embedding medium and then polymerized at 60°C for 2 days. The samples were cut on Leica EM UC6 (Leica, Wetzlar, German) at 80 nm thickness and stained with uranyl acetate and lead citrate. Images were acquired using a transmission electron microscope (Hitachi, Tokyo, Japan).

Ad-mCherry-GFP-LC3 transfection

HaCaT cells were transfected with mCherry-GFP-LC3 adenovirus when they grew to 60%–70% confluence on dishes for 12 h at 37°C. Following treatment with EGCG, LL-37, or BafA1, images were taken using a confocal microscope (Leica, Germany).

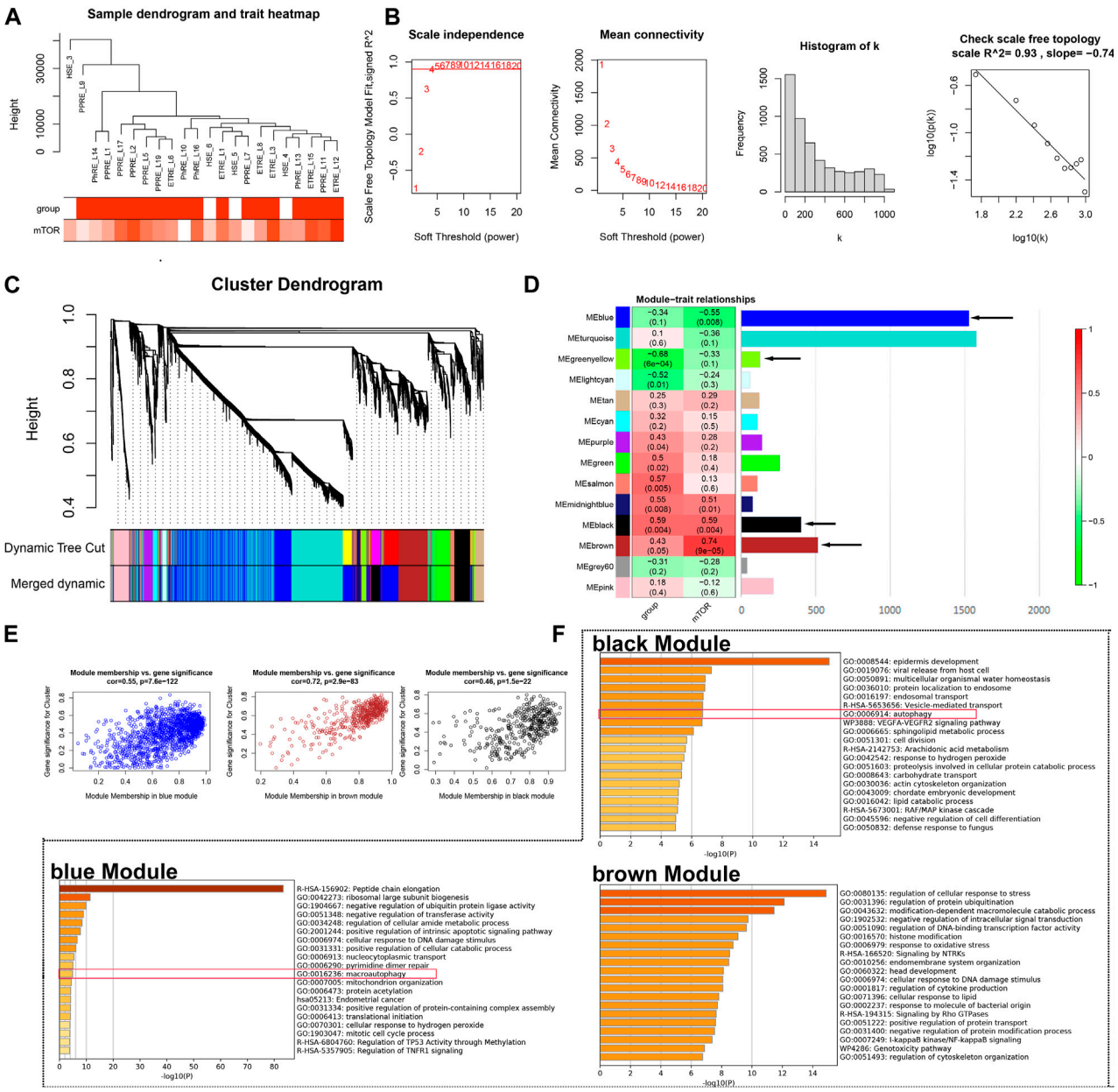

FIGURE 1
WGCNA. **(A)** Sample cluster analysis associated with clinical characters. **(B)** Scale-free fitting index analysis and the mean connectivity for various soft-threshold powers. **(C)** Gene dendrogram and module colors of WGCNA. **(D)** Correlation analysis between modules and clinical characters. **(E)** Relationship between GS and MM in the blue, brown, and black modules. **(F)** GO analysis of genes from blue, brown, and black modules, respectively.

Pharmacological targets of EGCG

We used accessible online tools to predict the potential pharmacological targets of EGCG, including TargetNet, Swiss, and TCMSP (Wishart et al., 2018). Then, the candidate targets were identified using the UniProt database (Li R. et al., 2021).

Molecular docking

The PubChem database (https://pubchem.ncbi.nlm.nih.gov/) was used to obtain the molecular structure of EGCG (CID-65064). The PDB database (https://www.rcsb.org/) was used for the protein structures of AKT1 (6HHG), MAPK1 (6DCG), and MMP9 (6ESM). Maestro software was used for molecular docking (Zhang H. et al., 2021).

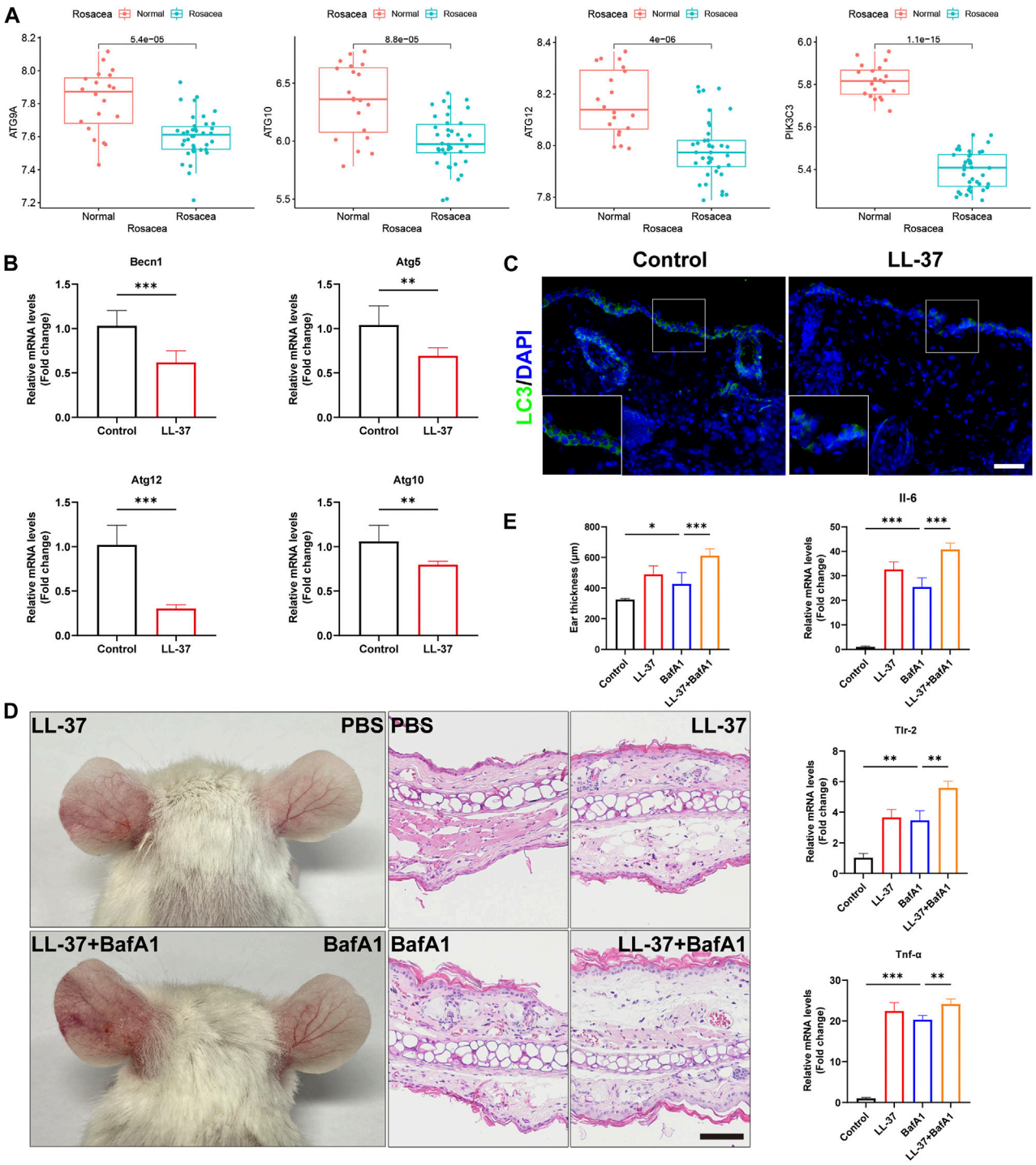

FIGURE 2
Autophagy was reduced in the keratinocytes and aggravated rosacea-like inflammation. **(A)** Expression of the autophagy markers, ATG9A, ATG10, ATG12, and PIK3C3, in the epidermis of rosacea patients and normal subjects. **(B)** mRNA expression levels of Becn1, Atg5, Atg10, and Atg12 in LL-37-induced mouse skin lesions. **(C)** Immunofluorescence analysis of LC3 in skin lesions from control mice and LL37-induced mice. Scale bar: 50 μm. **(D)** Representative images and HE straining of mice injected with BafA1 and/or LL-37 showing erythema on the ear. **(E)** Measurement of the mouse ear thickness. The mRNA expression levels of Il6, Tlr-2, and Tnf-α. (n = 5 for each group). All results are representative of at least three independent experiments. Data represent the mean ± SEM. One-way ANOVA with Bonferroni's *post hoc* test was used for statistical analyses. *$p < 0.05$, **$p < 0.01$, and ***$p < 0.001$.

Statistical analysis

Statistical analysis was conducted with GraphPad Prism (8.0.0) (San Diego, California United States). All data were displayed as the mean ± SEM of three independent experiments. Unpaired Student's t-test was used for the comparison of two groups, and one-way ANOVA followed by Dunnett's test was used for multiple comparisons. The level of statistical significance was set at $p < 0.05$.

Results

WGCNA identified the keratinocyte autophagy associated with the mTOR pathway in rosacea

Our previous study identified the important role of the mTOR pathway in rosacea; however, the potential mechanism remains unknown (Deng et al., 2021). Here, based on our previous epidermis transcriptome data, GSVA identified the activation of the mTOR pathway in rosacea (Supplementary Figure S1). Next, we used WGCNA to identify the rosacea-related and mTOR pathway-related genes in the epidermis of rosacea. A total of 5,278 genes were used for WGCNA, and one abnormality (HSE_3) was removed (Figure 1A). The soft threshold $\beta = 4$ and scale-free $R^2 = 0.93$ are shown in Figure 1B. After merging the similar modules, 14 modules were obtained as shown in Figure 1C. The relationships between the mTOR pathway and modules are shown in Figure 1D. The black module (r = 0.59, $p = 0.004$) and brown module (r = 0.74, P = 9e-5) were positively associated with the mTOR pathway, while the blue module (r = -0.55, $p = 0.008$) was negatively associated with the mTOR pathway. The relationship between GS and MM in black, brown, and blue modules is shown in Figure 1E. The GO enrichment analysis demonstrated that the genes in the blue and black modules were enriched in the autophagy-related signal pathways using Metascape (http://metascape.org/) (Figure 1F). These results indicated that the activated mTOR pathway could affect keratinocytes' autophagy in rosacea.

Autophagy was reduced in the keratinocytes and aggravated rosacea-like inflammation

To determine the roles of autophagy in rosacea, we analyzed the expression levels of the autophagy-related markers in rosacea lesion tissues and normal skin tissues. As shown in Figure 2A and Supplementary Figure S2, the expression of autophagy-related genes (ATG9A, ATG10, ATG12, and PIK3C3) was evidently decreased in rosacea lesions compared with normal skin tissues in the GSE65914 dataset. Immunofluorescence revealed decreased becline1 in the lesioned skin of rosacea patients (Supplementary Figure S3). These results were confirmed in LL-37-induced rosacea-like mouse models. We observed that the mRNA expressions of autophagy-related genes (Becn1, Atg5, Atg10, and Atg12) were decreased in LL-37-induced mouse skin tissue (Figure 2B). The immunofluorescence analysis also revealed that the LC3 expression was much lower in the epidermis of LL-37-induced rosacea-like lesioned skin than in control mouse skin tissues (Figure 2C).

Next, we investigated whether autophagy affects LL-37-induced rosacea-like inflammation. For that, 8-week-old BALB/c female mice were injected intradermally with LL-37 alone, bafilomycin A1 (autophagy inhibitor) alone, or co-injected with both LL-37 and bafilomycin A1. Enhanced ear redness and thickness were observed, accompanied by an increase in Il-6, Tlr-2, and Tnf-α (Figures 2D, E). We also found that Cxcl1, Cxcl15, Cd68, Itgam, Cma1, and Tpsab1 were increased when treated with BafA1 alone or with LL-37 + BafA1 (Supplementary Figure S4). In addition, in our previous studies, we observed that rapamycin, an agonist of autophagy, prevents the development of rosacea-like skin inflammation (Deng et al., 2021). In the present study, we found that the mRNA expression of autophagy-related genes Becn1, Atg5, Atg10, and Atg12 was significantly increased in LL37-induced rosacea lesions after topical rapamycin treatment (Supplementary Figure S5). Altogether, these results demonstrated that autophagy was reduced in keratinocytes of rosacea, and autophagy impairment/improvement aggravated/ameliorated rosacea-like skin inflammation.

EGCG was identified as a candidate drug for rosacea

To investigate the candidate drugs for rosacea, the hub genes from black and blue modules were input into DGIdb. In total, 190 drugs targeting 23 genes from the black module and 77 drugs targeting 15 genes from the blue module were identified, and 28 drugs overlapped (Figure 3A). The Sankey diagram revealed the detailed relationship between hub genes and 28 drugs (Figure 3B). Among them, EGCG has been reported to present anti-inflammatory and immunoregulatory effects and has been increasingly recognized worldwide for its low cost, easy-to-obtain nature, low toxicity, low side effects, and high tolerance. So, EGCG was selected for further study.

EGCG attenuated LL-37-induced rosacea-like dermatitis

We initially investigated the potential therapeutic effect of EGCG on rosacea in an LL-37-induced mouse model. As shown in Figure 4A, EGCG treatment significantly ameliorated the LL37-induced rosacea-like lesions. The average redness area and score were dramatically reduced in the EGCG group compared with the PBS group (Figures 4B, C). Histological analysis showed that treatment with EGCG resulted in the reduction of immune infiltration in the dermis (Figures 4A–D). Meanwhile, EGCG treatment also reduced the expression of pro-inflammatory cytokines, including Il-6, Tlr-2, and Tnf-α in LL-37-induced rosacea-like lesions (Figure 4E). Moreover, EGCG also reduced the expressions of the neutrophil-attracting chemokines (Cxcl15 and Cxcl1), macrophage markers (Cd68 and Itgam), and mast cell-related genes (Tpsab1 and Cma1) in LL-37-induced rosacea-like lesions (Supplementary Figure S6A). The infiltration of $CD4^+$ T cells and the expression of Stat1, Stat3, and IL-17A were repressed by EGCG treatment in rosacea-like mice (Supplementary Figures S6B–D). These results demonstrated the therapeutic effect of EGCG in rosacea-like dermatitis in mice.

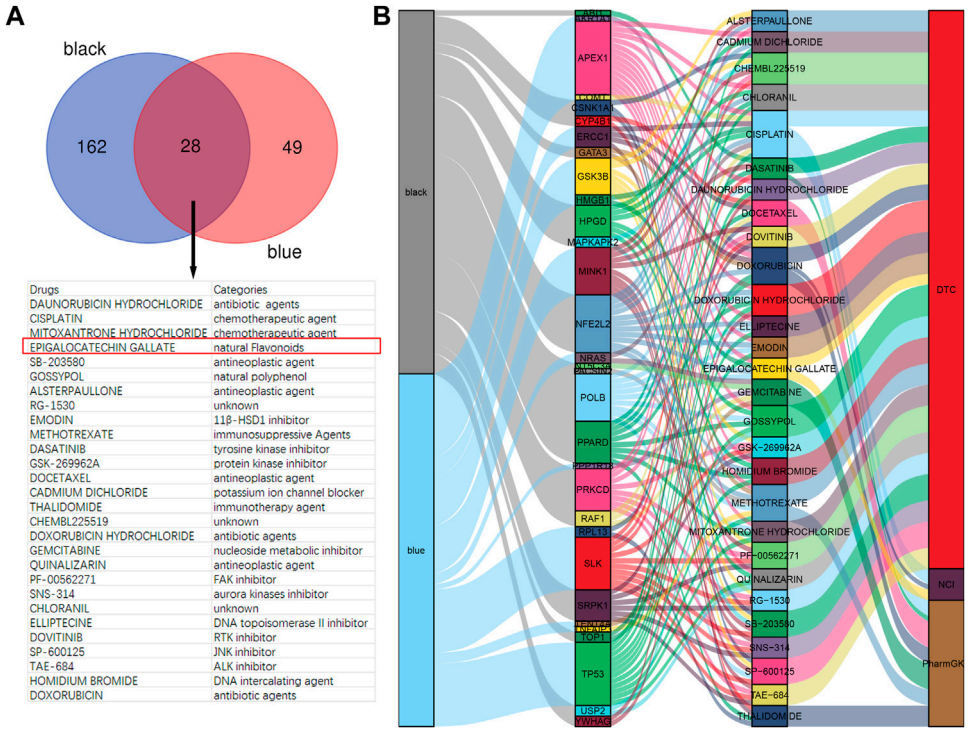

Drugs	Categories
DAUNORUBICIN HYDROCHLORIDE	antibiotic agents
CISPLATIN	chemotherapeutic agent
MITOXANTRONE HYDROCHLORIDE	chemotherapeutic agent
EPIGALOCATECHIN GALLATE	natural Flavonoids
SB-203580	antineoplastic agent
GOSSYPOL	natural polyphenol
ALSTERPAULLONE	antineoplastic agent
RG-1530	unknown
EMODIN	11β-HSD1 inhibitor
METHOTREXATE	immunosuppressive Agents
DASATINIB	tyrosine kinase inhibitor
GSK-269962A	protein kinase inhibitor
DOCETAXEL	antineoplastic agent
CADMIUM DICHLORIDE	potassium ion channel blocker
THALIDOMIDE	immunotherapy agent
CHEMBL225519	unknown
DOXORUBICIN HYDROCHLORIDE	antibiotic agents
GEMCITABINE	nucleoside metabolic inhibitor
QUINALIZARIN	antineoplastic agent
PF-00562271	FAK inhibitor
SNS-314	aurora kinases inhibitor
CHLORANIL	unknown
ELLIPTECINE	DNA topoisomerase II inhibitor
DOVITINIB	RTK inhibitor
SP-600125	JNK inhibitor
TAE-684	ALK inhibitor
HOMIDIUM BROMIDE	DNA intercalating agent
DOXORUBICIN	antibiotic agents

FIGURE 3
EGCG is a candidate drug for rosacea. **(A)** Overlapped drugs predicted by DGIdb. **(B)** Sankey diagram revealed the relationship between modules, hub genes, and drugs.

EGCG decreased LL-37-induced inflammation in keratinocytes

First, we detected the role of EGCG on keratinocytes *in vitro*. We found that the concentrations of 80 μM EGCG repressed the viability of HaCaT cells, and drug concentrations of 10, 20, and 40 μM were chosen in the following cell experiments (Figure 5A). Next, we demonstrated that EGCG treatment reduced LL37-induced TLR-2 and CAMP, the key rosacea markers (Yamasaki et al., 2007; Yamasaki et al., 2011; Zhang J. et al., 2021), and expression in the HaCaT cells (Figure 5B). Considering the pivotal role of keratinocytes in producing excessive pro-inflammatory cytokines and chemokines in the pathogenesis of rosacea (Steinhoff et al., 2011), we demonstrated the inhibitory effects of EGCG on cytokine and chemokine expression in HaCaT cells. The expressions of pro-inflammatory cytokines and chemokines, including CXCL10, CCL20, CCL3, CCL5, CXCL12, and CXCL13, were analyzed using the qPCR assay. All these genes except CCL5 were significantly reduced by EGCG treatment (Figure 5C). Thus, we concluded that EGCG repressed LL-37-induced keratinocyte inflammation.

EGCG reduced rosacea-like inflammation by inducing keratinocyte autophagy

It has been reported that autophagy effectively protects keratinocytes against injury in inflammatory skin diseases (Hou et al., 2020; Kim et al., 2021). To confirm whether the anti-inflammatory effect of EGCG could be due to the induction of autophagy in rosacea, we detected the autophagy levels in rosacea-like mice after EGCG treatment. Here, we found that EGCG could induce keratinocyte autophagy in LL37-induced rosacea-like mice (Figure 6A). Next, we detected the role of EGCG in autophagy in LL37-treated HaCaT cells. The HaCaT cells were treated with 10, 20, and 40 μM EGCG or rapamycin (autophagy agonist) in the presence of LL-37, and subsequent autophagy events were monitored by western blotting. As shown in Figures 6A, B, LC3-I gradually transformed into LC3-II with the increase in EGCG concentration and treatment time. To determine the role of EGCG-induced autophagy in LL37-induced keratinocyte inflammation, BafA1, an autophagy inhibitor, was included in the ensuing studies. qPCR analysis showed that EGCG-repressed pro-inflammatory cytokine and chemokine expression, including CCL3, CCL5, CCL20, CXCL10, CXCL12, and CXCL15, was reversed by BafA1 treatment (Figure 6C).

Meanwhile, to examine whether the mechanism of EGCG on autophagy was due to an increase in the autophagy level and not due to the blocking of autophagy flux, we further analyzed p62 protein expression, which reflects the level of autophagosome clearance and negatively correlates with autophagy (Lamark et al., 2017). After EGCG treatment, there was a significant decrease in the p62 expression level (Figure 6B). EGCG significantly reduced p62 expression but induced LC3-II levels in a dose- and time-dependent manner. Cytoplasmic LC3 puncta formation is the hallmark event of autophagy (Schaaf et al., 2016). Thus, we

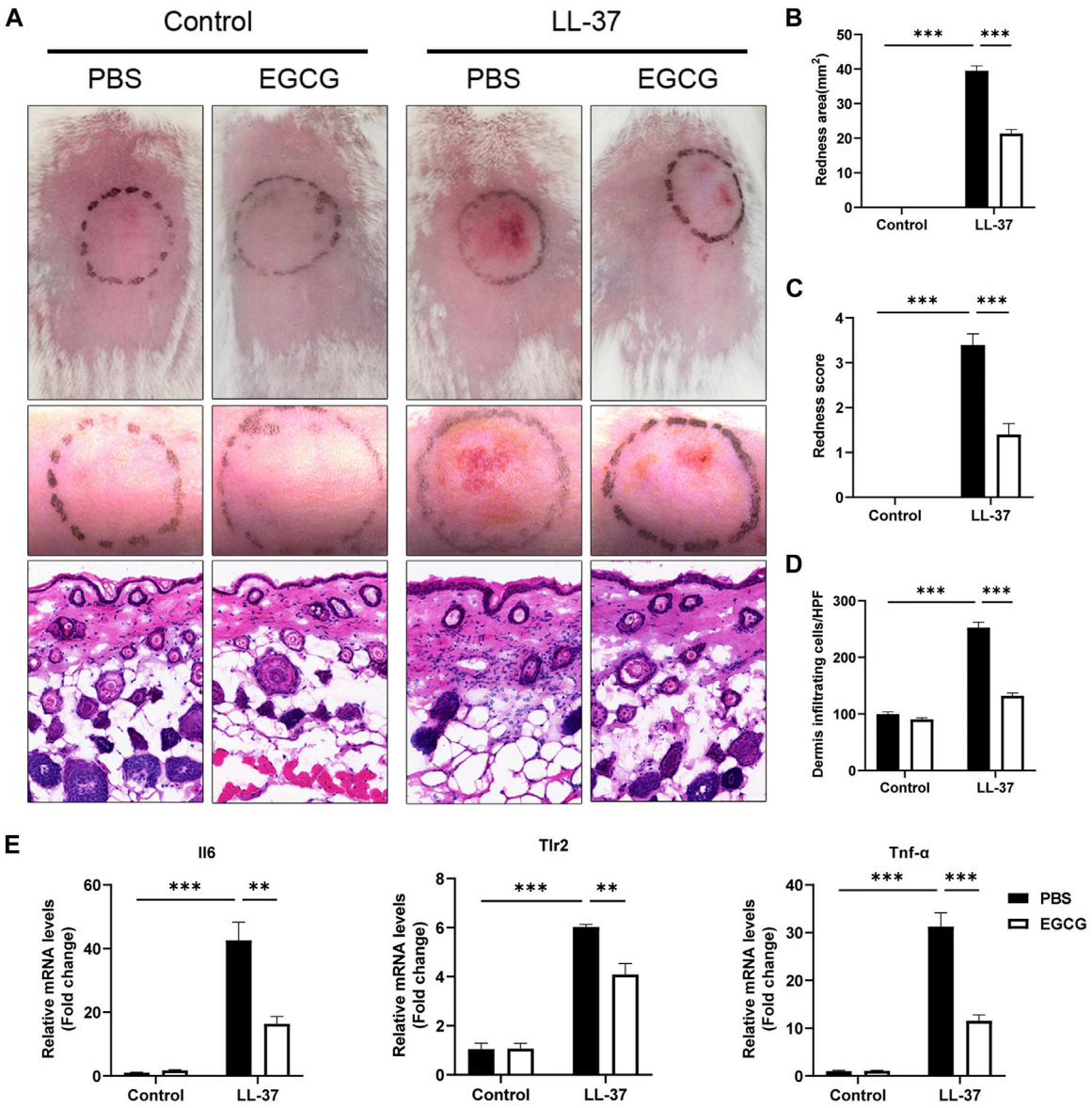

FIGURE 4
Effect of EGCG on LL37-induced rosacea-like mice. **(A)** Skin manifestation of different groups. Images were taken 48 h after the first LL37 administration. Scale bar: 50 μm. The severity of inflammatory responses on the skin was assessed in the redness area **(B)**, redness score **(C)**, and quantitative result of HE staining for dermal cellular infiltrates **(D)**. **(E)** mRNA expression levels of Il6, Tlr2, and TNF-α in skin lesions (n = 5 for each group). All results are representative of at least three independent experiments. Data represent the mean ± SEM. One-way ANOVA with Bonferroni's *post hoc* test was used for statistical analyses. $^{**}p < 0.01$ and $^{***}p < 0.001$.

examined EGCG induction of LC3 puncta formation after treating the HaCaT cells with EGCG by immunofluorescent staining. We observed that LC3 puncta formation was considerably augmented in the EGCG treatment group, while it was reduced in the LL-37-induced HaCaT cells compared with the untreated vehicle control (Figure 7A).

Furthermore, to clarify the correlation between EGCG and autophagy induction, 3-MA and bafilomycin A1 (BafA1), autophagy inhibitors, were employed in the subsequent studies. Immunoblot analysis showed that 3-MA and BafA1 blocked the EGCG-induced conversion of LC3-I to LC3-II, while p62 degradation induced by EGCG was impeded by autophagy inhibitors in LL-37-induced conditions (Figure 7B). Likewise, we found that the HaCaT cells co-treated with EGCG and LL-37 showed abundant autophagolysosomes under transmission electron microscopy. However, in contrast, the cells treated with merely LL-37 or BafA1 showed a limited number of autophagosomes and autophagolysosomes (Figure 7C). Next, tandem mCherry-GFP-LC3 fluorescence microscopy assay and transmission electron microscopy were performed to assess autophagosome and autophagolysosome formation. Our results indicated that the number of autophagosomes (green spots) and autolysosomes (yellow spots) in the EGCG treatment group was significantly increased compared to other groups, which suggested

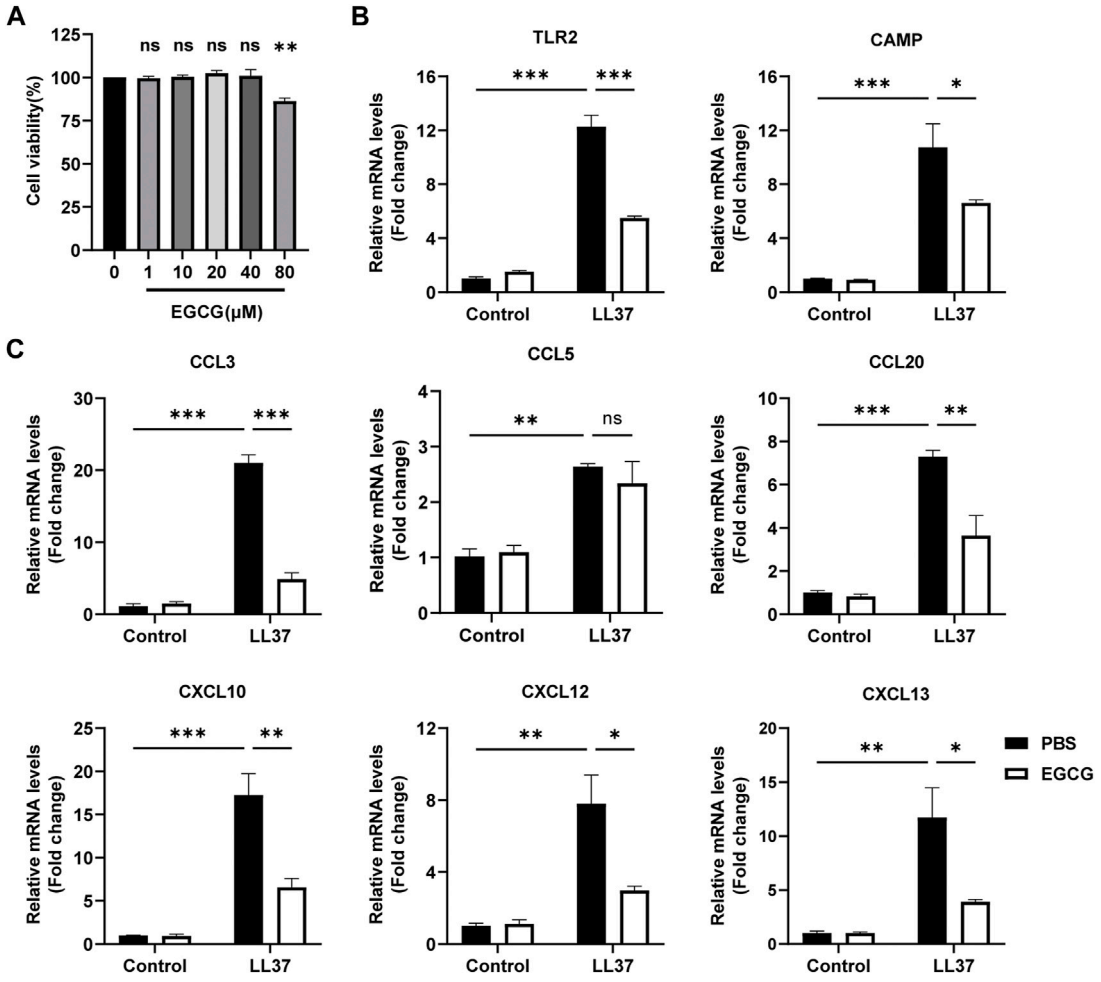

FIGURE 5
EGCG decreased the production of cytokines and chemokines related to rosacea in keratinocytes. **(A)** Effect of different concentrations of EGCG on cell viability is determined by CCK-8 assay. **(B)** mRNA expression levels of TLR2 and CAMP. **(C)** mRNA expression levels of CCL3, CCL5, CCL20, CXCL10, CXCL12, and CXCL13. All results are representative of at least three independent experiments. Data represent the mean ± SEM. One-way ANOVA with Bonferroni's *post hoc* test was used for statistical analyses. *$p < 0.05$, **$p < 0.01$, and ***$p < 0.001$. ns, no significance.

that EGCG enhanced autophagy flux in LL-37-induced HaCaT cells (Figure 7D).

Taken together, these data strongly suggested that EGCG attenuated LL-37-induced inflammation by increasing autophagy induction and autophagy flux in keratinocytes.

ATK1, MAPK1, and MMP9 could be direct targets of EGCG in rosacea

To explore the specific molecular mechanism of EGCG-induced autophagy, three databases (TargetNet, Swiss, and Tcmsp) were used to predict the target of EGCG in rosacea, and 95 target genes were predicted in two or more databases at the same time (Figure 8A). The GO analysis revealed the enrichment of these target genes in rosacea-related, autophagy-related, and mTOR-related pathways (Figures 8B, C). Among them, ATK1, MAPK1, and MMP9 were the key molecules in these pathways. Subsequent molecular docking was used to predict the binding of EGCG to ATK1, MAPK1, and MMP9 (Figure 8D). ATK/MAPK pathways were reported as a regulator of autophagy (Yuan et al., 2022). So, we speculated that EGCG could regulate autophagy by targeting ATK1, MAPK1, and MMP9 in rosacea.

Discussion

Although significant effort is devoted to revealing pathogenesis and developing new therapeutic agents, the current therapeutic strategies for rosacea are still unsatisfactory (Logger et al., 2020; Wang B. et al., 2021; Kim et al., 2022). In this study, we revealed the important role of epidermis autophagy in rosacea and demonstrated EGCG as an effective agent for rosacea treatment, which attenuated rosacea-like inflammation *via* inducing keratinocyte autophagy.

The mTOR pathway is a crucial signal transduction pathway implicated in various physiological and pathological processes (Deng et al., 2015; Fogel et al., 2015). Our previous work demonstrated the important role of hyperactivated mTOR

10.3389/fphar.2023.1092473

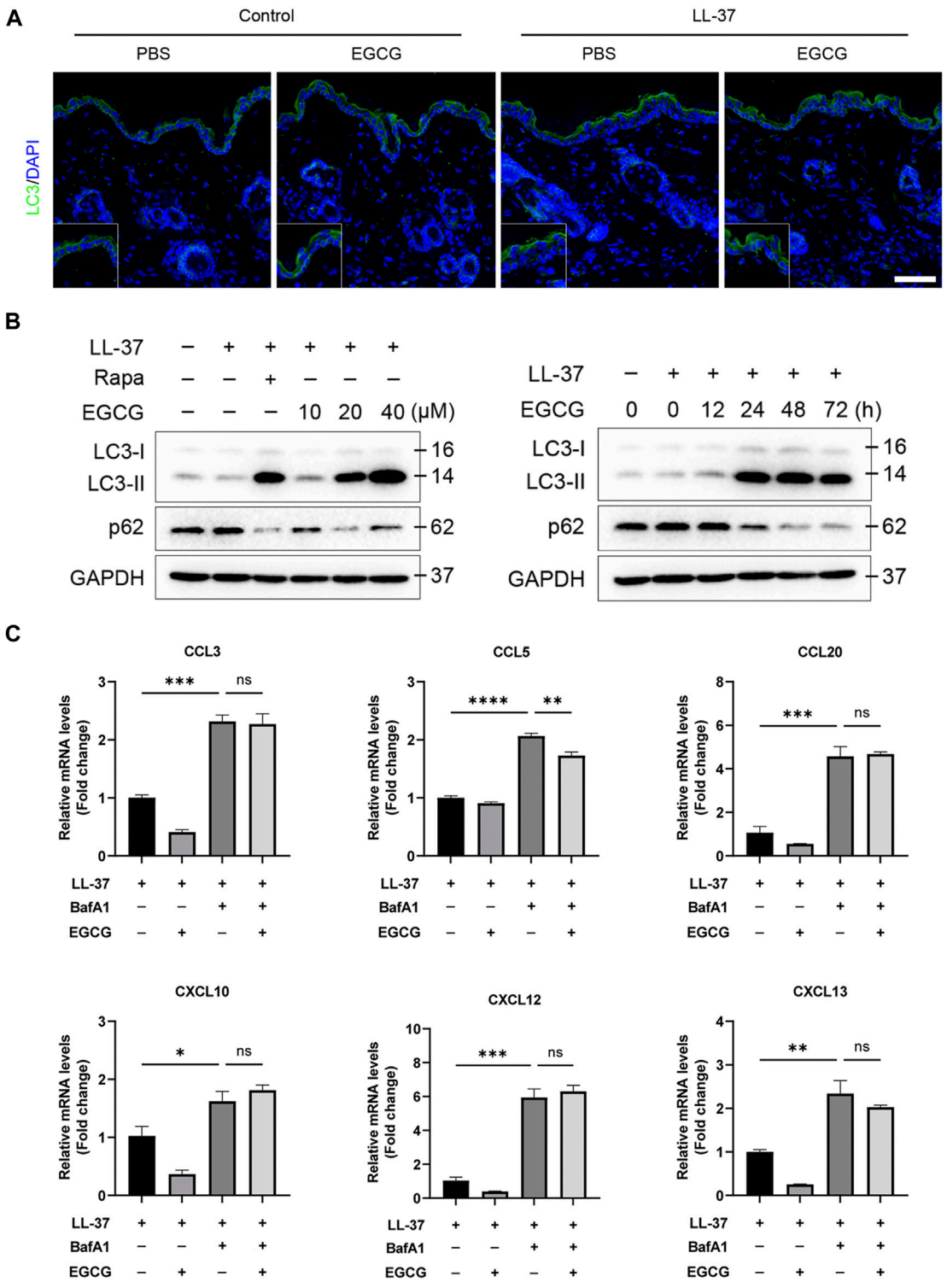

FIGURE 6
EGCG reduced rosacea-like inflammation by inducing keratinocyte autophagy. **(A)** LC3 immunofluorescence staining (green) in LL-37-induced mice treated with or without EGCG. DAPI staining (blue) indicates nuclear localization. Scale bar: 50 μm. **(B)** Representative immunoblot analysis for the expression of LC3 and p62 in a dose- and time-dependent manner of EGCG treatment. **(C)** Inhibition of autophagy impairs the anti-inflammatory role of EGCG in HaCaT cells. The mRNA expression levels of CCL3, CCL5, CCL20, CXCL10, CXCL12, and CXCL13. All results are representative of at least three independent experiments. Data represent the mean ± SEM. One-way ANOVA with Bonferroni's *post hoc* test was used for statistical analyses. *$p < 0.05$, **$p < 0.01$, and ***$p < 0.001$. ns, no significance.

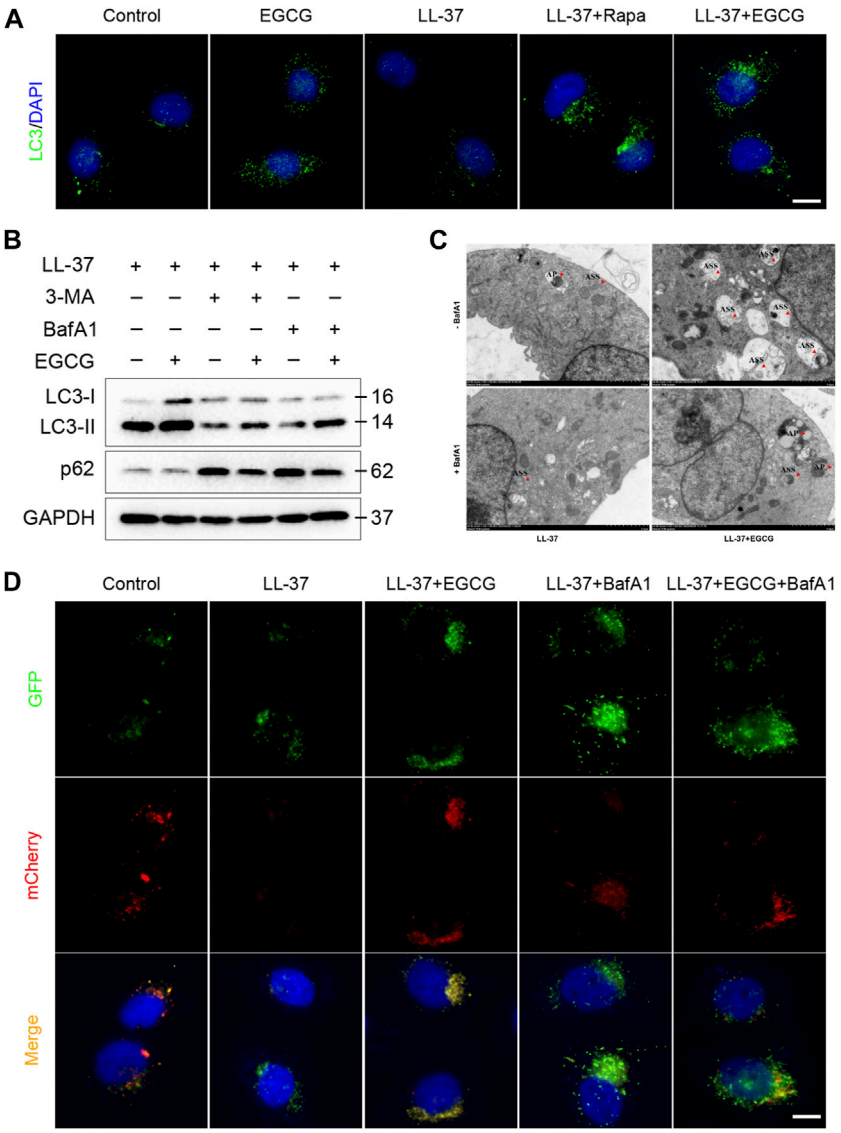

FIGURE 7
EGCG-induced autophagy in LL-37-induced HaCaT cells. **(A)** Immunostaining of LC3 in HaCaT keratinocytes treated with LL37 and/or EGCG for 24 h. DAPI staining (blue) indicates nuclear localization. Scale bar: 20 μm. **(B)** Representative immunoblot analysis of autophagy marker proteins in response to various treatments. **(C)** Representative TEM images showing the ultrastructure of HaCaT cells incubated with EGCG with or without BafA1 in the presence of LL-37. The red arrowheads indicate the autophagic vacuoles, respectively. AP, autophagosome; ASS, autolysosome. **(D)** HaCaT cells were transfected with the mCherry-GFP-LC3 plasmid and then treated with EGCG and/or BafA1 in the presence of LL-37 for 24 h. Nuclei were stained with DAPI. Scale bar: 20 μm. All results are representative of at least three independent experiments.

signaling in rosacea (Deng et al., 2021). In this study, an upregulated mTOR pathway in the epidermis of rosacea patients was confirmed using GSVA. Subsequently, WGCNA revealed the potential regulation of mTOR signaling on autophagy in the epidermis of rosacea. Autophagy is essential for the homeostasis of keratinocytes, and dysregulation of autophagy contributes to the pathogenesis of skin diseases and has been shown to play a critical role in inflammatory skin disorders, including atopic dermatitis, psoriasis, and allergic contact dermatitis (Cadwell, 2016). In this study, we found that autophagy was decreased and contributed to the progression of rosacea. mTOR is a well-known regulator of autophagy (Munson and Ganley, 2015). It has been shown that IL-17A-activated PI3K/AKT/mTOR signaling contributed to the inflammatory response of psoriasis partly by inhibiting autophagy in keratinocytes (Varshney and Saini, 2018). Rapamycin, a well-known mTOR inhibitor, alleviated psoriasis-like dermatitis by inducing autophagy (Kim et al., 2021). Our previous study revealed the therapeutic role of rapamycin in rosacea. We also revealed the induction of autophagy by rapamycin in rosacea-like dermatitis, implying that autophagy was a novel therapeutic target for rosacea.

In recent years, natural medicinal products and plant extracts have been highly sought after for therapeutic drugs with the advantages of cost effectiveness, high bioactivity, abundant content, and safety. EGCG, a

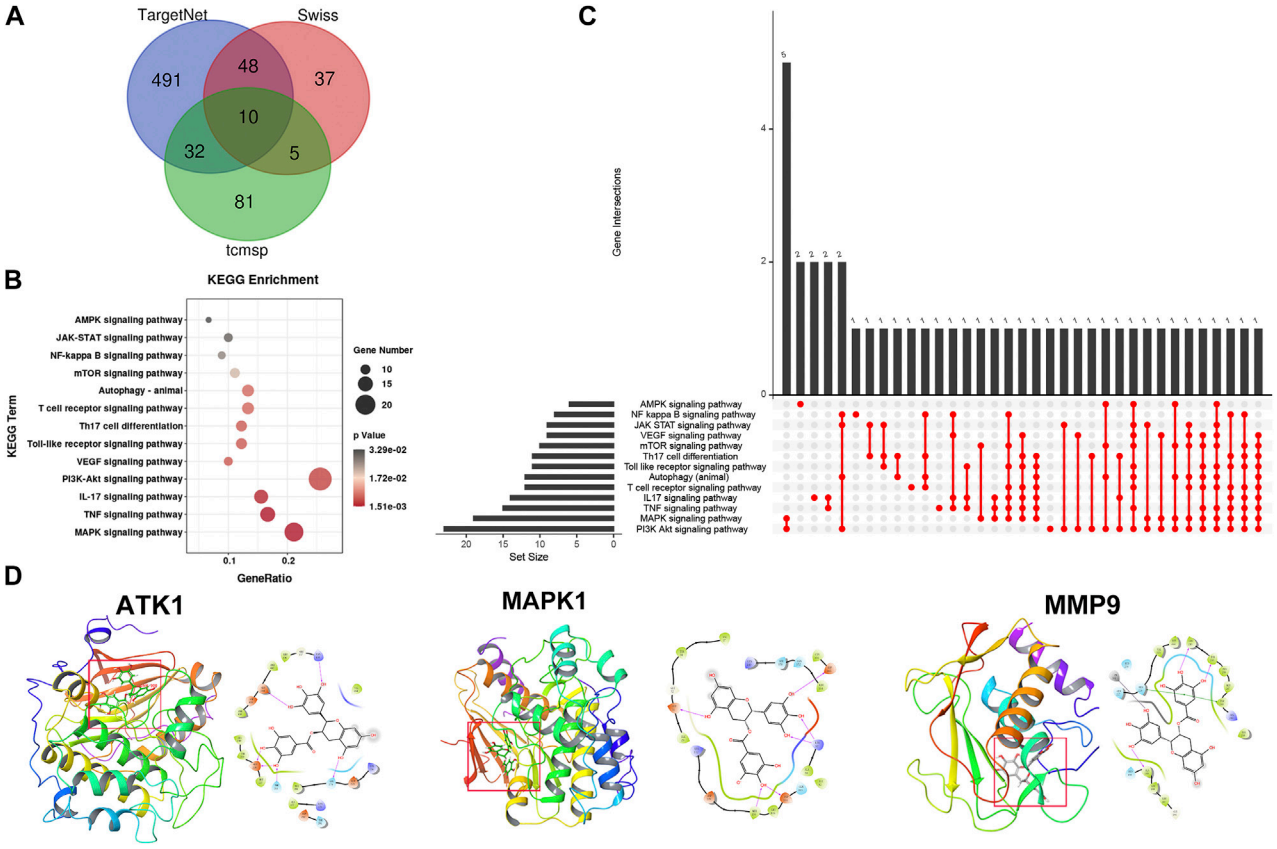

FIGURE 8
Pharmacological targets of EGCG in rosacea. **(A)** Overlapped target genes of EGCG in TargetNet, Swiss, and Tcmsp. **(B)** KEGG enrichment analysis of EGCG-targeted signaling pathways. **(C)** Upset diagram of EGCG-targeted signaling pathways. **(D)** Molecular docking revealed the binding targets of EGCG.

natural polyphenol found in green tea, has been reported to have many biological activities, including anti-inflammatory, antioxidant, cardioprotective, neuroprotective, and anticancer activities (Nan et al., 2019; Huang et al., 2020; Yi et al., 2020). In this study, based on the mTOR signal and autophagy-related genes, EGCG was predicted as a candidate drug for rosacea. The *in vivo* and *in vitro* experiments showed that EGCG attenuated rosacea-like inflammation by inducing keratinocyte autophagy. Consistent with our results, EGCG was proven therapeutic to various diseases by inducing cytoprotective autophagy (Wu et al., 2021). Cytoplasmic LC3 puncta formation is the hallmark of autophagy (Schaaf et al., 2016); the blocking of autophagy flux and an increase in the autophagy level lead to increased LC3-II (Lamark et al., 2017). In the present study, it was observed that EGCG promoted the formation of autophagosomes and autophagolysosomes accompanied in a dose- and time-dependent manner. Subsequently, the target prediction and molecular docking showed that ATK1, MAPK1, and MMP9 were the potential targets of EGCG. ATK/MAPK pathways were reported as a regulator of autophagy (Yuan et al., 2022).

Conclusion

In summary, we demonstrated a contribution of impaired autophagy in rosacea pathogenesis and implied EGCG as an effective treatment strategy for rosacea, which attenuated rosacea-like inflammation *via* inducting autophagy in keratinocytes.

Data availability statement

The original contributions presented in the study are included in the article/Supplementary Material; further inquiries can be directed to the corresponding authors.

Ethics statement

All studies and experimental procedures were approved by the Animal Ethics Committee of Xiangya Hospital of the Central South University (No. 201703211).

Author contributions

JL and YZ conceived this project; LZ, YZ, and YW performed and analyzed the experiments; YZ performed bioinformatics analyses; ZD, YH, HX, and QW gave critical comments; and LZ,

YZ, and JL wrote the manuscript with the approval of all other authors.

Funding

This work was supported by the National Key Research and Development Program of China (No. 2021YFF1201205), the National Natural Science Funds for Distinguished Young Scholars (82225039), and the National Natural Science Foundation of China (Nos. 82273557, 81703149, 81874251, and 82173448). This work was supported by the National Natural Science Foundation of Hunan Province (2020JJ5950).

Conflict of interest

Author QW was employed by Hunan Binsis Biotechnology Co., Ltd.

The remaining authors declare that the research was conducted in the absence of any commercial or financial relationships that could be construed as a potential conflict of interest.

Publisher's note

All claims expressed in this article are solely those of the authors and do not necessarily represent those of their affiliated organizations, or those of the publisher, the editors, and the reviewers. Any product that may be evaluated in this article, or claim that may be made by its manufacturer, is not guaranteed or endorsed by the publisher.

Supplementary material

The Supplementary Material for this article can be found online at: https://www.frontiersin.org/articles/10.3389/fphar.2023.1092473/full#supplementary-material

References

Agrahari, G., Sah, S. K., Nguyen, C. T., Choi, S. S., Kim, H.-Y., and Kim, T.-Y. (2020). Superoxide dismutase 3 inhibits LL-37/KLK-5-mediated skin inflammation through modulation of EGFR and associated inflammatory cascades. *J. investigative dermatology* 140 (3), 656–665.e8. doi:10.1016/j.jid.2019.08.434

Ahn, C. S., and Huang, W. W. (2018). Rosacea pathogenesis. *Dermatol. Clin.* 36 (2), 81–86. doi:10.1016/j.det.2017.11.001

Awosika, O., and Oussedik, E. (2018). Genetic predisposition to rosacea. *Dermatol. Clin.* 36 (2), 87–92. doi:10.1016/j.det.2017.11.002

Braegelmann, C., Niebel, D., Ferring-Schmitt, S., Fetter, T., Landsberg, J., Hölzel, M., et al. (2022). Epigallocatechin-3-gallate exhibits anti-inflammatory effects in a human interface dermatitis model-implications for therapy. *J. Eur. Acad. Dermatol Venereol.* 36 (1), 144–153. doi:10.1111/jdv.17710

Cadwell, K. (2016). Crosstalk between autophagy and inflammatory signalling pathways: Balancing defence and homeostasis. *Nat. Rev. Immunol.* 16 (11), 661–675. doi:10.1038/nri.2016.100

Chamcheu, J. C., Siddiqui, I. A., Adhami, V. M., Esnault, S., Bharali, D. J., Babatunde, A. S., et al. (2018). Chitosan-based nanoformulated (-)-epigallocatechin-3-gallate (EGCG) modulates human keratinocyte-induced responses and alleviates imiquimod-induced murine psoriasiform dermatitis. *Int. J. Nanomedicine* 13, 4189–4206. doi:10.2147/ijn.s165966

Cotto, K. C., Wagner, A. H., Feng, Y.-Y., Kiwala, S., Coffman, A. C., Spies, G., et al. (2018). DGIdb 3.0: A redesign and expansion of the drug-gene interaction database. *Nucleic acids Res.* 46 (D1), D1068–D1073. doi:10.1093/nar/gkx1143

Deng, Z., Chen, M., Liu, Y., Xu, S., Ouyang, Y., Shi, W., et al. (2021). A positive feedback loop between mTORC1 and cathelicidin promotes skin inflammation in rosacea. *EMBO Mol. Med.* 13 (5), e13560. doi:10.15252/emmm.202013560

Deng, Z., Lei, X., Zhang, X., Zhang, H., Liu, S., Chen, Q., et al. (2015). mTOR signaling promotes stem cell activation via counterbalancing BMP-mediated suppression during hair regeneration. *J. Mol. Cell. Biol.* 7 (1), 62–72. doi:10.1093/jmcb/mjv005

Domingo, D. S., Camouse, M. M., Hsia, A. H., Matsui, M., Maes, D., Ward, N. L., et al. (2010). Anti-angiogenic effects of epigallocatechin-3-gallate in human skin. *Int. J. Clin. Exp. pathology* 3 (7), 705–709.

Fogel, A. L., Hill, S., and Teng, J. M. C. (2015). Advances in the therapeutic use of mammalian target of rapamycin (mTOR) inhibitors in dermatology. *J. Am. Acad. Dermatology* 72 (5), 879–889. doi:10.1016/j.jaad.2015.01.014

Freshour, S. L., Kiwala, S., Cotto, K. C., Coffman, A. C., McMichael, J. F., Song, J. J., et al. (2021). Integration of the drug-gene interaction database (DGIdb 4.0) with open crowdsource efforts. *Nucleic acids Res.* 49 (D1), D1144–D1151. doi:10.1093/nar/gkaa1084

Gallo, R. L., Granstein, R. D., Kang, S., Mannis, M., Steinhoff, M., Tan, J., et al. (2018). Standard classification and pathophysiology of rosacea: The 2017 update by the national rosacea society expert committee. *J. Am. Acad. Dermatology* 78 (1), 148–155. doi:10.1016/j.jaad.2017.08.037

Gether, L., Overgaard, L. K., Egeberg, A., and Thyssen, J. P. (2018). Incidence and prevalence of rosacea: A systematic review and meta-analysis. *Br. J. dermatology* 179 (2), 282–289. doi:10.1111/bjd.16481

Huang, H.-T., Cheng, T.-L., Ho, C.-J., Huang, H. H., Lu, C.-C., Chuang, S.-C., et al. (2020). Intra-articular injection of (-)-Epigallocatechin 3-gallate to attenuate articular cartilage degeneration by enhancing autophagy in a post-traumatic osteoarthritis rat model. *Antioxidants (Basel, Switz.* 10 (1), 8. doi:10.3390/antiox10010008

Kim, H. R., Kim, J. C., Kang, S. Y., Kim, H. O., Park, C. W., and Chung, B. Y. (2021). Rapamycin alleviates 2,3,7,8-Tetrachlorodibenzo-p-dioxin-Induced aggravated dermatitis in mice with imiquimod-induced psoriasis-like dermatitis by inducing autophagy. *Int. J. Mol. Sci.* 22 (8), 3968. doi:10.3390/ijms22083968

Kim, J. S., Seo, B. H., Cha, D. R., Suh, H. S., and Choi, Y. S. (2022). Maintenance of remission after oral metronidazole add-on therapy in rosacea treatment: A retrospective, comparative study. *Ann. Dermatol* 34 (6), 451–460. doi:10.5021/ad.22.093

Kulkarni, N. N., Takahashi, T., Sanford, J. A., Tong, Y., Gombart, A. F., Hinds, B., et al. (2020). Innate immune dysfunction in rosacea promotes photosensitivity and vascular adhesion molecule expression. *J. Investigative Dermatology* 140 (3), 645–655.e6. doi:10.1016/j.jid.2019.08.436

Lamark, T., Svenning, S., and Johansen, T. (2017). Regulation of selective autophagy: The p62/SQSTM1 paradigm. *Essays Biochem.* 61 (6), 609–624. doi:10.1042/EBC20170035

Li, R., Li, Y., Liang, X., Yang, L., Su, M., and Lai, K. P. (2021). Network Pharmacology and bioinformatics analyses identify intersection genes of niacin and COVID-19 as potential therapeutic targets. *Brief. Bioinform* 22 (2), 1279–1290. doi:10.1093/bib/bbaa300

Li, Y., Yang, L., Wang, Y., Deng, Z., Xu, S., Xie, H., et al. (2021). Exploring metformin as a candidate drug for rosacea through network pharmacology and experimental validation. *Pharmacol. Res.* 174, 105971. doi:10.1016/j.phrs.2021.105971

Logger, J. G. M., Olydam, J. I., and Driessen, R. J. B. (2020). Use of beta-blockers for rosacea-associated facial erythema and flushing: A systematic review and update on proposed mode of action. *J. Am. Acad. Dermatology* 83 (4), 1088–1097. doi:10.1016/j.jaad.2020.04.129

Munson, M. J., and Ganley, I. G. (2015). MTOR, PIK3C3, and autophagy: Signaling the beginning from the end. *Autophagy* 11 (12), 2375–2376. doi:10.1080/15548627.2015.1106668

Nan, J., Nan, C., Ye, J., Qian, L., Geng, Y., Xing, D., et al. (2019). EGCG protects cardiomyocytes against hypoxia-reperfusion injury through inhibition of OMA1 activation. *J. Cell. Sci.* 132 (2), jcs220871. doi:10.1242/jcs.220871

Nan, S., Wang, P., Zhang, Y., and Fan, J. (2021). Epigallocatechin-3-Gallate provides protection against alzheimer's disease-induced learning and memory impairments in rats. *Drug Des. Dev. Ther.* 15, 2013–2024. doi:10.2147/DDDT.S289473

Noh, S. U., Cho, E. A., Kim, H. O., and Park, Y. M. (2008). Epigallocatechin-3-gallate improves Dermatophagoides pteronissinus extract-induced atopic dermatitis-like skin lesions in NC/Nga mice by suppressing macrophage migration inhibitory factor. *Int. Immunopharmacol.* 8 (9), 1172–1182. doi:10.1016/j.intimp.2008.04.002

Ohsumi, Y. (2014). Historical landmarks of autophagy research. *Cell Res.* 24 (1), 9–23. doi:10.1038/cr.2013.169

Qiang, L., Yang, S., Cui, Y. H., and He, Y. Y. (2021). Keratinocyte autophagy enables the activation of keratinocytes and fibroblastsand facilitates wound healing. *Autophagy* 17 (9), 2128–2143. doi:10.1080/15548627.2020.1816342

Schaaf, M. B. E., Keulers, T. G., Vooijs, M. A., and Rouschop, K. M. A. (2016). LC3/GABARAP family proteins: autophagy-(un)related functions. *FASEB J.* 30 (12), 3961–3978. doi:10.1096/fj.201600698R

Song, X., Narzt, M. S., Nagelreiter, I. M., Hohensinner, P., Terlecki-Zaniewicz, L., Tschachler, E., et al. (2017). Autophagy deficient keratinocytes display increased DNA damage, senescence and aberrant lipid composition after oxidative stress *in vitro* and *in vivo*. *Redox Biol.* 11, 219–230. doi:10.1016/j.redox.2016.12.015

Steinhoff, M., Buddenkotte, J., Aubert, J., Sulk, M., Novak, P., Schwab, V. D., et al. (2011). Clinical, cellular, and molecular aspects in the pathophysiology of rosacea. *J. investigative dermatology. Symposium Proc.* 15 (1), 2–11. doi:10.1038/jidsymp.2011.7

Varshney, P., and Saini, N. (2018). PI3K/AKT/mTOR activation and autophagy inhibition plays a key role in increased cholesterol during IL-17A mediated inflammatory response in psoriasis. *Biochimica Biophysica Acta. Mol. Basis Dis.* 1864, 1795–1803. doi:10.1016/j.bbadis.2018.02.003

Wang, B., Yuan, X., Huang, X., Tang, Y., Zhao, Z., Yang, B., et al. (2021). Efficacy and safety of hydroxychloroquine for treatment of patients with rosacea: A multicenter, randomized, double-blind, double-dummy, pilot study. *J. Am. Acad. Dermatology* 84 (2), 543–545. doi:10.1016/j.jaad.2020.05.050

Wang, Z., Zhou, H., Zheng, H., Zhou, X., Shen, G., Teng, X., et al. (2021). Autophagy-based unconventional secretion of HMGB1 by keratinocytes plays a pivotal role in psoriatic skin inflammationflammation. *Autophagy* 17 (2), 529–552. doi:10.1080/15548627.2020.1725381

Wishart, D. S., Feunang, Y. D., Guo, A. C., Lo, E. J., Marcu, A., Grant, J. R., et al. (2018). DrugBank 5.0: A major update to the DrugBank database for 2018. *Nucleic Acids Res.* 46 (D1), D1074–d1082. doi:10.1093/nar/gkx1037

Wu, D., Liu, Z., Wang, Y., Zhang, Q., Li, J., Zhong, P., et al. (2021). Epigallocatechin-3-Gallate alleviates high-fat diet-induced nonalcoholic fatty liver disease via inhibition of apoptosis and promotion of autophagy through the ROS/MAPK signaling pathway. *Oxid. Med. Cell Longev.* 2021, 5599997. doi:10.1155/2021/5599997

Yamasaki, K., Di Nardo, A., Bardan, A., Murakami, M., Ohtake, T., Coda, A., et al. (2007). Increased serine protease activity and cathelicidin promotes skin inflammation in rosacea. *Nat. Med.* 13 (8), 975–980. doi:10.1038/nm1616

Yamasaki, K., Kanada, K., Macleod, D. T., Borkowski, A. W., Morizane, S., Nakatsuji, T., et al. (2011). TLR2 expression is increased in rosacea and stimulates enhanced serine protease production by keratinocytes. *J. investigative dermatology* 131 (3), 688–697. doi:10.1038/jid.2010.351

Yi, J., Chen, C., Liu, X., Kang, Q., Hao, L., Huang, J., et al. (2020). Radioprotection of EGCG based on immunoregulatory effect and antioxidant activity against ^{60}Coγ radiation-induced injury in mice. *Food Chem. Toxicol.* 135, 111051. doi:10.1016/j.fct.2019.111051

Yuan, Q., Zhang, X., Wei, W., Zhao, J., Wu, Y., Zhao, S., et al. (2022). Lycorine improves peripheral nerve function by promoting Schwann cell autophagy via AMPK pathway activation and MMP9 downregulation in diabetic peripheral neuropathy. *Pharmacol. Res.* 175, 105985. doi:10.1016/j.phrs.2021.105985

Zhang, H., Zhang, Y., Li, Y., Wang, Y., Yan, S., Xu, S., et al. (2021). Bioinformatics and network pharmacology identify the therapeutic role and potential mechanism of melatonin in AD and rosacea. *Front. Immunol.* 12, 756550. doi:10.3389/fimmu.2021.756550

Zhang, J., Jiang, P., Sheng, L., Liu, Y., Liu, Y., Li, M., et al. (2021). A novel mechanism of carvedilol efficacy for rosacea treatment: Toll-like receptor 2 inhibition in macrophages. *Front. Immunol.* 12, 609615. doi:10.3389/fimmu.2021.609615

Frontiers in Pharmacology

Explores the interactions between chemicals and living beings

The most cited journal in its field, which advances access to pharmacological discoveries to prevent and treat human disease.

Discover the latest Research Topics

See more →

Frontiers

Avenue du Tribunal-Fédéral 34
1005 Lausanne, Switzerland
frontiersin.org

Contact us

+41 (0)21 510 17 00
frontiersin.org/about/contact